UNIVERSITAT POLITÈCNICA DE VALÈNCIA

HYDRAULIC AND ENVIRONMENTAL ENGINEERING DEPARTMENT

DOCTORAL PROGRAM OF WATER AND ENVIRONMENTAL ENGINEERING

Ph. D. THESIS

METHODOLOGY FOR ENERGY EFFICIENCY IMPROVEMENT ANALYSIS IN PRESSURIZED IRRIGATION NETWORKS. PRACTICAL APPLICATION

AUTHOR

MODESTO PÉREZ SÁNCHEZ

THESIS DIRECTOR

Ph. D. PETRA AMPARO LÓPEZ JIMÉNEZ

Ph. D. FRANCISCO JAVIER SÁNCHEZ ROMERO

Valencia, Spain

March, 2017

This page is intentionally left blank.

You left when I needed you most,
but I know that you gave me the necessary strength to do it.

In memoriam: Sergio

"When the man mixes faith in what he believes: study, effort, perseverance and long-term, the resultant fluid is constant, durable and wise"

Julio C. Trigo Sixto

Acknowledgements

A thesis should be considered a team sport in which the thesis' author is one more player. Therefore, many people are necessary to join the 'game' and another are essential to support for getting the challenge. Naming them all is impossible.

If there is an irreplaceable person in this team, she is my director Mrs Amparo López. She is the first to wear the overall and she is the last one to take it off her. Her ideas, professional and personal advice, reviews as well as our reflections have been fundamental along this thesis. Thanks so much, each day has its own eagerness.

I also want to thank another director, Mr Francisco J. Sánchez. His force, reflections and reviews were important to develop the methodologies. Along this stage, we had had time to study, enjoy, cry and smile together, but the good moments will only be remembered.

I want to give my special thanks to Prof. Helena Ramos, from IST, for her help in the reviews of different papers as well as for accepting me to do my research stay in her department. Her point of view improved the different developed researches of this thesis.

From IST, I want to thank Mohsen Besharat, Mariana Simão, and João Pedro. They help me to tune-up the experimental hydraulic facilities. However, the tests could be carried out thanks to the help of Bernardo Capello and João Fernandes, who made water and electricity friendly. Special gratitude for Prof. Paulo Branco who from the first day betted by my experimental tests, spending his bit free time in a Spanish he had just met.

I am grateful to all teachers from Primary to University, everyone of them contributed their sand grain in my academic training.

Also, I extend this gratitude to colleagues of Hydraulic and Environmental Engineering Department for the welcome from the first moment as well as to Andres, Batiste, Carlos, Javier, Miguel, Paco, Manolo, as well as the irrigation communities, which helped me.

Outside of the academic life, the unconditional support of my family (in special, my parent and sisters) and friends were crucial to obtain energy when it was necessary. I apologize for the time that the thesis deprived me of being with you.

I do not forget my friends Julio and Rovira. The first reminds me every morning that the life is wonderful, the second, at the monthly dinner, he makes me laugh with his happened adventures. Special consideration to Vero and Jose as well as their son, Diego, they are the real treasure which I discovered.

I will eternally be grateful to Pepe, I will never forget the protection you offered me when I was most vulnerable. Pepe, Tere, Rigo, and Rosa were the real props that made the boat didn't sink.

I apologize if someone has not been named. Thanks you all.

This page is intentionally left blank.

Abstract

Analyses of possible synergies between energy recovery and water management are essential for achieving sustainable improvements in the performance of pressurized irrigation networks. Improving the energy efficiency of water systems by hydraulic energy recovery is becoming an inevitable trend for energy conservation, emissions reduction, and increases in profit margins.

This *Ph.D.* research is focused on the proposal and development of an optimization methodology that improves energy efficiency in pressurized irrigation networks. To develop this methodology, the main objective of this *Ph.D.* thesis, the research is supported by secondary objectives. The first secondary objective overviews the state-of-the-art for different hydropower systems, paying attention to those systems in which residual energy can be considered for energy improvement. Furthermore, the need to analyze this energy improvement in pressurized irrigation networks is justified through enumerating the main advantages and disadvantages of these energy recoveries. This first objective establishes the contextualization stage of the thesis. The second part of this *Ph.D*. research, which develops the rest of the objectives, is called the procedural stage. This phase contains the analytical and experimental development of this research. The analytical phase develops the main steps of the optimization strategy. Each step comprises one methodology or method that is focused on the following objectives:

- To propose a methodology to determine the circulating flow over time in pressurized irrigation networks in any line depending on the agronomist intrinsic parameters of the established crops
- To develop a calibration strategy for the flow assignment in lines, which indicates the success of the proposed methodology
- To establish the energy balance as well as the involved energy terms to quantify the theoretical recoverable energy in pressurized water networks, particularly in irrigation networks
- To present a new methodology to maximize the recovered energy considering the actual feasibility to allocate pumps working as turbines (*PATs*) within pressurized water networks by using simulated annealing as a water management tool.

The analytical phase is complemented with an intensive experimental campaign in two different *PATs* (radial and axial) in steady and unsteady flow conditions. The campaign regarding steady flow conditions enables the study of the efficiency variations in the machine as a function of the flow and rotational speed. The experimental analysis as well as the modification of the classical affinity laws allows one to determine the best efficiency line (*BEL*) and the best efficiency head (*BEH*) based on Suter parameters. Both lines enable modelers to establish the optimal rotational speed as a function of the

flow during each instant to maximize the recovered energy. These new lines (*BEL* and *BEH*) should be incorporated within the optimization strategy, developing a procedure to recover energy as a function of the number of installed machines.

The developed methodologies for each defined objective are applied in three different case studies, in which specific software (*i.e., EPANET*, *WaterGEMS*) is used to develop the simulations. The methodology to determine the circulating flows is applied in small irrigation networks located in Vallada (Spain). The flow over time in any line is determined based on the farmers' habits. This methodology is validated by developing a calibration strategy that is adapted from traditional hydrological models, defining some particular key performance indicators. This calibration strategy is applied on a pressurized irrigation network located in Callosa d'en Sarrià (Spain). The obtained results for the calibration of the maximum flows are satisfactory in all intervals. Once the methodology is calibrated, an energy balance is developed in the network in Vallada. This balance establishes the potential margin of the energy improvement in the pressurized irrigation networks. The balance determines the values of the theoretically recoverable energy of 178.10 MWh/year (*i.e.,* 65% of the total improved energy in the network) when all irrigation points are considered or 89.99 MWh/year if the line with the greater theoretical recovered energy is only considered.

The development of the methodology to determine the circulating flows as well as the developed energy balance for an individual point (*i.e.,* line, hydrant or irrigation point) promote the need to maximize the theoretically recovered energy, considering the location of the hydraulic machinery. To establish the best location of the machines, a methodology based on a simulated annealing algorithm through two different objective functions, is proposed to optimize the emplacement of the recovery systems. This maximization is developed by considering the following:

- the demands of the farmers, which depend on the different habits of farmers (*i.e.,* irrigation amount, maximum days between irrigation, weekly irrigation trends, and irrigation duration patterns);
- the location of the *PATs* or turbines according to the number of selected recovery points;
- the type of machine installed (*i.e.,* specific speed, impeller diameter, rotational speed); and
- the analysis of the recovered energy considering the machine efficiency at each time point as a function of the circulating flow.

This maximization strategy is again applied in the Vallada network, resulting in a recovered energy value of 26.51 MWh/year (9.55% of the provided energy in the system).

The second case study analyzes a large pressurized system (Júcar-Vinalopó Transfer) to determine the energy balance. In the case study, twenty recovery points are technically and economically analyzed. When the payback period (*PSR*) and energy index (*EI*) are

taken into account, only five of the twenty systems are considered feasible. However, if these viable recovery points are considered, the total recovered energy represents 7% of the improved energy in the system.

The third case study analyzes the influence of the flow consumption patterns on the energy behavior of the pressurized water systems as well as the difference between the energy balances depending on the consumption flow patterns. To only compare the flow pattern influences, the case study is applied in a synthetic pump network, in which four different consumption patterns are studied. These patterns are obtained from flowmeter readings in two irrigation and two supply networks. Related to this case study, new parameters are presented in this research to establish the influence of the consumption patterns. These parameters are necessary because the proposed energy balance does not directly allow for the comparison between different case studies when recorded flows are very different between networks. These parameters are as follows: the nondimensional energy footprint of the water (EWF_A) and the nondimensional flow (Q_A). Both parameters allow establishing and comparing the energy footprint of the water between different systems (when the water manager is in the design or management phase). EWF_A is a powerful index for comparing different networks in energy audits. The developed analysis of EWF_A in this case study shows that the networks with less variability in their consumption flow patterns present smaller values of EWF_A. The proposed parameter (EWF_A) can also be used as a sustainability criterion during the initial design phase of pressurized water networks, in addition to the technical and economic criteria used, as long as its thresholds are previously defined.

Finally, to complement the developed analysis for the installation of the recovery systems in pressurized water systems, the unsteady flow in these facilities is also analyzed. The analysis of the obtained experimental data during the experimental campaign as well as the evaluation of the simulated data (which is conducted using *Allievi* software) allow for isolating the overspeed effect in the hydraulic machine when the recovery system reaches runaway conditions. The flow variation according to the head and rotational speed are analyzed for both machines, and the results are related with the best efficiency point (*BEP*) of the *PAT* (Q_{BEP}, H_{BEP}, N_{BEP}) through a mathematical transformation of the available pump data (based on experiments especially developed for this study) into characteristic curves of the discharge variation, Q/Q_{BEP}, with the rotating speed, N/N_{BEP}. If machine behavior is compared between both machines (radial and axial), there are differences between the radial and axial machines when the turbine operates under runaway conditions. In the radial *PAT*, the flow decreases as a constant value of h ($h=H/H_{BEP}$), while inverse results are obtained when the axial machine is analyzed.

This page is intentionally left blank.

Resumen

El desarrollo de los análisis de las posibles sinergias entre los sistemas de recuperación de energía y la gestión del agua es esencial, para poder lograr mejoras en la eficiencia energética de las redes de riego presurizadas a través de medidas sostenibles. La mejora de la eficiencia energética, mediante la recuperación de la energía hidráulica, se está convirtiendo en una tendencia inevitable para la conservación de la energía, la reducción de las emisiones de gases efecto invernadero y el aumento de los márgenes de beneficio en los sistemas de distribución de agua presurizados.

Esta tesis doctoral está centrada en la propuesta y desarrollo de una metodología de optimización, la cual, mejore la eficiencia energética en redes de riego presurizadas. Para desarrollar esta metodología, objetivo principal de esta tesis, la investigación está basada en diferentes objetivos secundarios. El primer objetivo secundario, estudia el estado del arte en los diferentes sistemas hidroeléctricos, prestando atención a aquellos sistemas en los que, la energía residual puede ser tenida en cuenta para mejorar la eficiencia energética. La necesidad de analizar esta mejora energética en las redes de riego presurizadas, se justifica mediante la enumeración de las principales ventajas y desventajas de estos sistemas de recuperación tienen sobre los sistemas de distribución. Este primer objetivo, establece la etapa de contextualización de la tesis. La segunda parte de la tesis, denominada fase procedimental o de procedimiento, desarrolla el resto de los objetivos y contiene, el desarrollo analítico y experimental de esta investigación. La fase analítica desarrolla los principales bloques que forman la estrategia de optimización. Estos bloques de contenido están constituidos, cada uno de ellos, por una metodología desarrollada o método aplicado, cubriendo los siguientes objetivos:

- Proponer una metodología que determine el caudal circulante a lo largo del tiempo, en cualquier línea, en función de los parámetros intrínsecos agronómicos.
- Desarrollar una estrategia de calibración para la asignación de caudales en líneas, que demuestre la bondad de la metodología propuesta.
- Establecer el balance energético, así como los términos energéticos involucrados, para cuantificar la energía recuperable teórica en redes presurizadas, particularmente en redes de riego.
- Presentar una nueva metodología de maximización de energía recuperada donde la viabilidad de asignar bombas trabajando como turbinas (*PATs*) dentro de redes de distribución sea considerada, mediante el uso de la herramienta 'simulated annealing' en la gestión del agua.

La fase analítica se complementa con el desarrollo de una campaña experimental en dos *PATs* diferentes (una de tipo radial y otra de tipo axial). Ambas máquinas han sido ensayadas en condiciones de flujo permanente y transitorio. El análisis experimental en

condiciones de flujo permanente ha permitido estudiar la variación de la eficiencia de la máquina en función del caudal y de la velocidad de rotación de la misma. Este análisis experimental, así como la modificación de las leyes clásicas de semejanza, han hecho posible la definición de la mejor línea de eficiencia (best efficiency line (*BEL)*) y la mejor eficiencia de altura recuperada (best efficiency head (*BEH)*). Ambas líneas están basadas en los parámetros de Suter, y permiten a los modeladores el establecimiento de la velocidad de giro óptima en función del caudal circulante en cada instante, maximizando la energía recuperada. Estas nuevas líneas (*BEL* y *BEH*) deben incorporarse a la estrategia de optimización, teniéndolas en cuenta a lo largo del proceso para recuperar energía en función del número de máquinas instaladas en el sistema.

Las metodologías desarrolladas en cada objetivo, se han aplicado en tres casos de estudios diferentes. En estos casos de estudio se ha utilizado software específico (*e.g., EPANET*, *WaterGEMS*) para desarrollar las simulaciones. La metodología para determinar los caudales circulantes a lo largo del tiempo se ha aplicado a una red de riego ubicada en Vallada (España). El caudal en función del tiempo, se ha determinado en base a los hábitos de riego de los agricultores, y la metodología ha sido validada mediante el desarrollo de una estrategia de calibración. Esta estrategia de calibración ha sido adaptada de los modelos hidrológicos tradicionales, definiendo algunos indicadores clave de rendimiento (*KPIFs*) y aplicándose en una red de riego situada en Callosa d'en Sarrià, Alicante (España). Los resultados obtenidos para caudales máximos han sido satisfactorios en todos los intervalos de tiempo de tiempo considerados. Una vez calibrada la metodología, el balance energético ha sido desarrollado en la red de riego de Vallada. Este balance ha permitido establecer el margen potencial de mejora de eficiencia energética en las redes de riego analizadas. En el caso concreto de Vallada, el balance energético determina que los valores de energía teóricamente recuperable son 178,10 MWh/año (valor que representa un 65% de la energía total aportada a la red) cuando todas las tomas de riego son consideradas, o 89,99 MWh/año si solamente la línea con mayor energía teóricamente recuperable es considerada.

El desarrollo de la metodología para determinar los caudales circulantes, así como el balance energético desarrollado para cada punto individual analizado (es decir, línea, hidrante o toma de riego) promueven la necesidad de maximizar la energía teórica recuperada, teniendo en cuenta la ubicación de las máquinas hidráulicas a instalar. Para establecer la mejor ubicación de éstas máquinas, se propone una metodología basada en el algoritmo de recocido simulado (*simulated annealing*) considerando dos funciones objetivo diferentes, optimizando el emplazamiento de los sistemas de recuperación. Esta estrategia de maximización ha sido desarrollada teniendo en cuenta:

- los hábitos culturales de los agricultores, los cuales dependen de los hábitos de la dotación, los días máximos entre riegos, la tendencia semanal de riego, así como el tiempo de riego.
- la ubicación de *PATs* o turbinas de acuerdo al número de puntos de recuperación seleccionados.

- el tipo de máquina instalada atendiendo a la velocidad específica, el diámetro del impulsor y/o la velocidad de rotación.
- el análisis de la energía recuperada considerando el rendimiento de la máquina en cada momento en función del caudal circulante.

Esta estrategia de maximización se aplica también en la red de Vallada, obteniendo un valor energético recuperado de 26,51 MWh/año (9,55% de la energía suministrada en el sistema).

El segundo caso de estudio analiza un sistema presurizado de mayor envergadura, concretamente el Post-Trasvase Júcar-Vinalopó, sobre el cual se ha aplicado del balance energético propuesto en esta tesis. En el caso de estudio se han analizado, técnica y económicamente, veinte posibles puntos de recuperación, teniendo en cuenta el período de amortización (*PSR*) y el índice de energía (*EI*). Cuando éstos índices son evaluados, sólo se consideran viables cinco de veinte emplazamientos. No obstante, considerados los puntos de recuperación viables, la energía total recuperada representa el 7% de la energía aportada en el sistema.

El tercer caso de estudio analiza la influencia de los patrones de consumo de caudal en el comportamiento energético de los sistemas de agua presurizada. Este caso de estudio también analiza la diferencia entre los balances energéticos de las diferentes redes analizadas, dependiendo de los patrones de caudal anuales. Con el fin de comparar sólo la influencia de los patrones de caudal, el caso de estudio es aplicado en una red de bombeo sintética, en la cual se estudian cuatro patrones de consumo diferentes. Estos patrones se han obtenido en dos redes de riego y dos redes de abastecimiento, mediante el registro de datos reales en función del tiempo mediante un caudalímetro. En relación con este caso de estudio, en esta tesis se han propuesto dos parámetros nuevos para analizar la influencia de los patrones de consumo en el consumo energético. Estos parámetros, permiten la comparación directa entre diferentes casos de estudio, cuando los caudales registrados son muy diferentes entre redes. Los nuevos parámetros definidos son: huella energética no dimensional del agua (EWF_A) y flujo no dimensional (Q_A). Ambos parámetros permiten establecer y comparar la huella energética del agua entre diferentes sistemas (cuando el gestor del agua está en una fase de diseño o gestión). EWF_A es un índice que permite comparar diferentes redes a través del desarrollo de auditorías energéticas. El análisis de EWF_A llevado a cabo en este caso de estudio, muestra que las redes con una menor variabilidad en los valores del patrón de caudal, presentan valores más pequeños de EWF_A. El parámetro propuesto (EWF_A) también puede ser utilizado como criterio de sostenibilidad en la fase de diseño inicial en redes de agua a presión, unido a los criterios técnicos y económicos normalmente utilizados, siempre que sus umbrales sean definidos previamente.

Finalmente, para complementar el análisis desarrollado de la instalación de sistemas de recuperación energética en redes de distribución, se ha analizado el régimen transitorio en estos sistemas cuando se producen las maniobras de apertura o cierre rápidas tienen lugar. Para desarrollar este análisis, se han utilizado tanto los datos experimentales

obtenidos a lo largo de la campaña experimental, así como datos simulados mediante el software *Allievi*. Ambos resultados, han permitido aislar el efecto de la sobrevelocidad en la máquina hidráulica cuando el sistema de recuperación alcanza dichas condiciones. En esta introducción al análisis del régimen transitorio, la variación del caudal según la altura recuperada y la velocidad de rotación han sido analizadas para ambas máquinas, relacionando los resultados obtenidos, con el punto óptimo de rendimiento (best efficiency point (*BEP)*) de la *PAT* (Q_{BEP}, H_{BEP}, N_{BEP}). Esta relación ha sido desarrollada, a través de una transformación matemática a partir de los datos disponibles curvas características bombas, en función de su variación de la descarga, Q/Q_{BEP}, con la velocidad de rotación, N/N_{BEP}. Cuando el comportamiento de la máquina es comparado atendiendo al tipo de impulsor (axial y radial), entre en ambas existen diferencias, cuando la turbina opera bajo condiciones de sobrevelocidad. En el caso de máquinas radiales, el caudal disminuye para un valor constante de h ($h = H/H_{BEP}$) mientras que los resultados son inversos si la máquina analizada es axial.

Resum

El desenvolupament de les anàlisis de les possibles sinergies entre els sistemes de recuperació d'energia i la gestió de l'aigua són essencials per a aconseguir millores en l'eficiència energètica de les xarxes de reg pressuritzades a través de mesures sostenibles. La millora de l'eficiència energètica, mitjançant la recuperació de l'energia hidràulica, s'està convertint en una tendència inevitable per a la conservació de l'energia, la reducció de les emissions de gasos efecte hivernacle i l'augment dels marges de benefici en els sistemes de distribució d'aigua pressuritzada.

Aquesta tesi doctoral està centrada en la proposta i desenvolupament d'una metodologia d'optimització, la qual millore l'eficiència energètica en xarxes de reg pressuritzades. Per a desenvolupar aquesta metodologia, objectiu principal d'aquesta tesi, la recerca ha estat basada en diferents objectius secundaris. El primer objectiu secundari estudia l'estat de l'art en els diferents sistemes hidroelèctrics, centrant-se en aquells sistemes en els quals l'energia residual pot ser tinguda en compte per a millorar l'eficiència energètica. La necessitat d'analitzar aquesta millora energètica en les xarxes de reg pressuritzades es justifica mitjançant l'enumeració dels principals avantatges i desavantatges que aquests sistemes de recuperació tenen sobre els sistemes de distribució. Aquest primer objectiu estableix l'etapa de contextualització de la tesi. La segona part de la tesi, denominada fase procedimental o de procediment, desenvolupa la resta dels objectius i conté(,)el desenvolupament analític i experimental d'aquesta recerca. La fase analítica desenvolupa els principals blocs que formen l'estratègia d'optimització. Aquests blocs de contingut estan constituïts cadascun d'ells per una metodologia desenvolupada o mètode aplicat, els quals cobreixen els següents objectius:

- Proposar una metodologia que determine el cabal circulant al llarg del temps, en qualsevol línia, en funció dels paràmetres intrínsecs agronòmics.
- Desenvolupar una estratègia de calibratge per a l'assignació de cabals en línies, que demostre la bondat de la metodologia proposada.
- Establir el balanç energètic, així com els termes energètics involucrats, per a quantificar l'energia recuperable teòrica en xarxes pressuritzades, particularment en xarxes de reg.
- Presentar una nova metodologia de maximització d'energia recuperada, on la viabilitat d'assignar bombes treballant com a turbines (*PATs*) dins de xarxes de distribució siga considerada, mitjançant l'ús de l'eina “simulated annealing” en la gestió de l'aigua.

La fase analítica es complementa amb el desenvolupament d'una campanya experimental en dues *PATs* diferents (una de tipus radial i una altra de tipus axial), les quals han sigut assajades en condicions de flux permanent i transitori. L'anàlisi experimental, en

condicions de flux permanent, ha permès estudiar la variació de l'eficiència de la màquina en funció del cabal i de la velocitat de rotació de la mateixa. Aquesta anàlisi experimental, així com la modificació de les lleis clàssiques de semblança, han fet possible la definició de la millor línia d'eficiència (*best efficiency line (BEL)*) i la millor eficiència d'altura recuperada (*best efficiency head (BEH)*). Ambdues línies estan basades en els paràmetres de Suter i permeten als modeladors l'establiment de la velocitat de gir òptima, en funció del cabal circulant en cada instant, maximitzant l'energia recuperada. Aquestes noves línies (*BEL* i *BEH*) han d'incorporar-se a l'estratègia d'optimització, tenint-les en compte al llarg del procés per a recuperar energia en funció del nombre de màquines instal·lades en el sistema.

Les metodologies desenvolupades en cada objectiu, s'han aplicat en tres casos d'estudis diferents. En aquests casos d'estudi s'ha utilitzat programari específic (*e.g., EPANET*, *WaterGEMS*) per a desenvolupar les simulacions. La metodologia per a determinar els cabals circulants al llarg del temps s'ha aplicat a una xarxa de reg situada a Vallada (Espanya). El cabal en funció del temps s'ha determinat sobre la base dels hàbits de reg dels agricultors i la metodologia s'ha validat mitjançant el desenvolupament d'una estratègia de calibratge. Aquesta estratègia de calibratge ha sigut adaptada dels models hidrològics tradicionals, definint alguns indicadors clau de rendiment (*KPIFs*) i aplicant-se en una xarxa de reg situada a Callosa d'en Sarrià, Alacant (Espanya). Els resultats obtinguts per a cabals màxims han sigut satisfactoris en tots els intervals de temps considerats. Una vegada calibrada la metodologia, el balanç energètic ha sigut desenvolupat en la xarxa de reg de Vallada. Aquest balanç ha permès establir el marge potencial de millora d'eficiència energètica en les xarxes de reg analitzades. En el cas concret de Vallada, el balanç energètic determina que els valors d'energia teòricament recuperable són 178,10 MWh/any (valor que representa un 65% de l'energia total aportada a la xarxa) quan es considered totes les preses de reg, o 89,99 MWh/any si solament es considera la línia amb major energia teòricament recuperable.

El desenvolupament de la metodologia per a determinar els cabals circulants, així com el balanç energètic desenvolupat per a cada punt individual analitzat (és a dir, línia, hidrant o presa de reg) promouen la necessitat de maximitzar l'energia teòrica recuperada, tenint en compte la ubicació de les màquines hidràuliques a instal·lar. Per a establir la millor ubicació d'aquestes màquines, es proposa una metodologia basada en l'algorisme de recuitat simulada (simulated annealing) considerant dues funcions objectiu diferents i optimitzant l'emplaçament dels sistemes de recuperació. Aquesta estratègia de maximització s'ha desenvolupat tenint en compte:

- els hàbits culturals dels agricultors, els quals depenen dels hàbits de la dotació, els dies màxims entre regs, la tendència setmanal de reg, així com el temps de reg.
- la ubicació de *PATs* o turbines d'acord al nombre de punts de recuperació seleccionats.

- el tipus de màquina instal·lada atenent a la velocitat específica, el diàmetre de l'impulsor i/o la velocitat de rotació.
- l'anàlisi de l'energia recuperada considerant el rendiment de la màquina a cada moment en funció del cabal circulant.

Aquesta estratègia de maximització s'aplica també en la xarxa de Vallada, obtenint un valor energètic recuperat de 26.51 MWh/any (9.55% de l'energia subministrada en el sistema).

El segon cas d'estudi analitza un sistema pressuritzat de major envergadura, concretament el Post-Transvase Xúquer-Vinalopó, sobre el qual s'ha aplicat el balanç energètic proposat en aquesta tesi. En el cas d'estudi s'han analitzat, tècnica i econòmicament, vint possibles punts de recuperació, tenint en compte el període d'amortització (*PSR*) i l'índex d'energia (*EI*). Quan aquests índexs són avaluats, només es consideren viables cinc de vint emplaçaments. No obstant açò, considerats els punts de recuperació viables, l'energia total recuperada representa el 7% de l'energia aportada en el sistema.

El tercer cas d'estudi analitza la influència dels patrons de consum de cabal en el comportament energètic dels sistemes d'aigua pressuritzada. Aquest cas d'estudi també analitza la diferència entre els balanços energètics de les diferents xarxes analitzades, depenent dels patrons de cabal anuals. Amb la finalitat de comparar només la influència dels patrons de cabal, el cas d'estudi és aplicat en una xarxa de bombament sintètica, en la qual s'estudien quatre patrons de consum diferents. Aquests patrons s'han obtingut en dues xarxes de reg i dues xarxes de proveïment, mitjançant el registre de dades reals en funció del temps mitjançant un cabalímetre. En relació amb aquest cas d'estudi, en aquesta tesi s'han proposat dos paràmetres nous per a analitzar la influència dels patrons de consum en el consum energètic. Aquests paràmetres permeten la comparació directa entre diferents casos d'estudi quan els cabals registrats són molt diferents entre xarxes. Els nous paràmetres definits són: petjada energètica no dimensional de l'aigua (EWF_A) i flux no dimensional (Q_A). Tots dos paràmetres permeten establir i comparar la petjada energètica de l'aigua entre diferents sistemes (quan el gestor de l'aigua està en una fase de disseny o gestió). EWF_A és un índex que permet comparar diferents xarxes a través del desenvolupament d'auditories energètiques. L'anàlisi de EWF_A dut a terme en aquest cas d'estudi mostra que les xarxes amb una menor variabilitat en els valors del patró de cabal, presenten valors més xicotets de EWF_A. El paràmetre proposat (EWF_A) també pot utilizar-se com a criteri de sostenibilitat en la fase de disseny inicial en xarxes d'aigua a pressió, unit als criteris tècnics i econòmics normalment utilitzats, sempre que els seus llindars siguen definits prèviament.

Finalment, per a complementar l'anàlisi desenvolupada de la instal·lació de sistemes de recuperació energètica en xarxes de distribució, s'ha analitzat el règim transitori en aquests sistemes quan es produeixen les maniobres d'obertura o tancament ràpides. Per a desenvolupar aquesta anàlisi, s'han utilitzat tant les dades experimentals obtingudes al

llarg de la campanya experimental, així com dades simulades mitjançant el programari *Allievi*. Tots dos resultats han permès aïllar l'efecte de la sobrevelocitat en la màquina hidràulica quan el sistema de recuperació aconsegueix aquestes condicions. En aquesta introducció a l'anàlisi del règim transitori, la variació del cabal segons l'altura recuperada i la velocitat de rotació han sigut analitzades per a ambdues màquines, relacionant els resultats obtinguts amb el punt òptim de rendiment (best efficiency point (*BEP)*) de la *PAT* (Q_{BEP}, H_{BEP},N_{BEP}). Aquesta relació ha sigut desenvolupada, a través d'una transformació matemàtica a partir de les dades disponibles corbes característiques bombes, en funció de la seua variació de la descàrrega, Q/Q_{BEP}, amb la velocitat de rotació, N/N_{BEP}. Quan el comportament de la màquina és comparat atenent al tipus d'impulsor, (axial i radial), entre en ambdues existeixen diferències quan la turbina opera sota condicions de sobrevelocitat. En el cas de màquines radials, el cabal disminueix per a un valor constant d' h ($h = H/H_{BEP}$) mentre que els resultats són inversos si la màquina analitzada és axial.

Contents

Figures index

Table index

Abbreviations

BEH	best efficiency head
BEL	best efficiency line
BEP	best operation point
CFD	computational fluid dynamics
C_{RT}	recovery coefficient
e	efficiency ratio
E	Nash-Sutcliffe coefficient
E_{FR}	friction energy
E_R	real recovered energy
E_{RI}	energy required for irrigation
E_T	total energy
E_{TA}	theoretically available energy
E_{TN}	theoretically energy necessary
E_{TR}	theoretically recoverable energy
E_{TR}^{S}	total recovered energy with '*n*' installed turbine in series
E_{NTR}	theoretically non-recoverable energy
EI	energy index
EWF	energy water footprint
EWF_A	dimensional energy footprint of water
$F_{100\%}$	cumulated demand in all consumption points of the network
FP	annual flow pattern
h	head Suter parameter
h_{min}	minimum level fixed for the reservoir
h_{min_r}	minimum level fixed to active groundwater resources
H_0	recovered head when the opening degree valve is total
H_{BEP}	recovered head when turbine operates in the best efficiency point

h_{UR}	level in the head reservoir
H_{RW}	recovered head in runaway conditions
i	irrigation amount
j	each day of year
KPIF	key performance indicators
L_0	number of transition in simulated annealing process
N_{BEP}	rotational speed of the machine when turbine operates in the best efficiency point
N_0	rotational speed of the machine when the opening degree valve is total
n	number of turbines or *PATs*
n_s	specific rotational speed
p	power coefficient
p_{cm}	cumulative probability
P_I	irrigation probability
PAT	pump as working turbine
PBIAS	percent bias
PRV	pressure reduction valves
PSR	payback simple period
q	flow Suter Parameter
Q_A	non-dimensional flow
Q_{BEP}	flow when turbine operates in the best efficiency point
Q_0	flow when the opening degree valve is total
Q_{RW}	flow runaway
RRSE	root relative square error
SCADA	supervisory control and data acquisition
T_i	initial temperature in simulated annealing process
T_f	final temperature in simulated annealing process
T_t	transition temperature in simulated annealing process
V_{Na}	volume balance between irrigated volume and irrigation needs

V_{IR}	irrigated Volume
VOS	variable operation strategies
x_i	line where each turbine is located
X	initial combination $X = (x_1, x_2, .., x_n)$
Y	new combination generated in simulated annealing process
α_c	cooling rate
ψ_i	objective function

Chapter 1
Introduction

1.1. Scope and motivation

Currently, society has become aware of the need to increase the energy efficiencies of different processes as well as the renewable energy processes used (*e.g.,* photovoltaic, wind, tidal, hydraulic). Water distribution systems have not gone unnoticed in this trend, considering that these infrastructures are high energy consumers regarding the catchment, distribution and reuse of hydric resources. An example of the importance of hydraulic systems as energy consumers is that energy consumption in water supply networks represents 7% of the worldwide consumption of energy [1], in which distribution is approximately one-third (2-3%) of this consumption [2]. Therefore, considering the need to develop sustainable growth, new strategies should be introduced for water management systems to improve energy efficiency, to reduce the carbon footprint [3] and to consider newly available technologies, depending on the field of study [4]. In this sense, the installation of recovery systems is one of the strategies to use in places where the energy is dissipated (*e.g.,* pressure reduction valves (*PRVs*) or hydraulic jumps).

A deep knowledge of the water-energy nexus in hydraulic systems is essential to define and to introduce new action lines for their water management [5] in order to define performance indicators [6]. The analysis of the water-energy nexus, which depends on intrinsic factors of the hydraulic systems, defines the potential energy recovery in any hydraulic system. Once the water-energy nexus is known, performance indicators can be

established, quantifying energy savings and contributing to the improvement of the sustainable, environmental, economic, and management terms [7–9].

Although the recovery system in open channel flow is also important, the establishment of water pressurized systems in any scope (*i.e.,* urban, irrigation, industrial use) has promoted the development of energy recovery strategies that are mainly focused on water supply networks. Regarding energy recovery in water supply networks, Ramos and Borga (1999) were pioneers in the development of an unconventional solutions [10]. Their solution replaced *PRVs* with pumps as working as turbines (*PATs*) in pressurized water supply networks, keeping the advantages of leakage reduction [11] and pipe breakage reduction as well as introducing an improvement in the renewable energy generation. Since then, the energy recovery in water supply systems has been studied by different authors in terms of selecting the type of hydraulic machines for which *PATs* can provide a feasible solution [12–14], modeling and maximizing the theoretical energy available with the average flow modulation curve [15].

The development of these energy recovery solutions is currently underdeveloped for irrigation pressurized networks as a result of the following:

(i) irrigation modernization is currently carried out by replacing gravity irrigation with water pressurized networks (*e.g.,* sprinkler or drip irrigation);

(ii) an area of 324 million hectares are provided to the world through irrigation installations. This large irrigated area is distributed with gravity irrigation (86%), sprinkler irrigation (11%), and drip irrigation (3%) [16]. Particularly, Spain represents 1.09% of the worldwide irrigated area with a consumed volume equal to 16344 hm^3/year.

(iii) agricultural processes have less economic resources than supply networks that can be allocated to research studies;

(iv) resource management is more singular in the irrigation framework, which affects its social and cultural aspects.

If previously cited bulletins and the annual irrigation percentage of the consumed volume (2729 km^3/year) are considered, studying energy efficiency improvement through the installation of energy recovery systems in pressurized networks is interesting, considering that the irrigation volume represents 69.53% of the total consumed volume worldwide compared to 11.77% for drinking systems or 18.70% for industrial use [17]. This highlights the paramount importance of studying energy efficiency improvement through the installation of energy recovery systems in pressurized irrigation networks.

Related to the improvement of the sustainability indexes for irrigation networks, different researchers have analyzed the optimization of energy consumption in pump systems [18–20], while others have developed strategies to perform energy audits in pressurized systems [11, 20–22]. Nevertheless, an analysis of the potential recovered

energy has not been comprehensively performed, as far as the consulted references indicate. Regarding this topic, only average flow studies have been conducted [23].

Therefore, the current development of energy recovery for water supply systems as well as the high-energy potential in irrigation networks have incited development studies in this field. These studies should try to increase the knowledge of the actual behavior of pressurized water networks (*e.g.,* the determination of flow over time) to analyze the theoretically recoverable energy and the behavior of the recovery systems in these networks.

1.2. Thesis structure

This document is organized into six chapters and eight appendices.

In Chapter 1, an introduction is presented, and the main motivation of this research is described.

Chapter 2 contains the proposed objectives to develop this research.

In Chapter 3, the Material and Methods used to develop the methodology are enumerated.

Chapter 4 summarizes the Results and Discussion, enumerating the main results of each one of the objectives.

In Chapter 5, the chief conclusions are described, defining future research lines to continue improving the energy recovery in pressurized water networks.

Chapter 6 collects the references used in the different chapters of the thesis.

Finally, eight appendices are attached. Each appendix corresponds to the author's version of the submitted review articles, which have been created through the development of this thesis. The papers submitted throughout the development of this thesis are listed below:

1. Energy recovery in existing water networks: towards greater sustainability
   a. *Co-authors:*
      Pérez-Sánchez, M; Sánchez-Romero FJ; Ramos, HM; López-Jiménez PA.
   b. *Journal:*
      Water ISSN 2073-4441
      Impact Factor 1.687. Position 33/85 (Q2). Water Resources
   c. *State*:
      Published [Water 2017, 9, 97; doi:10.3390/w9020097]

2. Modelling irrigation networks for the quantification of potential energy recovering: A case study.
   a. *Co-authors:*
      Pérez-Sánchez, M; Sánchez-Romero FJ; Ramos, HM; López-Jiménez PA.
   b. *Journal:*
      Water ISSN 2073-4441.
      Impact Factor 1.687. Position 33/85 (Q2). Water Resources.
   c. *State*:
      Published [Water 2016, 8, 1–26. doi:10.3390/w8060234]
3. Calibrating a flow model in an irrigation network: Case study in Alicante, Spain
   a. *Co-authors:*
      Pérez-Sánchez, M; Sánchez-Romero FJ; López-Jiménez PA.; Ramos, HM.
   b. *Journal:*
      Spanish Journal of Agricultural ISSN 2171-9292
      Impact Factor 0.76. Position 24/57 (Q2). Multidisciplinary
   c. *State*:
      Published [*Spanish J. Agric. Res.*, 2017, 15, 1, e1202,.doi:10.5424/sjar/2017151-10144]
4. Water-Energy nexus. Energy optimization in water distribution system. Case study 'Postrasvase Júcar Vinalopó' (Spain).
   a. *Co-authors:*
      Pérez-Sánchez, M; Sánchez-Romero FJ; López-Jiménez PA.
   b. *Journal:*
      Tecnologías y Ciencias del Agua ISSN 2007-2422.
      Impact Factor 0.760108. Position 83/85 (Q4). Water Resources
   c. *State*:
      Accepted to publish [Accepted Data: 27/03/2017, Vol VIII (4) July-August 2017].
5. Energy footprint of water depending on consumption patterns.
   a. *Co-authors:*
      Pérez-Sánchez, M; Sánchez-Romero FJ; López-Jiménez PA.
   b. *Journal:*
      Ingeniería del Agua ISSN 1134-2196.
      Extended JCR.
   c. *State*:
      Accepted with changes [Registered Date: 10/01/2017]

6. PATs' selection towards sustainability in irrigation networks: Simulated annealing as water management tool.
   a. *Co-authors:*
      Pérez-Sánchez, M; Sánchez-Romero FJ; López-Jiménez PA.; Ramos, HM.
   b. *Journal:*
      Renewable Energy ISSN 0960-1481
      Impact Factor 3.404. Position 24/88 (Q2). Energy&Fuels
   c. *State*:
      Submitted [Registered Data: 10/09/2016]
7. Modified affinity laws in hydraulic machines towards the Best Efficiency Line.
   a. *Co-authors:*
      Pérez-Sánchez, M; López-Jiménez PA.; Ramos, HM.
   b. *Journal:*
      Water Resources Management ISSN 0920-4741
      Impact Factor 2.437. Position 12/85 (Q1). Water Resources
   c. *State*:
      Submitted [Registered Data: 08/12/2016]
8. PATs operating in water networks under unsteady flow conditions: control valve maneuver and overspeed effect.
   a. *Co-authors:*
      Pérez-Sánchez, M; López-Jiménez PA.; Ramos, HM.
   b. *Journal:*
      Renewable Energy ISSN 0960-1481
      Impact Factor 3.404. Position 24/88 (Q2). Energy&Fuels
   c. *State*:
      Submitted [Registered Data: 20/02/2017]

This page is intentionally left blank.

Chapter 2
Objectives

The presented thesis is focused on contributing to the knowledge pertaining to the operating mode of energy recovery systems when they are installed in pressurized water networks (particularly, irrigation networks). The main aim of this thesis is centered on the proposal and development of a methodology that improves energy efficiency in pressurized irrigation networks.

The main objective is supported by secondary objectives, which complement the development of this thesis and contribute to developing the main aim. Therefore, other complementary objectives in this thesis are as follows:

1. To study the state-of-the-art of different hydropower systems, paying attention to those systems in which residual energy can be considered for energy improvement, such as water supply networks and irrigation networks in particular.
2. To propose a methodology to determine the circulating flow over time in pressurized irrigation networks in any line depending on the agronomist intrinsic parameters of the established crops.
3. To develop a calibration strategy for flow assignment in lines, which shows the success of the proposed methodology.
4. To establish an energy balance methodology as well as the involved energy terms to quantify the theoretical recoverable energy in pressurized water networks, particularly in irrigation networks.

5. To present a new methodology for maximizing the recovered energy considering the actual feasibility to allocate pumps as turbines (*PATs*) within pressurized water networks by using simulated annealing as a water management tool.
6. To apply both proposed methodologies (*i.e.,* flow and energy balance) in two different cases of the study. The first case corresponds to a pressurized irrigation network (here, referred to as small systems), and the second case study corresponds to a pressurized distribution water system to transfer a water volume between basins (here, referred to as large systems).
7. To analyze the water-energy coupling, which considers the energy consumption as a cubic meter distribution (energy footprint of water, *EWF*) in a pressurized water network depending on the consumption flow patterns (*e.g.,* supply and irrigation).
8. To carry out an experimental campaign that enables defining the hydraulic machine behavior, particularly for pumps as turbines (*PATs*), when these machines operate with variable circulating flow in steady flow conditions.
9. To introduce the transient phenomena in *PATs* through the analysis of the experimental data, which are experimentally obtained in unsteady flow conditions.

Chapter 3
Materials and Methods

This *Ph.D.* research looks for the development of a methodology to optimize the energy recovery in pressurized water systems, when they are applied on irrigation networks particularly. Therefore, the *Ph.D.* research is defined by an ensemble of methods, methodologies and materials, in which the results obtained and their connection between them, constitute the methodology to optimize the energy recovery in the pressurized water systems. Each one of the objectives, which is included in each intermediate result, is defined by one method or methodology at least, reaching the aim proposed in each phase of the optimization strategy. The material and methods used in this PhD research are enumerated in the following paragraph and further described.

The used methods are focused on (i) definition of the analytical model to determine the flows over time; (ii) strategy to validate the methodology to estimate the flow in each line of the network; (iii) optimization of the recovered energy by an analytical strategy; (iv) study of analytical models to know the efficiency in steady flow conditions as well as the behaviour of the machine in unsteady flow regime. The analysis of the machine in steady flow is developed through affinity laws and Suter parameters, while the unsteady flow analysis is based on dynamic behavior of the machine depending on the type of closure valve, damping effects, and specific rotational speed of the machine; and (v) simulation of the analytical method by using of numerical model through specific software to know the obtained values.

The definition of the analytical model to determine the flows over time is focused on the determination of the opening or closure in each irrigation point depending on balance between irrigation needs and irrigation cumulated volume. The opening of the irrigation point is established on different patterns. These patterns show the irrigation trends of the

farmers (*i.e.,* weekly trend, maximum days between irrigation, irrigation duration). The definition of these patterns enables to determine the time in which the irrigation starts. This methodology was completely developed in Appendix II of this research.

The calibration strategy, defined in Appendix III, was based on key performance indicators (*KPIFs*), coming from traditional hydrological models [24, 25]. The *KPIFs* were Nash-Sutcliffe (*E*), root relative square error (*RRSR*), and percent of bias (*PBIAS*), which allowed for the determination of the goodness of fit between estimated and registered flow.

The optimization developed by an analytical strategy, was carried out in two phases. The first phase was focused on the integral balance of the energy in a control volume [26]. The energy terms were defined by equations, distinguishing between recoverable and non-recoverable energy, depending on the required energy for irrigation. This energy balance was defined in Appendix II. The second phase was to develop an optimization strategy through a heuristic algorithm, which is based on the analogy with the physics process of annealing of metals and inspired in Monte-Carlo's method [27]. The optimization strategy was developed on Appendix VI.

The recovered energy by a recovery system depends on the efficiency of the hydraulic machine. As the flow varies over time, the strategies of regulation, defined by Carravetta *et al.,* (2013) [13], were considered to determine the recovered energy through affinity laws and Suter parameter of the hydraulic machines. The objective was to analyze the variation of head and efficiency curve as a function of the rotational speed when the machine operates under steady flow conditions. This method was described on Appendix VII. Also, the machine can be subjected to variable conditions of the flow, and therefore, the opened or closure maneuvers cause unsteady flow conditions of the machine. Short introduction of the phenomena was included in this research, when fast closure or opened maneuvers were done. The development of the analysis was attached in Appendix VIII.

Once the used analytical method was defined, the simulations were developed to be applied on different case studies. The used software was *EPANET* [28], *WaterGEMS* [29], and *Allievi* [30]. *EPANET* software is public domain software that models water distribution in pipe systems. Different elements can be represented: pipe networks composed by pipes, nodes (junctions), pumps, valves, and storage tanks or reservoirs. The model can simulate extended-period hydraulic analysis by simulating by sort of pipes systems, computing friction and minor losses, representing various types of valves, junctions, tanks and pumps, considering multiple patterns at nodes consumption with time variation, and system operation on simple tank level, timer controls or complex rule-based controls. *WaterGEMS* is a private domain software that provides to users a decision support tool for water distribution networks improving the knowledge of how infrastructure behaves as a system. This software can represent different elements (*e.g.,* pipes, joints, pumps, turbines, valves) as well as optimization strategies to minimize consumed energy in pumped systems or determining pipe sizes as function of the investment cost, circulating flows and restriction of pressure by means use of genetic

algorithm. The software has others utilities to improve the water management. Finally, *Allievi* software is a public domain software for calculating and simulating of the unsteady flow conditions in pressurized water systems and open channels flows.

However, the analysis of the used methods cannot be developed whether there are no materials to be introduced in the different analytical methods. In this case, these materials are the experimental data, which were obtained along the development of this research. The materials were: (i) development of interviews to know the farmers' habits, which were used as inputs data in the analytical model developed for the estimation of the flow over time; (ii) data of registered flow over time of the different irrigation networks, which were analyzed in each case study developed; (iii) the obtained experimental data in two different *PATs*, which were tested in the *CERIS*-Hydraulic Lab of Instituto Superior Técnico (*IST*) at the University of Lisbon.

The interviews to farmers were developed in different irrigation communities. The results of these interviews were afterwards used in the development of the case study for determining the patterns to estimate the flows by proposed methodology. The obtained patterns of the interviews were described in Appendix II and Appendix III.

The registered flow data were used to carry out the case study of the calibration strategy in Appendix III. The data were obtained on a flowmeter, which was installed in the main line of the irrigation network of the Callosa d'en Sarrià (Alicante, Spain).

The last materials used in this research were the experimental texts were carried out for a radial and an axial machine installed at *IST* in Lisbon. In both cases the discharge was measured by an electromagnetic flowmeter; the pressure was registered by pressure transducers, through the Picoscope data acquisition system; the power was measured by a multimeter which was connected to the generator; and the rotational speed was measured by a frequency meter. The used machines were a radial pump working as turbine (*PAT*), with a rotational specific speed of 51 rpm (in m, kW); and an axial one, with a rotational specific speed of 283 rpm (in m, kW). The hydraulic machines were analyzed both steady and unsteady flow conditions. The results, obtained for each flow conditions (steady and unsteady), were used in Appendix VII and VIII.

The cited material and methods were implemented in the different developed phases to optimize the energy recovery, using the output of the results of each one of the steps as input data in the next optimization phase, such as it is described in the following Chapter. In this section (Results and discussion), the work structure of the Ph. D. is presented, as well as the relationship between the objectives, the used methods and the obtained results are summarized as each step of the research is contained in each one of the attached manuscripts, which can be found in the eight appendices of this document. Furthermore, the used methods and the obtained results are summarized and contained in each one of the attached research manuscripts, which can be found in the eight appendices of this document.

This page is intentionally left blank.

Chapter 4
Results and Discussion

The development of each one of the objectives of this *Ph.D.* research leads to the design of an optimization strategy for pressurized irrigation networks through different results and discussions, which are obtained in each phase of this thesis. Each one of the objectives is interrelated. Commonly, their results are the initial assumptions to develop the next phase or objective of the thesis.

The results of the present research are obtained according to the flowchart depicted in Figure 1. The flowchart contains two main stages for developing and obtaining the defined aims. Each bullet point of the figure is enumerated according to different sections described in Chapter 4, which will be discussed below. At the same time, each section indicates the submitted manuscript in which the objective is completely developed, describing the methodology or method applied as well as showing some results and the conclusions reached.

The first stage (4.1 Contextualization Stage) is focused on the development of a review of different hydropower systems according to their installed power (*e.g.,* large and small hydropower). This phase describes a general vision (*i.e.,* generation, location, technical, environmental, and economic aspects) for these recovery systems. An analysis of the energy recovery potential by using a hydraulic machine is also developed, considering pressurized water networks (*e.g.,* supply and irrigation). This analysis serves as a starting point for studying the possibility of improving the energy efficiency as well as considering the positive and negative characteristics of the micro and pico recovery systems.

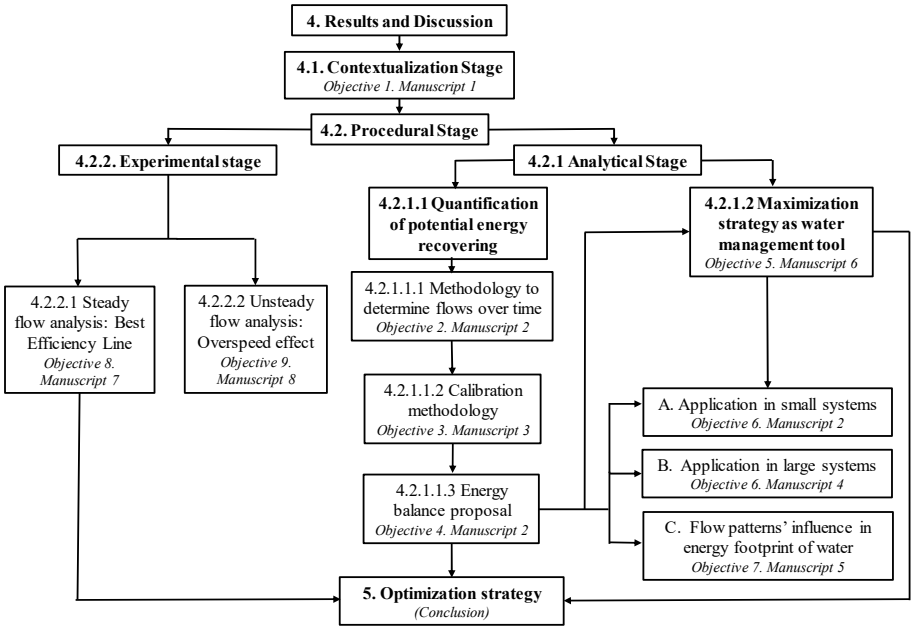

Figure 1 Flowchart with different stages to develop the proposed objectives

The second stage (4.2. Procedural stage) encompasses the main part of the thesis. This phase is divided in two content blocks: the analytical (Point 4.2.1) and experimental stage (Point 4.2.2). The analytical stage contains the numeric development for quantifying the potential recovery (Point 4.2.1.1) and the maximization strategy to recover energy (Point 4.2.1.2).

The quantification of the potential recovery is structured based on the developed methodology to determine the circulating flows (Point 4.2.1.1.1), the calibration of the circulating flows (Point 4.2.1.1.2), and the proposal of the energy balance to analyze the theoretically recovered energy in any pressurized water network (Point 4.2.1.1.3) based on flow over time. The development of the last point enables the application of the energy balance in two different case studies: a small irrigation network (A.) and a large pressurized water system (B.). To finish the quantification stage, the energy footprint of water (*EWF*) is analyzed based on the proposed methodology to determine the flow pattern influence in the dissipated friction energy for the flow distribution (C.). All case studies are supported by a software application, *EPANET*, to develop the necessary simulations. The proposal of energy balance ensures the possibility of the developing the maximization strategy as a water management tool.

The developed strategy based on simulated annealing maximizes the actual recovered energy depending on hourly flow consumption patterns and selected hydraulic machines

(*i.e.,* specific rotational speed, impeller diameter, rotational speed). This strategy is simulated using *WaterGEMS* software.

Parallel to the development of the analytical stage, the experimental phase is performed. This phase is based on the development of experimental tests in recovery hydraulic machines. The first experimental stage (Point 4.2.2.1) is focused on efficiency variation when the rotational speed is changed in two different *PATs* in steady flow conditions. The second experimental phase (Point 4.2.2.2) introduces the transient behavior of the *PATs* according to the specific rotational speed using an unsteady flow analysis in two different *PATs* and comparing the experimental results *versus* the obtained values for simulations performed with *Allievi* software.

The main landmarks reached in the different papers submitted (consigning the presented research) are summarized in the following sections.

4.1 Contextualization stage

The Contextualization phase is based on published paper (Appendix I):

Energy recovery in existing water networks: towards greater sustainability

Co-authors: Pérez-Sánchez, M; Sánchez-Romero FJ; Ramos, HM; López-Jiménez PA.
Journal: Water ISSN 2073-4441.
Impact Factor 1.687. Position 33/85 (Q2). Water Resources.
State: Published [*Water 2017, 9, 97; doi:10.3390/w9020097*]

The synergistic analysis between the energy recovery and water management are necessary to consider the energy efficiency improvement in the different hydraulic systems. These systems are classified for different scales according to the installed capacity (*i.e.,* large, small, micro, and pico hydropower systems).

The attached research document (Appendix I), in its first part, establishes a global summary of the generation levels (*e.g.,* worldwide, Europe, and Spain) according to the type of resource used to generate renewable energy (*i.e.,* solar, wind, hydropower), mainly focused on hydropower generation.

The second part of the manuscript analyzes a review of large and small hydropower systems. This analysis is established for each scale, considering the geographical locations, production levels, and environmental, and economic aspects. Inside of this part, a hydraulic machine classification is developed in one specific section that considers the type of energy recovery system (*e.g.,* open channel flow or pressurized systems). The selected machines are presented as a function of flow and the available head, commenting on the progress and efficiency of these machines over time.

In the third part, the state-of-the-art contextualization depicts a deep analysis of micro and pico hydropower systems because there is large interest for understanding the current

situation of these schemes due to pressurized water networks (particularly, irrigation systems). The consulted references helped to establish and to comment on the different analyzed topics, which are structured on the following:

- used machines in pressurized networks (*e.g., PATs*);
- description and operation of *PATs* according to available technologies;
- performance and modeling of *PATs*;
- installation of recovery systems;
- implementation of simulations to determine the theoretically recovered energy;
- design of variable operating strategies;
- environmental and economic advantages;
- development of policies applied in different countries; and
- analysis of actual pilot plants and theoretical case studies proposed in pressurized water networks.

Finally, the document concludes by enumerating the advantages and disadvantages of energy recovery systems in pressurized water networks as well as defining some aspects that should be considered to improve the implantation of *PATs* inside of networks. Aspects such as the determination of the recovered energy depending on circulating flow, the improvement of strategies to recover energy with changeable flows, and the development of sustainable and feasible electric systems (grid connections or a stand-alone operations) are considered as work lines to enhance the improvement of energy recovery system in pressurized water networks.

4.2 Procedural stage

The second phase of the present thesis contains the main block of the research, which is divided into an analytical and experimental phase. The development of both stages as well as the analyses and discussion of the obtained results enables the proposal of the present methodology for improving the energy efficiency analysis for pressurized irrigation networks.

4.2.1 Analytical stage

The numeric development for quantifying the potential recovery as well as the maximization strategy for recovering energy are described in this section.

4.2.1.1 Quantification of potential energy recovery in irrigation water networks

The proposed methodology for determining the circulating flows, calibration strategy for the consumed flow patterns, and energy balance proposal and three case studies are described in this section. The researches are based on submitted papers, which are summarized in the follow sections.

4.2.1.1.1 Methodology to determine circulating flow with time depending on assigned consumption pattern

The methodology is totally defined on published paper (Appendix II; Section 1 and 2.1):

Modelling irrigation networks for the quantification of potential energy recovering: A case study

Co-authors: Pérez-Sánchez, M; Sánchez-Romero FJ; Ramos, HM; López-Jiménez PA.
Journal: Water ISSN 2073-4441.
Impact Factor 1.687. Position 33/85 (Q2). Water Resources.
State: Published [*Water 2016, 8, 1–26. doi:10.3390/w8060234*]

The determination of circulating flows over time is crucial for approximating the simulated values with the real values. Considering the average flows can be useful when preliminary studies are performed. However, their use is not recommended if water managers require more accuracy because the definition of the hydraulic machine to be selected as well as its operating point cannot be precisely defined and guaranteed.

The proposed methodology is based on the determination of the flows in any line or consumption node over a year in an irrigation network, considering the needs of the crop, the historic consumption and the irrigation farmers' habits. The possibility of determining the circulating flow over time using the volume consumed and farmers' habits presents a great advantage for irrigation networks. This advantage exists because the majority of irrigation networks do not have measurement flow devices in their lines because the idiosyncrasy of irrigation networks has not caused the need to control the distributed volume (*i.e.,* leakage, non-registered, evaporated, and consumed volume) until now. This is different in dissimilar supply systems, which normally track readings of flows and pressures at all times.

The methodology (Figure 2) determines the random openings or closures in each consumption node according to the farmer's habits (*i.e.,* irrigation needs or consumed volume, Input 1; weekly trend of irrigation, Input 2; days between irrigation, Input 3; and irrigation duration patterns, Input 4).

The first step (Step 1) is the estimation of the cumulative volume consumed by the irrigation point. The decision to irrigate depends on the balance (V_{Na}) between the previous irrigated volume and the consumption assigned (needs) to the irrigation point (Input 1). Once irrigation is required ($V_{Na}<0$), the irrigation probability (P_I) is randomly determined, according to Input 2 and Input 3 (Step 2). If the methodology through P_I proposes the decision to irrigate, the determination of the irrigation duration is established depending on Input 1, the irrigation amount, and the irrigated area (Step 3).

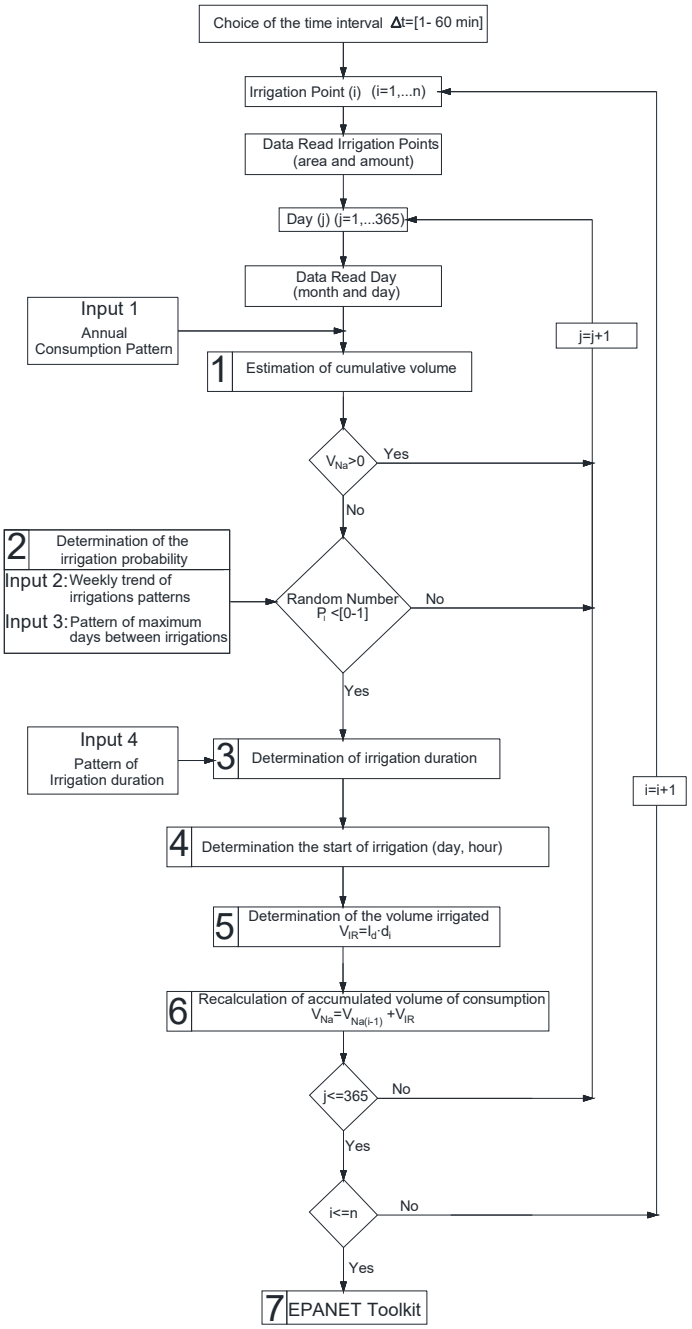

Figure 2. Schematic description of the methodology for flow estimation [31]

The next stage (Step 4) randomly determines the time interval to start the irrigation depending on Input 4 and the cumulative probability (p_{cm}) and calculates the irrigation volume (Step 5). When the irrigation volume is known, the methodology updates the water volume available for the plant (Step 6). The cycle from Step 1 to Step 6 is performed for each consumption point and for every day of the year. Once all consumption node states are known (*i.e.,* opened or closed), the pressure and flow are calculated for all consumption points and lines using the *EPANET* Toolkit (Step 7).

The proposed methodology is applied in two different cases studies. The first case study is developed in Appendix II, and the second case study is used to calibrate the methodology (Appendix III). The calibration strategy (described in the next section) shows the robustness of the methodology, demonstrating that the randomness of the irrigation point openings does not affect the obtained flow results.

4.2.1.1.2 Calibration strategy for consumption flow pattern assignation

This phase of the research is based on published paper (Appendix III):

Calibrating a flow model in an irrigation networks: Case study in Alicante, Spain

Co-authors: Pérez-Sánchez, M; Sánchez-Romero FJ; Ramos, HM; López-Jiménez PA..
Journal: Spanish Journal of Agricultural ISSN 2171-9292.
Impact Factor 0.76. Position 24/57 (Q2). Multidisciplinary.
State: Published [*Spanish J. Agric. Res.*,2017, 15, 1, e1202,. doi:10.5424/ sjar/2017151-10144]

The calibration of models is crucial when their use is involved in decision support tools. Therefore, the proposal of any methodology has to be subjected to a calibration process, which guarantees the goodness success of the obtained results. The consulted references in the manuscript are focused on calibration processes for determining the pressure and roughness of the networks, which are supported by supervisory control and data acquisition (*SCADA*). This type of calibration process is used often for water management to improve the output results of simulations. Considering that the consulted calibration models were focused on the pressure, a calibration strategy for the flows is proposed and applied in a case study in the present research.

The submitted manuscript contains the calibration strategy for the flow assignments in the lines. As a novelty, we defined some particular key performance indicators (*KPIFs*) imported from the hydrologic models. These *KPIFs* include the Nash-Sutcliffe coefficient (*E*: non-dimensional index), root relative square error (*RRSE*: the error index), and percent bias (*PBIAS*: the tendency index). The characterization of the goodness of fit was divided into very good, good, satisfactory, and unsatisfactory depending on the *KPIF* values (Table 1).

Table 1. Classification of the goodness of fit [32]

Goodness Fit	***E***	***RRSE***	***PBIAS* (%)**
Very Good	$E>0.6$	$0.00\leq RRSE\leq 0.50$	$PBIAS < \pm 10$
Good	$0.40<E\leq 0.60$	$0.50< RRSE \leq 0.60$	$\pm 10 \leq PBIAS < \pm 15$
Satisfactory	$0.20<E\leq 0.40$	$0.60< RRSE \leq 0.70$	$\pm 15 \leq PBIAS < \pm 25$
Unsatisfactory	$E< 0.20$	$RRSE >0.70$	$PBIAS > \pm 25$

The previously described calibration strategy was applied for an actual case study in a small irrigation network. Particularly, the calibration was developed in a water system that is located in Callosa d'En Sarrià (Alicante, Spain). Initially, defining the calibration parameters was necessary. The possible parameters depended on the farmer's habits (*i.e.,* irrigation requirements, weekly irrigation trends, maximum days between irrigation, and irrigation amount). The irrigation requirements and weekly irrigation trends were intrinsic to the crops and farmer, respectively. The different habits of the farmer (maximum days between irrigation and the irrigation amount) were compared, obtaining a great sensibility of the estimated flows when the irrigation amount was varied. As an example, if the irrigation amount as increased up to 100%, the variation in the maximum flows was 15.49%. In the meantime, if the maximum days between irrigation were increased to 100%, the variation in the maximum flow was 2.15%; the irrigation amount was the more sensitive parameter in this calibration process

The proposed calibration was developed for maximizing the circulating flows. Knowledge of the range of flows enables selecting the optimal hydraulic machines for the recovery system, considering not only the maximum flow but also the more frequent operating point. However, the *KPIF* parameters were also determined for both the average flows and maximum flows, considering the reduction in the input data in the methodology (simplification of the farmer's habits) and discussing their variation. For all cases, the *KPIF* parameters showed satisfactory results. If the irrigation required a change, the calibration was good. For the rest of the cases, when the farmers' habits varied, the *KPIFs* were very good for the average estimated flows. In contrast, for the farmers' habits, if the maximum flows were considered, the *KPIF* parameters did not show satisfactory results when the irrigation amount was inaccurate, showing the sensibility of this parameter, as it was exposed in the previous paragraph.

The goodness of fit results was satisfactory for time intervals lower than two and four hours. The intervals of one hour and eight hours had satisfactory indexes. If greater time intervals were considered (up to 8 hours), the values of *E* and *PBIAS* continued to be positive and satisfactory, but the *RRSE* exhibited unsatisfactory values. This endorses the possibility to use the methodology for determining the circulating flows over time, knowing the trends in the variation of the flows in any line.

Finally, because consequence of the methodology for determining the circulating flows is based on randomness of the opening or closure of each consumption node, the variability of the goodness of fit was analyzed to consider how the randomness affects the flow determination. The model was run 200 times for the same irrigation scenario (*i.e.,* the annual consumption pattern, weekly irrigation pattern trends, maximum days between irrigation, and pattern of irrigation time) to analyze the variability. In the case study, if the variability of the maximum flow was determined in the main line, the obtained flow range varied between 47.67 and 54.09 l/s, with an average value of 50.17 l/s and a variance 1.08 l/s. If the maximum flow was compared to the obtained values using Clément's Method (for the maximum requirements per month, the maximum flow was 52.87 l/s) the results were similar, but when the cumulative frequency was determined, the proposed methodology presented a better fit than Clement's Method using the actual circulating flows (Figure 3).

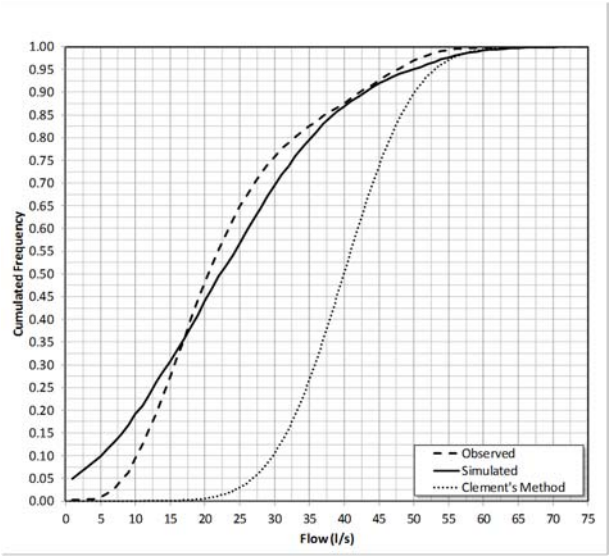

Figure 3. Comparison of the cumulated frequency between the observed, simulated and Clément's Method results for the maximum irrigation requirements on June [32]

4.2.1.1.3 Energy balance proposal in irrigation networks

This stage is based on published paper (Appendix II; Section 1 and 2.2):

Modelling irrigation networks for the quantification of potential energy recovering: A case study

Co-authors: Pérez-Sánchez, M; Sánchez-Romero FJ; Ramos, HM; López-Jiménez PA.
Journal: Water ISSN 2073-4441.
Impact Factor 1.687. Position 33/85 (Q2). Water Resources.
State: Published [*Water 2016, 8, 1–26. doi:10.3390/w8060234*]

An energy balance was required for the present stage. The obtained results for the methodology of determining the flow over time (Section 4.2.1.1.1), as previously described, are required for this step.

The objective of the proposed energy balance is to help water managers quantify the potential energy recovery of a pressurized water network (the balance is particularized for an irrigation network) with adequate conditions for topography distribution, considering the service conditions of minimum pressure and flow in all consumption nodes.

The balance will help modelers to determine the energy balance in any line, hydrant or irrigation point (Figure 4). The total energy (E_T), friction energy (E_{FR}), theoretical energy necessary (E_{TN}), energy required for irrigation (E_{RI}), and theoretical available energy (E_{TA}) can be discretized in any line or point of the pressurized water network. This balance, which was determined for the considered time interval (*e.g.,* hourly), considers the opening or closure state of the downstream consumption nodes in the analyzed point (*e.g.,* line, hydrant or irrigation point) for each time point. Knowledge of friction energy enables the calculation of the energy footprint of water (*EWF*).

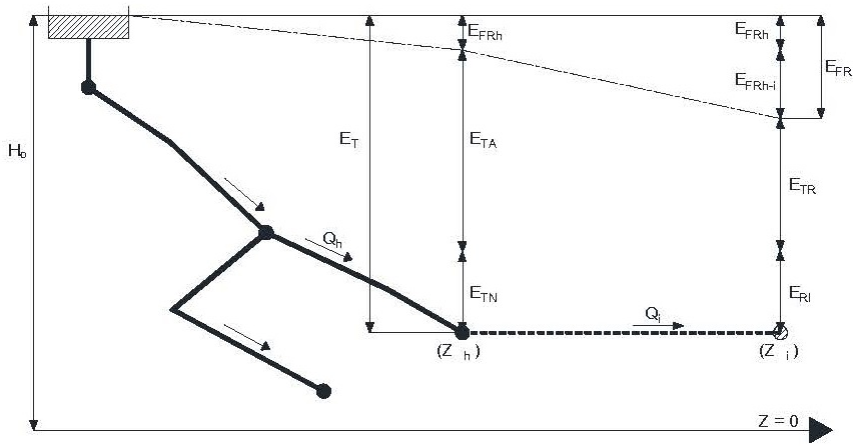

Figure 4. Scheme of hydraulic energy grade lines [31]

As a novelty, the balance includes the possibility divide the theoretically available energy into theoretically recoverable energy (E_{TR}) and theoretically non-recoverable energy (E_{NTR}; which is E_{TA} - E_{TR}) in any line or point. This discretization allows the determination of the recovery coefficient (C_{RT}). This parameter represents the proportion of the theoretically recovered energy over the available energy in an irrigation point, hydrant or line of the network. C_{RT} can be used in future optimization strategies.

The application of the balance allows the determination of a theoretic value for the recovered energy (total and discretized) as well as the developed power in each instant.

Knowing the flow, head and power enables the possibility of selecting the pertinent hydraulic machine, considering the repeatability of values over a year with the supported information through the relative and cumulative frequency.

The following sections (from A, B, and C) apply the proposed balance to determine energy balance as well as energy indicators in each analyzed case study.

A. *Case study applied to small irrigation water systems*

This case study is based on published paper (Appendix II; Section 3 and 4):

Modelling irrigation networks for the quantification of potential energy recovering: A case study

Co-authors: Pérez-Sánchez, M; Sánchez-Romero FJ; Ramos, HM; López-Jiménez PA.
Journal: Water ISSN 2073-4441.
Impact Factor 1.687. Position 33/85 (Q2). Water Resources.
State: Published [*Water 2016, 8, 1–26. doi:10.3390/w8060234*]

A case study is presented in this paper. The analyzed irrigation network is located on Vallada (Valencia, Spain). The existent irrigation network was used to apply the proposed methodology (Section 4.2.1) for determining circulating flow with the farmer's habits. These habits were obtained from interviews with the farmers and consumption data provided by the water manager of the irrigation community. During the data collection, the determination of the irrigation amount was very accurate because it was a very sensitive parameter in the calibration process. The first results (flow and pressure) were determined in any line of the system, according to the irrigation trends and based on the historical series of records between 2003 and 2014 (17808 records).

Regarding the flows, the frequency histograms displayed a large variability in the flows over the course of a year. The histograms show that the flows behave in a different way than those in drinking systems. Supply networks (except for touristic cities) have monthly seasonal consumption patterns between 0.8 and 1.2, oscillating their daily flow patterns between 0.7 and 1.5 with respect to the average value. If the seasonal flows were analyzed in the irrigation systems, the results were opposite and much larger than those of the drinking systems. Particularly, if the crop was citrus, the seasonality pattern varied between 0.14 and 2.36 when each hourly pattern was compared to the average value. In the presented case study, the estimated variability oscillated between 0.1 and 2.54 times the average flow. This different behavior of the consumption pattern is analyzed in section C of the present document, considering the energy implications related to the influences of the flow pattern.

Related to the energy balance, all energy components (*i.e.,* E_T, E_{FR}, E_{TN}, E_{RI}, E_{TA}, E_{TR}, E_{NTR}) were determined for all irrigation points (371), hydrants (70), and lines (85); the average consumption was 925427 m^3/year. The global energy balance in the network established an ET of 274.00 MWh/year. This energy was distributed as 11.25 MWh/year

(4.10%) for friction energy, 74.52 MWh/year (27.20%) for energy required for irrigation, and 188.23 MWh/year (68.70%) in theoretically energy recoverable if the sum of the total individual recovered energies is considered.

If the balance was also established for the hydrants (Figure 5), the friction energy from the hydrants was 6.20 MWh/year, the energy required for irrigation was 75.20 MWh/year, the theoretically recoverable energy was 178.10 MWh/year (*i.e.,* 65% of the total energy), and the theoretically non-recoverable energy was 14.50 MWh/year.

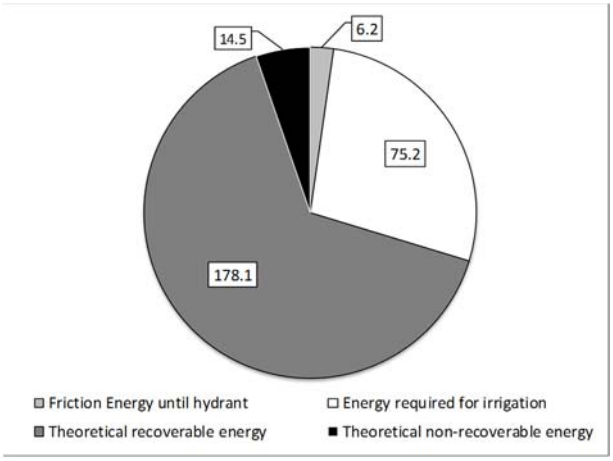

Figure 5. Annual energy balance in the hydrants [31]

Considering the estimated values, the operation work (the pairs of the data flow *versus* the available head) was determined (Figure 6).

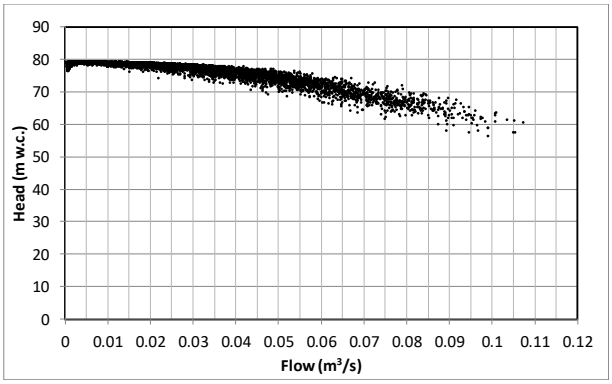

Figure 6. Pairs of the data flow versus the available head in line 38 [31]

Knowing these pairs of data enables the selection of the best machine according to the power frequency histogram. The obtained results allow for determining the payback simple period (*PSR*) and energy index (*EI*) of the investment depending on the analyzed point (*e.g.,* in line 38, the theoretically recoverable energy was 89.99 MWh/year, the *PSR* was 5.9, and the EI was 0.22, showing the feasibility investment). Finally, the possibility recovering the total estimated energy in all irrigation points has a positive environmental impact, contributing to a theoretical reduction of 137.4 tonnes of CO_2/year when the renewable generation was compared to non-renewable resources (*e.g.,* coal and gas) or 216.2 tonnes of CO_2/year if the renewable energy was compared to fuels in this case study.

B. Case study applied to larger water distribution systems

This case study is based on submitted paper (Appendix IV):

Water-Energy nexus. Energy optimization in water distribution system. Case study 'Postrasvase Júcar Vinalopó' (Spain)

Co-authors: Pérez-Sánchez, M; Sánchez-Romero FJ; López-Jiménez PA.
Journal: Tecnologías y Ciencias del Agua ISSN 2007-2422.
Impact Factor 0.108. Position 83/85 (Q4). Water Resources
State: Accepted to publish [Accepted Data: 27/03/2017, Vol VIII (4) Julio-Agosto 2017]

The lack of hydric resources in some locations causes the need to install large hydraulic infrastructures to transfer water volumes from surplus to shortfall zones. These transfers are performed using open channels flow (*e.g.,* James Bay Project, Quebec, Canada; Central Valley Project, California, United States; Tajo-Segura Transfer, Spain) or large pressurized water systems (*e.g.,* Hetch Hetchy Aqueduct, California, United States; Júcar-Vinalopó Transfer, Spain).

These transfers are characterized as having a main distribution system and secondary distribution systems. The main distribution systems correspond to flow transport between the zones, which often have large hydropower systems installed to take advantage of the high transferred volumes. The secondary distribution systems are used for flow transportation near final uses (*e.g.,* supply or irrigation communities), transferring smaller volumes compared to the flow distributed in main distribution systems. Currently, these systems normally do not have recovery systems.

The Jucar-Vinalopó Transfer is analyzed in this research. This transfer connects the Jucar River Basin (Valencia, Spain) with an irrigated area that is located on the Vinalopó River Basin (Alicante, Spain). The case study presented mainly focused on two topics. Initially, the study optimizes the volume transfer to minimize the groundwater extraction through control rules established using *EPANET*. Later, an energy balance is developed.

The control rules were declared for all reservoirs integrated on the 'Júcar-Vinalopó Post-Transfer'. These operating laws, whose constraints are defined in Figure 7, depended on

the reservoir levels and interval times. The following parameters are defined for the operating laws:

- the volume transferred from the 'Júcar-Vinalopó Transfer';
- the operating time of the groundwater resources, distinguished from the interval time contained in the electric contract rate; and
- the volume provided from other input flow lines from resources from the irrigation communities (*e.g.,* wastewater, regenerated water, surface water resources).

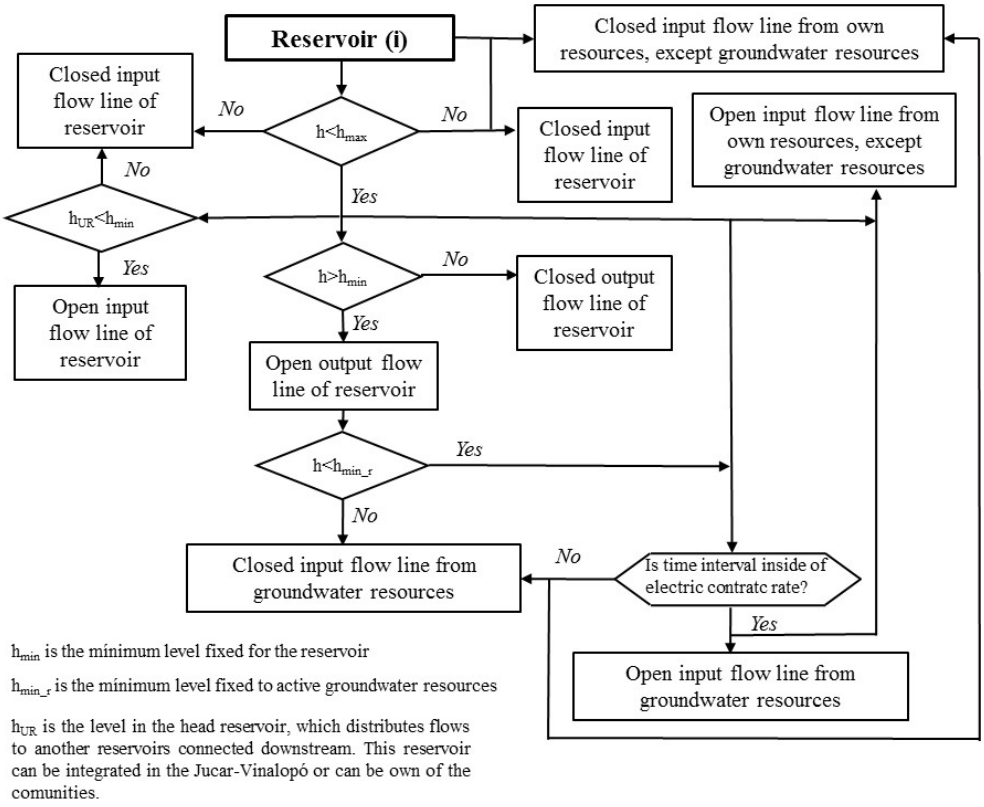

Figure 7. Control rules to optimize the flow distribution in Júcar-Vinalopó Post-Transfer [33]

In contrast, this research analyzed the potential energy recovered in the system, when the resources were distributed to both the small reservoir or final user demands (supply or agricultural). Considering such described topics, five stages were developed in this research:

(i) To study the exploitation conditions, including the data acquisition (*e.g.,* storage, consumption volume, infrastructures) of 50000 hectares inside of the system;

(ii) To model the infrastructures and demands (drinking and agricultural) using *EPANET*, developing control rules according to the level of the reservoir, levels between the head and recipient reservoir, hourly discrimination in the pump systems, groundwater concessions, and hourly demands;

(iii) To analyze the viability of actual infrastructure to satisfy the demands according to different scenarios;

(iv) To plan and analyze possible improvements for maximizing the use of resources and built infrastructures; and

(v) To consider the possibility to leverage the piezometric head of the small reservoir to install an energy recovery system, increasing the energy efficiency in the system.

Regarding the hydraulic modeling, the study concluded that there were not enough objective criteria for closing the wells when the provided volume was not greater than 50 hm^3/year.

Regarding the study of the recovered energy, based on the proposed energy balance as well as the economic feasibility indexes, the maximum theoretically recoverable energy was 18418 MWh/year. The study established that five of twenty possible energy recovery systems were feasible. If these facilities for energy recovery were installed, the recovered energy would contribute to recover 7% of the consumed energy (Figure 8) to pump water from the origin (Marquesa Dam) to the head reservoir (San Diego Reservoir).

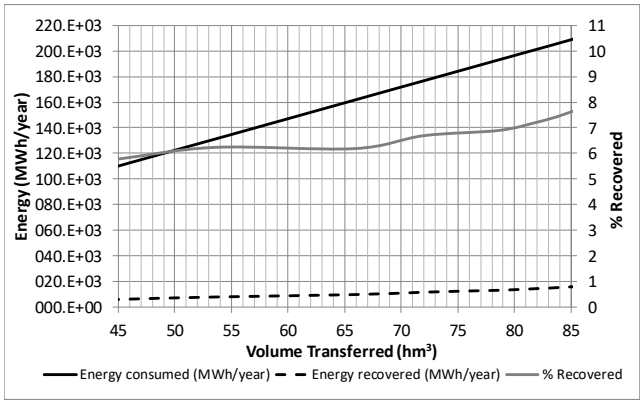

Figure 8. Consumed vs recovered energy depending on the volume transferred [33]

C. ***Flow pattern influences on the energy footprint of water in the pressurized water networks***

The proposed method and case study are based on submitted paper (Appendix V):

Energy footprint of water depending on consumption patterns

Co-authors: Pérez-Sánchez, M; Sánchez-Romero FJ; López-Jiménez PA.
Journal: Ingeniería del Agua ISSN 1134-2196.
Extended JCR.
State: Accepted with changes [Registered Data: 10/01/2017].

Flow consumption patterns have a great influence on the energy behavior of the pressurized water systems. This difference causes the need to work with discretized patterns over time (*e.g.,* hourly) if water managers want to perform deeper energy studies or if they want to establish thresholds for the efficiency indexes (*e.g.,* the energy footprint of water) during an energy audit.

The manuscript analyzed the differences between the energy balances depending on the consumption flow patterns. To only compare the flow pattern influences, the case study was applied in a synthetic pump network, in which four different consumption patterns were studied. These patterns were actual values that were obtained from flowmeter readings in two irrigation and two supply networks. The irrigation networks were called Network A and Network B. Network A corresponded to a crop with typical irrigation needs, and Network B represented a crop with a high irrigation frequency. Networks C and D corresponded to supply networks. Network C represented a supply network in which the consumption was uniform, while Network D belonged to a touristic township in which the demand grew from May to October. Therefore, the patterns analyzed for each network were different from each other, representing different behaviors in the demanded flow.

In this research, a methodology was described to develop a synthetic network with the same design criteria according to the consumption flow patterns. This methodology was structured using five stages:

(i) the determination of the annual flow pattern. The annual flow pattern (*FP*) was defined, which established the ratio between the hourly demanded flow and total demand of the consumption nodes. The *FP* was determined by the registered flow data over time and the cumulated demand in all consumption points of the network ($F_{100\%}$).

(ii) the flow normalization. The objective of this phase was to compare the same consumption situations in each analyzed pattern.

(iii) the generation of operating assumptions for each normalized flow depending on the opening and closure of the consumption nodes.

(iv) the network sizes. To compare the energy balances between networks, all networks compared had the same design criteria. This phase determined the pipe sizes, according to the maximum flow calculated in each case study.

(v) the energy balance. When the pipes for the synthetic were sized, the energy balance was developed according to section 4.2.1.1.3. The energy footprint of the water was then determined using the energy balance in each network.

The balance developed in stage (v) did not directly allow for the comparison between different case studies because the circulating flows were defined by very different *FP* values. Therefore, new parameters were presented in this research. These parameters were as follows: the non-dimensional energy footprint of water (EWF_A) and the non-dimensional flow (Q_A). Both parameters allowed establishing and comparing the energy footprint of water between different systems in the design or management phase.

The EWF_A analysis (Figure 9) applied in the developed cases concluded that networks with less *FP* variability consumed less total energy (5.22, 3.21, and 4.01%) and friction energy (28.57, 21.42 and 25%) than the networks with greater *FP* variability. If the EWF_A was analyzed, the average EWF_A values of the three networks with greater *FP* variability were 31.53, 149.38, and 42.59% higher when compared to the network with a more uniform *FP*.

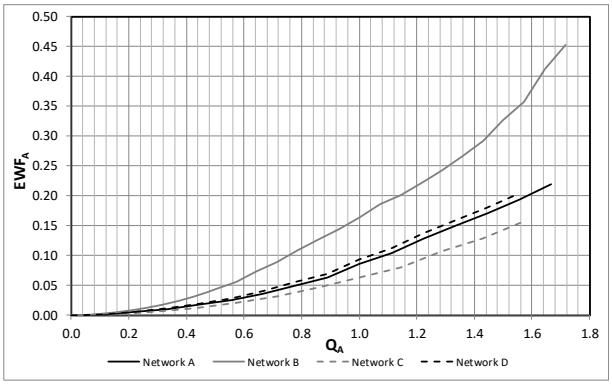

Figure 9. EWF_A versus Q_A depending on the case study [34]

The proposed parameter (EWF_A) can be used for developing energy audits, enabling a comparison between networks. The EWF_A can also be used as a sustainability criterion during the initial design phase for pressurized water networks. This index can be introduced in addition to the technical and economic criteria used to size pipelines in networks, if its thresholds are predefined by analyzing actual networks that are currently operating.

4.2.1.2 Maximization strategy as a water management tool in water distribution systems

The maximization strategy as water management tool described in this section is based on submitted paper (Appendix VI):

PATs' selection towards sustainability in irrigation networks: Simulated annealing as water management tool

Co-authors: Pérez-Sánchez, M; Sánchez-Romero FJ; López-Jiménez PA.; Ramos, HM.
Journal: Renewable Energy ISSN 0960-1481
Impact Factor 3.404. Position 24/88 (Q2). Energy&Fuels
State: Submitted [Registered Data: 10/09/2016]

The development of the methodology to determine the circulating flow as well as the energy balance developed for an individual point (*i.e.,* line, hydrant or irrigation point) promote the need to maximize the theoretical energy recovered, considering the location of the recovery machine. This maximization was developed by considering the following:

(i) the demands of the farmer, which depend on the different habits of the farmer (*i.e.,* the irrigation amount, maximum days between irrigation, weekly irrigation trends, and irrigation duration patterns);

(ii) the location of the PATs or turbines according to the number of selected recovery points;

(iii) the type of machine installed (*i.e.,* specific speed, impeller diameter, rotational speed); and

(iv) the analysis of the recovered energy considering the machine efficiency in each time point as a function of the circulating flow.

The influence of farmer's demands (i) is discussed in section 4.2.1.1.2, based on a submitted paper (Appendix II). The rest of the bullet points cited in the previous paragraphs are proposed, analyzed, and discussed in the submitted manuscript in Appendix VI, and they are summarized below. To establish the best location of the machines, a methodology based on a simulated annealing algorithm was proposed to optimize the emplacement of the recovery systems (Figure 10).

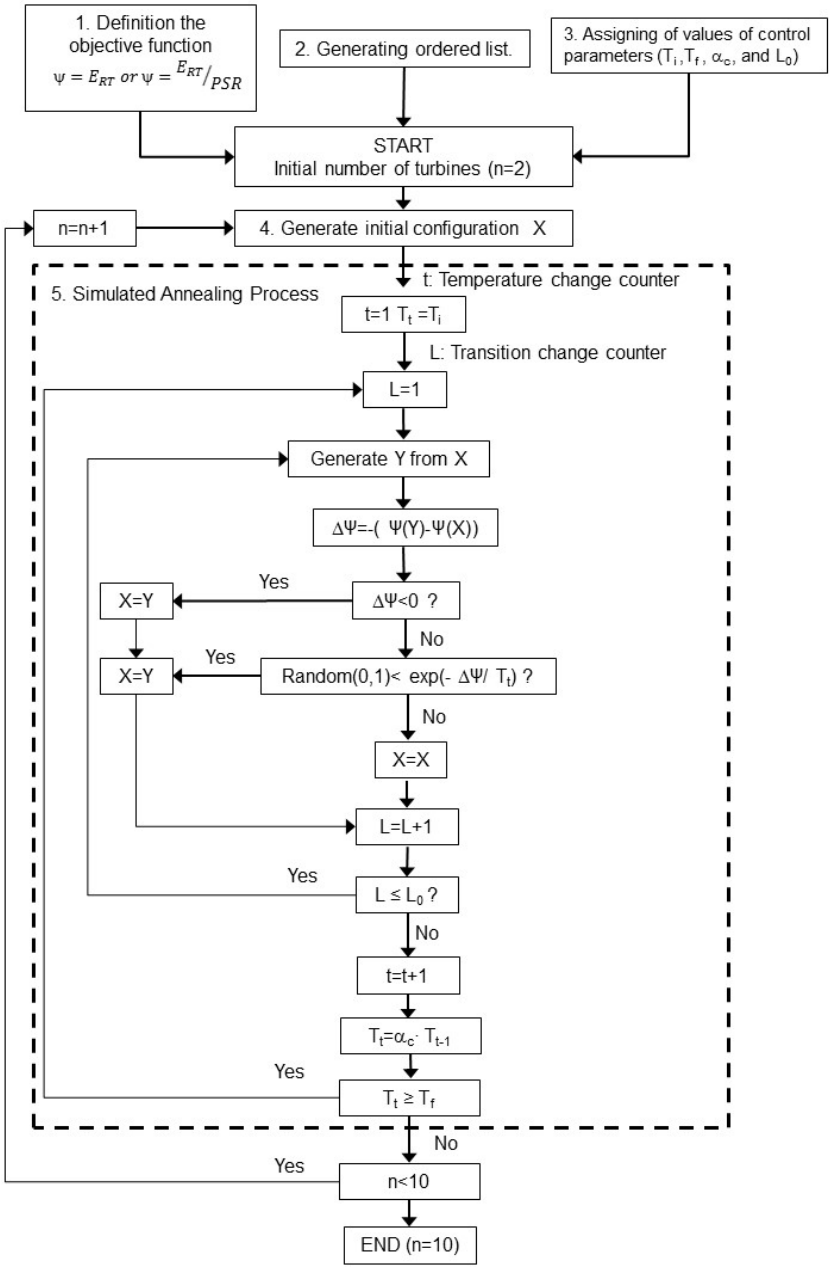

Figure 10. Flowchart for optimizing the networks in the energy recovery process with "n" installed turbines or *PATs* [35]

This methodology was applied to the irrigation network in Vallada (Figure 11). The optimization methodology was developed for two objective functions, E_{TR}^{S} and $\frac{E_{TR}^{S}}{PSR}$, where E_{TR}^{S} is the total recovered energy with "n" serial installed machines. In this case, the maximum number of lines considered for each objective function was fixed to ten, although as novelty, the proposed methodology enabled a great number of studied lines without increasing the computational cost . Once the network was maximized, the four best results were used for simulated annealing using *WaterGEMS*, considering the recovery from one to four lines with a fixed rotational speed. Another additional simulation was developed by installing a group of *PATs* in one line with a variable rotational speed (fifth simulation).

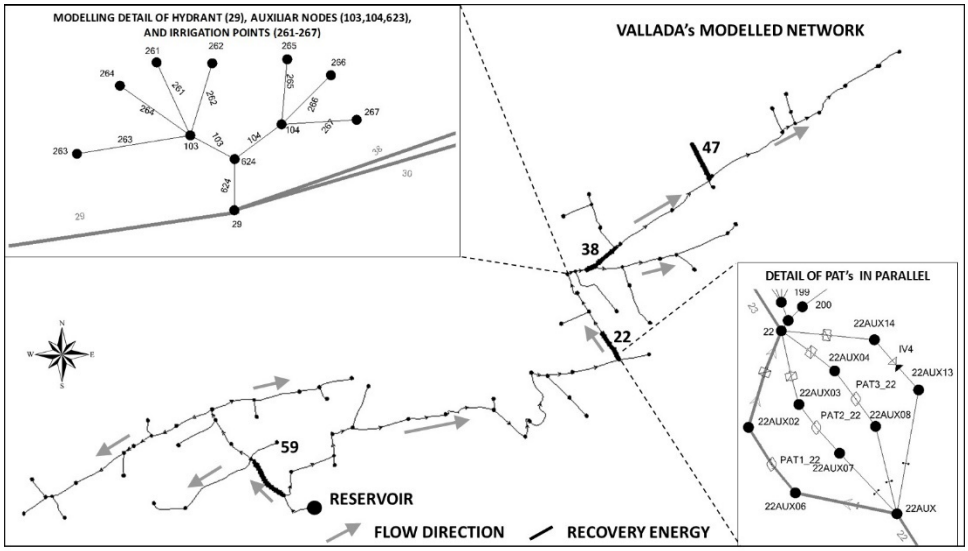

Figure 11. Case study Vallada (Spain) [35]

This software simulated the hourly flow depending on the consumption patterns, hydraulic machine characteristics (*e.g.,* the efficiency and recovered head according to the circulating flow, number of machines installed in parallel, and fixed or variable rotational speed), and operating flow range (Figure 12). The operating flow range was required to guarantee the minimum pressure and flow conditions for the user, as the energy generation was not a priority objective in this type of pressurized network. The used machines, their characteristic parameters (*e.g.,* rotational speed, discharge number, and head number), and their efficiency were obtained based on the experimental tests according to a specific speed.

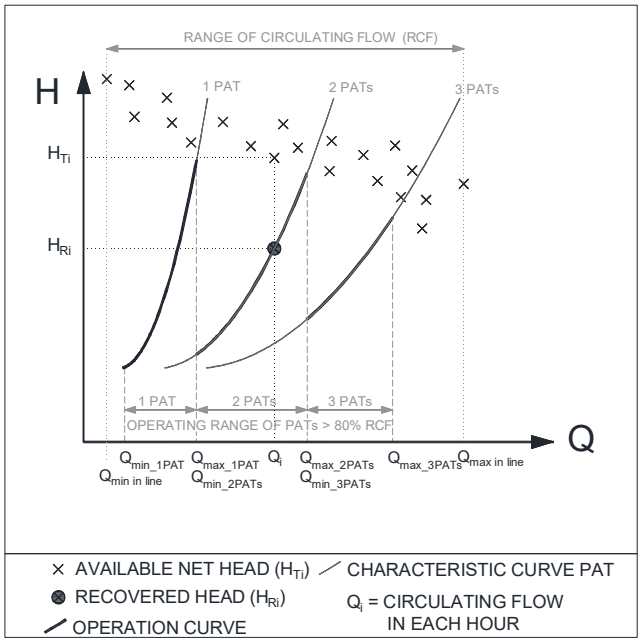

Figure 12. Scheme of the operation zone when a parallel *PAT* group was simulated [35]

The five simulations were analyzed by determining the theoretical recovered energy (E_{TR}), which was determined from the simulated annealing; the actual recovered energy (E_R), considering the *PAT* simulation in *WaterGEMS*; the payback period (*PSR*); and the efficiency index (*EI*). This analysis was developed for both obtained solutions (the simulated annealing and *WaterGEMS* simulation). The best obtained solution occurred when one group of *PATs* was installed in only one line, with consideration of its rotational speed variable. For this simulation, the recovered energy was 26.51 MWh/year (9.55% of the provided energy in the system, considering the efficiency variation of the machine according to the flow). If the *PAT* performance was considered to be uniform (equal to 0.55), the recovered energy increased up to 49.66 MWh/year. When the *PAT* performance was considered to be ideal (the efficiency was one), the recovered energy was 89.99 MWh/year (this value is based on the obtained results in Appendix II).

The previously enumerated values, which belonged to the same line, show the need to develop recovery studies by adding different strategies. These strategies should consider the following:

- variable operation strategies (*VOS*), which establish the best rotational speed according to the flow;
- the efficiency variation as a function of flow; and
- the optimization of the system according to the number of installed machines.

4.2.2 Experimental stage

The present part of the research focuses on the experimental research conducted to analyze the behavior of the hydraulic machines in steady and unsteady flow conditions. Some particular experimental tests were carried out in the *CERIS*-Hydraulic Lab of Instituto Superior Técnico at the University of Lisbon. The analysis was performed with two different *PATs* (radial and axial, with specific speeds of 51 and 283 (m, kW, respectively). The first aim of this phase was to analyze the efficiency and head variation when the machines were operated with variable flows in steady flow conditions. Additionally, the second objective was to introduce the characterization of the transient phenomenon during the design of *PAT* systems in order to emphasize transient events that could occur during normal operation (*e.g.,* fast openings or closures).

4.2.2.1 Steady Flow analysis: best efficiency line (BEL)

This experimental stage, proposal of modified affinity laws, and analysis are described on submitted manuscript (Appendix VII):

Modified affinity laws in hydraulic machines towards the Best Efficiency Line

Co-authors: Pérez-Sánchez, M; López-Jiménez PA.; Ramos, HM.
Journal: Water Resources Management ISSN 0920-4741
Impact Factor 2.437. Position 12/85 (Q1). Water Resources
State: Submitted [Registered Data: 08/12/2016]

When *PATs* are installed within pressurized water systems, the variability of the flow rates in the pipes or hydrants brings to light the need to operate with variable operation strategies (*VOSs*). *VOSs* enable the variation of the rotational speed of the hydraulic machine as a function of flow, considering the best rotational speed for each time point. The determination of the efficiency, head, and power of the machine according to rotational speed is normally carried out using classical affinity laws. These laws are theoretical, and their use can cause erroneous results when determining the head and efficiency values.

This research shows the need to know the efficiency of the hydraulic machine as a function of its rotational speed. The presented research in this section pursues two objectives:

(i) the calculation and analysis of errors between the measured and calculated efficiency when classical affinity laws are applied.

(ii) the development of modified affinity laws to establish the best efficiency line (*BEL*) and best efficiency head (*BEH*) as a function of the flow in each tested machine (axial and radial). Knowing the *BEH* and *BEL* allows water managers to determine the best operation point (*BEP*) for each flow value.

This methodology proposes the modification of affinity laws using the Suter parameter and theoretical affinity laws. Their validation with experimental data is also proposed. These modified affinity laws were applied to two different *PATs* (axial and radial).

The error analysis shows that the obtained errors between the experimental and estimated data in this particular case with classical affinity laws could reach 10% in both machines for the head and efficiency values, presenting mean square errors between 0.04 and 0.09 according to the analyzed *PAT*. If newly modified functions were proposed to determine the flow (q), head (h), power (p), and efficiency (e) using Suter parameters for both machines, the mean errors were reduced between 50 and 83.33%, depending on the Suter parameters and the analyzed machine; these errors were compared to the obtained values after applying the classical affinity laws. If the proposed functions were obtained as a function of the rotational speed, the *BEL* and *BEH* could be defined depending on the flow (Figure 13).

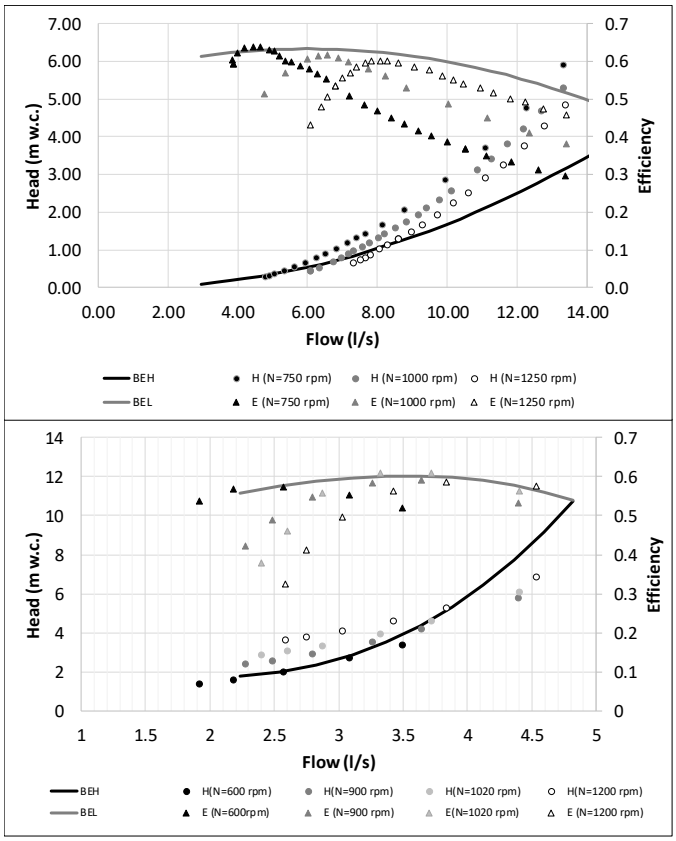

Figure 13. *BEH* and *BEL* for the axial (up) and radial (bottom) hydraulic machines [36]

Knowing the *BEL* enables defining operation rules to determine the *BEP* for each flow, determining the best rotational speed of the machine in each instant and, therefore, maximizing the machine performance.

Finally, the need to correlate the rotational speed and the specific speed with the different characteristic parameters (q, h, p, and e) is of utmost importance. The development of similar studies for different specific speeds will define the *BEL* and *BEH* as a function of the Suter parameters. This knowledge will help modelers to choose the best hydraulic machine for each system according to the hydraulic characteristics (*e.g.,* flow, available head, power frequency), improving the simulations developed. This improvement of the energy studies promotes the determination of more accurate energy recovery values.

4.2.2.2 Unsteady flow analysis: Overspeed effects

This experimental stage is based on submitted paper (Appendix VIII):

PATs operating in water networks under unsteady flow conditions: control valve maneuver and overspeed effect

Co-authors: Pérez-Sánchez, M; López-Jiménez PA.; Ramos, HM.
Journal: Renewable Energy ISSN 0960-1481
Impact Factor 3.404. Position 24/88 (Q2). Energy&Fuels
State: Submitted [Registered Data: 20/02/2017]

All previous sections considered *PATs* operating under steady flow conditions. However, if a *PAT* is installed within a pressurized water system, the recovery system will be affected by unsteady flow conditions when flow variations occur (*e.g.,* a change in the demanded flow, a closure shutdown). These flow variations give rise to a transient state in the network. Therefore, knowing the transient conditions in hydraulic systems equipped with *PATs* is of the utmost importance. This must become a priority for safety reasons and for the successful implementation of these new renewable solutions, as far as the consulted references indicate.

This study proposed the characterization of the water hammer phenomenon for the design of *PAT* systems in order to emphasize the effects of transient events that can occur during a normal operation (*e.g.,* control maneuvers (fast openings or closures), overspeed effects).

The obtained results from the experimental campaigns developed for both *PATs* (axial and radial) were described. The transient phenomenon was measured in terms of the flow, head (upstream and downstream of the hydraulic machine), and rotational speed of each machine. The tests were developed for different initial operating conditions (Q_0, H_0, N_0) when the opening degree of the valve was maximum. The experimental schemes were also simulated using *Allievi* software, which determined the maximum and minimum pressure waves in both analyzed *PATs*. The more determinant parameters (*i.e.,* the damping effect, effective time of the closure valve, and overspeed effect) in the

transient study were correctly calibrated. These parameters were mathematically defined by their dependent variables and constants in the different sections of the manuscript.

The analysis of the experimental and simulated data allowed isolating the overspeed effects in the machine when the recovery system reached runaway conditions. The flow variation according to the head and rotational speed were analyzed for both machines, and the results were related to the best efficiency points of the *PAT* (Q_{BEP}, H_{BEP}, N_{BEP}). If the behaviors of both machines were compared, some differences arose between the radial and axial machines under runaway conditions. In the radial *PAT*, the flow decreased for a constant value of h ($h=H/H_{BEP}$). As an example, in the tested radial machine, the flow reduction was approximately 50% if the flow runaway (Q_{RW}) was compared to Q_0, while the ratio H_{RW}/H_0 (upstream and downstream) remained constant during overspeed conditions for different tested conditions (Figure 14).

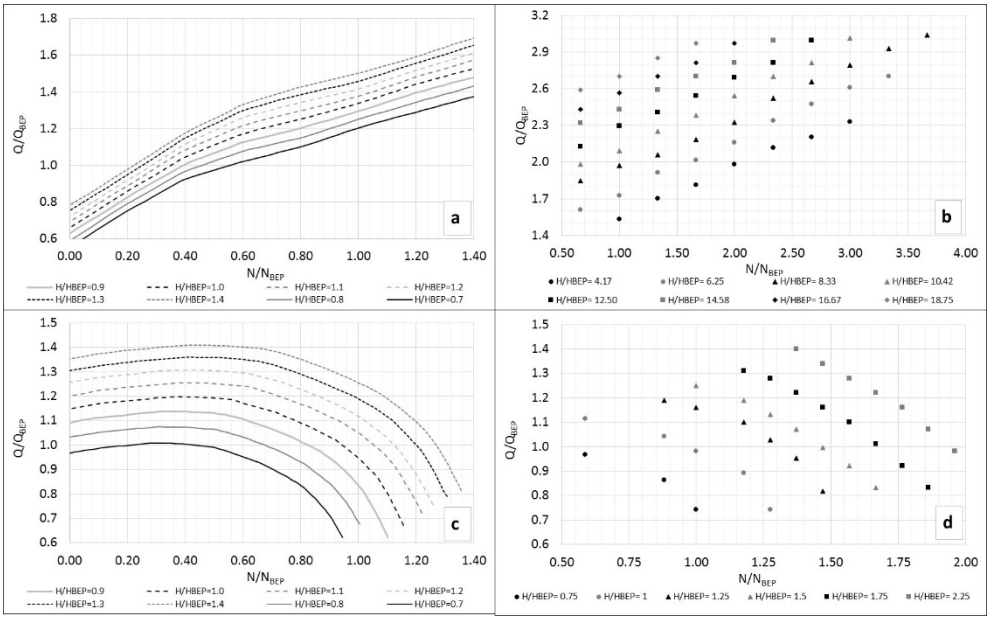

Figure 14. Q/Q_{BEP} as a function of N/N_{BEP} and $h=H/H_{BEP}$ for axial classical turbine (a), axial *PAT* (b), radial classical turbine (c) and radial *PAT* (d)

Inverse results were obtained when the axial machine was studied. In this case, if the rotational speed increased, the flow also increased for a constant value of *h*. If this behavior was analyzed for different values of *h* (H/H_{BEP}), the same trend was observed. For axial *PAT*, the Q_{RW}/Q_0 approximately increased by 150%, while the H_{RW}/H_0 (upstream and downstream) remained constant for different tested conditions.

Based on the data obtained during this intensive experimental campaign, important information was presented and utilized for some specific *PAT* transient state conditions.

This analysis required a mathematical transformation of the available data for the pumps (based on experiments especially developed for this study) into characteristic curves of the discharge variation, Q/Q_{BEP}, with the rotating speed, N/N_{BEP}. This mathematical transformation facilitated the understanding of the behavior of the dynamic pump as a turbine under unsteady conditions.

The feasibility of the pumps operating as turbines was proven, based on the typical performance control analyses, because their dynamic behavior was quite similar to that of the classical reaction turbines, regarding the flow variation due to the runner type that was characterized by its specific rotational speed (n_s).

Therefore, the installation of *PATs* can be adopted in pressurized water networks, considering the water hammer phenomenon introduced by these recovery systems in the network when maneuvers are performed. This phenomenon can be analyzed with specific software (*e.g., Allievi*) provided that water managers have perfectly defined and calibrated their model according to the damping effects of the system, the maneuver type (*e.g.,* effective closure time), and the machine characteristics (*e.g.,* inertia, specific rotational speed).

Chapter 5
Conclusions and Future Developments

The present thesis determined the energy consumption in pressurized irrigation networks. To analyze this energy use as well as try to improve the energy efficiency, a methodology for improving energy efficiency analyses in pressurized irrigation networks was proposed. This methodology was based on different strategies to estimate the actual operation of a network. The conclusion and main findings as well as future developments are discussed in the present chapter.

5.1 Conclusions and mine findings

The main conclusion of this thesis is the proposal of a methodology to improve the energy efficiency in pressurized irrigation networks through contextualization stages developed. Each stage developed in the present thesis establishes one step in defining the optimization strategy. These stages were described and summarized in Chapter 4 and developed in their pertinent appendices. Therefore, the conclusion is structured on six different bullet points:

1. The contextualization stage permitted the analysis of different alternatives for hydropower production from large to pico facilities, according to the production levels, economic and environmental points of view, and classification of the hydraulic machines. Considering the evolution of these energy recovery strategies, **achieving energy recovery using *PATs* in pressurized water networks is an alternative solution that improves the sustainability and efficiency in these water systems**. This conclusion is related to Objective 1 and its analysis can establish the main positive and negative aspects of *PATs*.

1.1 The favorable main aspects of recovery systems using *PATs* are focused on the following:

(ii) the installation of a *PAT* enables the replacement of any *PRV* to dissipate excess flow energy and, therefore, reduce leakages;

(iii) satisfactory efficiency values that vary between 0.60-0.70 in the best efficiency point of the machine are achieved when the *PAT* operates in the reverse mode;

(iv) theoretical behavior studies can be easily developed with current technology (*e.g.,* computational fluid dynamics (*CFD*)) based on the classical theory for hydraulic machines (*i.e.,* Euler's Theorem) for comparison with existent experimental tests;

(v) the advantages of low investment costs and a high number of available machines allow water managers to promote the installation of these machines in pressurized water systems.

1.2 The unfavorable main aspects of *PATs* are related to the following:

(i) the low efficiency when a PAT operates out of the best efficiency point due to variability of the circulating flows in the line. Operating with different flows can be solved by developing new regulation techniques (*e.g.,* variable operation strategies (*VOS*)) through the use of electronic regulation. The positive resolution of this aspect is a crucial point for the expanded use of *PATs* in water distribution networks.

(ii) the use of the generated energy has to be bound for self-consumption and storage in batteries and integrated in a similar way with renewable energy with other supplementary sources (*e.g.,* solar, wind). However, the generated energy can directly be sold in grid systems in which the contractual conditions are more flexible.

2. Regarding the used software for simulating these recovery strategies, **the implementation of specific operation rules for these machines in specific algorithms is necessary and is a key point in the development of optimized techniques,** enabling similar studies to those developed for water pump systems.

3. **The development of an optimization strategy to improve the energy efficiency in pressurized irrigation networks makes sense** because the long list of consulted references for the contextualization stage is not explicitly developed, showing that there are still a few references that can be related to agricultural water networks and energy recovery. Therefore, this field is a barely explored subject. The procedural stage contains steps developed in this research. These phases define the methodology for energy efficiency improvement (Figure 15). Each step is related to one of the objective of the thesis.

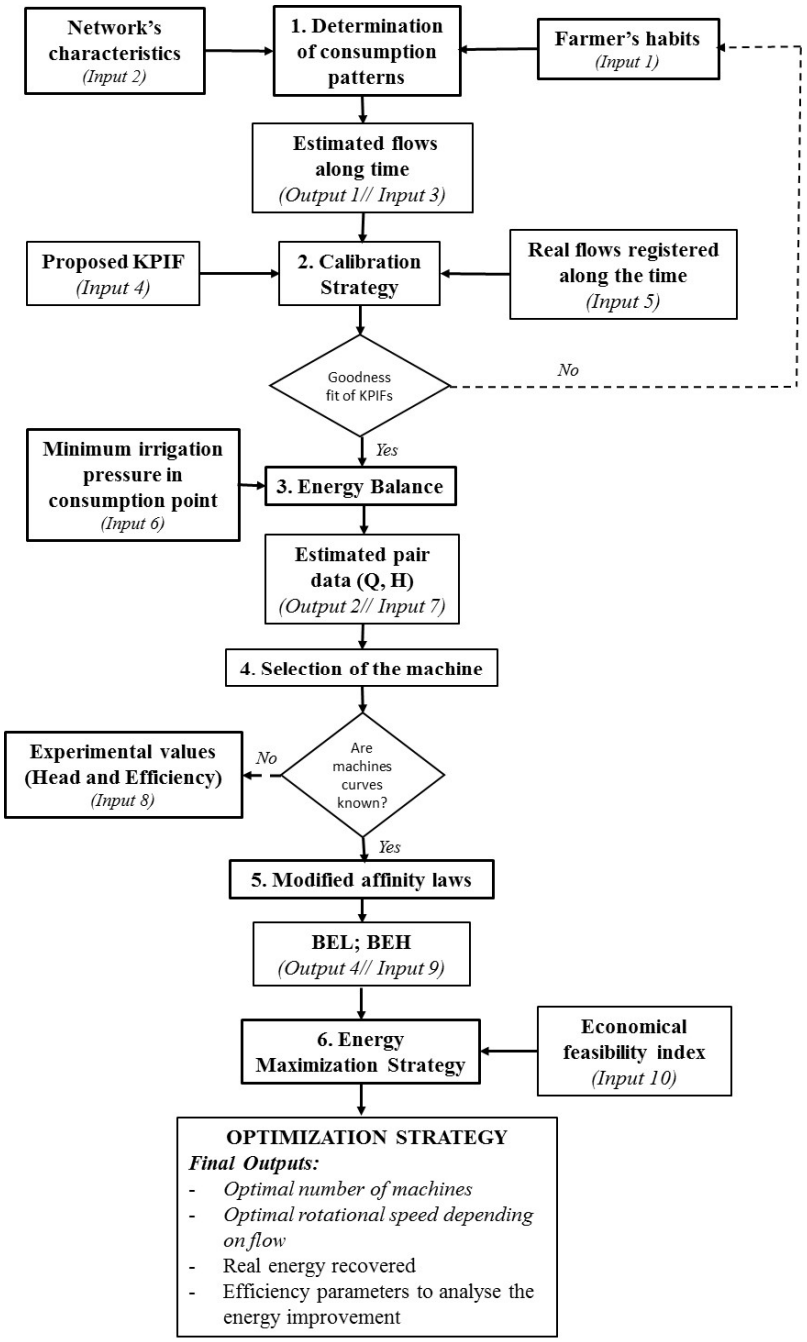

Figure 15. Optimization strategy proposed through developed stages in the thesis

3.1 **A methodology was proposed to determine the consumption flow patterns due to a farmer's habits and characteristics of the network**. This methodology estimates the circulating flow over time in any line of the network. This conclusion is related to Objective 2.

3.2 **A calibration strategy was proposed using key performance indicators (*KPIF*) that were adapted from traditional hydrological models.** The comparison with actual recovered data determined the success of the fit. If the calibration is satisfactory, the energy balance (Step 3) can be approached. Regarding the calibration strategy, which was applied to a real case study, some conclusions were achieved for the particular analyzed case:

i. when maximum flows were compared, *KPIF* values were satisfactory for time intervals lower than eight hours. If greater time intervals were considered (up to 8 hours), the values of *E* and *PBIAS* remained positive and satisfactory in the entire range, but the *RRSE* values became unsatisfactory. This shows the possibility of using the methodology to determine the circulating flow in any line.

ii. when the average flow was analyzed considering that a farmers' habits could be uniform or unknown, the *KPIF* results were satisfactory.

iii. the variability of the goodness of fit was analyzed as a consequence of the methodology to determine the circulating flows, which was based on randomness in the opening or closure of each consumption node. To check this variability, the model was run 200 times for the same irrigation scenario (*i.e.,* annual consumption patterns, weekly irrigation pattern trends, the maximum days between irrigations, and patterns of irrigation times), and robust and low variability results were obtained.

iv. if maximum flow was determined in the main line using the proposed methodology and it was compared to the maximum flow obtained by Clément's Method (for the maximum needs per month), the result was similar. However, if the cumulative frequency was determined, the proposed methodology presented a better fit with the observed flows when it was compared to Clement's Method in the case study analyzed.

This conclusion is related to Objective 3.

3.3 **An energy balance was proposed when the flows were estimated and their goodness of fit was checked**. The energy balance is able to discretize different energy terms (*e.g.,* total, irrigation, friction) and to differentiate the terms for the theoretically available energy between the theoretically recoverable energy and theoretically non-recoverable energy, considering the minimum irrigation pressure at each consumption point. Knowing the theoretically available energy allows for being able to determine the theoretical recovery coefficient at any line, hydrant or consumption point. In addition, the energy balance allows the

estimation of the recovered head for each flow over time. Knowing these pairs of data enables selecting the most suitable machine at each study point. This conclusion is related to Objective 4.

3.4 **Knowing the flow and recoverable head over time from the energy balance allows the selection of the machine type** (*e.g.,* radial, axial) according to the frequency histogram of the power generated among other conditions. To develop a guaranteed estimation of the recovered energy, the head and efficiency curve should be known for different rotational speeds. If this information is not provided by the manufacturer, experimental tests are recommended to obtain the efficiency variation depending on the flow and for different rotational speeds. On a related note, in the present thesis, an intensive campaign was developed in the *CERIS*-Hydraulic Lab of Instituto Superior Técnico at the University of Lisbon in which two different *PATs* (one radial and another axial) were tested in steady flow conditions; the experimental data of the efficiency as a function of flow and rotational speed were obtained. This conclusion is related to Objective 8.

3.5 **A proposal using modified affinity laws was applied for two different *PATs* (radial and axial) through classical affinity laws based on Suter parameter variation depending on the rotational speed**. Based on these new laws, two new concepts (the best efficiency line, *BEL* and best head line, *BEH*) were defined. The *BEL* adapts the rotational speed as a function of the flow, adjusting the maximum efficiency in each time point and, therefore, maximizing the energy recovered. This conclusion is related to Objective 8.

3.6 **The proposal of a strategy to maximize the energy recovered was developed** by using *PATs*, considering the theoretically recovered energy and economic feasibility indexes. This strategy makes use of a simulated annealing algorithm that considers the following:

i. the installation of turbines in series affects the operation zone of the machine, and this type of connection causes a greater dispersion in the pairs of data (*Q, H*), reducing the operation time of the machine.

ii. as a novelty, the maximization is performed with an objective function that takes into account both maximum recovered energy and the feasibility index (*PSR*).

iii. the use of *PSR* can be introduced in the maximization strategy when the modeler knows the exact market prices and characteristic curves of the available machines. The precise knowledge of the machine curves allows water managers to differentiate between positions in which the machine cannot be installed due to fact that the theoretical pairs of data (*i.e.*, Q and H) are not inside of the operating range of the manufactured machine.

This conclusion is related to Objective 5.

4. **The development of this strategy (Step 3. Maximization) enables developing an energy analysis method for any pressurized irrigation network, obtaining the optimal number of machines to install and the optimal rotational speed depending on the flow, and determining the real recovered energy as well as the efficiency parameters to analyze the energy improvement in the studied network**. Based on the presented steps of this strategy (Figure 15), three particular case studies were analyzed.

4.1 In the first case study, which corresponded to a small irrigation network, the methodology, the energy balance, and the maximization strategy were applied, obtaining interesting recovery values that improved the energy efficiency of the network. The methodology and energy balance were performed using *EPANET* software, while the maximization was developed using *WaterGEMS* software. For the best situation, the recovered energy was 26.51 MWh/year (9.55% of the provided energy in the network, considering the variation of the performance according to the circulating flow as well as the variable operating strategies (*VOS*)).

4.2 In the second case study, a large pressurized water system (Júcar-Vinalopó Transfer) was analyzed. The study optimized the volume transfer to minimize the groundwater extraction through a strategy of control rules established on *EPANET*. In addition, based on the energy balance proposed, the theoretically recoverable energy and selection of the machine were analyzed. The maximum recovered energy was 18418 MWh/year when the volume transferred was 85 hm^3/year (approximately 7% of the energy consumed by the pumps installed in the water system). In both cases, (4.1 and 4.2) the values of the energy recovered were interesting from sustainable and economic points of view.

4.3 In the third case study, using the proposed energy balance, different bullet points could be enumerated.

i. A new methodology was developed to compare the energy footprint of the water through the flow patterns, showing the existent differences between the supply and irrigation consumption patterns.

ii. The comparison of the energy footprint of water along the flow distribution using four different real consumption patterns was achieved. This analysis was developed through two new defined parameters (the non-dimensional energy footprint of water, EWF_A and the non-dimensional flow, Q_A).

iii. In the comparison developed, the irrigation patterns with high variability over time presented higher values of EWF_A than those of the more uniform patterns.

iv. The EWF_A can be introduced in sizing methodologies as a sustainability index in addition to the design and economic criteria. However, this parameter should be prechecked to establish the necessary thresholds.

This fourth conclusion is related to Objectives 6 and 7.

5. **To complement the optimization strategy, the behavior of the *PATs* was analyzed in unsteady flow conditions** when these machines were operated in pressurized water systems. Related to this phenomenon,

5.1 another intensive experimental campaign was conducted in the *CERIS*-Hydraulic Lab in which two different *PATs* (one radial and another axial) were tested in unsteady flow conditions. Experimental data of the pressure, flow and rotational speed over time were recorded through fast maneuvers (closure or opening). These maneuvers caused *PAT* start up or *PAT* shutdown conditions that generated overspeed effects in the machine.

5.2 the experimental data were supported with simulations developed on *Allievi* software, which obtained very interesting and quite accurate results.

5.3 the obtained data in addition to the mathematical transformation of the available data for pumps enabled the analysis of the characteristic curves of the discharge variation (Q/Q_{BEP}) as a function of the rotating speed (N/N_{BEP}) for the radial and axial machines, respectively.

5.4 This procedure elucidated the dynamic *PAT* behavior under unsteady conditions, which was quite similar to the classical reaction turbines regarding the flow variation due to the runner type.

This conclusion is related to Objective 9.

6. **The implementation of this strategy** and the knowledge of the behavior of *PATs* in unsteady flow conditions **will improve** the use of reverse pumps for drinking, irrigation and drainage water systems, increasing **the energy efficiency and**, therefore, the **sustainability in pressurized water systems**.

5.2 Future developments

This research contributes to the progress for theoretically approximating the energy analysis in pressurized irrigation networks through the installation of recovery systems, particularly *PATs*. However, new research lines have been created, providing an opportunity to develop new research studies. Some of these lines are described as follows:

(i) Regarding the proposed methodology, future research should focus on the flow estimation in any line through supply consumption nodes. The knowledge of the flow over time will allow the development of more exact energy studies for supply networks.

(ii) Related to the proposed methodology, other future research should focus on validating the methodology used during the design phase in the gravity system as well as optimizing the pump systems considering the flow frequency histograms. This validation should be developed by increasing the number of

case studies analyzed for pressurized irrigation networks and checking them using the calibration strategy presented.

(iii) Related to the optimization strategy, future research should focus on the implementation of these developed strategies (*i.e.,* methodology of the flows, calibration strategy, and maximization by simulated annealing) using specific software (*e.g., WaterGEMS*, *EPANET*) as water management tools. This strategy will allow the development of more accurate energy studies.

(iv) Related to the optimization strategy, other future research should focus on the development of similar optimization strategies using meshed water networks. These optimization strategies determine the operating network when recovery systems are installed and the difficult to define the flow directions in each network when demands vary.

(v) Related to the machine selection, future research should focus on the need to correlate the rotational speed and the specific speed using Suter parameters (q, h, p, and e); this is of utmost importance. The development of similar studies for different specific rotational speeds will define the *BEL* and *BEH* and determine the best hydraulic machine for different system characteristics, integrating the *BEL* and *BEH* as a function of flow in the specific software.

(vi) Related to the unsteady flow conditions, future research should focus on increasing the knowledge of transient phenomena in pressurized water networks when recovery systems are installed in these water systems. The studies should analyze the hydraulic behavior as well as the electric behavior in the hydraulic machine, depending on flow variations.

(vii) Related to the electronic regulation, future research should focus on the development of regulation strategies using electronic operations. These operations should select the best rotational speed for the machine depending on the *BEL* and type of connection of the machine (*i.e.,* connected to the grid or isolated from the grid). In this last case (isolated from the grid), the development of studies to minimize the reactive energy to excite the machine is necessary, considering that the increase in the number of capacitors causes a decrease in the efficiency of the machine.

(viii) Related to the electric connection, future research should focus on improving the storage systems and developing sustainable and feasible electric systems (grid connections or stand-alone operations). These electric systems will increase the viability of selling the energy to the national grid or using it for self-consumption. This generated energy can be combined with other renewable energies (*e.g.,* solar, wind), integrating the generated energy in water management to improve the sustainability of its utilization.

Chapter 6
References

[1] Coelho B, Andrade-Campos A. Efficiency achievement in water supply systems—A review. Renew Sustain Energy Rev. 2014;30:59-84. doi:10.1016/j.rser.2013.09.010.

[2] Nogueira M, Perrella J. Energy and hydraulic efficiency in conventional water supply systems. Renew Sustain Energy Rev. 2014;30:701-714. doi:10.1016/j.rser.2013.11.024.

[3] Pasten C, Santamarina JC. Energy and quality of life. Energy Policy. 2012;49:468-476. doi:10.1016/j.enpol.2012.06.051.

[4] Huesemann MH. The limits of technological solutions to sustainable development. Clean Technol Environ Policy. 2003;5(1):21-34. doi:10.1007/s10098-002-0173-8.

[5] Gilron J. Water-energy nexus: matching sources and uses. Clean Technol Environ Policy. 2014;16(8):1471-1479. doi:10.1007/s10098-014-0853-1.

[6] Emec S, Bilge P, Seliger G. Design of production systems with hybrid energy and water generation for sustainable value creation. Clean Technol Environ Policy. 2015;17(7):1807-1829. doi:10.1007/s10098-015-0947-4.

[7] Baki S, Makropoulos C. Tools for Energy Footprint Assessment in Urban Water Systems. Procedia Eng. 2014;89:548-556. doi:10.1016/j.proeng.2014.11.477.

[8] Okadera T, Chontanawat J, Gheewala SH. Water footprint for energy production and supply in Thailand. 2014;77:49-56.

[9] Herath I, Deurer M, Horne D, Singh R, Clothier B. The water footprint of hydroelectricity: a methodological comparison from a case study in New Zealand. J Clean Prod. 2011;19(14):1582-1589. doi:10.1016/j.jclepro.2011.05.007.

[10] Ramos H, Borga A. Pumps as turbines: an unconventional solution to energy production. Urban Water. 1999;1(3):261-263. doi:10.1016/S1462-0758(00)00016-9.

[11] Cabrera E, Cobacho R, Soriano J. Towards an Energy Labelling of Pressurized Water Networks. Procedia Eng. 2014;70:209-217. doi:10.1016/j.proeng.2014.02.024.

[12] Carravetta A, Del Giudice G, Fecarotta O, Ramos H. Pump as Turbine (PAT) Design in Water Distribution Network by System Effectiveness. Water. 2013;5(3):1211-1225. doi:10.3390/w5031211.

[13] Carravetta A, Del Giudice G, Fecarotta O, Ramos H. PAT Design Strategy for Energy Recovery in Water Distribution Networks by Electrical Regulation. Energies. 2013;6(1):411-424. doi:10.3390/en6010411.

[14] Ramos H, Mello M, De PK. Clean power in water supply systems as a sustainable solution: from planning to practical implementation. Water Sci Technol Water Supply. 2010;10(1):39-49. doi:10.2166/ws.2010.720.

[15] Samora I, Franca M, Schleiss A, Ramos H. Simulated Annealing in Optimization of Energy Production in a Water Supply Network. Water Resour Manag. 2016;30(4):1533-1547. doi:10.1007/s11269-016-1238-5.

[16] FAO. Agua Y Cultivos. Rome, Italy; 2002. http://www.fao.org/docrep/005/y3918s/y3918s10.htm.

[17] FAO. Aquastat. http://www.fao.org/nr/water/aquastat/data/query/results.html?regionQuery=true&yearGrouping=SURVEY&showCodes=false&yearRange.fromYear=1958&yearRange.toYear=2017&varGrpIds=4250%2C4251%2C4252%2C4253%2C4257&cntIds=&regIds=9805%2C9806%2C9807%2C9808%2C9809&edit. Published 2015. Accessed June 9, 2015.

[18] Jiménez-Bello MA, Royuela A, Manzano J, Prats AG, Martínez-Alzamora F. Methodology to improve water and energy use by proper irrigation scheduling in pressurised networks. Agric Water Manag. 2015;149:91-101. doi:10.1016/j.agwat.2014.10.026.

[19] Moreno MA, Planells P, Córcoles JI, Tarjuelo JM, Carrión PA. Development of a new methodology to obtain the characteristic pump curves that minimize the total cost at pumping stations. Biosyst Eng. 2009;102(1):95-105. doi:10.1016/j.biosystemseng.2008.09.024.

[20] Pardo MA, Manzano J, Cabrera E, García-Serra J. Energy audit of irrigation networks. Biosyst Eng. 2013;115(1):89-101. doi:10.1016/j.biosystemseng.2013.02.005.

[21] Rodriguez-Diaz JA, Camacho-Poyato E, Carrillo-Cobo MT. The role of energy audits in irrigated areas. The case of "Fuente Palmera" irrigation district (Spain). Spanish J Agric Res. 2010;8(2):152-161.

[22] Abadia R, Rocamora MC, Corcoles JI, Ruiz-Canales A, Martinez-Romero A, Moreno MA. Comparative analysis of energy efficiency in water users associations. Spanish J Agric Res. 2010;8(S2):134. doi:10.5424/sjar/201008S2-1356.

[23] Estrada F, Ramos H. Micro-hydro solutions in Alqueva Multipurpose Project (AMP) towards water-energy-environmental efficiency improvements. Dissertation Project at IST. 2015.

[24] Cabrera J, 2009. Calibración de modelos hidrológicos. Instituto para la Mitigación de los Efectos del Fenómeno el Niño, Lima, Perú.

[25] Moriasi DN, Arnold JG, Van Liew MW, Binger RL, Harmel RD, Veith TL. Model evaluation guidelines for systematic quantification of accuracy in watershed simulations. T ASABE. 2007; 50: 885-900.

[26] White, F.M., 2008. Fluid Mechanics, Sixth edit. ed. McGrau-Hill.

[27] Kirkpatrick, S., Gelatt, C., Vecchi, M. Optimization by simulated annealing. Science 1983; 80. 220, 671–680.

[28] Rossman LA. EPANET 2: User's Manual. U.S. EPA. Cincinnati; 2000.

[29] Nazari A, Meisami H. Instructing WaterGEMS Software Usage. ((INRC) D of P and TA of INRC, ed.). Tehran; 2008.

[30] ITA. Allievi. 2010. www.allievi.net. Universitat Politècnica de Valencia.

[31] Pérez-Sánchez M, Sánchez-Romero F, Ramos H, López-Jiménez P. Modeling Irrigation Networks for the Quantification of Potential Energy Recovering: A Case Study. Water. 2016;8(6):1-26. doi:10.3390/w8060234.

[32] Pérez-Sánchez M, Sánchez-Romero F, Ramos H, López-Jiménez P. Calibrating a flow model in an irrigation network: Case study in Alicante, Spain. Spanish J Agric Res. 2017;15(1): e1202. doi: 10.5424/sjar/2017151-10144.

[33] Pérez-Sánchez M, Sánchez-Romero F, López-Jiménez P. Water-Energy nexus. Energy optimization in water distribution system. Case study "Postrasvase Júcar Vinalopó" (Spain). Tecnol y Ciencias del Agua. (2007-2422): Submitted (30-03 - 2016).

[34] Pérez-Sánchez M, Sánchez-Romero F, López-Jiménez P. Energy footprint of water depending on consumption patterns. Rev Ing del Agua. (1134-2196): Submitted 10-01 - 2017.

[35] Pérez-Sánchez M, Sánchez-Romero F, Ramos H, López-Jiménez P. PATs' selection towards sustainability in irrigation networks: Simulated annealing as water management tool. Renew Energy. (0960-1481):Submitted 10-09 - 2016.

[36] Pérez-Sánchez M, López-Jiménez P, Ramos H. Modified affinity laws in hydraulic machines towards the Best Efficiency Line. Water Resour Manag. (0920-4741): Submitted 08-12 - 2016.

Appendices

Appendix I

ENERGY RECOVERY IN EXISTING WATER NETWORKS: TOWARDS GREATER SUSTAINABILITY

Author version document which was published in index JCR Journal "Water" ISSN 2073-4441. Impact Factor 1.687. Position 33/85 (Q2). Water Resources

Pérez-Sánchez, M., Sánchez-Romero, F., Ramos, H., López-Jiménez, P.A., 2017. Energy Recovery in Existing Water Networks: Towards Greater Sustainability. Water 9, 97-117. doi:10.3390/w9020097

This page is intentionally left blank.

ABSTRACT

Analyses of possible synergies between energy recovery and water management are essential for achieving sustainable improvements in the performance of irrigation water networks. Improving the energy efficiency of water systems by hydraulic energy recovery is becoming an inevitable trend for energy conservation, emissions reduction, and the increase of profit margins as well as for environmental requirements. This paper presents the state of the art of hydraulic energy generation in drinking and irrigation water networks through an extensive review and by analyzing the types of machinery installed, economic and environmental implications of large and small hydropower systems, and how hydropower can be applied in water distribution networks (drinking and irrigation) where energy recovery is not the main objective. Several proposed solutions of energy recovery by using hydraulic machines increase the added value of irrigation water networks, which is an open field that needs to be explored in the near future.

Keywords: irrigation water networks; water-energy nexus; renewable energy; sustainability and efficiency; hydropower solutions; water management

1. Hydropower Generation

Society's energy consumption worldwide has increased by up to 600% over the last century. This increase has been a direct result of population growth since the industrial revolution, in which energy has been provided mainly by fossil fuels. Nevertheless, today and in the near future, renewable energies are expected to be more widely implemented to help maintain sustainable growth and quality of life and, by 2040, to reduce energy consumption down to the 2010 levels [1]

Sustainability must be achieved by using strategies that do not increase the overall carbon footprint, considering all levels of production (macro- and microscale) of the different supplies. These strategies' development has to be univocally linked to new technologies [2]. Special attention must be paid to those new strategies that are related to energy recovery. These new techniques have raised interesting environmental and economic advantages. Therefore, a deep knowledge of the water-energy nexus is crucial for quantifying the potential for energy recovery in any water system [3], and defining performance indicators to evaluate the potential level of energy savings is a key issue for sustainability, environmental, or even management solutions [4].

Energy recovery, with the aim of harnessing the power dissipated by valves (in pressurized flow) or hydraulic jumps (in open channels), is becoming of paramount

importance in water distribution networks. Recovery will allow the energy footprint of water (*i.e.,* the energy unit cost needed to satisfy each stage of the water cycle: catchment, pumping, treatment, and distribution) to be reduced, even considering that energy generation is not a priority for these systems [5–7], although this recovery contributes to the development of more sustainable systems. This production could also contribute to the exploitation costs reduction in these systems, increasing the feasibility of drinking and irrigation water exploitation.

Among all of the different types of renewable energy (*e.g.,* photovoltaic, solar thermal, tidal, and wind), the hydropower plant stands out for its feasibility. Historically, large installations can be found in dams around the world to take advantage of the potential energy created by different water levels. The most important hydropower plants are located in countries such as China, the United States, Brazil, and Canada. Currently, China has the greatest installed capacity (exceeding 240 GW), with production greater than 800 TWh in 2012 and an average growth of capacity of 20 GW/year [8]. In Brazil and Canada, hydropower plants represent 84% and 56% of the total energy consumption, respectively. The production of this type of energy in these countries reaches 16% of the total consumed energy [9,10]. Figure 1 shows the technical, economic and exploited potential on each continent.

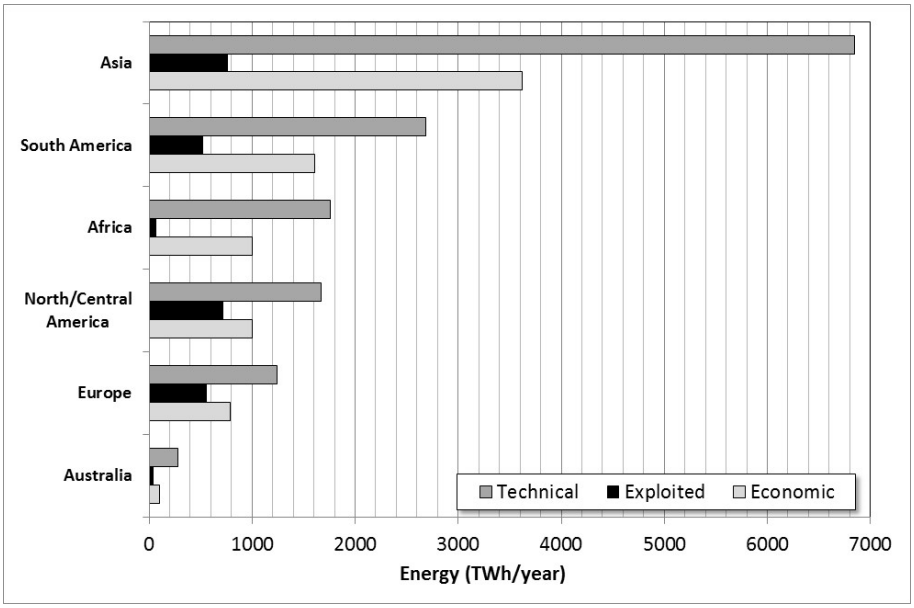

Figure 1. Worldwide hydraulic potential (adapted from [11])

Going further, Spänhoff [12] performed a worldwide projection of the installed capacity of renewable energy for the United States Energy Information Administration.

Hydropower has been the largest renewable source of energy in the period 2004–2010, and it will probably have the highest installed capacity in 2035. According to these forecasts, the installed capacity of hydropower will exceed 1400 GW. This installed capacity will be three times higher than that of wind energy and more than fifteen times greater than that of photovoltaic energy (Figure 2). The actual implementation of these renewable energy systems (solar and wind) in 2016 has been lower than the predicted values (Figure 2). The installed solar capacity is only 30% of the predicted capacity; the wind capacity is only 70% of the predicted value, and the hydropower capacity is approximately the value indicated in Figure 2 [13].

In Europe, renewable energy generation has increased by 96.17% in the period 2002–2013, with production equal to 2232.5 TWh in 2013 [14]. In this decade, the power produced by hydropower plants increased only 16.38%, but other sorts of energy (*e.g.,* solar, wind, and biomass) have experienced greater increases. For instance, in Spain, the increase in renewable energy generation was 152% in this period, but the increase was 73% for Spanish hydropower production.

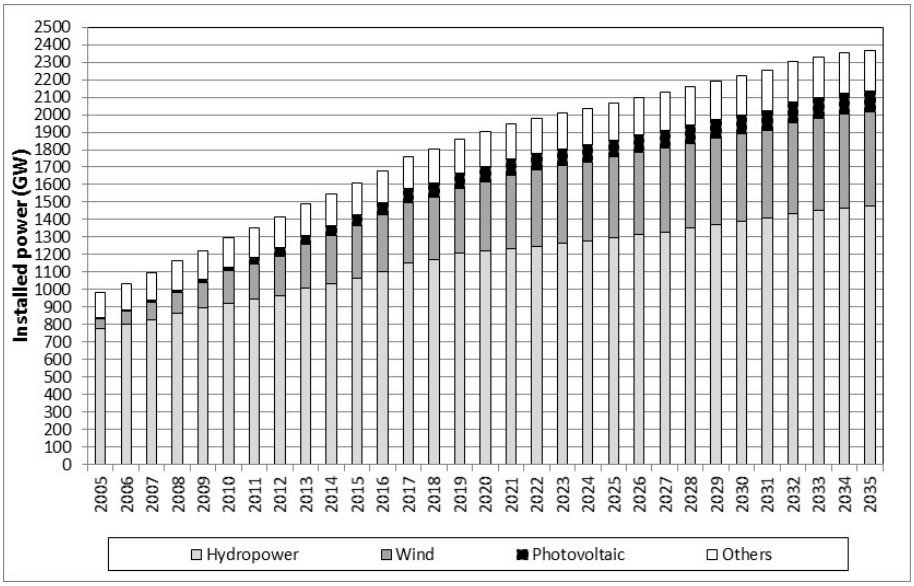

Figure 2. Trends for worldwide renewable energy (adapted from [13])

Considering all of these renewable energy systems, wind energy has increased by 477%, with a total generation of 53.90 TWh/year. Photovoltaic energy has increased by 4300%, producing 22.85 TWh in 2013 [14]. Nevertheless, the growth of hydropower production has been uneven due to the irregularity of rainfall in the Iberian Peninsula, although the trend is upward [15]. In Spain, the Institute for Energy Diversification and Saving estimated that the untapped generation potential of small hydropower is 1000 MW [16]. Therefore, the development of renewable energy has a promising future, if the potential

exploitation is considered. This promising development has positive aspects (*e.g.,* lower environmental impact and generation of stable electrical supply) compared to other renewable energies (*e.g.,* intermittent generation, such as solar or wind) [17]. In addition, this type of energy generation can be very important in the development of multipurpose water systems, where generation is another possible water use [18].

In the near future, part of the growth of hydropower production must come from the retrieval of potential energy embedded in water distribution networks. Considering the potential reduction of natural resources due to extensive agriculture or unsustainable water use on a global level, any investment in energy water recovery is crucial. Therefore, the whole water cycle must be included in the process of energy recovery, including both drinking and irrigation systems. This coupled water-energy nexus will allow the consideration of these systems as a new sustainable and efficient source of energy.

In this framework, the state of the art in the traditional field of hydropower (installed capacity) with a more advanced vision of the energy implications in drinking and irrigation systems is presented, considering the possibility of installing energy recovery in water distribution networks. The objective is to show the hydropower potential in water distribution networks. The installation of these systems will help increase energy efficiency. In the particular case of irrigation, improving the efficiency will allow the reduction of exploitation costs, decreasing pressure on the profit margin, as well as the environmental [19] and economic aspects [20].

2. Energy Recovery in Water Networks

Although there is not a consensus at the European level, the accepted demarcation between large and small hydro by the European Commission is whether the installed power capacity exceeds 10 MW [21]. When the installed capacity is below 100 kW, the generation system is called micro hydropower and when the generated power is below 10 kW, it is called pico hydropower.

2.1. Large Hydropower

Large hydropower in developed (20th century) and developing countries (*e.g.,* China, Brazil, and South Africa) in the early 21st century has been very large, with this generation system providing the main energy source in those countries where topography, hydrology and climatology allow hydropower recovery.

Although China began to develop its hydropower strategic plan in the 1950s, it has quickly overtaken other countries. Its development started with the Liujiaxia dam, which was completed in 1974 and has an installed capacity of 1250 MW. In 2012, China finished the Three Gorges Dam, which has a total installed capacity of over 20,000 MW. A project is currently being developed in the Yarlon Tsagpo Canyon with an installed capacity of over 40,000 MW, double the installed power in the Three Gorges Dam [8].

China has far exceeded the milestone achieved by the Hoover Dam (Colorado River, United States) in 1936, where 2000 MW were installed; or the 12,000 MW installed in the Itaipu Dam (Parana River, Brazil and Paraguay) in 1966, now with 14,000 MW. In Spain, up to 2013, the installed capacity is approximately 18,000 MW, and the hydropower installations do not exceed 400 MW on average.

Ansar [22] made an inventory of the 245 largest hydropower sites in the world (1934–2007). Among them, 72 are located in East Asia, 50 in Latin America, 40 in North America, 29 in Africa, 29 in Europe and 25 in South Asia. Of these, 97 dams are producing electricity, 89 are multipurpose (including hydropower) and 59 are devoted to irrigation and other uses. These plants are occasionally reversible to take advantage of the available volume of water, adjusting the electric energy injected to the grid according to the energy demand. Rehman et al. [10] established that the worldwide installed capacity of reversible plants is 104 GW (presently, the total installed capacity of hydropower is 1000 GW), of which 22.2 GW are installed in North America, 44 GW in Europe (5.3 GW in Spain), 33 GW in Asia, and the remainder in Africa and Russia. These authors refer to efficiencies between 70% and 80%.

Regarding environmental performance indicators of hydropower solutions, these plants have a positive impact on global climate change [23], based on the carbon footprint, which is the parameter used to determine the environmental impact, which has taken on special importance since the 1990s. This parameter is defined as the sum of the greenhouse gases emitted by an organization, event or product, expressed in terms of CO_2 equivalent units ($CO_{2\text{-}e}$) [24]. According to Zhang and Xu [25], the influence of the carbon footprint depends on many factors, most importantly the construction and maintenance costs (because these represent more than 60% in earthen dams and 50% in concrete dams) [9]. The range of emissions for these systems is between 2 and 240 $gCO_{2\text{-}e}$/kWh [9,26], with the carbon footprint in hydropower plants being smaller than that in coal plants. These non-renewable energy plants have emissions above 890 $gCO_{2\text{-}e}$/kWh [26–28]. Considering these emissions, hydropower plants saved 3.3 billion tons of CO_2 emissions in 2014 and will help reduce emissions by over 120 billion tons between 2015 and 2050 [13] compared to coal plants.

Regarding the economic aspects of large hydropower, the investment ratio (€/kW) decreases as the installed capacity increases, reaching values from 2170 to 470 €/kW for power ranges between 200 and 1400 MW [29,30]. Civil works represent between 70% and 80% of the total investment, and the remaining costs are devoted to electro-mechanics and hydraulic equipment [10].

2.2. Small Hydropower

The expansion of these installations was due to the development of the Francis turbine (for medium heads) [31], contributing both to the reduction of greenhouse gases and to the establishment of electrical service in remote rural areas or consumption points located away from supply points. This ‘social contribution’ should be taken into account

in viability studies in developing countries. As in large hydropower, the leading countries in small hydropower energy are China, Brazil, India, Canada, and some European countries. In 2013, China had a total installed capacity above 80 GW, which supplied more than 650 rural areas [8], with a range of installed power between 0.5 and 10 MW in each plant [32]. Brazil had 397 power plants in operation in 2011, with an installed capacity of 3.5 GW. Currently, the potential capacity is equal to 25.9 GW [33]. The United States Department of Energy tabulated more than a half million sites, with an installed potential of 100 GW [34], representing 10% of the current generation in the United States.

Currently, Australia has 60 small hydropower plants with a total installed capacity of 0.15 GW, which is 10% of the potential capacity. Australian Administration has projected three new plants with an installed capacity of 20, 8.4, and 7 MW, which will be developed in the future [35]. In India, the potential capacity is 15 GW, of which 2.4 GW are currently installed in 674 plants, with an expected increase of 9.4 GW in 2017 [36]. Ushiyama [37] established an installed power capacity of 30 GW for Japan in 2010, where small hydropower was practically non-existent. However, Japan has already started to develop projects in remote areas with a rate of capacity installation greater than 300 MW per year, with an installed power and potential capacity in the near future of 3.52 and 6.82 GW, respectively [38]. Across the African continent, small hydropower is also being developed in rural zones, where these plants are generating significant social benefits with a lower installed capacity of 300 kW [39].

According to the European Small Hydropower Association (*ESHA*), the total installed capacity in 2005 was 12.4 GW, of which six European Union members (Italy, France, Spain, Germany, Austria, and Sweden) in addition to Switzerland and Norway possess more than 90% of the installed capacity [40]. Alonso-Tristán *et al.* [41] presented the distribution of the small hydropower installed in Spain using data from Red Eléctrica de España (*REE*). This country represented 23.1% of the hydropower generation in European small hydropower in 2008 [42]. The potential growth in installed power capacity is 10 GW, with an annual production above 38,000 GWh [30], and the installed power will reach 17.3 GW (an increment of 39.51%) [41] in the period 2005–2020, as depicted in Figure 3.

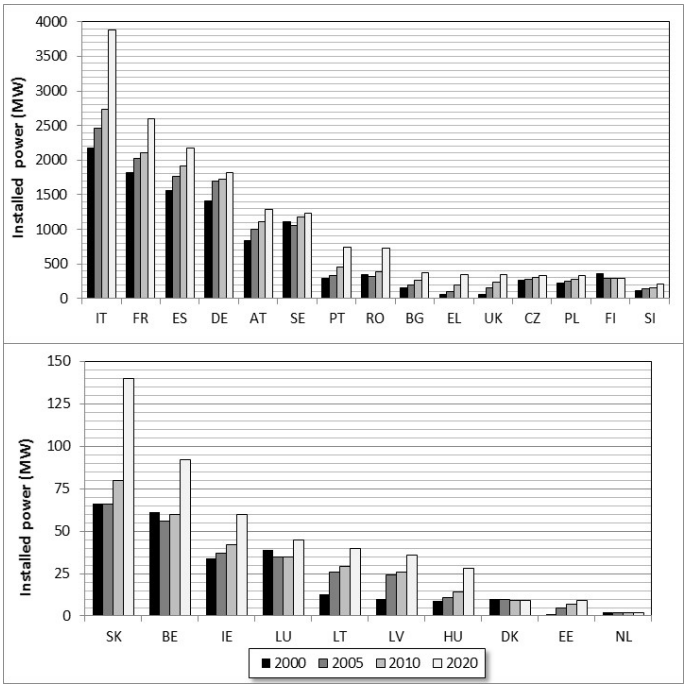

Figure 3. Planned installation of small hydropower capacity in 2005–2020 by European Union countries (adapted from [40])

Small hydropower has several advantages: less negative impacts than large hydropower and available potential to increase renewable energy production. ESHA estimated an annual reduction of 29×10^6 tonnes of CO_2 as a result of the 13 GW installed capacity in Europe [43]. Amponsah *et al.* [44] analyzed different values of the carbon footprint of small hydropower and established a range between 2 and 74.9 $gCO_{2\text{-}e}$/kWh based on the installation and the type of plant. In the particular case of micro-hydropower, Gallagher *et al.* [45] analyzed the carbon footprint of three plants with installed capacities of 15, 90 and 140 kW. The results of this analysis were 2.14, 4.39, and 2.78 $gCO_{2\text{-}e}$/kWh, respectively. These values emphasize the positive environmental impact of hydropower solutions.

Regarding economic aspects, Kosnik [34] developed an economic analysis based on several small plants, obtaining a non-linear relationship between the cost of implementation and installed power (small, micro or pico). Ogayar and Vidal [46] also analyzed the distribution of costs for small hydropower, which are distributed among civil work (40%), turbine (30%), electro-mechanical and regulation equipment (22%), and construction management (8%). This type of renewable energy project is viable when the required investment is below 2000 $/kW [47], although special attention should be paid to the environmental and social benefits provided by these installations. At the

European level, according to the General Direction for Environment, the average cost of investment for plants with an installed capacity below 10 MW is between 2941 and 4072 €/kW, depending on the characteristics of the system (*e.g.,* flow, head, orography) [40]. Mishra *et al.* [48] proposed formulas that use the turbine, installed power capacity, and net head to estimate the required investment. These expressions can be used to determine the associated costs.

Finally, the classification of these installations is referenced in European legislation [47] according to the installed power. However, other classifications have been proposed that depend on the type of plant from an operational point of view [16,49,50].

1) Power plant in flow or run-of-river: This system has no regulation reservoir and only takes advantage of the hydraulic head when the flow circulates. In mountain areas, with medium heads, the flow is diverted through a weir and a penstock carries the flow to the power house. If the topography does not allow it, the hydraulic head must be created by building a higher dam.

2) Power plant at the foot of a dam: The flow is regulated by a reservoir. In the case of small hydropower, reservoirs or dams are used to ensure project viability.

3) Power plant in water distribution network: The distribution network is used to take advantage of available pressure or kinetic energy, depending on the system characteristics.

2.3. Type of Hydraulic Machines

Hydraulic machines are classified according to the system (pressurized or open channels) in which they are installed (Figure 4). In open channels, all types of hydraulic wheels have been traditionally used to take advantage of waterfalls. According to the type of energy used (potential, pressure, or kinetic), the machines are classified as gravitational, hydrostatic, or kinetic. Gravitational machines take advantage of different water levels to extract energy from the flow (*e.g.,* Archimedes screw or waterwheel). Hydrostatic machines operate by the difference of hydrostatic pressures on both faces of a blade (*e.g.,* hydrostatic pressure wheel). Finally, if a wheel uses the velocity of the flow to move the axis of the machine, this type of machine is called a kinetic machine. There are many different types of kinetic machines (*e.g.,* helical turbine with vertical or horizontal axis, overshot wheel, and ducted turbine) [51].

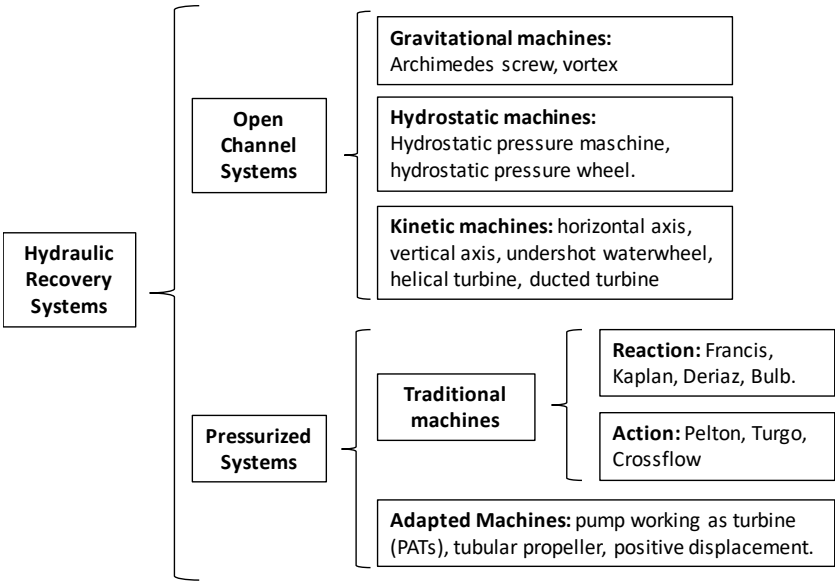

Figure 4. Classification of hydraulic machines

In pressurized water systems, the most frequently used machines can be grouped into traditional machines (which are categorized as action and reaction machines) and adapted machines. The last group includes hydraulic machines that normally work not as turbines but as pumps. In reaction machines, the hydraulic power is transmitted to the axis of the machine by varying the pressure flow between the inlet and outlet of the impeller, which depends on the specific speed of the machine (*e.g.,* Francis and Kaplan). In action turbines, the energy exchange (hydraulic to mechanical) is carried out at atmospheric pressure, and the hydraulic power is due to kinetic energy of the flow (*e.g.,* Pelton and Turgo).

These types of machines are used in large and small hydropower, depending on the nominal flow and the available head (Figure 5).

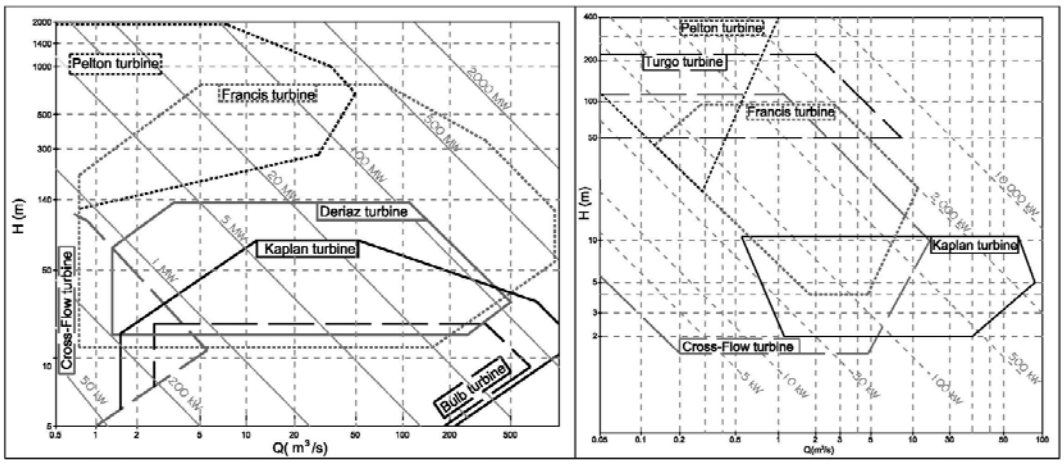

Figure 5. Selection of turbine depending on head and flow in: large (left); and small (right) hydropower [16,31]

Currently, most of the turbines installed for large hydropower are Pelton, Francis, Kaplan, or Deriaz turbines [31]. These turbines present different performance curves, which depend on their specific speed and discharge number [21,52]. Gordon [53] analyzed both the efficiency of 107 turbines that had been installed since 1908 and the increase in efficiency obtained with replacement impellers in 22 power plants, evaluating the improvement in the performance of propellers over time. Increases in the performance of the machines were obtained, rising from efficiencies lower than 50% in 1920 to above 96% in some current cases.

Regarding hydraulic machines installed for small hydropower, Paish [47] established the efficiency of these machines according to the type and head ratio. The efficiency has values of approximately 90% for Pelton turbines over a wide head ratio (0.2–0.8). In crossflow turbines, the values of efficiency are close to 80% for a head ratio (0.2–1). Francis and propeller turbines present efficiencies of approximately 85% for a head ratio (0.9–1).

The development and improvement of large and small hydropower systems have allowed the adaptation of the machines to water distribution networks, establishing the group called ‘adapted machines’ (Figure 4). This group of machines is used in micro and pico hydropower plants. Pump as turbine (*PAT*) [54], tubular propeller [55], and positive displacement machine [56] are included in this group (Figure 6).

Figure 6. Hydraulic machines at IST-Universidade de Lisboa: *PAT* (left); and tubular propeller (right)

This group of machines can be installed in places where energy is currently dissipated for specific flow and pressure operating conditions. These conditions mainly depend on user demand and the minimum pressure required (when the machine is installed in a pressurized water network). The existing demand establishes the circulating flow over time in the line, whereas a required pressure establishes the maximum recovered head. In pressurized water networks, the excess of energy is dissipated with pressure reduction valves. In open channel flows, this dissipation of energy is carried out by means of hydraulic jumps. In micro and pico systems, conventional machines can be installed according to installed power and head characteristics (*e.g.,* micro Francis, Pelton, Turgo, and Cross-Flow), but the high investment cost makes the installation not viable.

In 1931, Thoma [54] implemented the first pump working as a turbine (*PAT*). Later, other authors presented more research that presented the description, operation, performance, and theoretical model of these machines [57–64]. *PATs* are normally used in pressurized water networks but they can also be used in open channel flows when complementary civil works are carried out to adapt to *PAT* operating conditions. These machines present a high range of flow and head for installation according to the typology of the machine (Figure 7). The best efficiencies vary between 40% and 70% as a function of the specific speed [58].

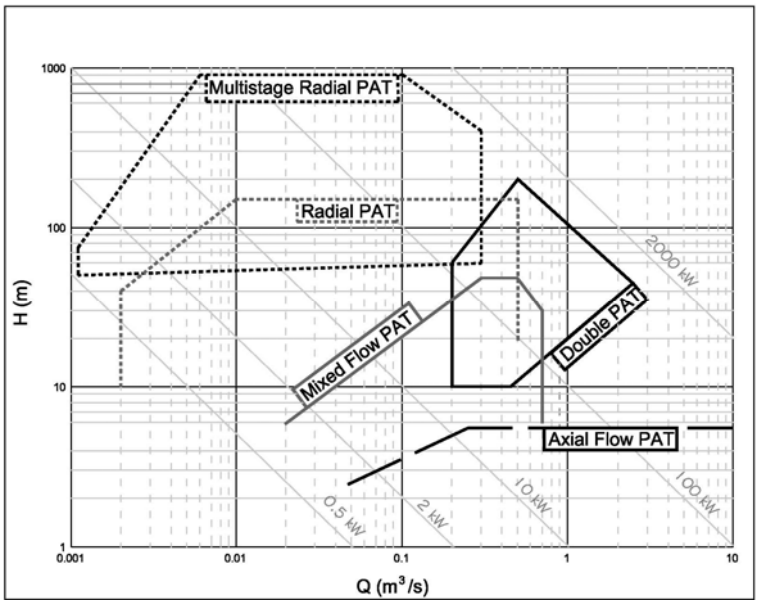

Figure 7. Range of application of PATs (adapted from [54])

PATs become the technological solution to efficiently recover energy in water distribution networks. The main advantage of these machines is their immediate availability for installation and lower cost compared with conventional machines. Nourbakhsh and Jahangiri [65] established that the payback period of these machines is less than two years for installed capacities between 5 and 500 kW. These payback values make micro generation in water distribution networks feasible.

Elbatran *et al.* [64] listed the advantages of these machines in micro hydropower plants, such as a 50% reduction in the cost of the machine compared to a conventional turbine; the existence of a large availability of operating ranges depending on the hydraulic head and flow; simple management and operation; and a lifespan of twenty-five years. Furthermore, they have lower installation costs, which can improve the viability of small projects [60].

3. Micro and Pico Hydropower Solutions

3.1. Energy Recovery in Open Channel Networks

Micro hydropower can use different hydraulic heads or diversion schemes in small dams in rivers and ravines, in open irrigation channels and in drainage systems. Some examples of these systems can be found in several regions, such as the western part of the Himalayas [66], Bangladesh [67], Nigeria [68], Laos [69], Europe [41], or Lithuania [70]. Although it might seem that the development of these hydropower plants has been

recent, this is not true because watermills were present in all continents many years ago, were fundamental to moving other machines in the Industrial Revolution, and can still be found operating in some countries (*e.g.,* United Kingdom, France, Spain, USA, Africa, and part of Asia) [71,72]. This technology is currently essential to generate electrical energy in rural areas and to support the social and economic development of these isolated regions.

Water wheels can also be used in other open channel flows. For example, these solutions can be located in water treatment plants. These elements can also be installed in urban infrastructure, where energy recovery systems are established to reduce the energy footprint of urban water systems [73]. In these facilities, Ramos *et al.* [28] proposed the use of an urban storm-water drainage system to take advantage of storm retention ponds and to develop energy recovery systems using the rain storage volume. This solution contributes a new source of clean energy, which is involved with the water drainage system. An example of energy recovery is analyzed by Novara *et al.* [74] in a wastewater treatment plant in the city of Asti (Italy). The flow in this channel oscillates between 0.07 and 0.83 m^3/s, while the available head changes between 0.062 and 0.744 m w.c.. With these values, a hydrostatic pressure machine (*HPM*) is proposed to be installed. This wheel is an experimental waterwheel specifically designed for application in open channels with reduced head, developed and improved by Senior *et al.* [75], patented by Austrian inventor Adolf Brinnich, and tested under the *HYLOW* project as part of EU's Seventh Framework Program between 2008 and 2013 [76]. If the energy balance is carried out, the maximum electrical power is approximately 650 W with a flow equal to 0.29 m^3/s, for a daily power of 10.9 kWh. In these conditions, 48% of the hydrostatic energy is converted into electrical power, 40% is mechanical loss, and 12% is electrical loss in the generator and transmission.

Similarly, in open channel irrigation systems, energy recovery can also be implemented by installed turbines in small dams or irrigation reservoirs [77,78]. An example of these installations is the analysis made by Butera and Balestra [79], who determined the potential generation by hydropower plants for the Piedmont region (Italy). This region has an installed capacity of 46 MW, of which 45% is pico hydropower, 49% is micro and 6% is small, with an average hydraulic potential of 1.5–2 kW/ha. Tarragó *et al.* [26] developed a preliminary study in the Alqueva's irrigation system, where twenty-two hydrostatic pressure machines were studied in different locations with hydraulic heads below three meters. Using this assumption, the theoretical energy recovery reached 406.64 MWh/year in 67,932 ha of this region.

3.2. Energy Recovery Water Pipe and Irrigation Systems

Currently, energy recovery in pressurized water distribution networks (both urban or irrigation water supply) has great significance. Relative to urban supply systems, the energy consumption in water supply networks represents 7% of the world's consumption of energy [80]. Water distribution involves an energy footprint between 0.18 and 0.32

kWh/m^3, according to the California Energy Commission [81]. In addition to energy consumption, energy analysis of these networks has shown that an increase of pressure is correlated with increased leakage [82]. This problem justifies the installation of pressure reduction valves (*PRVs*) in many water distribution networks. These valves reduce pressure and, therefore, leakage volume. This directly proportional correlation between leakage and pressure caused the pioneering study of alternatives to leverage the dissipated energy by *PRVs* in water supply systems [57]. An unconventional solution was considered: replacing *PRVs* by *PATs* [57,59]. Ferracota *et al.* [60] studied leakage reduction. They presented and integrated a new technical solution with economic and system flexibility benefits, replacing pressure reduction valves by pumps used as turbines (*PATs*). The optimal operating point of the *PATs* was selected by using a variable operating strategy. Carraveta *et al.* [63] established a *PAT* operating scheme with a *PRV* in parallel. This operating scheme and the variability of flows over time in network pipelines due to user demand have fostered leading studies to develop variable operating strategies in these machines. These strategies allow the variation of the rotational speed of the hydraulic machine [83,84]. Ferracota *et al.* [85] have begun studies to improve efficiency prediction in the machine through experimental tests in semi-axial machines when the rotational speed varies. Preliminary studies in drinking water systems have been developed through computational simulations [59,60,86]. These studies considered average flows or hourly uniform patterns in all consumption joints for the development of simulations of water supply networks [87,88]. These energy recovery studies have promoted the use of water supply networks to generate clean energy, using the dissipated energy in *PRVs* [91]. These studies have resulted in some pilot installations emerging for evaluation (*e.g.,* Murcia (Spain) [89], Portland (Oregon) [90], Hong Kong [91], and Kildare (Ireland) [92]).

In addition to water supply systems, water irrigation networks are very important for the improvement of energy efficiency in the water cycle. Worldwide water consumption is 3 925 km^3/year [93], which is distributed such that 69.53% of water is used for irrigation, 18.70% is used for industry, and 11.77% is used for drinking water systems. In Spain, water consumption is distributed as follows: 80% for irrigation, 15% for drinking, and 5% for industry. The annual volume used for agriculture equals 16 344 hm^3 [94].

Hence, because the volume of water consumed for irrigation is higher than in urban systems, the modernization of irrigation should not only be associated with high technology and automation but also with water management that accounts for the sustainability of this infrastructure. The study of the installation of micro and pico hydropower is necessary because the irrigated surface area is huge (approximately 324 million hectares in the world are provided with irrigation installations, of which 86% are gravity irrigation, 11% sprinkler irrigation and 3% drip irrigation [95]). In Spanish economic terms, the irrigation water distribution cost was €1285 million in 2012. This value represents 20% of the total cost of the water supply service in Spain [96], considering that the irrigated surface area in Spain is 3.54 million hectares (1.09% of the worldwide irrigated area) [97].

Therefore, if the annual volume of water consumed in irrigation networks worldwide is measured, the development of systems to reduce the energy consumption is of the utmost importance. These new solutions should also try to improve, as much as possible, the environmental and economic sustainability of irrigation, considering that the modernization of irrigation water systems introduces an average increase of installed power equal to 2 kW/ha [98].

3.3. Strategies for Sustainability and Energy Efficiency in Pressurized Water Networks

3.3.1. Pumped Water Systems

Pumped water systems have been analyzed by different authors [99–103] whose main objective has been to minimize the energy costs. Rodriguez-Diaz *et al.* [99] proposed a new methodology with energy savings between 10% and 30% in real case studies, considering the most critical consumption points, which depend on needs and location. Moreno *et al.* [100] developed a methodology in which characteristic and efficiency curves are optimized depending on the recorded flows, obtaining a 32.33% average reduction of installed power in the studied networks.

In other research, energy reduction has been carried out using strategies to minimize energy consumption through optimal operating schedules, reducing energy footprints by 36.4% [101,102]. Costa *et al.* [103] presented a general optimization routine integrated with *EPANET* [104]. This routine allows the determination of strategic optimal rules of operation for any type of water distribution system. Cabrera *et al.* [105] developed a methodology to carry out an energy audit, which detects weaknesses in pressurized water networks. This methodology is applied in a real case, obtaining energy savings above 40%. In all of the cited cases, energy savings correspond to an economic reduction between 35% and 50% of the energy costs. Ferracota *et al.* [60] integrated a new technical solution with economic and system flexibility benefits, which replaces pressure reduction valves by pumps as turbines. In the majority of methods, when energy optimization is carried out in pumped water systems, the objective is easily defined as minimizing the energy consumption, with the solution being the establishment of optimized irrigation schedules according to the minimum necessary pressure and irrigation needs at each consumption point.

3.3.2. Gravity Water Systems

If an irrigation network is a gravity system, the best solution is not to convert an on-demand water irrigation into a scheduled network because this decision can irritate farmers, and reduce their operational freedom. Therefore, if a water manager wants to increase the system sustainability and energy efficiency of a network by the installation of energy recovery systems, the manager should know the flow distribution over time. The analysis of water distribution systems allows the establishment of some crucial

aspects of the recovery system, such as the type of hydraulic machine, the best efficiency point (*BEP*) and the range of operating conditions for the energy converters [64].

Preliminary values of recoverable energy have been obtained using average circulating flows for both irrigation [26] and water supply networks [106] in some studies. The authors have used daily patterns in these studies. To analyze the variation of flows over time, Pérez-Sánchez *et al.* [107] developed a new methodology to estimate the hourly circulating flows in any line based on the opening probability of the irrigation points, which depends on farmers' habits (*i.e.,* irrigation duration, maximum days between irrigation, weekly irrigation trend, and irrigation start). This methodology can also be used in water supply networks when behavioral patterns are known. These demand patterns allow the water network to be simulated and the energy balance to be calculated to determine the percentage of energy dissipated by friction losses, the energy necessary for irrigation, the non-recoverable energy, and the theoretically available energy. In the case of Vallada (Spain) [107], the energy dissipated by friction is approximately 4.10% of the provided energy (with a maximum energy footprint of 2.85 kWh/m^3), with the theoretical recoverable energy in the network equal to 68.70%, when all of the irrigation points are considered elective places of recovery.

The feasibility of an energy project is not guaranteed when a high number of machines is installed in the network; thus, an analysis of the water network is needed to maximize the energy recovery. Samora *et al.* [108] developed a methodology that uses simulated annealing to maximize recovered energy in a water supply network [109]. This methodology selects the lines depending on the recovered energy, and considering the feasibility of the facilities according to an economic criterion. For these preliminary studies of feasibility, Castro [16] proposed a simple economic balance where the payback period is only determined through the investment cost, incomes and maintenance cost, which depend on the installed power. In an advanced or existing project, other more complex and detailed methods can be used, which consider the annual interest and the inflation rate [110,111].

Therefore, if the feasibility is studied, knowledge of the performance and head curves as functions of the flow in the selected machine is necessary to determine the real recovered energy. The proposed *PAT* curves by Rawal and Kshirsagar [112] and Singh [113] (Figure 8) can be used in the analysis to help select a *PAT*. These curves allow the impellers' diameter to be selected as a function of the specific rotational speed (n_s), the discharge number (φ), and the head number (ψ). These parameters are defined by Equations from (1) to (3) [24]:

$$n_s = N\frac{\sqrt{P_R}}{H_R^{1.25}} \quad (1)$$

$$\varphi = \frac{Q}{ND^3} \quad (2)$$

$$\psi = \frac{H}{N^2D^2} \quad (3)$$

where N is the rotational speed (rpm); P_R is the rated power (kW); R is the pump design point or the best efficiency condition; H_R is the rated head (m w.c.); Q is the circulating flow (m^3/s); H is the recovered head of the machine (m w.c.); and D is the impeller diameter (m).

If the previous premises are used, different studies have been developed in water systems (irrigation and drinking networks), considering strategies to maximize the energy efficiency. In the particular case study of Vallada (Spain) [107], where the annual water consumption is 930 000 m^3/year, the actual recovered energy is 26.51 MWh/year. This recovery represents 9.55% of the energy provided to the network, with a simple payback period of 5.28. In a preliminary study of Alqueva (Portugal) [26], the theoretical energy recovery is at least 2.12 MWh/year in 68 ha of pressurized irrigation, for a water consumption of 179 000 m^3/year.

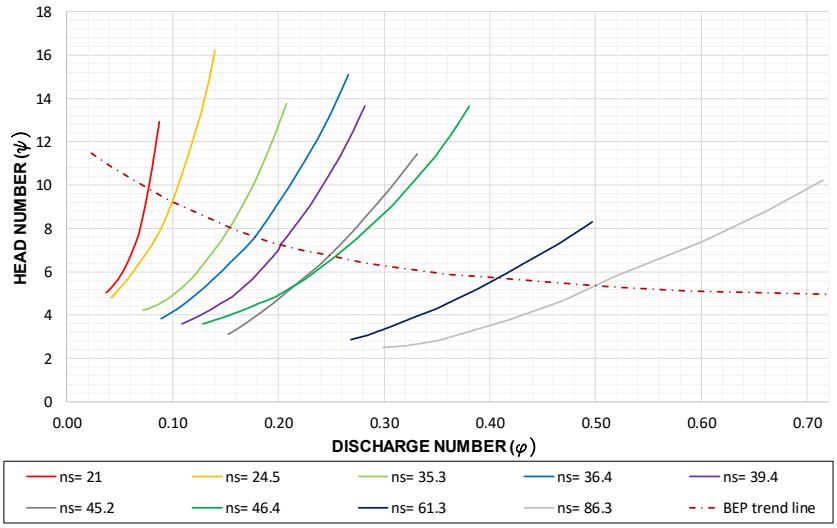

Figure 8. Head number depending on the discharge number (adapted from [112,113])

In water supply systems, a case study of Lausanne (Switzerland) [106] finds that the real recovered energy represents up to 5% of the available energy. In a case study of Fribourg in the same country, the recovered energy reaches 10% of the available energy [114]. Another energy study developed in collaboration with the Consortium of Commons for the Monferrato Aqueduct (Italy) [74] determines an energy recovery equal to 9585 kWh/year when the pressure reducing valve is replaced by a *PAT* with a constant flow of 7 l/s and head of 75 m w.c.. These examples show the importance of this type of solution for economic and environmental sustainability in water systems, if similar solutions are implemented.

From the economic point of view, the benefits of selling energy and generating income can be quite significant in some cases (although this generation is irregular over time because it depends on the flow, which varies as a function of consumption in water networks). Some particular analyses of these systems (and, more specifically, of *PATs*) present payback periods less than five years, with an installed capacity between 5 and 500 kW [8]. However, the importance of these solutions consists in the generation of energy for self-consumption by the local communities, i.e., for extracting water from their own water wells, electric supply in irrigation communities, or individual use at the irrigation points, avoiding investment in the electric grid.

From the environmental point of view, the use of these renewable energy sources reduces the emission of greenhouse gases when they are compared with non-renewable energy (*e.g.,* fuel, usually used in electric generators installed in irrigation communities or irrigation points). Therefore, these recovery systems can supply the users' demand for low energy consumption in their facilities. Regarding the environmental added value, the theoretical reduction of CO_2 emission is 216.2 t/year in Vallada's network.

The development of studies to install energy recovery in pressurized water networks (mainly in supply systems) has been important, as previously discussed. The development of these studies has focused on the use of non-conventional hydraulic machines to generate energy and on energy analyses using different installation schemes for these machines. Table 1 summarizes the current development of small energy recovery in pressurized water supply networks.

Table 1 shows different topics related to *PATs* that have been studied by different authors. The description, operating mode, characteristic curves (theoretical and experimental), and simulations (for hourly uniform patterns in all consumption joints) of *PATs* have been developed, enumerating the advantages (such as good efficiency values and low price) and limitations. The main limitations are lower efficiency when the system operates with oscillating flows and the irregular generation of energy due to variable flow, which hinders both sale and self-consumption.

Table 1. Analyzed topics related to recovery systems in water supply networks

Analyzed Topic	Reference
First *PAT*	[54]
Reduction of leaks, decreasing the pressure in water supply systems and increasing the efficiency	[57,60,80,82,84,87]
Proposal to use adapted machines (*PATs* and tubular propeller) in water supply systems to reduce the pressure	[55,57]
Description and operation of a *PAT* with a review of available technologies	[56,64,67,75,76]
Performance and modeling *PAT*	[56,58,61,65,85]
Installation of recovery systems in water supply networks	[59,79]
Implementation of simulations to determine the theoretical recovered energy in water supply and irrigation systems	[26,74,77,86,106–108]
Design of variable operating strategies to maximize the recovered energy	[59,60,62,84]
Economic cost of implementing recovery systems in water supply and irrigation networks	[8,16,64,84]
Environmental advantages	[66,78,88]
Policies and analyses to help the development of rural areas	[41,58,68–72]
Pilot plants built in water supply networks	[89–92]
Optimization to maximize recovered energy in water supply systems	[106]

The development of different research is necessary to solve the previously cited limitations. Future work should focus on obtaining better knowledge of recorded flows over time in any line; improving the variable operating strategies to adapt the rotational speed of machines in each time step; and developing sustainable and feasible electric systems (grid connection or stand-alone operation). These electric systems will increase the viability of selling the energy to the national grid or using it for self-consumption.

4. Conclusions

There are several related scales for the management of the hydraulic energy generation, including local, regional, national and international, when considering water as a resource. However, even today, energy recovery is a very attractive possibility in water networks, with small additional costs for managers and investors. The success of this novel use depends on the experience acquired in hydropower plants with higher installed power.

A deep review has been presented, analyzing the different alternatives for hydropower production from large to pico facilities, according to the production levels, the economic and the environmental points of view, as well as the classification of the hydraulic machines. Considering the evolution of these energy solutions, energy recovery in water distribution networks is an alternative for the development of systems towards more sustainable and efficient solutions. Technological, economic and environmental implications of hydropower systems for energy recovery around the world have to be considered. Despite the large list of references, only a few can be related to agricultural water network energy recovery because this subject has not yet been explored.

Analysis of the references cited in this document establishes that recovery systems in pressurized water networks are:

1) Recovery systems with less installed power, called mini and pico hydropower plants. These energy recovery systems appeared due to the need to replace waste or non-renewable energy devices with renewable energy solutions. The building of large hydropower plants has been maximized in different developed countries and the development of new large hydropower plants is currently limited due to environmental and social factors. However, the experience in these facilities (*i.e.,* large and small hydropower) has contributed to the development of new recovery systems in pressurized water networks. The most important transfer has been advances in possible recovery machines and improvement in the efficiency of impellers and in water pipe systems as a whole.

2) The description of machines used in different hydropower plants (*i.e.,* pressurized and open channel flows) has shown that on the one hand, classical machines cannot directly be used or scaled to pico hydropower plants because the adaptation of flow and head presents some difficulties in terms of viability. In contrast, similar or adapted machines can be developed based on classical machines (*e.g.,* Francis turbine vs. radial and mixed *PATs*; axial turbine vs. tubular propeller or axial *PATs*). The development of new adapted machines and improvement in the efficiency of the current ones are fundamental challenges for increasing the installation of recovery energy systems in water pipe networks in the near future.

3) For energy recovery in pico hydropower plants, the *PAT* is currently the most successful machine to be adapted to these systems, according to previous studies and installed pilot plants. The main positive aspects of these machines are that: (i) the installation of a *PAT* allows the replacement of a *PRV* to dissipate excess flow energy; (ii) the *PATs*' efficiency values vary between 0.40 and 0.70, operating in reverse mode; (iii) theoretical studies can be developed with the current technology (*e.g.,* computational fluid dynamics (*CFD*)) based on the classical theory of hydraulic machines (*i.e.,* Euler's Theorem), for comparison with existing experimental tests; and (iv) they have low investment costs and a high number of available machines. These advantages allow the installation of these machines in

water pipe systems to be promoted. The main aspects negative of *PATs* are related to their low efficiency when operating outside their best efficiency point. Operation with different flows can be solved by the development of new regulation techniques (*e.g.,* variable operation strategies (*VOS*)) with electronic regulation. The positive resolution of this aspect is a crucial point for expanding use of *PAT*s in water distribution networks. Issues related to the use of the generated energy for self-consumption may include storage in batteries and integrating this renewable energy in a similar manner as other supplementary sources (*e.g.,* solar and wind).

4) Different case studies have been developed using specific software (*e.g., EPANET* and *WaterGEMS*), which have been combined with optimization methodologies to maximize the recovered energy. Future simulations should take into account the integration of *VOS* as well as the variation of the machine efficiency with the rotational speed. These simulations should consider discretized demand over time to improve the analyzed energy values because the majority of studies only consider the mean demand value or modulation curves. The development of a specific methodology to determine this variation of flow over time in water supply networks is crucial to improve the fit between theoretical and real values of recovered energy. Regarding the software used, it is necessary to implement operation rules for these machines in specific algorithms. This implementation is the key point in the development of optimized techniques, making possible studies similar to those with water pump systems. The primary need is for correct machine selection and establishment of the rotational speed as a function of the flow, maintaining the maximum efficiency at each operation point of the machine.

Therefore, hydraulic recovery in water networks is a real and necessary alternative to improve the energy efficiency of the whole system. By means of implementing energy converters, the energy efficiency will be increased and operating costs will be reduced (*i.e.,* the energy footprint of water). The implementation of these systems will essentially depend on the physical characteristics of the systems. The orography, topology, and volumes of water consumed establish the economic viability of these recovery strategies in water distribution networks. When the investment analyses are developed, recovery systems have acceptable values of economic feasibility indexes (*e.g.,* payback value and internal rate of return). A better understanding of the operation of each recovery system in terms of water-energy management is needed that considers the high global volume distributed in pressurized water networks (*i.e.,* drinking and irrigation) each year. This understanding will positively contribute to the sustainability and efficiency of near future recovery system applications.

Acknowledgments: No additional funds have been received for this research.

Author Contributions: All the authors have participated in any step of this research. Particularly a brief description is attached: Helena M. Ramos has contributed by

supervising the state of the art and revision of the whole paper. Francisco Javier Sánchez-Romero developed the study of large and small hydropower. Modesto Pérez-Sánchez wrote and analyzed the state of the art in water networks taking account the energy recovery. P. Amparo López-Jiménez supervised the whole research and she was involved in conclusions determination.

Conflicts of Interest: The authors declare no conflict of interest. The founding sponsors had no role in the design of the study, in the collection, analyses, or interpretation of data, in the writing of the manuscript, and in the decision to publish the results.

References

1. Pasten, C.; Santamarina, J.C. Energy and quality of life. *Energy Policy* 2012, *49*, 468–476.
2. Huesemann, M.H. The limits of technological solutions to sustainable development. *Clean Technol. Environ. Policy* 2003, *5*, 21–34.
3. Gilron, J. Water-energy nexus: Matching sources and uses. *Clean Technol. Environ. Policy* 2014, *16*, 1471–1479.
4. Emec, S.; Bilge, P.; Seliger, G. Design of production systems with hybrid energy and water generation for sustainable value creation. *Clean Technol. Environ. Policy* 2015, *17*, 1807–1829.
5. Fontanazza, C.; Freni, G.; Loggia, G.; Notaro, V.; Puleo, V. Evaluation of the Water Scarcity Energy Cost for Users. *Energies* 2013, *6*, 220–234.
6. Herath, I.; Deurer, M.; Horne D.; Singh R.; Clothier B. The water footprint of hydroelectricity: A methodological comparison from a case study in New Zealand. *J. Clean. Prod.* 2011, *19*, 1582–1589.
7. Mushtaq, S.; Maraseni, T.N.; Reardon-Smith, K.; Bundschuh, J.; Jackson, T. Integrated assessment of water–energy–GHG emissions tradeoffs in an irrigated lucerne production system in eastern Australia. *J. Clean. Prod.* 2015, *103*, 491–498.
8. Hennig, T.; Wang, W.; Feng, Y.; Ou, X.; He, D. Review of Yunnan's hydropower development. Comparing small and large hydropower projects regarding their environmental implications and socio-economic consequences. *Renew. Sustain. Energy Rev.* 2013, *27*, 585–595.
9. Zhang, S.; Pang, B.; Zhang, Z. Carbon footprint analysis of two different types of hydropower schemes: Comparing earth-rockfill dams and concrete gravity dams using hybrid life cycle assessment. *J. Clean. Prod.* 2014, *103*, 854–862.
10. Rehman, S.; Al-Hadhrami, L.M.; Alam, M.M. Pumped hydro energy storage system: A technological review. *Renew. Sustain. Energy Rev.* 2015, *44*, 586–598.
11. Paish, O. Micro-hydropower: Status and prospects. *Proc. Inst. Mech. Eng. Part A J. Power Energy* 2005, *216*, 31–40.
12. Spänhoff, B. Current status and future prospects of hydropower in Saxony (Germany) compared to trends in Germany, the European Union and the World. *Renew. Sustain. Energy Rev.* 2014, *30*, 518–525.

13. Hans-Wilhelm, S. *World Energy Scenarios—The Role of Hydropower in Composing Energy Futures to 2050*; World Hydropower Congress: Beijing, China, 2015; pp. 40–46.
14. Eurostat. 2015. Available online: http://ec.europa.eu/eurostat/tgm/refreshTableAction.do?tab=table&plugin=1&pcode=ten00081&language=en (accessed on 31 May 2015).
15. López-González, L.M.; Sala-Lizarraga, J.M.; Míguez-Tabarés, J.L.; López-Ochoa, L.M. Contribution of renewable energy sources to electricity production in the autonomous community of Navarre (Spain): A review. *Renew. Sustain. Energy Rev.* 2007, *11*, 1776–1793.
16. Castro, A. *Minicentrales Hidroeléctricas*; Instituto para la Diversificación y Ahorro de la Energía: Madrid, Spain, 2006. Available online: http://www.energiasrenovables.ciemat.es/adjuntos_documentos/Minicentrales_hidroelectricas.pdf (accessed on 10th September 2016).
17. Gaudard, L.; Romerio, F. Reprint of "The future of hydropower in Europe: Interconnecting climate, markets and policies". *Environ. Sci. Policy* 2014, *43*, 5–14.
18. Choulot, A. *Energy Recovery in Existing Infrastructures with Small Hydropower Plants*; FP6 Project Shapes (Work Package 5—WP5); European Directorate for Transport and Energy: Brussels, Belgium, 2010.
19. Huisingh, D.; Zhang, Z.; Moore, J.C.; Qiao, Q.; Li, Q. Recent advances in carbon emissions reduction: Policies, technologies, monitoring, assessment and modeling. *J. Clean. Prod.* 2015, *103*, 1–12.
20. Ihle, C.F. The need to extend the study of greenhouse impacts of mining and mineral processing to hydraulic streams: Long distance pipelines count. *J. Clean. Prod.* 2014, *84*, 597. http://dx.doi.org/10.1016/j.jclepro.2012.11.013
21. Ramos, H.M.; Almeida, A. *Small Hydro as One of the Oldest Renewable Energy Sources*; Water Power and Dam Construction; Small Hydro: Lisbon, Portugal, 2000.
22. Ansar, A.; Flyvbjerg, B.; Budzier, A.; Lunn, D. Should we build more large dams? The actual costs of hydropower megaproject development. *Energy Policy* 2014, *69*, 43–56.
23. Hamududu, B.; Killingtveit, A. Assessing Climate Change Impacts on Global Hydropower. *Energies* 2012, *5*, 305–322.
24. Chakraborty, D.; Roy, J. Energy and carbon footprint: Numbers matter in low energy and low carbon choices. *Curr. Opin. Environ. Sustain.* 2013, *5*, 237–243.
25. Zhang, J.; Xu, L. Embodied carbon budget accounting system for calculating carbon footprint of large hydropower project. *J. Clean. Prod.* 2015, *96*, 444–451.
26. Tarragó, E.F.; Ramos, H. Micro-Hydro Solutions in Alqueva Multipurpose Project (AMP) towards Water-Energy-Environmental Efficiency Improvements. Bachelor's Thesis, Universidade de Lisboa, Lisboa, Portugal, 2015.
27. Pacca, S. Impacts from decommissioning of hydroelectric dams: A life cycle perspective. *Clim. Chang.* 2007, *84*, 281–294.
28. Ramos, H.M.; Teyssier, C.; López-Jiménez, P.A. Optimization of Retention Ponds to Improve the Drainage System Elasticity for Water-Energy Nexus. *Water Resour. Manag.* 2013, *27*, 2889–2901.

29. Steffen, B. Prospects for pumped-hydro storage in Germany. *Energy Policy* 2012, *45*, 420–429.
30. Deane, J.P.; Gallachóir, B.P.; McKeogh, E.J. Techno-economic review of existing and new pumped hydro energy storage plant. *Renew. Sustain. Energy Rev.* 2010, *14*, 1293–1302.
31. Mataix, C. *Turbomáquinas Hidráulicas*; Universidad Pontificia Comillas: Madrid, Spain, 2009.
32. Cheng, C.; Liu, B.; Chau, K.W.; Li, G.; Liao, S. China's small hydropower and its dispatching management. *Renew. Sustain. Energy Rev.* 2015, *42*, 43–55.
33. Pereira, A.O.; Cunha, R.; Costa, V.; Marreco, J.; Rovere, E.L. Perspectives for the expansion of new renewable energy sources in Brazil. *Renew. Sustain. Energy Rev.* 2013, *23*, 49–59.
34. Kosnik, L. The potential for small scale hydropower development in the US. *Energy Policy* 2010, *38*, 5512–5519.
35. Bahadori, A.; Zahedi, G.; Zendehboudi, S. An overview of Australia's hydropower energy: Status and future prospects. *Renew. Sustain. Energy Rev.* 2013, *20*, 565–569.
36. Nautiyal, H.; Singal, S.K.; Sharma, A. Small hydropower for sustainable energy development in India. *Renew. Sustain. Energy Rev.* 2011, *15*, 2021–2027.
37. Ushiyama, I. Renewable energy strategy in Japan. *Renew. Energy* 1999, *16*, 1174–1179.
38. Liu, H.; Masera, D.; Esser, L. World Small Hydropower Development Report 2013. United Nations Industrial Development Organization; International Center on Small Hydro Power. Available online: www.smallhydroworld.org (accessed on 13th September 2016).
39. Miller, C.A.; Altamirano-Allende, C.; Johnson, N.; Agyemang, M. The social value of mid-scale energy in Africa: Redefining value and redesigning energy to reduce poverty. *Energy Res. Soc. Sci.* 2015, *5*, 67–69.
40. ESHA. Statistical Releases. 2012. Available online: http://streammap.esha.be/ (accessed on 13th September 2016).
41. Alonso-Tristán, C.; González-Peña, D.; Díez-Mediavilla, M.; Rodríguez-Amigo, M.; García-Calderón, T. Small hydropower plants in Spain: A case study. *Renew. Sustain. Energy Rev.* 2011, *15*, 2729–2735.
42. Instituto para la Diversificación y Ahorro de la Energía. *National Action Plan for Renewable Energy in Spain (PANER) 2011–2020*; Ministerio Industria, Turismo y Comercio Madrid, Spain, 2010. http://www.idae.es/uploads/documentos/documentos_11227_per_2011-2020_def_93c624ab.pdf
43. European Small Hydropower Association *Current Status of Small Hydropower Development in the EU-27*. ⟨http://www.streammap.esha.be/fileadmin/documents/Raising_awareness_doc___press_release/FINAL_SHP_Awareness_2011. pdf⟩ (accessed on 15th September 2016).
44. Amponsah, N.Y.; Troldborg, M.; Kington, B.; Aalders, I.; Hough, R.L. Greenhouse gas emissions from renewable energy sources: A review of lifecycle considerations. *Renew. Sustain. Energy Rev.* 2014, *39*, 461–475.
45. Gallagher, J.; Styles, D.; McNabola, A.; Williams, A.P. Life cycle environmental balance and greenhouse gas mitigation potential of micro-hydropower energy recovery in the water industry. *J. Clean. Prod.* 2015, *99*, 152–159.

46. Ogayar, B.; Vidal, P.G. Cost determination of the electro-mechanical equipment of a small hydro-power plant. *Renew. Energy* 2009, *34*, 6–13.
47. Paish, O. Small hydro power: Technology and current status. *Renew. Sustain. Energy Rev.* 2002, *6*, 537–556.
48. Mishra, S.; Singal, S.K.; Khatod, D.K. Optimal installation of small hydropower plant—A review. *Renew. Sustain. Energy Rev.* 2011, *15*, 3862–3869.
49. European Small Hydropower Association. Guía Para El Desarrollo de Una Pequeña Central Hidroeléctrica. European Small Hydropower Association. 2006. Available online: www.esha.be/fileadmin/esha_files/.../GUIDE_SHP_ES_01.pdf (accessed on 15th September 2016).
50. Ramos, H. *Guidelines for Design of Small Hydropower Plants*; WREAN (Western Regional Energy Agency &Network) and DED (Department of Economic Development), Belfast, North-Ireland. 2000.
51. Yuce, M.I.; Muratoglu, A. Hydrokinetic energy conversion systems: A technology status review. *Renew. Sustain. Energy Rev.* 2015, *43*, 72–82.
52. Ramos, H.M.; Almeida A. *Caracterização Dinâmica Global do Funcionamento de Aproveitamentos Hidroeléctricos*; IV SILUSBA – Simpósio de Hidráulica e Recursos Hídricos dos Países de Língua Oficial Portuguesa. Lisboa, Portugal, 1999. (In Portuguese)
53. Gordon, J.L. Hydraulic turbine efficiency. *Can. J. Civ. Eng.* 2001, *28*, 238–253.
54. Chapallaz J.M. *Manual on Pumps Used as Turbines*; Vieweg: Braunschweig, Germany, 1992.
55. Caxaria, G.; Mesquita, D.; Ramos, H.M. *Small Scale Hydropower: Generator Analysis and Optimization for Water Supply Systems*; World Renewable Energy Congress: Linköping, Sweden, 2011; pp. 1386–1393.
56. Simão, M.; Ramos, H.M.Hydrodynamic and performance of low power turbines: Conception, modelling and experimental tests. *Int. J. Energy Environ.* 2010, *1*, 431–444.
57. Ramos, H.; Borga, A. Pumps as turbines: An unconventional solution to energy production. *Urban Water* 1999, *1*, 261–263.
58. Arriaga, M. Pump as turbine—A pico-hydro alternative in Lao People's Democratic Republic. *Renew. Energy* 2010, *35*, 1109–1115.
59. Carravetta, A.; Fecarotta, O.; Del Giudice, G.; Ramos, H. Energy Recovery in Water Systems by PATs: A Comparisons among the Different Installation Schemes. *Procedia Eng.* 2014, *70*, 275–284.
60. Fecarotta, O.; Aricò, C.; Carravetta, A.; Martino, R.; Ramos, H.M. Hydropower Potential in Water Distribution Networks: Pressure Control by PATs. *Water Resour. Manag.* 2014, *29*, 699–714.
61. Derakhshan, S.; Nourbakhsh, A. Experimental study of characteristic curves of centrifugal pumps working as turbines in different specific speeds. *Exp. Therm. Fluid Sci.* 2008, *32*, 800–807.
62. Carravetta, A.; Del Giudice, G.; Fecarotta, O.; Ramos, H. Pump as Turbine (PAT) Design in Water Distribution Network by System Effectiveness. *Water* 2013, *5*, 1211–1225.

63. Carravetta, A.; Del Giudice, G.; Fecarotta, O.; Ramos, H.M. Energy Production in Water Distribution Networks: A PAT Design Strategy. *Water Resour. Manag.* 2012, *26*, 3947–3959.
64. Elbatran, A.H.; Yaakob, O.B.; Ahmed, Y.M.; Shabara, H.M. Operation, performance and economic analysis of low head micro-hydropower turbines for rural and remote areas: A review. *Renew. Sustain. Energy Rev.* 2015, *43*, 40–50.
65. Nourbakhsh, A.; Jahangiri, G. Inexpensive small hydropower stations for small areas of developing countries. In Proceedings of the Conference on Advanced in Planning-Design and Management of Irrigation Systems as Related to Sustainable Land Use, Louvain, Belgium, 14–17 September 1992; pp. 313–319.
66. Kumar, D.; Katoch, S.S. Small hydropower development in western Himalayas: Strategy for faster implementation. *Renew. Energy* 2015, *77*, 571–578.
67. Razan, J.I.; Islam, R.S.; Hasan, R.; Hasan, S.; Islam, F. A Comprehensive Study of Micro-Hydropower Plant and Its Potential in Bangladesh. *Renew. Energy* 2012, *2012*, 635396.
68. Ohunakin, O.S.; Ojolo, S.J.; Ajayi, O.O. Small hydropower (SHP) development in Nigeria: An assessment. *Renew. Sustain. Energy Rev.* 2011, *15*, 2006–2013.
69. Vicente, S.; Bludszuweit, H. Flexible design of a pico-hydropower system for Laos communities. *Renew. Energy* 2012, *44*, 406–413.
70. Punys, P.; Dumbrauskas, A.; Kasiulis, E.; Vyčienė, G.; Šilinis, L. Flow Regime Changes: From Impounding a Temperate Lowland River to Small Hydropower Operations. *Energies* 2015, *8*, 7478–7501.
71. Abbasi, T.; Abbasi, S.A. Small hydro and the environmental implications of its extensive utilization. *Renew. Sustain. Energy Rev.* 2011, *15*, 2134–2143.
72. Punys, P.; Dumbrauskas, A.; Kvaraciejus, A.; Vyciene, G. Tools for Small Hydropower Plant Resource Planning and Development: A Review of Technology and Applications. *Energies* 2011, *4*, 1258–1277.
73. Vilanova, M.R.; Balestieri, J.A. Hydropower recovery in water supply systems: Models and case study. *Energy Convers. Manag.* 2014, *84*, 414–426.
74. Novara, D.; Stanek W.; Ramos, H. Energy Harvesting from Municipal Water Management Systems: From Storage and Distribution to Wastewater Treatment. Master's Thesis, Universidade de Lisboa, Lisboa, Portugal, 2016.
75. Senior J.A.; Muller, G.; Wiemann, P. The development of the rotary hydraulic pressure machine. In Proceedings of the Congress IAHR, Venice, Italy, 1–6 July 2007.
76. Senior, J.A.; Saenger, N.; Müller, G. New hydropower converters for very low-head differences. *J. Hydraul. Res. 2010*, *48*, 703–714.
77. Adhau, S.P.; Moharil, R.M.; Adhau, P.G. Mini-hydro power generation on existing irrigation projects: Case study of Indian sites. *Renew. Sustain. Energy Rev.* 2012, *16*, 4785–4795.
78. Tilmant, A.; Goor, Q.; Pinte, D. Agricultural-to-hydropower water transfers: Sharing water and benefits in hydropower-irrigation systems. *Hydrol. Earth Syst. Sci.* 2009, *13*, 1091–1101.
79. Butera, I.; Balestra, R. Estimation of the hydropower potential of irrigation networks. *Renew. Sustain. Energy Rev.* 2015, *48*, 140–151.

80. Coelho, B.; Andrade-Campos, A. Efficiency achievement in water supply systems—A review. *Renew. Sustain. Energy Rev.* 2014, *30*, 59–84.
81. Klein, G.; Krebs, M.; Hall, V.; O'Brien, T.; Blevins, B.B. *California's Water—Energy Relationship*; California Energy Commission: Sacramento, CA, USA, 2005.
82. Almandoz, J.; Cabrera, E.; Arregui, F.; Cobacho, R. Leakage Assessment through Water Distribution Network Simulation. *J. Water Resour. Plan. Manag.* 2005, *131*, 458–466.
83. Carravetta, A.; Del Giudice, G.; Oreste, F.; Ramos, H. PAT design strategy for energy recovery in water distribution networks by electrical regulation. *Energies* 2013, *6*, 411–424.
84. Colombo, A.F.; Karney, B.W. Energy and Costs of Leaky Pipes: Toward Comprehensive Picture. *J. Water Resour. Plan. Manag.* 2002, *128*, 441–450.
85. Fecarotta, O.; Carravetta, A.; Ramos, H.M.; Martino, R. An improved affinity model to enhance variable operating strategy for pumps used as turbines. *J. Hydraul. Res.* 2016, *54*, 332–341.
86. Sitzenfrei, R.; von Leon, J. Long-time simulation of water distribution systems for the design of small hydropower systems. *Renew Energy* 2014, *72*, 182–187.
87. Fontana, N.; Giugni, M.; Portolano, D. Losses Reduction and Energy Production in Water-Distribution Networks. *J. Water Resour. Plan. Manag.* 2012, *138*, 237–244.
88. Ramos, H.; Mello, M.; De, P.K. Clean power in water supply systems as a sustainable solution: From planning to practical implementation. *Water Sci. Technol. Water Supply* 2010, *10*, 39–49.
89. Imbernón, J.A.; Usquin, B. Sistemas de generación hidráulica. Una nueva forma de entender la energía. In Proceedings of the II Congreso Smart Grid, Madrid, Spain 27-28th October 2014. https://www.smartgridsinfo.es/biblioteca/libro-de-comunicaciones-del-ii-congreso-smart-grids
90. Lisk, B.; Greenberg, E.; Bloetscher, F. *Implementing Renewable Energy at Water Utilities*; Case Studies; Water Research Foundation: Denver, CO, USA, 2012.
91. Hong Kong Polytechnic University, Novel Inline Hydropower System for Power Generation from Water Pipelines. Available online: http://phys.org/news/2012-12-inline-hydropower-power-pipelines.html (accessed on 16 August 2016).
92. McNabola, A.; Coughlan, P.; Williams, A.P. Energy recovery in the water industry: An assessment of the potential of micro hydropower. *Water Environ. J.* 2014, *28*, 294–304.
93. Food and Agriculture Organization (FAO). Aquastat. 2015. Available online: http://www.fao.org/nr/water/aquastat/data/query/results.html?regionQuery=true&yearGrouping=SURVEY&showCodes=false&yearRange.fromYear=1958&yearRange.toYear=2017&varGrpIds=4250%2C4251%2C4252%2C4253%2C4257&cntIds=&regIds=9805%2C9806%2C9807%2C9808%2C9809&edit (accessed on 9 June 2015).
94. Seoane, P.; Allué, R.; Postigo, M.J.; Cordón, M.A. *Boletín Mensual de Estadística*; Instituto Nacional de Estadística: Madrid, Spain, 2013. (In Spanish)
95. Food and Agriculture Organization (FAO). Agua Y Cultivos, 2002. Available online: http://www.fao.org/docrep/005/y3918s/y3918s10.htm (accessed on 19th September 2016). (In Spanish)

96. Maestu, J.; Villar, A. Precios Y Costes de Los Servicios Del Agua En España, Madrid, Spain, 2007. Available online: http://hispagua.cedex.es/sites/default/files/especiales/Tarifas_agua/precios_costes_servicios_agua.pdf (accessed on 19th September 2016). (In Spanish)
97. MAGRAMA. El Riego Localizado Alcanza el 48.23% de la Superficie Regada en España. Minist Agric Aliment y Medio Ambient. 2014. 4. Available online: http://www.magrama.gob.es/gl/prensa/noticias/el-riego-localizado-alcanza-el-4823--de-la-superficie-regada-en-espa%C3%B1a-/tcm7-312671-16 (accessed on 9 June 2015). (In Spanish)
98. Instituto para la Diversificación y Ahorro de la Energía. *Ahorro Y Eficiencia Energética En Agricultura de Regadío*; Ministerio Industria, Turismo y Comercio; Madrid, Spain, 2005. (In Spanish)
99. Rodríguez-Díaz, J.A.; Montesinos, P.; Poyato, E.C. Detecting Critical Points in On-Demand Irrigation Pressurized Networks—A New Methodology. *Water Resour. Manag.* 2012, *26*, 1693–1713.
100. Moreno, M.A.; Planells, P.; Córcoles, J.I.; Tarjuelo, J.M.; Carrión, P.A. Development of a new methodology to obtain the characteristic pump curves that minimize the total cost at pumping stations. *Biosyst. Eng.* 2009, *102*, 95–105.
101. Jiménez-Bello, M.A.; Royuela, A.; Manzano, J.; Prats, A.G.; Martínez-Alzamora, F. Methodology to improve water and energy use by proper irrigation scheduling in pressurised networks. *Agric. Water Manag.* 2015, *149*, 91–101.
102. Prats, A.G.; Picó, S.G.; Alzamora F.M.; Bello, M.A. Random Scenarios Generation with Minimum Energy Consumption Model for Sectoring Optimization in Pressurized Irrigation Networks Using a Simulated Annealing Approach. *J. Irrig. Drain. Eng.* 2012, *138*, 613–624.
103. Costa, L.; de Athayde-Prata, B.; Ramos, H.; de Castro, M. A Branch-and-Bound Algorithm for Optimal Pump Scheduling in Water Distribution Networks. *Water Resour. Manag.* 2015, *30*, 1037–1052.
104. Rossman, L.A. *EPANET 2 User's Manual*; U.S. Environmental Protection Agency (EPA): Cincinnati, OH, USA, 2000.
105. Cabrera, E.; Cobacho, R.; Soriano, J. Towards an Energy Labelling of Pressurized Water Networks. *Procedia Eng.* 2014, *70*, 209–217.
106. Samora, I.; Franca, M.; Schleiss, A.; Ramos, H.M. Simulated Annealing in Optimization of Energy Production in a Water Supply Network. *Water Resour. Manag.* 2016, *30*, 1533–1547.
107. Pérez-Sánchez, M.; Sánchez-Romero, F.; Ramos, H.; López-Jiménez, P. Modeling Irrigation Networks for the Quantification of Potential Energy Recovering: A Case Study. *Water* 2016, *8*, 234.
108. Samora, I.; Manso, P.; Franca, M.J.; Schleiss, A.J.; Ramos, H.M. Opportunity and Economic Feasibility of Inline Microhydropower Units in Water Supply Networks. *J. Water Resour. Plan. Manag.* 2016, *142*, 04016052.

109. Kirkpatrick, S.; Gelatt, C.; Vecchi, M. Optimization by simulated annealing. *Science* 1983, *220*, 671–680.
110. Forouzbakhsh, F.; Hosseini, S.M.H.; Vakilian, M. An approach to the investment analysis of small and medium hydro-power plants. *Energy Policy* 2007, *35*, 1013–1024.
111. Zema, D.A.; Nicotra, A.; Tamburino, V.; Zimbone, S.M. A simple method to evaluate the technical and economic feasibility of micro hydro power plants in existing irrigation systems. *Renew. Energy* 2016, *85*, 498–506.
112. Rawal, S.; Kshirsagar, J. Simulation on a pump operating in a turbine mode. In Proceedings of the 23rd International Pump Users Symposium, Houston, TX, 5–8 March 2007; Texas A&M University: College Station, TX, USA, 2007; pp. 21–27.
113. Singh, P. *Optimization of the Internal Hydraulic and of System Design in Pumps as Turbines with Field Implementation and Evaluation*; Karlsruhe 2005.
114. Samora, I.; Manso, P.; Franca, M.; Schleiss, A.; Ramos, H. Energy Recovery Using Micro-Hydropower Technology in Water Supply Systems: The Case Study of the City of Fribourg. *Water* 2016, *8*, 344–360.

This page is intentionally left blank.

Appendices

Appendix II

MODELING IRRIGATION NETWORKS FOR THE QUANTIFICATION OF POTENTIAL ENERGY RECOVERING: A CASE STUDY

Author version document which was published in index JCR Journal "Water" ISSN 2073-4441. Impact Factor 1.687. Position 33/85 (Q2). Water Resources

Pérez-Sánchez, M., Sánchez-Romero, F., Ramos, H., López-Jiménez, P., 2016. Modeling Irrigation Networks for the Quantification of Potential Energy Recovering: A Case Study. Water 8, 1–26. doi:10.3390/w8060234

This page is intentionally left blank.

ABSTRACT

Water irrigation systems are required to provide adequate pressure levels in any sort of network. Quite frequently, this requirement is achieved by using pressure reducing valves (*PRVs*). Nevertheless, the possibility of using hydraulic machines to recover energy instead of *PRVs* could reduce the energy footprint of the whole system. In this research, a new methodology is proposed to help water managers quantify the potential energy recovering of an irrigation water network with adequate conditions of topographies distribution. *EPANET* has been used to create a model based on probabilities of irrigation and flow distribution in real networks. Knowledge of the flows and pressures in the network is necessary to perform an analysis of economic viability. Using the proposed methodology, a case study has been analyzed in a typical Mediterranean region and the potential available energy has been estimated. The study quantifies the theoretical energy recoverable if hydraulic machines were installed in the network. Particularly, the maximum energy potentially recovered in the system has been estimated up to 188.23 MWh/year) with a potential saving of non-renewable energy resources (coal and gas) of CO_2 137.4 t/year.

Keywords: smart water; water-energy nexus; energy efficiency; sustainable water management; energy recovering

1. Introduction

Water and its management is one of the more important current and future global challenges. Its variability can cause cloudbursts, making sewers to overflow, while the scarcity of water in other components involves public services and reduces irrigation [1]. Hence, an efficient management of water irrigation networks is crucial for facing future challenges related to the energy-water nexus, considering the importance of irrigation in the whole planet [2]. The development of the modernization of irrigation systems in agriculture (replacing open channel with pressurized irrigation) has considerably increased energy consumption in recent years [3]. Nevertheless, the establishment of drip irrigation has made more efficient systems in water consumption but not in energy demand.

Spain is not an exception: The annual irrigation volume consumed in Spain is 16.344 km^3/year [4] and the global irrigation consumption in pressure systems approaches 3925 km^3/year [5]. Consequently, the theoretical energy recoverable could be a significant amount.

In Spain, the drip irrigated area (*i.e.,* 1.7 of 3.54 million of hectares are irrigated by pressure systems) [6] represents 17.56% of the world's surface irrigated by localized drip (approximately 9 million hectares) [7]. The high energy consumption and the rising cost of tariff have reduced profits or even the viability of farms [8]. The need to study strategies to decrease the energy consumption in these installations is pointed out in the consulted references. Regarding this issue, Coehlo *et al.* established the need to study the recovery in water distribution systems for increasing the energy efficiency, since the energy consumption in water networks involves 7% of the global energy consumption [9]. The objectives of this recovery are: to reduce the energy footprint of water in irrigation system and to lessen greenhouse emissions compared with other non-renewable energy sources.

Water-energy nexus analysis has become a crucial issue in recent years [3,10–13]. Baki *et al.* [10] studied water-energy interactions in water systems in Athens. Okadera et al. [11] and Herath *et al.* [12] analyzed water footprints of hydroelectricity. Water management improvement in irrigation networks have also been analyzed in [14], where a 40% irrigation reduction volume was achieved.

Sustainable social and economic growth based on renewable energy sources forces water networks to work as multipurpose systems [15], where power generation is not the first objective but an important complementary one [16].

Some studies and prototypes of recovering energy with small turbines can be found in the literature for power less than 100 kW [17–22]. The previous publications of Carravetta *et al.* [17,18] compare the feasible regulation systems for pump as turbines (*PATs*). These authors [19,20] determined performance of *PATs* installed in drinking systems. The efficiency oscillates between 0.4 and 0.6. Ramos *et al.* [21,22] proposed new design solutions to energy production in water pipe systems. These solutions are focused on the installing of *PATs* with electrical or hydraulic regulation within network. Additionally, to the previous referenced authors, the variability of the flow along time is studied as an objective in the present research. Here, a deep analysis of theoretical recovery energy in the network is proposed (*i.e.,* distinguishing values of dissipated energy, necessary energy and losses in lines and consumption points).

Particularly in irrigation networks, some studies of recovering energy in open channels flow [23–25] and preliminary studies in pressure pipe systems are described. These show the importance to analyze these networks in terms of recovery energy. An example of these studies is the network of Alqueva in Portugal [26]. In that contribution, authors analyzed the recovery energy with average steady state flows. A discretized analysis in short time intervals is proposed for determining the theoretical energy recoverable in a part of the Alqueva distribution network. This analysis was made with average consumption demands.

The present research determines the variability of flows and pressure in any point or line on the network depending on irrigation habits. This advantage (determining instant

values of flows and pressure) allows performing the analysis of energy recovery in any point on the network. The methodology obtains the data pairs of flow (Q) and head (H) of the working area of the hypothetical installed machine.

Furthermore, the methodology determines the variation of flow in a network based on the habits of irrigation in order to perform energy analyzes. The application of this methodology in irrigation networks aims to complement previous studies for *PATs* efficiency in dinking supply networks, extending its use.

The variation of flow is based on random demand of the users and the real irrigation allocations. Depending on these parameters, the proposed methodology estimates the energy dissipated by friction losses, the energy required for irrigation, and the recoverable energy in the irrigation network. The discretization of the flows leads managers to analyze power generation depending on irrigation time periods. Accordingly, the present analysis has the following objectives:

1) Proposing a new methodology for determining the flows throughout the year in an irrigation network demand, considering the need of the crop, the historic consumption and the irrigation farmers' habits.

2) Estimating the flow rate and pressures with the time.

3) Quantifying the energy balance in pressurized irrigation distribution systems to determine the energy footprint of water in the distribution system, and the estimated recoverable energy.

4) Applying these procedures to a real case study.

2. Methods and Materials

2.1. Methodology for Determining the Flow

In this section, the proposed methodology to determine the time-dependent flow throughout the year is described. In order to analyze any pressurized irrigation network from the energy point of view, the flow and pressure along pipelines are determinant variables. The requirements of the minimum pressure at any consumption point are also fundamental. Pressures are different depending on the location of irrigation points. Therefore, the spatial and timing distribution of these consumptions are important aspects to take into consideration.

The flows are variable over any irrigation campaign, depending on many factors such as distribution of crops in the irrigation area, crop maturity, weather conditions, soil characteristics, efficiency of drippers (ranging from 0.90 to 0.95), and the habits of farmers, among others.

Traditionally, the Clement's methodology has been used for irrigation network sizing [27–29]. This methodology allows determining the maximum flow circulating in a network line. This maximum flow rate is calculated by assuming a binomial distribution

flow. The mathematical expectation and standard deviation of the binomial probability distribution depends on the opening point of consumption. Clement assumed that this probability was uniform and equal over time. This uniform probability consideration can lead to underestimating the flows. Consequently, the Clement methodology cannot be used for analyzing potential energy recovery. Probability of irrigation at any point is non-uniform, and depends on the habits of irrigation farmers. Therefore, it varies throughout the day, week, and month. This underestimation leads to the proposal of different methodologies for estimating flows in irrigation networks. The most common are those that use statistical methods [27–29], or models based on the random opening of irrigation points by means of computer simulations [30–33]. A new methodology considering both strategies is here proposed.

Flow and energy implications are therefore separately considered and described.

The majority of water distribution networks only have water meters in each irrigation point for billing and controlling the consumed volumes. Unfortunately, it is not usual that the irrigation network has readings of flows and pressures at any time. For this reason, the proposed methodology simulates the operation of any irrigation network based on the random generation of consumption in irrigation points.

The day, start, and duration of irrigations (as function of the habits of the farmers) are considered in this research as factors for irrigation probability and flows. Furthermore, the real consumption probability weights (obtained from historical archives of the irrigation entities) can be assigned to consumptions, and the network can be very precisely simulated.

Hence, for any day of the year, consumptions can be estimated in any irrigation point by following these steps (Figure 1).

1. Estimation of cumulative volume consumed by the irrigation point

The decision to irrigate depends on the balance (V_{Na}) between the previous irrigated volume and the consumption assigned (needs) of the irrigation point (Input 1). If the volume of cumulative consumption is positive, automatically the methodology indicates that this is not an irrigation day. Only when this volume is negative, irrigation is possible. If the volume of cumulative consumption is negative, the methodology determines the irrigation probability.

2. The determination of the irrigation probability (P_I)

To randomly determine if crops are irrigated or not during a particular day, two types of weight functions are assigned. These functions are obtained from interviews with farmers. According to Figure 1, Input 2 determines the irrigation weekly pattern (w_{dj}), prioritizing the irrigation days per week. Input 3 determines the maximum days between irrigations for each month of the year (i). If in previous days no irrigation has been performed, watering is forced.

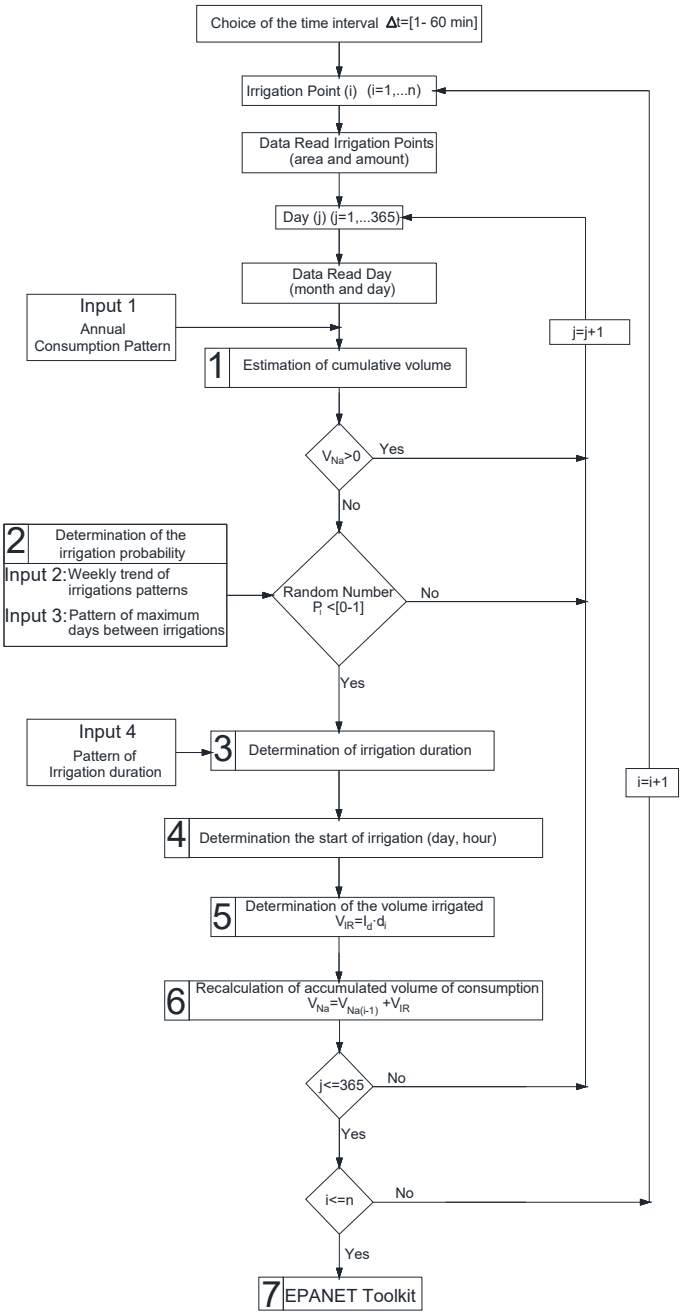

Figure 1. Schematic description of the methodology for flow estimation

The methodology generates a random number (*RN*) between zero and one associated with an irrigation probability. If $RN_j \leq P_I$ irrigation is assigned to this consumption point.

$$P_I = \frac{w_{dj}}{\sum_{n=1}^{n=i-j+1} w_{dn}} \quad (1)$$

where:

i is the numbers of days inside of interval;

j is the day of decision making;

w_{dj} is the pattern to irrigate one particular day inside the interval;

$\sum_{n=1}^{n=i-j+1} w_{dn}$ is the total addition of patterns.

3. The determination of the irrigation duration

The methodology allows determining the estimated time based on irrigation habits of farmers to satisfy irrigation needs (Input 1). This value depends on irrigation amount and type of crop.

4. The start of irrigation

The irrigation duration randomly determines the start of irrigation as a function of the daily probability curves of irrigation time (Input 4). When the methodology determines that a consumption point has to be irrigated, the start time of irrigation is determined. Therefore, the cumulative probability must be used for starting irrigation. This curve is defined by twenty-four sections (one per hour). When no irrigation exists, the irrigate weight (w_h) in this interval is assigned to be zero.

The probability in the time interval (p_h) is:

$$p_h = \frac{w_h}{\sum_{h=0}^{h=23} w_h} \quad (2)$$

where w_h is the defined pattern (Input 2) to irrigate one particular hour inside the interval.

The cumulative probability (p_{cm}) is:

$$p_c = \sum_{h=0}^{h=m} p_h \ (m = 0, \dots, 23) \quad (3)$$

where *m* is the number of intervals in one day.

A new *RN* is generated, ranging from 0 to 1. It is compared with the values of cumulative probability (p_{cm}) and the start irrigation period is established. For this particular time period, the methodology selects within this period the start interval from zero to value equal to $\frac{60}{\Delta t}$ (where Δt is the time interval in which the simulated flow is discretized). When this step is completed, the day and hour of starting irrigation is known.

5. Determination of irrigation volume

The irrigation supply (agronomic known parameter, which depends on: framework plantation, number of dripper per plant and flow of the dripper) and the duration (Input 4) are known and the irrigation volume can be calculated for that day.

6. Calculation of cumulative consumption

When the irrigation volume is known, the methodology updates the water volume available for the plant.

7. The pressure and flow modelled for each node in the network

They are calculated for every irrigation points and each day using Epanet Toolkit. Epanet is public domain software [34] that models water distribution in pipe systems. Different elements can be represented: pipe networks composed by pipes, nodes (junctions), pumps, valves, and storage tanks or reservoirs. The model can simulate extended-period hydraulic analysis by simulating by sort of pipes systems, computing friction and minor losses, representing various types of valves, junctions, tanks and pumps, considering multiple patterns at nodes consumption with time variation, and system operation on simple tank level, timer controls or complex rule-based controls.

2.2. Balance of Energy

Once flows and pressures are estimated along the time in the whole network, the energy equation (Reynolds Theorem) must be implemented to consider the energy balance in the system [35].

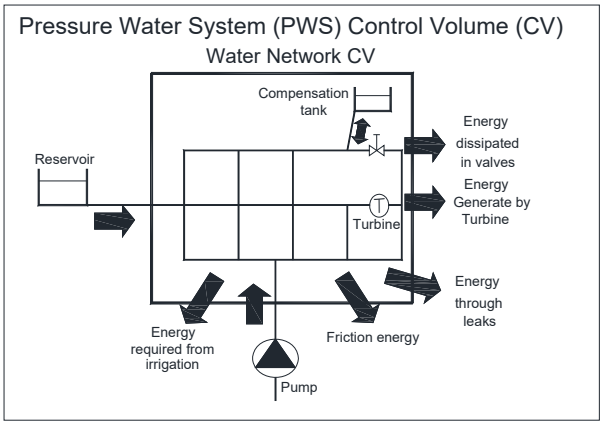

Figure 2. Energy balance in the pressurized irrigation water network adapted from [36]

According to Figure 2, a generic irrigation network with all possible elements (reservoir, pumps, turbines, and compensation tanks) is presented. The conservation of energy equation is defined as:

$$\frac{dE}{dt} = \frac{dQ}{dt} + \frac{W_{shaft}}{dt} = \frac{d}{dt}\iiint_{CV} \rho\left(gz + u + \frac{v^2}{2}\right) dV + \iint_{CS}\left(gz + u + \frac{P}{\rho} + \frac{v^2}{2}\right)\rho\left(\vec{v}\cdot d\vec{A}\right) (4)$$

where:

$\frac{dE}{dt}$ is the exchange of energy per unit time in the control system;
$\frac{dQ}{dt}$ is the exchange of heat per unit of time (heat power);
$\frac{W_{shaft}}{dt}$ is the power transmitted directly to or from the fluid (*e.g.,* pump);
dV is the differential volume of control volume for integration;
$\vec{v}$ is the velocity vector of fluid;
$d\vec{A}$ is the differential area of control surface for integration;
ρ is the fluid density;
gz is the potential energy per unit mass;
u is the internal energy per unit mass;
$\frac{v^2}{2}$ is the kinetic energy per unit mass;
$\frac{P}{\rho}$ is the height of pressure per unit mass;

Within the control system, the following simplifications can be made:

- The water density is constant.
- Flow is uniform in each interval.
- Exchange of heat between fluid and surroundings is negligible (adiabatic system).
- The shaft work is the power transmitted directly to/from the fluid in the case that a pump or turbine exists in the network.
- There is no compensation tank in the network, therefore, the time energy variation inside of the control volume as function of time is negligible.

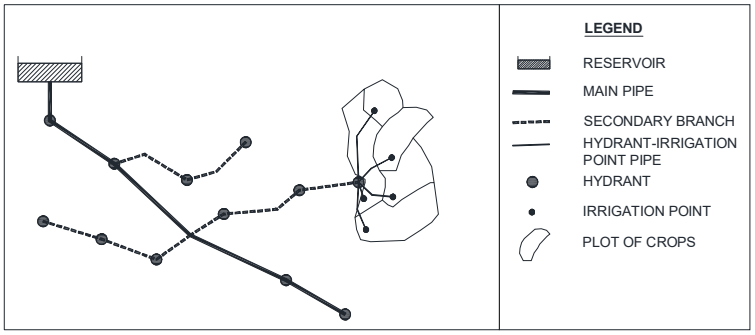

Figure 3. Scheme of irrigation network

If an irrigation system operates by gravity (Figure 3), the equation of energy applied to any control system along a time interval is defined by Equation (5):

$$\gamma Q_D H_D \Delta t = \sum_{i=1}^{n} \gamma Q_{oi} H_{oi}\, \Delta t + \rho(\sum_{i=1}^{n}(Q_{oi} u_{oi} - Q_{Di} u_{Di}))\Delta t \quad (5)$$

where:

Δt is the time interval (s);
n is the total number of irrigation points;
i is the individual irrigation points;
γ is the specific weight of the fluid (N/m^3);
Q_D is the total flow demanded by the network (m^3/s);
H_D is the = piezometric head of the reservoir. For a pumped system, the value is the manometric height;
Q_{oi} is the flow demanded by each irrigation point (m^3/s);
H_{oi} is the piezometric head of the consumption node (m);
$\gamma Q_D H_D$ is the total energy (kW) supplied to the system. This term is equal to E_T, which is later defined;
$\sum_{i=1}^{n} \gamma Q_{oi} H_{oi}$ is the energy consumed by all irrigation points (kW). This term will be defined as E_{RI} plus E_{TRI};
$\rho(\sum_{i=1}^{n}(Q_{oi} u_{oi} - Q_{Di} u_{Di}))$ is the exchange of internal energy. In an adiabatic system, it is equal to friction losses. This term will be defined as E_{FR}.

Leakages are not considered in this analysis because the drip irrigation network is still new (minimum leakages), the maintenance and repair plans are usually undertaken (which reduce possible losses), and finally, these networks are not as automated as drinking systems so unmeasured volumes and leakages are difficult to discern. If an energy audit were made, this volume should be considered or estimated [6, 36]. Furthermore, the installation of hydraulic machines does not affect the water quality of the final use (*i.e.,* irrigation).

When a global energy balance of the network is established, it is possible to define different terms of energy. Such as lines, hydrants and irrigation points, as follow (Figure 4):

- *Total Energy (E_{Ti}):* potential total energy in an irrigation point when the consumption is null in the entire network. It corresponds to the static energy (i.e., potential) of the node. For an irrigation point along a time interval, the value is:

$$E_{T_i}(kWh) = \frac{9.81}{3600} Q_i (z_o - z_i) \Delta t \quad (6)$$

where Q_i is the flow circulating by a line that supplies to more unfavorable irrigation point (most disadvantageous consumption node in terms of need of the pressure) (m^3/s); z_i is the geometry level above reference plane of the irrigation point. In this case, the reference is sea level (m); z_0 is the geometry

level above reference plane of the free water surface of the reservoir. In this case, the reference is sea level (m); and Δt is the time interval (s).

- *Friction Energy (E_{FRi}):* for a time interval, it is the energy dissipated in the network by the water coming from head until the irrigation point.

$$E_{FR_i}(kWh) = 2.725 \cdot 10^{-3} Q_i \big(z_o - (z_i + P_i)\big) \Delta t \quad (7)$$

where P_i is the service pressure in any point of the network when consumption exists. The units are meter water column (m w.c.).

Minor losses (pressure loss in particular network components like tees, valves, and similar) are considered as a percentage of friction losses. Associated with this term, the Energy Footprint of Water (*EFW*) can be calculated. Energy Footprint of Water is defined as the ration between energy dissipated due to friction losses (E_{FRi}) over the distributed volume on the network (kWh/m^3).

- *Theoretical Energy Necessary (E_{TNi}):* it is the minimum energy required in a hydrant or line to ensure the minimum pressure of irrigation in the more unfavorable point. The value is:

$$E_{TN_i}(kWh) = 2.725 \cdot 10^{-3} Q_i P_{min_i} \Delta t \quad (8)$$

where P_{min_i} is the minimum pressure of service of a line or hydrant to ensure the minimum pressure in the most disadvantageous consumption node. The units are meter water column (m w.c.).

- *Energy Required for Irrigation (E_{RIi}):* during an interval of time, it is the minimum energy required at an irrigation point to ensure the irrigation water evenly. The value is:

$$E_{RI_i}(kWh) = 2.725 \cdot 10^{-3} Q_i P_{minI_i} \Delta t \quad (9)$$

where P_{minI_i} is the minimum pressure of service of an irrigation point required to ensure the irrigation water evenly. The units are meter water column (m w.c.).

- *Theoretical Available Energy (E_{TAi}):* it is the available energy for recovery in a hydrant or line. The recovery coefficient in a hydrant or line (C_{RT}) depends on losses existent between the hydrant (or pipeline) and the most disadvantageous consumption node. It is equal to the sum of the theoretical energy recoverable plus the theoretical energy unrecoverable (E_{NRT}). The value of this energy for a particular time duration, is defined as:

$$E_{TA_i}(kWh) = 2.725 \cdot 10^{-3} Q_i \big(P_i - P_{min_i}\big) \ \Delta t \quad (10)$$

- *Theoretical Recoverable Energy (E_{TRi}):* it is the maximum theoretical recoverable energy in an irrigation point, hydrant or line of the network, ensuring at downstream the minimum pressure of irrigation.

$$E_{TR_i}(kWh) = 2.725 \cdot 10^{-3} Q_i \left(P_i - \max\left(P_{min_i}; P_{minI_i}\right)\right) \ \Delta t = \\ = 2.725 \cdot 10^{-3} Q_i H_i \Delta t \quad (11)$$

where H_i is the value of head in irrigation point, hydrant or line (m w.c.), obtained as:

$$H_i = P_i - \max\left(P_{min_i}; P_{minI_i}\right) \quad (12)$$

- *Theoretical unrecoverable Energy (E_{NTRi}):* it is the energy in a hydrant or line on the network that cannot be recovered. This energy is necessary to assume the losses from the line or hydrant to the more unfavorable irrigation point.

$$E_{NTR_i} = E_{TA_i} - E_{TR_i} \quad (13)$$

- *Recovery coefficient in hydrant or line (C_{RTi}):* it is the quotient between E_{TRi} and E_{TAi} in an irrigation point, hydrant or line of the network. It represents the proportion of recovery energy over available energy.

$$C_{RT_i} = \frac{E_{TRi}}{E_{TAi}} \quad (14)$$

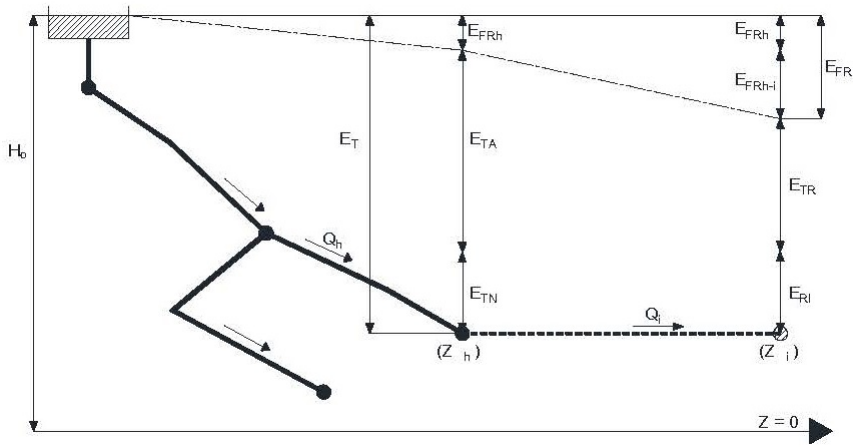

Figure 4. Scheme of hydraulic energies grade line

Q_h (Figure 4) is the flow circulating in a line or consumed by a hydrant in m^3/s, z_h is the geometry level above reference plane of the line or hydrant in meters. H_0 is the piezometric height of the reservoir that supplies the network in m w.c. The units are meter water column (m w.c.). If reservoir is open, H_0 is equal to z_0.

When Equation (5) is applied in a point of the network, it is defined by Equation (15):

$$E_{Ti} = E_{FRi} + E_{RIi} + E_{TRi} \quad (15)$$

When all irrigation points are considered (z_i in Figure 4), the annual balance of energy is defined by Equation (16):

$$\sum_{i=1}^{n} E_{Ti} = \sum_{i=1}^{n} (E_{FRi} + E_{RIi} + E_{TRi}) \quad (16)$$

In the case of lines and hydrants (z_h in Figure 4), the annual balance of energy is defined by Equation (17):

$$E_T = E_{FRh} + E_{TA} + E_{TN} = E_{FRh} + E_{RI} + E_{TR} + E_{NTR} \quad (17)$$

The energy footprint of water and the theoretical recoverable energy are crucial for the energy balance. The energy footprint on the network distribution can be obtained along the year and compared with average values analyzed in other distribution systems. Some of these values are: 0.31 kWh/m^3 in injected irrigation network [36], 0.18–0.32 kWh/m^3 according to California Energy Commission [37], 0.081 kWh/m^3 in Bangkok, 0.5 kWh/m^3 in Delhi and 0.13 kWh/m^3 in Tokyo [38].

Regarding the theoretical recoverable energy in a network, it mainly depends on the orography of the irrigation area. The networks with larger gradients between the supply and the consumption points have greater possibility to recover energy, if the appropriate machine is selected. The energy recovery can be analyzed in different parts of the network:

i. In plot of cultivation; in this case, the private user needs to reduce pressure down to 30 m w.c. to carry out drip irrigation. Generally, the user installs a pressure reducer to dissipate the excess energy. This element can be replaced by a pico-turbine to generate energy for self-consumption. This energy can be used in remote-control system, cleaning of filters, lighting and others similar consumptions.

ii. In the hydrant pipe; when the hydrant supplies to flat topography, reduction of pressure can be done. In an operating network, this reduction is carried out with a pressure reducing valve. This recovery could potentially be done if a suitable turbine could be installed.

iii. In pipe branch; in networks with large extension and irregular orography, some parts of the network can achieve higher pressure than necessary, forcing pressure to be reduced on a pipe branch. Currently, this reduction is possible by using a reducing valve installed on this branch. These valves can be replaced by turbines or pumps as turbines (PAT) [14] depending on the system characteristics to increase the energy efficiency of the network.

The presented methodology helps managers to estimate the theoretical recoverable energy in irrigation points, hydrants and branches (pipelines). According to Spadaro *et al.* [39], this recovery can contribute with a theoretical average reduction of greenhouse gases emission between 582 and 877 gCO_2/kWh when compared to non-renewable energy solutions (*e.g.,* coal and gas) and 1150 gCO_2/kWh when compared to emissions of fossil fuel [40]. However, this reduction will depend on the water source

(groundwater, superficial or residual water) and distribution (gravity or pumped) [41]. Future research should try to integrate all applications together (supply, irrigation and wastewater for better water management) in a strategy to improve system efficiency, thus reducing greenhouse gases [42].

The viability of these installations is subject to economic evaluation (incomes vs. costs). Zema *et al.* [43] proposed a simple method to evaluate the economic feasibility of micro-hydropower plants in irrigations systems. In preliminary studies, these methods are good indicators for taking decisions to develop more detailed projects. These decisions are focused on the selection of machine efficiency, temporal distribution of energy produced and investment analyzes. Similarly, Castro [44] proposed the period simple return (PSR) and energy index (*EI*) as indicators of investment viability. These sorts of installations are viable if the *PSR* is less than six years and the energy index smaller than 0.6 €/kWh. *PSR* and *EI* are defined by the following equations:

$$PSR = \frac{IC}{I-C} \tag{18}$$

$$I = P_E E\eta \tag{19}$$

$$C = C_0 E\eta \tag{20}$$

$$EI = \frac{IC}{E} \tag{21}$$

where *IC* is the investment cost (€); *C* is the annual operating cost (€/year); C_0 is the unit operating cost (€/kWh); *I* is the annual income (€/year); *PE* is the energy price (€/kWh); *E* is the theoretical energy recovery by the turbine (kWh/year) and η is the machine efficiency.

The investment cost using *PAT* is 50% lower than the cost of traditional turbines [45]. Carravetta *et al.* [20] estimated *IC* of 545 €/kW if the machine is electrically regulated. Incomes depend on generated energy, which depends on the price of energy, recovery energy and the efficiency of the machine. Based on the specific speed, expert literature indicates that efficiency varies between 50%–60% [20,46]. Castro [44] established a sales price (*PE*) of 0.0842 €/kWh and C_0 of 0.0145 €/kW. These solutions, due to the smaller cost of *PATs*, present a lower payback period.

3. Case Study

3.1. Description

In order to apply the developed methodology, a drip irrigation network located in Vallada (Valencia, Spain) is proposed (Figure 5). The network covers 290.2 hectares, with water coming from a well. The main crop is citrus, although there is a small area of olive trees. The water is accumulated in a reservoir with a 7000 m^3 capacity. The topography varies between 378 and 248 m above sea level. The pond is located sufficiently high (399 m above sea level) to ensure the minimum pressure of 30 m w.c. in all irrigation points.

The pipelines of the network are built on asbestos cement pipes (diameters between 300 and 500 mm), polyvinyl chloride (diameters between 250 and 125 mm) and ductile iron (diameter of 150 mm). The installation has seventy multiuser hydrants. A manifold is installed in each hydrant to connect pipes of polyethylene with irrigation points. Inside the hydrant, meters are placed to read the consumption volume.

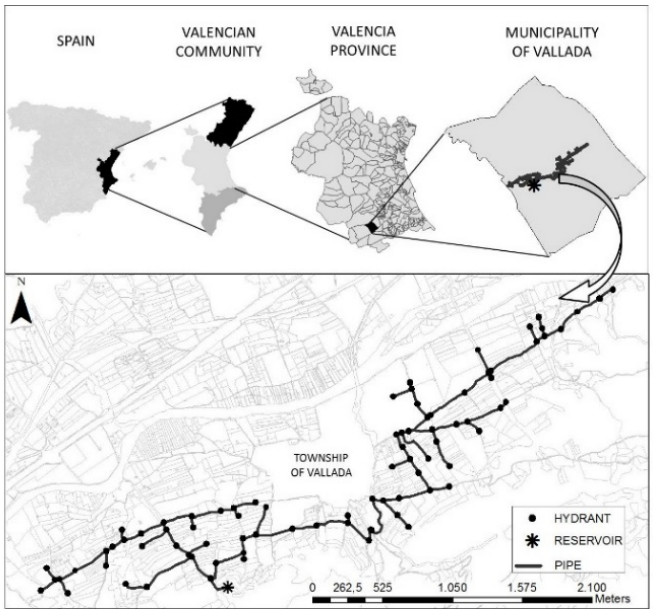

Figure 5. Study area in Vallada case study network

The next steps are necessary to apply the proposed methodology:

a) To make use of records of the water metered in the irrigation points. There are records since 2003 (year that network began to operate). In each plot, registers were taken quarterly corresponding to the months of March, June, September and December.

b) To calculate the flow design (water requirements) for each of the considered plot, according to the crop and characteristics of the irrigation installation (distance between drippers and type). The number of sectors is established depending on the area of plots. This has allowed an allocation of irrigation according to the existing installation (Figure 1).

c) To perform interviews of users and operating staff for estimating farmer habits. The type of irrigation management at the annual, monthly, weekly and daily levels has been analyzed in this questionnaire. Based on these interviews, different consumption patterns have been established. These patterns take in to account the irrigation habits of farmers: weekly trend, maximum days between irrigations and irrigation duration (Inputs 2, 3 and 4 in Figure 1).

3.2. Methodology

3.2.1. Historical Consumption Data and Probability Function

Based on the total consumption provided by the entity, an average consumption of 3189 m^3/ha has been estimated. Therefore, the annual average consumption is 925427 m^3 in the time series studied from 2003 to 2014 (Figure 6).

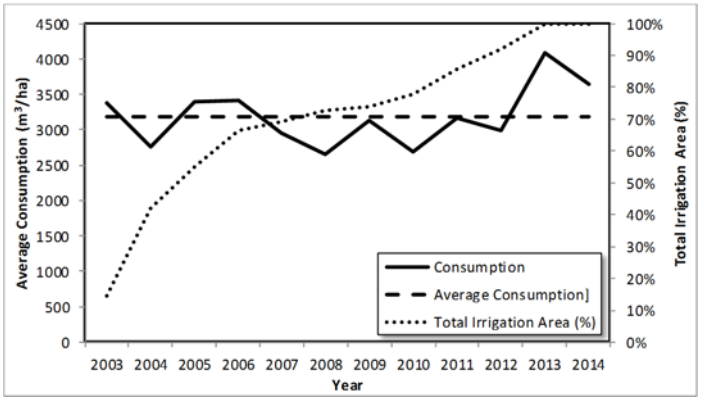

Figure 6. Measured Annual Consumption in Vallada case study network

The next steps allow establishing consumption patterns:

1. The annual consumption is estimated for each irrigation point, grouping them in terms of similar consumptions. This classification has provided the distribution presented in Figure 7.

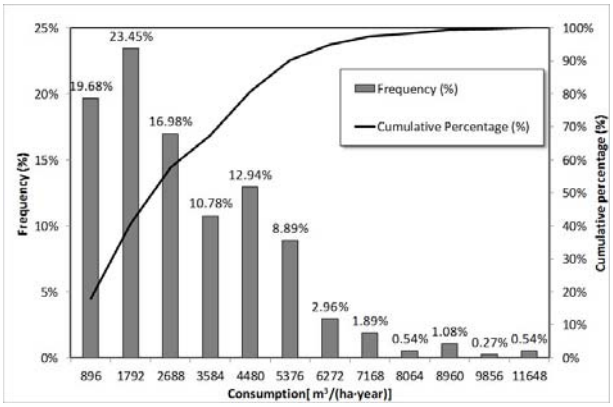

Figure 7. Distribution of annual consumptions in Vallada case study

2. In order to determine the distribution of daily consumption, specific weights for crops of citrus and olive needs to be considered, according to the registered consumptions. The monthly pattern of irrigation needs has been set taking into

account consumer groups (Figure 7). On the one hand, the irrigation points with consumptions lower than 3584 m^3/ha have been assigned the patterns of consumption under the name "Crop of Olive" (Figure 8). On the other hand, the irrigation points with consumptions higher than 4480 m^3/ha have been assigned the patterns of consumption under the name "Crop of Citrus" (Figure 8).

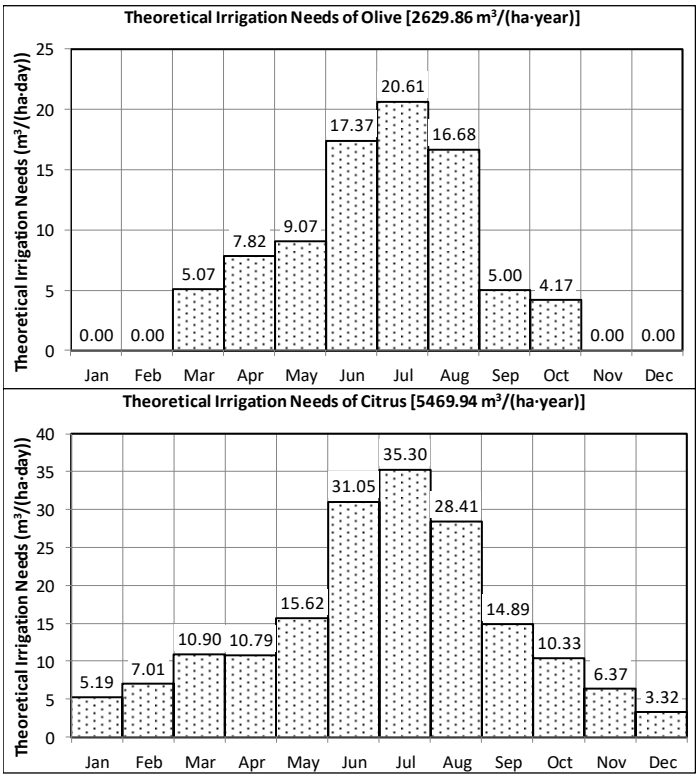

Figure 8. Pattern of irrigation needs: Top-Crop of olive. Bottom-Crop of citrus

3.2.2. Pattern of irrigation habits

Habit patterns of farmers obtained by interviews, are defined as follows:

1. Analyzing the information obtained from interviews, two trends of irrigations have been depicted. Small farmers avoid Sunday as irrigation day and Saturday appears with double preference than the rest of the days (Figure 9a). Big farmers also have double preference for Saturday, but do not avoid irrigation on Sunday (Figure 9b).

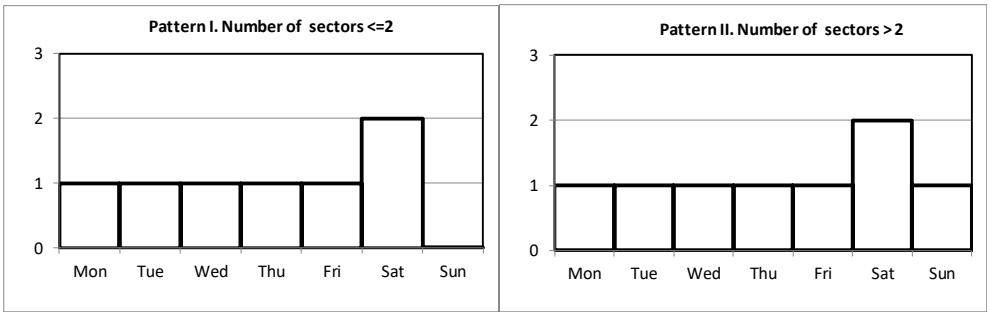

Figure 9. Weekly trend of irrigation pattern according to the number of sectors in the plot areas [Left Figure (a). Right Figure (b)]

2. Distribution of maximum days between irrigations: these patterns refer to the maximum interval between watering. Irrigation occurs every day during the months of higher consumption (May, June, July, August and September). In remaining months, the intervals of irrigation increase, being not a clear and well-defined pattern for all farmers. Each farmer chooses the interval according to different factors (*e.g.,* rain, availability and soil properties). Based on the results of the interviews, four distributions have been defined. According to the results of the requested data for farmer habits across surveys, patterns have been assigned. Pattern I has been assigned approximately to 40% of the irrigation points, pattern II to 20%, pattern III to 20% and pattern IV to the other 20%. This assignment has been carried out randomly (Figure 10).

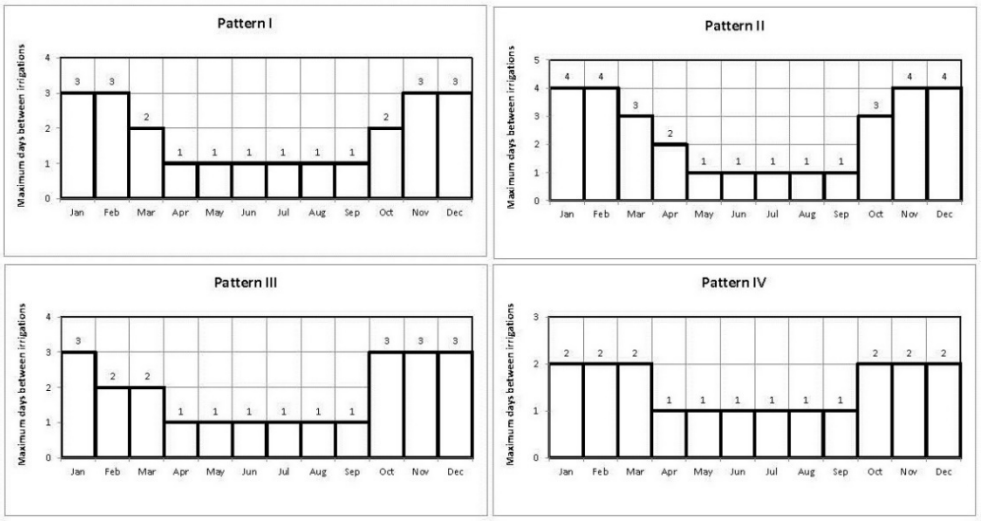

Figure 10. Patterns of maximum days between irrigations

3. Patterns of irrigation duration: based on the requested information four distributions have been proposed. Again, pattern I has been assigned approximately to 40% of the irrigation points, pattern II to 20%, pattern III to 20% and pattern IV to other 20%. This assignment has been carried out randomly (Figure 11).

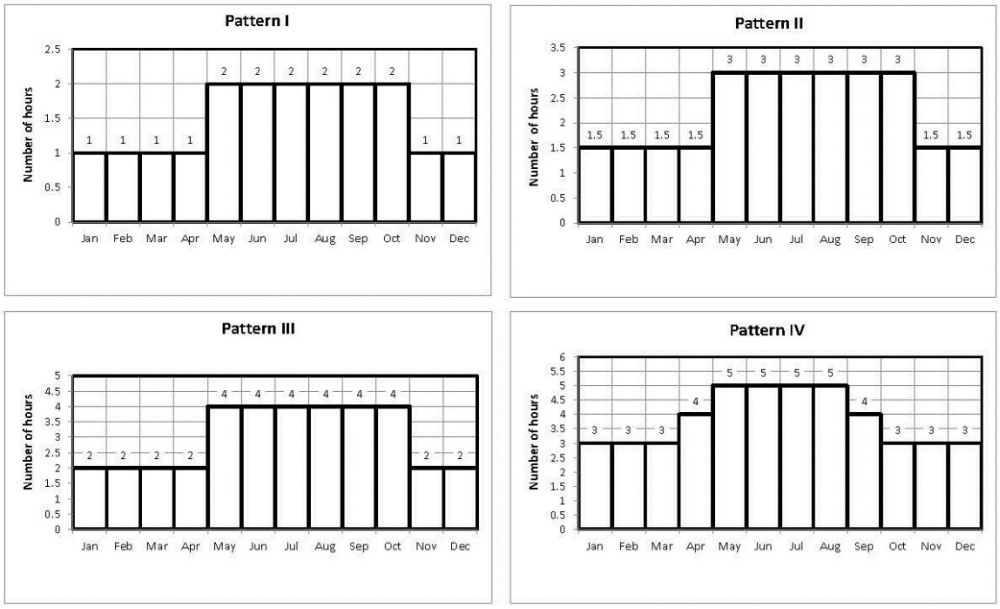

Figure 11. Patterns of irrigation duration.

4. Distribution of irrigation start probability: farmers tend to irrigate in certain particular hours of the day. This aspect is considered in this methodology by using the patterns for the probability of starting irrigation in the different schedules. The watering schedule between 10 am and 4 pm is chosen in the months of January, February, March, April, October, November and December. However, farmers irrigate in different light hours in summer months to avoid warmer hours and night. Therefore, three patterns have been developed to define the probability (see Figure 1, step 4).

A first pattern is assigned to the winter months from October to April and considers that the irrigation starts between 8 am and 6 pm. A second pattern is assigned to the summer months, from May to September, where the irrigation avoids hours of day with higher temperatures. The watering schedule starts between 4 am and 12 pm and from 6 pm until 12 am. Finally, a third pattern function is defined for irrigating plots with more of two sectors, at any time of the day along the year.

4. Results

4.1. Basic Characteristics

Following the methodology, an analysis for flows and pressures is necessary for energy consideration in the network based on hydraulic simulations. These simulations have been run with the *EPANET* software.

The model of the developed network by means of the *EPANET* software has been run for each day along one year. In this case, these calculations have been repeated 20, 40 and 60 times with different scenarios represented. Nevertheless, comparing these simulations, the variability obtained when the flow in the main line is compared to the average flow is smaller than 5%. As this deviation remains similar, no more repetitions are considered.

This methodology has been calibrated in other networks by the authors. The calibration has been performed with measured flow every five minutes. The results have been satisfactory with Nash-Sutcliffe index upper to 0.40, root relative squared mean error below 0.7 and percent bias below 5%, as indicated in [47].

Figures 12 and 13 depict the topology of the network to be considered and analyzed in further sections.

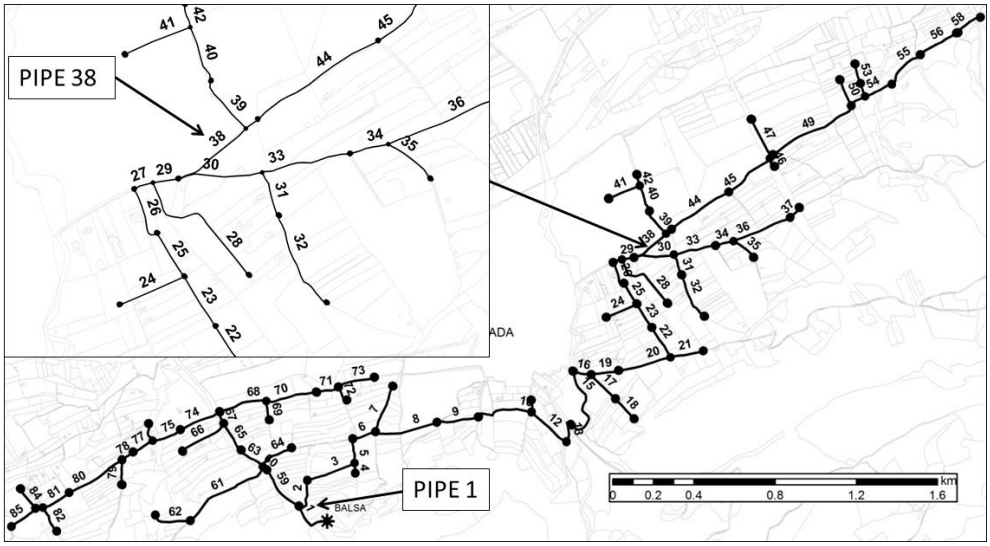

Figure 12. Identification of pipes in the irrigation network

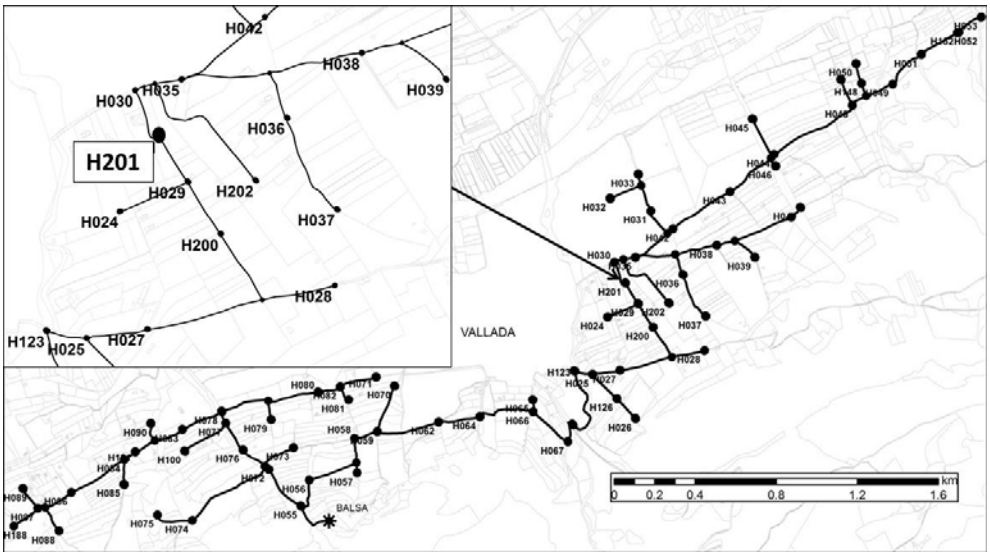

Figure 13. Identification of hydrants in the irrigation network

4.2. Flows in the Network

Flow and pressure have been obtained along the time, based on the historical series of records registered between 2003 and 2014, in any line of the system, according to the irrigation trends. These time series of data collected in those 12 years (17808 records), flow in the main line (see Figure 12, line 1) and hydrant 201 (see Figure 13, H201) are depicted in Figure 14.

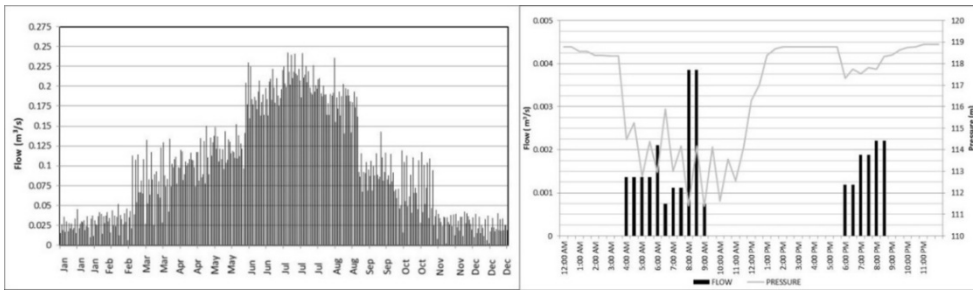

Figure 14. Flow in the main line (pipe 1) along the year (Left). Flow and pressure variation in the hydrant (H201) over time (Right)

The frequency histogram (Figure 15) displays the large variability of flows along the year. Hence, irrigation networks behave in a different way than drinking systems: monthly seasonal ratios range between 0.8–1.2 in drinking networks (except for touristic cities) and its variability of flows during the day varies between 0.7–1.5 of the average value. Opposite to this, the flow seasonality factor in irrigation systems is much larger

than in drinking systems. In the case of citrus, seasonality factor varies between 0.14 and 2.36 times relative to the annual average consumption volume. According to this, the estimated variability in this network case study ranges between 0.1 and 2.54 times the average flow.

Additionally, there is a very high frequency of very low flows (Figure 15). Flows below 0.05 m^3/s (25% of the maximum flow rate) arise up to 80% times in the main line of the network. These small flows will become of utmost importance to be used for energy recovery.

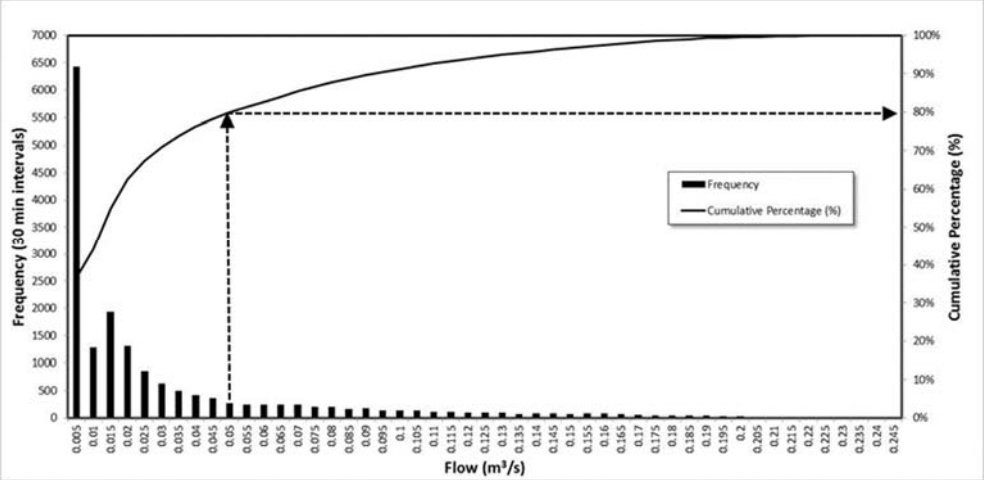

Figure 15. Histogram of flow in the main line

4.3. Water-Energy Nexus Estimation

This section analyzes the estimation of energy dissipated in the network as a result of friction losses. Figure 16 shows the variation of the energy footprint based on time. The network is working 5943 hours during of the year. Figure 16 shows the energy footprint during the distribution of flows in the water network. As shown in the histogram, 99.7% of the time the network has an energy footprint below 2 kWh/m^3. The maximum value obtained is 2.87 kWh/m^3 for a July day. However, 58.5% of the time the network has an energy footprint below 0.1 kWh/m^3.

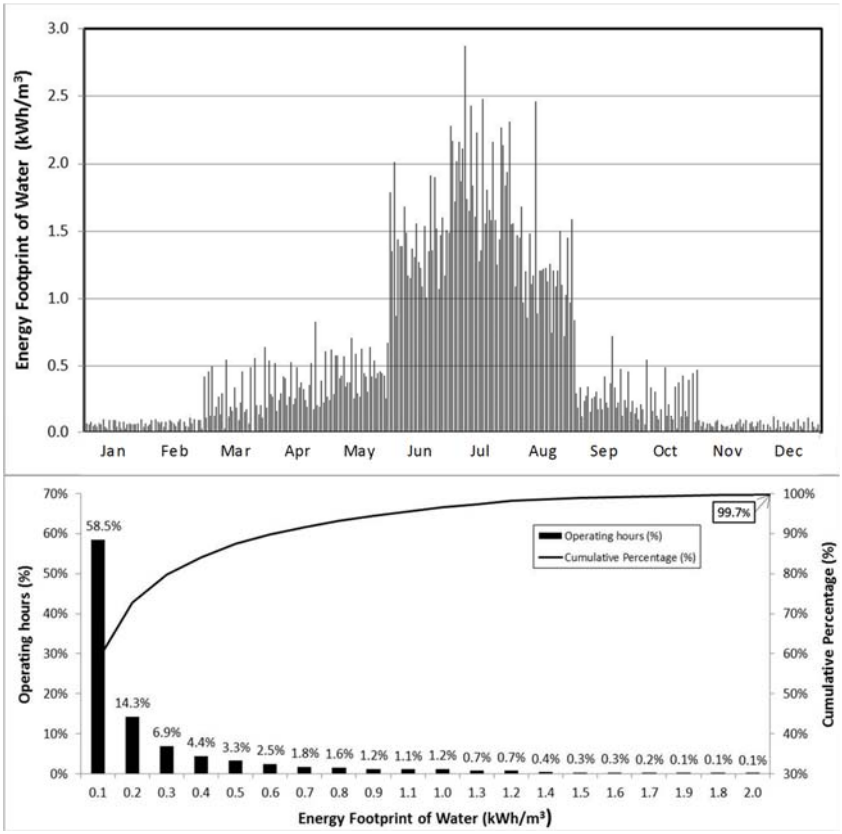

Figure 16. Network energy footprint of water

4.4 Theoretical Recoverable Energy

If the results are analyzed in irrigation points, the total theoretical recoverable energy is 188.23 MWh/year (*i.e.,* 68.7% of the total energy supplied to the network). In these nodes, the theoretical coefficient of recovery (C_{RT}) is equal to one, as E_{RT} is equal to E_{TA}.

Figure 17 shows a detail of instantaneous power along data registered for the month of July for the analyzed time series, and the distribution of instant power frequencies over time for an irrigation point. In these points, the frequency at which the value of instantaneous power appears is practically constant because the consumption flow is uniform and only pressure varies due to the use of pressure-compensating drippers.

As an example, in irrigation point 303, the annual operating time is 2957 hours. The instantaneous power oscillates between 9.96 kW and 11.64 kW. The maximum power occurs 44.2% of time, and the theoretical total energy is 33.80 MWh/year (Figure 17).

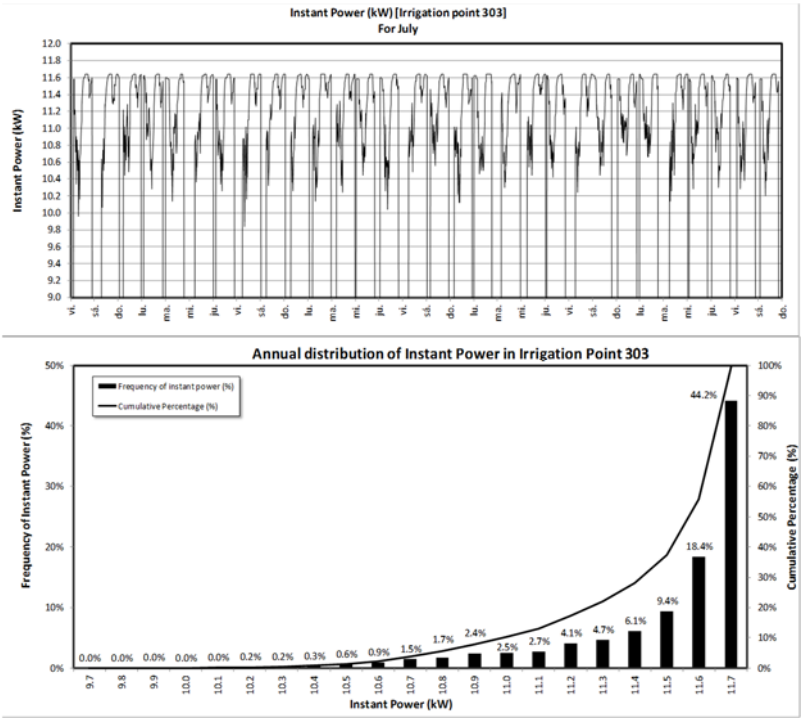

Figure 17. Potential Power in the irrigation point 303

In the case of hydrants, the result is similar where the sum of the theoretical recoverable energy is 178.1 MWh/year. Figure 18 shows analogous results to those exposed in the irrigation points. Particularly, a maximum instantaneous power of 4.64 kW is achieved in hydrant H201, with an annual operating time of 1460 h and total energy of 1.59 MWh/year. The average weighted coefficient of recovery in this hydrant is 0.68 (*i.e.,* 9.68% of the total energy could be recovered if turbines had 100% efficiency). The maximum recovery occurs in the hydrant H045 with 16.12 MWh/year, with a recovery rate of 0.83 (Figure 18).

The values of theoretical energy recoverable in all hydrants are detailed in Table 1, as well as their recovery coefficients. The theoretical maximum recoverable energy is obtained in hydrant H042 with a total energy of 33.73 MWh/year, and a coefficient of recovery of 0.80. The theoretical energy ranges between 0.01 (H056) and 33.73 MWh/year. The recovery coefficient ranges between 0.14 (H055) and 0.84 (H053). The weighted average recovery coefficient is 0.75.

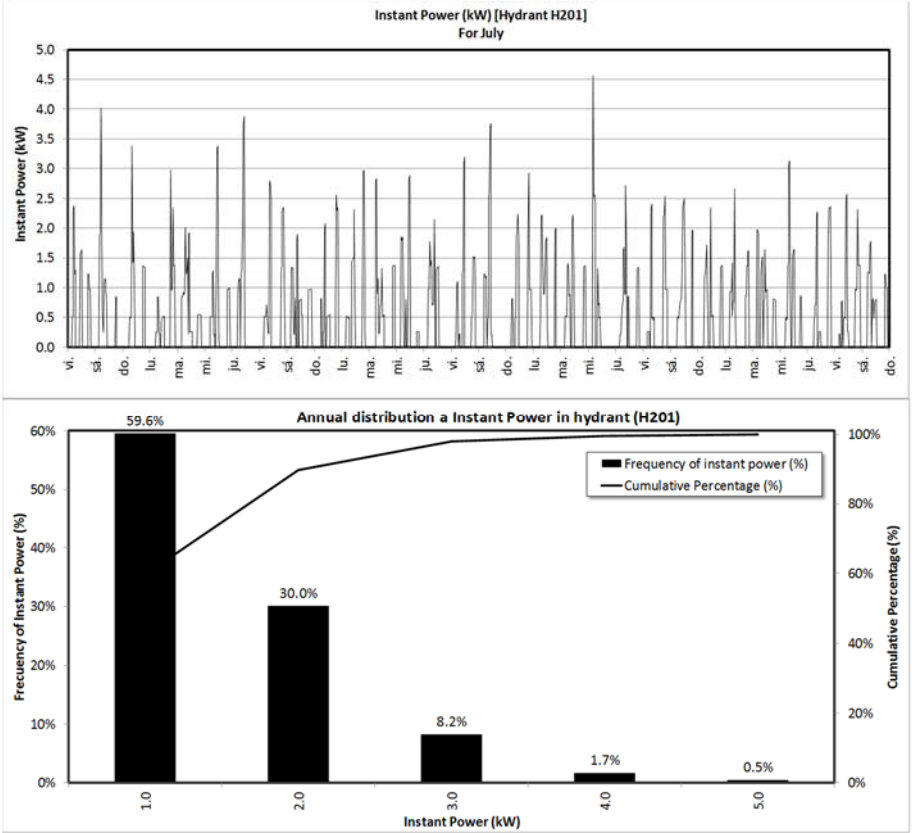

Figure 18. Potential Power in hydrant H201

Table 1. Theoretical energy recoverable in hydrants on the irrigation network

HYDRANT	E_{RT} MWh/year	C_{RT}	HYDRANT	E_{RT} MWh/year	C_{RT}
H024	1.99	0.66	H065	0.80	0.63
H025	1.56	0.76	H066	0.13	0.57
H026	0.48	0.59	H067	0.22	0.53
H027	1.92	0.67	H070	1.40	0.69
H028	0.12	0.46	H071	0.40	0.72
H029	2.27	0.72	H072	0.28	0.35
H030	0.77	0.80	H073	0.22	0.45
H031	1.36	0.81	H074	0.64	0.40

Table 1. (*Cont.*)Theoretical energy recoverable in hydrants on the irrigation network

HYDRANT	E_{RT} MWh/year	C_{RT}	HYDRANT	E_{RT} MWh/year	C_{RT}
H032	3.94	0.73	H075	0.31	0.54
H033	4.19	0.81	H076	1.34	0.55
H035	3.57	0.79	H077	0.52	0.64
H036	2.50	0.76	H078	3.68	0.69
H037	1.12	0.69	H079	0.76	0.53
H038	3.54	0.71	H080	1.41	0.66
H039	0.64	0.69	H081	0.40	0.72
H040	3.57	0.65	H082	1.28	0.71
H042	33.73	0.80	H083	0.87	0.72
H043	9.13	0.81	H084	0.80	0.67
H044	5.60	0.78	H085	1.50	0.58
H045	16.12	0.83	H086	0.48	0.52
H046	5.14	0.72	H087	0.27	0.58
H047	5.03	0.80	H088	0.51	0.26
H048	13.37	0.80	H089	0.73	0.59
H049	0.26	0.82	H090	0.59	0.69
H050	1.93	0.77	H100	0.89	0.65
H051	2.67	0.59	H101	1.05	0.63
H052	0.86	0.77	H123	1.78	0.79
H053	11.05	0.84	H126	0.47	0.68
H055	0.04	0.14	H140	0.73	0.74
H056	0.01	0.28	H148	0.32	0.82
H057	0.55	0.26	H152	2.47	0.72
H058	0.99	0.60	H188	2.81	0.68
H059	0.46	0.61	H200	1.35	0.77
H062	2.32	0.57	H201	1.58	0.68
H064	0.22	0.28	H202	2.08	0.76

The line that presents the maximum recoverable energy is depicted in Figure 19 and Table 2. This condition is set on line 38, with maximum recoverable energy of 89.99 MWh/year and an average weighted recovery rate of 0.64. The maximum instantaneous power is 63.7 kW. The histogram presented in Figure 19 shows that during 918 hours of the operating time (17.1%), the instantaneous power arises up to 10 kW.

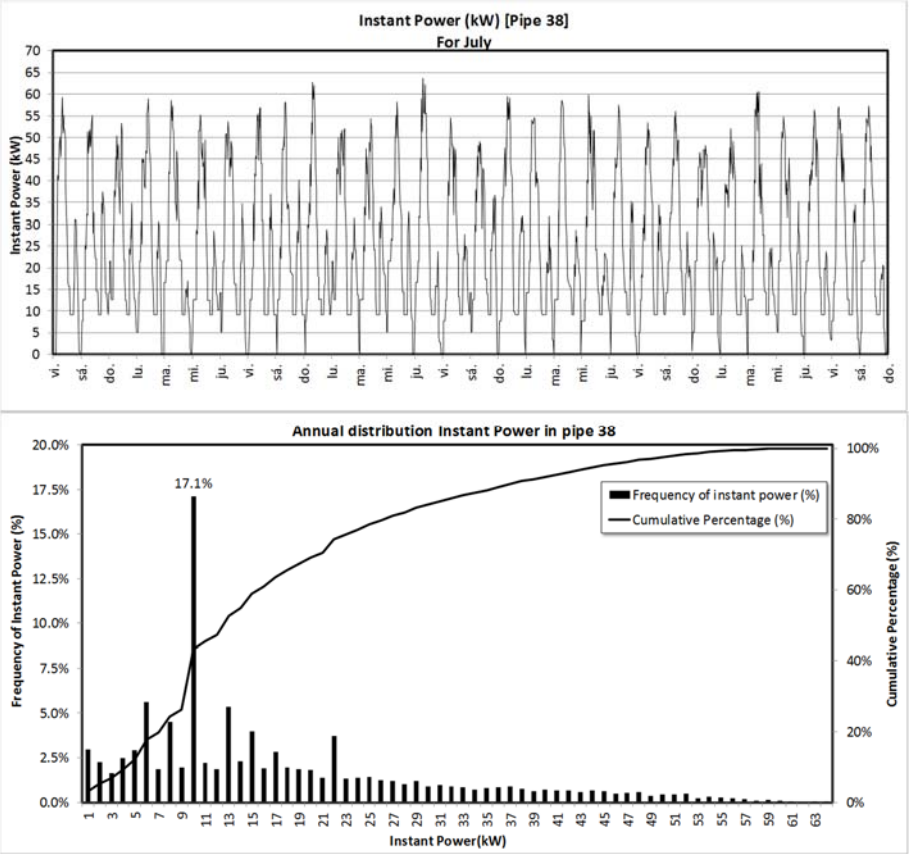

Figure 19. Potential Power in line 38

Table 2 shows that the maximum recoverable energy is obtained in line 38 with total energy of 89.99 MWh/year and a coefficient of recovery 0.64. The estimated energy (E_{RT}) ranges between 0.12 (line 21) and 89.99 MWh/year, the range of recovery coefficient can be found between 0.15 (line 74) and 0.84 (line 58) and the weighted average coefficient is 0.48.

Table 2. Estimated energy recoverable in lines on the irrigation network

PIPE	E_{RT} MWh/year	C_{RT}	PIPE	E_{RT} MWh/year	C_{RT}
1	4.29	0.16	44	55.58	0.64
2	17.56	0.29	45	48.35	0.63
3	18.64	0.23	46	5.14	0.72
4	0.55	0.26	47	16.12	0.83
5	26.83	0.26	48	32.61	0.62
6	26.41	0.25	49	28.13	0.60
7	1.40	0.69	50	5.03	0.80
8	25.85	0.25	51	14.49	0.60
9	24.84	0.29	52	2.24	0.81
10	41.64	0.40	53	1.93	0.77
11	0.80	0.63	54	12.88	0.58
12	41.10	0.33	55	12.70	0.59
13	40.96	0.28	56	12.62	0.72
14	40.96	0.28	57	0.86	0.77
15	40.96	0.25	58	11.05	0.84
16	40.42	0.24	59	10.56	0.46
17	0.77	0.42	60	10.18	0.43
18	0.48	0.59	61	0.85	0.39
19	39.40	0.27	62	0.31	0.54
20	38.64	0.35	63	5.79	0.21
21	0.12	0.46	64	0.22	0.45
22	83.51	0.57	65	5.27	0.17
23	82.51	0.52	66	0.89	0.65
24	1.99	0.66	67	4.90	0.16
25	79.32	0.50	68	3.01	0.47
26	78.15	0.50	69	0.76	0.53
27	77.67	0.49	70	3.29	0.66
28	2.08	0.76	71	1.96	0.66
29	76.15	0.48	72	0.40	0.72
30	9.88	0.48	73	0.40	0.72
31	2.84	0.52	74	3.08	0.15

Table 2. (Cont.) Estimated energy recoverable in lines on the irrigation network

PIPE	E_{RT} MWh/year	C_{RT}	PIPE	E_{RT} MWh/year	C_{RT}
32	1.12	0.69	75	2.90	0.16
33	7.68	0.57	76	0.59	0.69
34	4.83	0.59	77	2.78	0.16
35	0.64	0.69	78	2.51	0.17
36	4.20	0.64	79	1.50	0.58
37	3.57	0.65	80	1.78	0.19
38	**89.99**	**0.64**	81	1.60	0.21
39	8.86	0.75	82	0.51	0.26
40	7.59	0.72	83	2.98	0.59
41	3.94	0.73	84	0.73	0.59
42	4.19	0.81	85	2.81	0.68
43	82.74	0.64	--	--	--

The pairs of flow, Q_i, and head, H_i, defined in Equation (11) for any point of the network are crucial to determine energetic aspects. With these data (flow and head), the estimated area of operation of the future selected machine could be determined. This cloud of point pairs is depicted in Figure 20 for an irrigation point, a hydrant and two of the lines with the maximum theoretical recoverable energy.

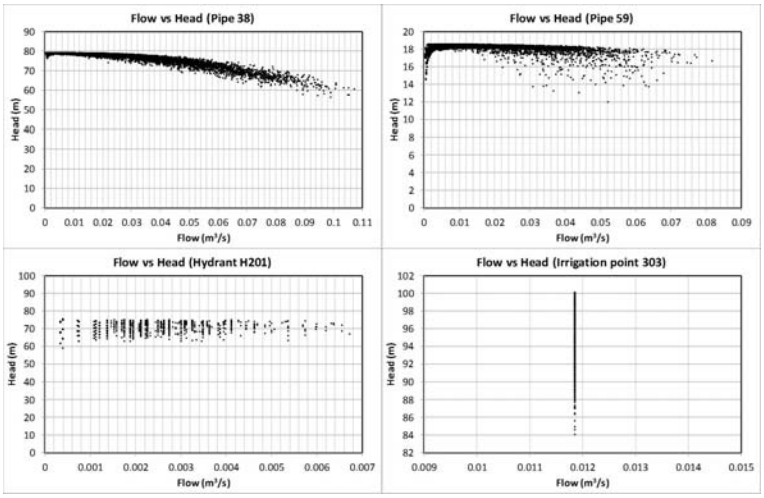

Figure 20. Representation of flow *versus* head for ideal turbine characteristics in irrigation point, hydrant and lines 38 and 55

Figure 20 shows that not all lines have narrow operating point intervals. Line 59 has a large dispersion of operating points in the flow range. Similar circumstances occur in hydrant H201 with a wide range of flow, making the choice of a unique turbine difficult. In the case of recovery in irrigation points, the flow is constant with an interval of pressure according to the demand of the network. This becomes an additional advantage in which the performance of the chosen machine could be easily optimized.

4.5. Global Energy Balance

The global energy network analysis in this case study, shows that with a total of 274.00 MWh/year of the network (E_T), the energy dissipated by friction (E_{FR}) is 11.25 MWh/year (4.10%), the energy required for irrigation (E_{RI}), is 74.52 MWh/year and the theoretical energy recoverable (E_{TR}) is 188.23 MWh/year (considering the sum of total individual recovery in all irrigation points).

If total energy balance in hydrants is calculated, the distribution of energy in the network is defined by Figure 21. This graphic shows that in the case of carrying out energy recovery at all hydrants, theoretical energy recoverable would be 75.2 MWh/year (27.4% compared to the total energy E_T).

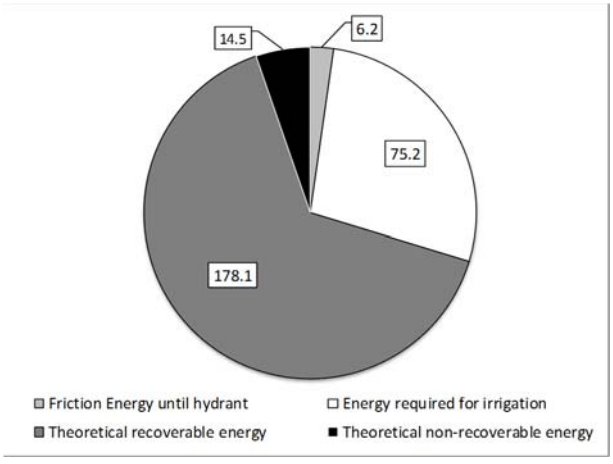

Figure 21. Annual Balance Energy in hydrants

Finally, the virtual possibility of recovering all of the estimated energy in all irrigations points is 188.23 MWh/year. In this case, the environmental impact versus generation with non-renewable resources (*e.g.,* coal and gas) would be a theoretical reduction of 137.4 t of CO_2/year or 216.2 t of CO_2/year with fuels.

4.6. Economic Feasibility

In a first economical approach, the maximum theoretical recovery line is analyzed (line 38). The corresponding *PAT* proposed for line 38 would have a *PSR* value of 5.9 years and *EI* of 0.22 €/kWh (Equation (18) and (21)). In this case, these results are established by considering a machine of 30 kW peak power with efficiency of 50 % and the economic parameters defined in section 2.2.

5. Conclusions

In this research, a methodology for quantifying the potential recovered energy for an average year in an irrigation network has been presented. Even nowadays, some irrigation networks do not have flowmeters. In these cases, a flow estimation method must be implemented: the flow is assigned to pipes along time depending on registered volumes, irrigation trends, and consumption patterns.

Once flows are known, the *EPANET* toolkit is used for estimating pressures in different scenarios along the year in order to determine pressure and energy balance for each point. Hence, it is possible to discriminate the energy needed for irrigation, friction head losses, non-recoverable energy, and potentially recoverable energy in any line or hydrant in a network.

The method was demonstrated as applied to a real case. Considering consumption records from 2003 to 2014, an irrigation network in Valencia (Spain) has been analyzed in order to determine the dissipated and recoverable energy, observing that the energy footprint achieves maximum values of 2.85 kWh/m^3, being 79.7% of time under 0.3 kWh/m^3. The potential recoverable energy, instant power, recovering coefficients relating total with recoverable energy and frequency histogram of power are studied for any irrigation point, hydrant or line.

The maximum estimated potential recoverable energy sums to 188.23 MWh/year considering all the consumption points, and 178.1 MWh/year considering all the hydrants. If only one turbine were to be installed, the more convenient location is line 38, with a potential recovery of 89.99 MWh/year.

Future works should be undertaken to analyze the performance of real turbines in lines in order to propose a method to optimize the selection of turbines and the technical and economic involvements of such installations in different irrigation networks.

Acknowledgments: This paper has been possible with the free collaboration of the “Comunidad de Regantes Virgen de Gracia”. No additional funds have been received for this research. Authors thank the reviewers for their valuable comments, which have greatly contributed in the improvement of the document.

Author Contributions: All the authors have participated in any step of this research. Particularly a brief description is attached: The author Helena M. Ramos has contributed

supervising the state of the art description, flow assignation and energy implications of the present study. The author Francisco Javier Sánchez-Romero has been involved in the conception of the methodology for flow assignation and computational programming for *EPANET* Toolkit. The author Modesto Pérez-Sánchez has analyzed the flow data for proposing the final flow distribution, has implemented the data for *EPANET* Toolkit and analyzed the results for energy determination. The author: P. Amparo López-Jiménez has supervised the whole research and document and has been involved in final energy analysis of results and conclusions.

Conflicts of Interest: The authors declare no conflict of interest. The founding sponsors had no role in the design of the study; in the collection, analyzes, or interpretation of data; in the writing of the manuscript, and in the decision to publish the results.

References

1. Kahil, M.; Albiac, J.; Dinar, A. Improving the performance of water policies: Evidence from drought in Spain. *Water* **2016**, *8*, 34.
2. Llop, M.; Ponce-Alfonso, X. Water and agriculture in a Mediterranean region: The search for a sustainable water policy strategy. *Water* **2016**, *8*, 66.
3. Corominas, J. Agua y Energía en el riego en la época de la sostenibilidad. *Ing. Agua.* **2010**, *17*, 219–233.
4. Seoane, P.; Allué, R.; Postigo, M.J.; Cordón, M.A. *Boletín Mensual de Estadística*; Ministerio de Agricultura, Alimentación y Medio Ambiente; Madrid, Spain; 2013.
5. FAO. Agua Y Cultivos. Rome, Italy; 2002. Availiable online: http://www.fao.org/docrep/005/y3918s/y3918s10.htm. (accessed on 30 April 2016)
6. MAGRAMA. El riego localizado alcanza el 48.23% de la superficie regada en España. Minist Agric Aliment y Medio Ambient. Available online: http://www.magrama.gob.es/gl/prensa/noticias/el-riego-localizado-alcanza-el-4823--de-la-superficie-regada-en-espa%C3%B1a-/tcm7-312671-16. (accessed on 15 April 2016)
7. FAO. Superficie equipada para el riego. Available online: http://www.fao.org/nr/water/aquastat/infographics/Irrigation_esp.pdf. (accessed on 15 April 2016)
8. Pardo, M.A.; Manzano, J.; Cabrera, E.; García-Serra, J. Energy audit of irrigation networks. *Biosyst. Eng.* **2013**, *115*, 89–101.
9. Coelho, B.; Andrade-Campos, A. Efficiency achievement in water supply systems—A review. *Renew Sustain. Energy. Rev.* **2014**, *30*, 59–84.
10. Baki, S.; Makropoulos, C. Tools for energy footprint assessment in urban water systems. *Procedia Eng.* **2014**, *89*, 548–556.
11. Okadera, T.; Chontanawat, J.; Gheewala, S.H. Water footprint for energy production and supply in Thailand. *Energy* **2014**, *77*, 49–56.
12. Herath, I.; Deurer, M.; Horne, D.; Singh, R.; Clothier, B. The water footprint of hydroelectricity: A methodological comparison from a case study in New Zealand. *J. Clean. Prod.* **2011**, *19*, 1582–1589.

13. Endo, A.; Burnett, K.; Orencio, P. Methods of the water-energy-food nexus. *Water* **2015**, *7*, 5806–5830.

14. Mendoza-Grimón, V.; Hernández-Moreno, J.; Palacios-Díaz, M. Improving water use in fodder production. *Water* **2015**, *7*, 2612–2621.

15. Ramos, H.M.; Vieira, F.; Covas, D.I.C. Energy efficiency in a water supply system: Energy consumption and CO_2 emission. *Water Sci. Eng.* **2010**, *3*, 331–340.

16. Choulot, A. *Energy Recovery in Existing Infrastructures with Small Hydropower Plants*; FP6 Project Shapes (Work Package 5—WP5); European Directorate for Transport and Energy: Brussels, Belgium, 2010.

17. Carravetta, A.; Fecarotta, O.; Del Giudice, G.; Ramos, H. Energy recovery in water systems by PATs: A comparisons among the different installation schemes. *Procedia Eng.* **2014**, *70*, 275–284.

18. Carravetta, A.; Del Giudice, G.; Fecarotta, O.; Ramos, H. Pump as turbine (PAT) design in water distribution network by system effectiveness. *Water* **2013**, *5*, 1211–1225.

19. Carravetta, A.; Del Giudice, G.; Fecarotta, O.; Ramos, H.M. Energy production in water distribution networks: A PAT design strategy. *Water Resour. Manag.* **2012**, *26*, 3947–3959.

20. Carravetta, A.; Del Giudice, G.; Oreste, F.; Ramos, H. PAT design strategy for energy recovery in water distribution networks by electrical regulation. *Energies* **2013**, *6*, 411–424.

21. Ramos, H.; Borga, A. Pumps as turbines: an unconventional solution to energy production. *Urban Water* **1999**, *1*, 261–263.

22. Ramos, H.; Borga, A.; Simão, M. New design solutions for low-power energy production in water pipe systems. *Water Sci. Eng.* **2009**, *2*, 69–84.

23. Adhau, S.P.; Moharil, R.M.; Adhau, P.G. Mini-hydro power generation on existing irrigation projects: Case study of Indian sites. *Renew. Sustain. Energy Rev.* **2012**, *16*, 4785–4795.

24. Butera, I.; Balestra, R. Estimation of the hydropower potential of irrigation networks. *Renew. Sustain. Energy. Rev.* **2015**, *48*, 140–151.

25. Tilmant, A.; Goor, Q.; Pinte, D. Agricultural-to-hydropower water transfers: sharing water and benefits in hydropower-irrigation systems. *Hydrol. Earth Syst. Sci.* **2009**, *13*, 1091–1101.

26. Tarragó E., F.; Ramos, H. Micro-hydro solutions in Alqueva multipurpose project (AMP) towards water-energy-environmental efficiency improvements. Bachelor's Thesis, Universidade de Lisboa, Lisboa, Portugal, 2015.

27. Clément, R. Calcul des débits dans le réseaux d'irrigation fonctionnant á la demande. *La Houille Blanche.* **1966**, *5*, 553–575.

28. Mavropoulos, T.I. Sviluppo di una nuova formula per il calcolo delle portate di punta nelle reti irrigue con esercizio alla domanda. *Riv. Irrig. Dren.* **1997**, *44*, 27–35.

29. Maidment, D.R.; Hutchinson, P.D. Modeling water demands of irrigation projects. *J. Irrig. Drain. Eng.* **1983**, *109*, 405–418.

30. Alandi, P.P.; Pérez, P.C.; Álvarez, J.F.O.; Hidalgo, M.; Martín-Benito, J.M.T. Pumping selection and regulation for water-distribution networks. *J. Irrig. Drain. Eng.* **1997**, *131*, 273–281.

31. Aliod, R.; Eizaguerri, A.; Estrada, C. Dimensionado y análisis hidráulico de redes de distribución a presión en riego a la demanda: aplicación del programa GESTAR. *Riegos Dren. XXI* **1997**, *92*, 22–38.

32. Pereira, L.S.; Teixeira, J.L. *Modelling for Irrigation Delivery Scheduling: Simulation of Demand at Sector Level with Models ISAREG and IRRICEP*; FAO: Rome, Italy, 1994.

33. Lamaddalena, N.; Sagardoy, J.A. *Performance Analysis of On-Demand Pressurized Irrigation Systems*; FAO: Roma, Italy, 2007.

34. Rossman, L.A. *EPANET 2 User's Manual*; U.S. Environmental Protection Agency (EPA): Cincinnati, OH, USA, 2000.

35. White, F.M. *Fluid Mechanics*, 6th ed.; McGrau-Hill: Madrid, Spain, 2008.

36. Cabrera, E.; Cobacho, R.; Soriano, J. Towards an energy labelling of pressurized water networks. *Procedia Eng.* **2014**, *70*, 209–217.

37. Klein, G.; Krebs, M.; Hall, V.; O'Brien, T.; Blevins, B.B. *California's Water–Energy Relationship*; California Energy Comission: California, United States, 2005.

38. Shrestha, S.; Dhakal, S.; Shrestha, A.; Kaneko, S.; Kansal, A. Water-Energy-Carbon Nexus in Cities: Cases from Bangkok, New Delhi, Tokyo. In *Water Energy Food Nexus: International Cooperation and Technology Transfer*; Asian Institute of Technology: Paris, France, 2015.

39. Spadaro, J.V.; Langlois, L.; Hamilton, B. Greenhouse Gas Emissions of Electricity Generation Chains: Assessing the Difference. *IAEA Bull.* **2000**, *42*, 19–28.

40. Weisser, D. A guide to life-cycle greenhouse gas (GHG) emissions from electric supply technologies. *Energy* **2007**, *32*, 1543–1559

41. Arora, M.; Aye, L.; Malano, H.; Ngo, T. Water-energy-GHG emissions accounting for urban water supply: A case study on an urban redevelopment in Melbourne. *Water Util. J*. **2013**, *6*, 9–18.

42. Nair, S.; George, B.; Malano, HM.; Arora, M.; Nawarathna, B. Water–energy–greenhouse gas nexus of urban water systems: Review of concepts, state-of-art and methods. *Resour. Conserv. Recycl*. **2014**, *89*, 1–10.

43. Zema, D.A.; Nicotra, A.; Tamburino, V.; Zimbone, S.M. A simple method to evaluate the technical and economic feasibility of micro hydro power plants in existing irrigation systems. *Renew. Energy* **2016**, *85*, 498–506.

44. Castro, A. *Minicentrales Hidroeléctricas*. Instituto para la Diversificación y Ahorro de la Energía: Madrid, Spain, 2006.

45. Elbatran, A.H.; Yaakob, O.B.; Ahmed, Y.M.; Shabara, H.M. Operation, performance and economic analysis of low head micro-hydropower turbines for rural and remote areas: A review. *Renew. Sustain. Energy Rev.* **2015**, *43*, 40–50.

46. Derakhshan, S.; Nourbakhsh, A. Experimental study of characteristic curves of centrifugal pumps working as turbines in different specific speeds. *Exp. Therm. Fluid Sci.* **2008**, *32*, 800–807.

47. Moriasi, D.N.; Arnold, J.G.; Van Liew, M.W.; Binger, R.L.; Harmel, R.D.; Veith, T.L. Model evaluation guidelines for systematic quantification of accuracy in watershed simulations. *Trans. ASABE* **2007**, *50*, 885–900.

This page is intentionally left blank.

Appendices

Appendix III

CALIBRATING A FLOW MODEL IN AN IRRIGATION NETWORKS: CASE STUDY IN ALICANTE

Author version document which was published in index JCR Journal "Spanish Journal of Agricultural" ISSN 2171-9292. Impact Factor 0.76. Position 24/57 (Q2). Multidisciplinary.

Pérez-Sánchez, M., Sánchez-Romero, F., Ramos, H., López-Jiménez, P., 2017. Calibrating a flow model in an irrigation networks: Case study in Alicante. *Spanish J. Agric. Res.*, 15, 1, e1202,. doi:10.5424/ sjar/2017151-10144

This page is intentionally left blank.

ABSTRACT

The usefulness of models depends on their validation in a calibration process, ensuring that simulated flows and pressure values in any line are really occurring and, therefore, becoming a powerful decision tool for many aspects in the network management (*i.e.,* selection of hydraulic machines in pumped systems, reduction of the installed power in operation, analysis of theoretical energy recovery). A new proposed method to assign consumptions patterns and to determine flows over time in irrigation networks is calibrated in the present research. As novelty, the present paper proposes a robust calibration strategy for flow assignment in lines, based on some key performance indicators (*KPIF*) coming from traditional hydrological models (Nash-Sutcliffe coefficient (non-dimensional index), root relative square error (error index) and percent bias (tendency index)). The proposed strategy for calibration was applied to a real case in Alicante (Spain), with a goodness of fit considered as 'very good' in many indicators. *KPIF* parameters observed present a satisfactory goodness of fit of the series, considering their repeatability. Average Nash-Sutcliffe coefficient value oscillated between 0.30 and 0.63, average percent bias values were below 10% in all the range, and average root relative square error values varied between 0.65 and 0.80.

Keywords: water management; calibration model, Key Performance Indicators (*KPIF*);

1. Introduction

Currently, the management of water distribution networks (*WDNs*) is increasingly based on use of models as decision support tools, particularly in performance and energy efficiency implications (Rodriguez-Diaz *et al*., 2010; Arbat *et al*., 2013; Cabrera *et al*., 2014). When different database and mathematical algorithms are combined, these hydraulic models are an useful tool to analyze WDNs, if these models are properly calibrated.

Water management becomes more efficient when a deep knowledge of the network is done by modelling (Carravetta *et al*., 2012; Pardo *et al*., 2013; Cabrera *et al*., 2014; Butera & Balestra, 2015; Emec *et al*., 2015; Delgoda *et al*., 2016), increasing the sustainability of the whole system and decreasing the water footprint (Corominas, 2010; Ramos *et al*., 2010a,b). This knowledge of the network (mainly flows and pressure) allows the design of strategies to transform the WDNs in multipurpose systems (Choulot, 2010). For instance, the replacement of pressure reducing valves by hydraulic machines is an efficient solution, considering the feasibility in the investment (Ramos & Borga,

1999; Ramos *et al*., 2010a; Carravetta *et al*., 2012, 2013, 2014). The installation of hydraulic machines in existing networks is cheaper than the development of small similar hydropower stations. When already installed machines are used, the facilities (*e.g.,* reservoir, pipes, and excavation) are already done for satisfying the demand to users (Ramos & Borga, 1999).

Particularly, models become necessary to analyze the flow distribution over time at each pipe of the irrigation network. If discretized flows and pressures are known, energy balance can be obtained in any WDN. Throughout the 20th century, different authors have proposed and revised different methodologies to determine the maximum flows in on-demand irrigation networks and to design the pipe sizes (Clément, 1955; Boissezon & Haït, 1965; Granados, 1986; Lamaddalena & Sagardoy, 2000). Clèment (1955) develops the so called expression Clément's first formula, one of the most used to design on-demand irrigation networks. Boissezon & Haït (1965) introduce new terms in the Clément's first formula, in which the irrigation probability depends on crop rotation over year, with a mathematical method similar to Clément. Later, Clément (1966) developed the Clément´s second formula. This new method considers the time as variable. Both methods (Boissezons' methods and Clément´s second formula) do not provide great accuracy in the calculation, being the Clement´s second formula more complex than the first one (Clément, 1955; Granados, 2013). Afterwards, new methodologies have been developed by different authors, requiring a high database treatment. These methods are based on increasing computers capacity. For instance, Moreno *et al*., (2007) propose random generation of scenarios with different hydrants opened in the network. In other cases, flows are determined by computational neural networks or genetic algorithms (Pulido *et al*., 2003; Martínez-Solano *et al*., 2008).

The need for determining flows and pressure over time at any line or joint has contributed to the use of models, which are increasingly getting common (Ritter *et al*., 2009). Nevertheless, the reliable use of these models must be exposed to a correct and systematic calibration process, generally related with the study of pressures and roughness (Braun *et al*., 2010; Tabesh *et al*., 2011). Some models for determining flows can be found in the references consulted (*e.g.,* the method presented by Preis *et al*. (2009)). This method uses a statistical data-driven algorithm to estimate the circulating flow, being necessary that an SCADA (supervisory control and data acquisition) is installed in the irrigation network. Other similar studies have been developed by different researchers (Datta & Sridharan, 1994; Clark & Wu, 2006; Davidson & Bouchart, 2006; Ghiassi *et al*., 2008; Sanz & Perez, 2014, 2015).

Generally, these systems have pressure and flow sensors installed, which is located in different points of the network. These sensors transmit to *SCADA* the registered data. Existence of these measurement devices allows the application of computational methods, which determine the flows using the database of *SCADA* to correct the predicted values by the analytical methods. Unfortunately, most of irrigation networks do not generally have these control elements installed as consequence as idiosyncrasy of

the agricultural sector. This fact hinders the flow control along the water management process.

When the water managers do not have information about the flows in the network, other strategies for calibrating the model must be developed. A calibration is defined as a process of changing values for certain input parameters in an attempt to match some reference conditions within acceptable criteria (Mulligan & Brown, 1998). This is a difficult task, as a model is an idealization of the reality, in which the real behavior is hoped to be simulated by mathematical modelling. Thus, calibration is of utmost importance in determining the reliability of any method to ensure its future use as a decision tool.

A strategical method for calibration is therefore needed to avoid trial and error procedures. To determine the goodness fit of model, some indicators must be used to estimate errors between observed estimated values. The evaluation of the ability prediction in a particular a model should contain an error index, a non-dimensional index and a graphic method between the observed values (O) and simulated values (P) (Legates & McCabe, 1999).

In this research, a new methodology to determine distribution flows over time in any line by a numerical model is presented. This method which is based on farmers' habits, allows the knowledge of flows over time, when no sufficient measurement devices are installed in the network. Unfortunately, the lack of flow measurement devices is a very common situation in irrigation networks, especially in systems older than 20 years as consequence as technology was more expensive two decades ago and water managers were not aware of the need to increase hydraulic efficiency in the *WDN*. As novelty in this manuscript, the calibration process of this method is described, dealing with time series of values. To do so, the implementation of calibration indexes adopted from traditional hydrological studies is proposed. Different authors (Nash & Sutcliffe, 1970; Willmott, 1981; Gupta *et al*., 1999; Legates & McCabe, 1999; Singh *et al*., 2005; McCuen *et al*., 2006;) proposed different statistical indexes of 'goodness of fit', which were applied in this strategy. This calibration method, as far as the consulted references depict, is initially applied to calibrate flows in irrigation water distribution networks. This calibration was based on flow time series registered, contrasting estimated with measured data set. The results were very promising for calibrating of this model, transforming the model in a reliable decision making tool for water managers.

The proposed strategy was used to determine the assignment of flow in a particular case study focused on an irrigation network allocated in the township of Callosa d'en Sarrià, in Alicante (Spain).

2. Material and methods

2.1 Methodology for flow assignation

In this section, the assignation flows method was described as well as calibration strategy was also proposed. Flows variability in the irrigation network was high as the consumption, which depended on many factors along the year (*e.g.,* weather conditions, type of crops, habits of farmers, among others).

The method determined the irrigation probability (P_I) at each irrigation point of the network and simulated the operation of any network, which was based on the generation of demand in consumption points (Pérez-Sánchez *et al*., 2016). The method considered the irrigation needs of the crops and the farmers' habits to generate the P_I (*e.g.,* weekly trend of irrigation, watering duration, maximum days between irrigations and hour of time start irrigation). Farmers' habits were obtained from: interviews to farmers, records of water meter, and records of flowmeters installed in the network. The information asked in interviews (*e.g.,* irrigation crop, maximum days between irrigation, irrigation weekly trend) were described by Pérez-Sánchez *et al*., 2016. The aim of the method was to generate the consumption patterns for all irrigation points over year by following the next steps (Figure 1).

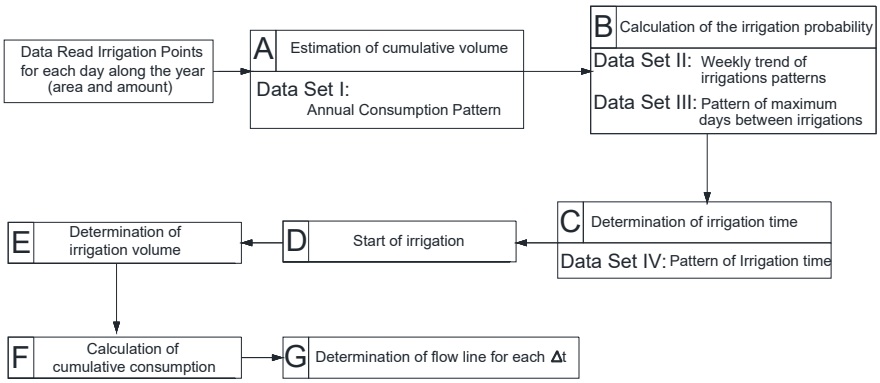

Figure 1. Schematic description of the method for flow estimation at each irrigation point

A. Estimation of the cumulative volume consumed in the irrigation point

The cumulative volume consumed was estimated by the comparing the previous irrigated volume and the irrigation needs. This volume was individually assigned to all the irrigation points (Data Set I). If the balance (V_{Na}) at each irrigation point was positive, the method established that this was not an irrigation day. If the balance was negative, the method goes to step *B*, and the P_I was calculated in this consumption point. The calculus of irrigation needs was developed according to Allen *et al*., (2006). In this case,

the climatic data (*i.e.,* temperature, wind, humidity, and rainfall) have been obtained from their own weather station, installed within the irrigated surface.

B. Calculation of the irrigation probability (P_I)

The P_I was based on two functions: irrigation weekly pattern (w_{dj}, Data Set II), and patterns of maximum days between irrigations (d_d, Data Set III). Both functions were obtained from interviews. Furthermore, the method generated a random number (*RN*) between zero and one. The generation of this *RN* is uniform, but the opened law was established by the function irrigation weekly trend (Data Set II) and maximum days between irrigation (Data Set III). The irrigation was only carried out if $RN \leq P_I$ (Pérez-Sánchez *et al*., 2016). The P_I is defined by equation (1).

$$P_I = \frac{w_{dj}}{\sum_{n=1}^{n=d-j+1} w_{dn}} \quad (1)$$

where *d* is the numbers of days inside of irrigation interval, and j is the day of decision making. On the one side, w_{dj} is the pattern to irrigate one particular day inside the interval. This pattern is an integer number which shows the irrigation trend of that day related to the rest of days of the week. This trend was defined according to farmer's habits (Data II). On the other side, $\sum_{n=1}^{n=d-j+1} w_{dn}$ is the total addition of patterns of the days included in the irrigation interval, according to Data Set III.

C. Determination of the irrigation time

The interviews allowed to establish the irrigation time. This value depends on irrigation needs (Data Set I) and irrigation amount (i_i). This irrigation amount is considered as the average flow rate unit of consumption in each irrigation plot of the irrigated surface.

The method considered the number of on-farm irrigation sectors. On the one hand, the number of sectors has been considered to develop the trends of irrigation. On the other hand, the number of sectors was implicit in the irrigation time, because the irrigation needs of the crops and the average unit consumption flow had units of volume per surface.

The irrigation unit discharge (i_i) depends on the planting layout (area defined by the space between rows of the plantation), determining the number of plants per hectare (n_p), the number of drippers per plant (n_d) and the dripper discharge (d_d) in l/h. This parameter was defined by equation. [2]

$$i_i(l/(s \cdot ha)) = n_p \cdot n_d \cdot d_d \cdot \frac{1}{3600} \quad (2)$$

The irrigation time (t_r) depends on daily irrigation needs of crops (V_c) and the irrigation unit discharge (i_i). Both parameters define the irrigation time in each hydrant by equation (3):

$$t_r(s) = \frac{V_c}{i_i} \quad (3)$$

D. Start of irrigation

The method determined the start time of irrigation for each irrigation point. The cumulative probability pattern was used in this step. These patterns were defined by twenty-four intervals (one per hour) and they were also defined from interviews performed to farmers. A new *RN* was generated between zero and one, and it was compared with cumulative probability patterns. This *RN* established the start irrigation period, considering the irrigation time within the selected day and the maximum days between irrigations (Data Set III). The irrigation time depended on daily irrigation needs of crops (V_c) and the irrigation unit discharge (i_i), as was described in Step C. After this step, the day and hour for the irrigation to start is known for each consumption point.

E. Determination of irrigation volume

In this step, the irrigation volume was determined from the irrigation supply and the irrigation time (step C).

F. Calculation of cumulative consumption

The volume of cumulative consumption was calculated.

G. Determination of flow line

When all consumption patterns have been determined during the year, the flow was calculated by *EPANET* toolkit (Rossman, 2000). This tool calculated the circulating flow in each line considering the demanded flow of the opened irrigation points downstream in each instant. The demanded flow at each irrigation point depends on irrigation unit discharge (i_i) and surface of the opened tap, being the addition of these flows in each hydrant equal to the circulating flow by the same in each interval time.

2.2. Evaluation of goodness of fit

The method used to evaluate the goodness of fit, is focused on:

1. Graphic representation of the observed values (O) vs simulated values (P).
2. Determination of the Nash-Sutcliffe coefficient (E). This non-dimensional index is a fit indicator, which is recommended in the calibration of hydrologic models and simulations of temporal series. The value of E can oscillate within the interval $-\infty \leq E \leq 1$. The goodness of fit is optimal if $E=1$. If the index was inside of a range between zero and one, E was accepted as good indicator. Negative values of E are considered poor. The Nash-Sutcliffe index is defined by equation (4):

$$\mathrm{E} = 1 - \frac{\sum_{i=1}^{N}[O_i - P_i]^2}{\sum_{i=1}^{N}[O_i - \bar{O}_i]^2} \quad (4)$$

where O_i is the observed value in each interval; $\bar{O}_i$ is the average of the observed values; and P_i is the simulated value in each interval. These values were obtained from the model.

3. Determination of the root relative squared error (*RRSE*). This non-dimensional index quantifies the prediction error of the model with the normalized variable. If *RRSE* is zero, this value indicates a perfect fit. Low values of *RRSE* indicate that the root mean square error (*RMSE*) is minor, meaning the performance of the model simulation is better. *RRSE* is defined by equation (5):

$$RRSE = \sqrt{\frac{\sum_{i=1}^{N}[O_i - P_i]^2}{\sum_{i=1}^{N}[O_i - \bar{O}_i]^2}} \quad (5)$$

4. Determination of bias percentage (*PBIAS*). This parameter measures the tendency of the simulation and determines if the simulated values are smaller or larger than observed values. Negative values indicate that the model overestimates the variable analyzed; positive values indicate that the variable is underestimated, and a *PBIAS* equal to zero is optimal. This index is defined by equation (6):

$$PBIAS\ (\%) = \frac{\sum_{i=1}^{N}[O_i - P_i] * 100}{\sum_{i=1}^{N}[O_i]} \quad (6)$$

The goodness analysis of the temporal simulated series is established in Table 1, according to developed analyses by researches of Moriasi *et al*., (2007) and Cabrera (2009). These authors classified the goodness of fit in four categories: very good, good, satisfactory, and unsatisfactory. These categories depend on the value of previously enumerated parameters (*i.e., E*, *RRSE*, and *PBIAS*). Furthermore, the estimations of *E*, *RRSE*, and *PBIAS* will be nominated as key performance indicators for goodness of fit (*KPIF*) in this calibration strategy.

Table 1. Classification of goodness of fit, according to Moriasi et al. (2007) and Cabrera (2009)

Goodness of fit	**Nash-Sutcliffe (*E*)**	**Root Relative Squared Error (*RRSE*)**	**BIAS Percentage (*PBIAS*)**
Very good	$E>0.6$	$0.00 \leq RRSE \leq 0.50$	$PBIAS < \pm 10$
Good	$0.40 < E \leq 0.60$	$0.50 < RRSE \leq 0.60$	$\pm 10 \leq PBIAS < \pm 15$
Satisfactory	$0.20 < E \leq 0.40$	$0.60 < RRSE \leq 0.70$	$\pm 15 \leq PBIAS < \pm 25$
Unsatisfactory	$E<0.20$	$RRSE>0.70$	$PBIAS > \pm 25$

The goodness of fit in the calibration was based on the peak flows value for different time intervals. This time interval was the step in which the developed model was discretized, and it can oscillate between 1 h and 336 h. Simulated values reached then the maximum observed values.

Finally, variability of the goodness of fit indexes was analyzed in the calibration proposed. This analysis was of paramount importance, as the proposed method was based on randomness in the opening at each irrigation point. To analyze this variability, the model was run 200 times for the same irrigation scenario (*i.e.,* annual consumption pattern, weekly trend of irrigation patterns, maximum days between irrigations, and pattern of irrigation time). The repetition allowed the analysis of average and standard deviation of the sample.

2.3 Case study

A drip irrigation network located in Callosa d'en Sarrià (Alicante, Spain) was proposed to illustrate the calibration procedure method for the flow assignment model. The network supplies 120 hectares, with water coming from a well (Figure 2).

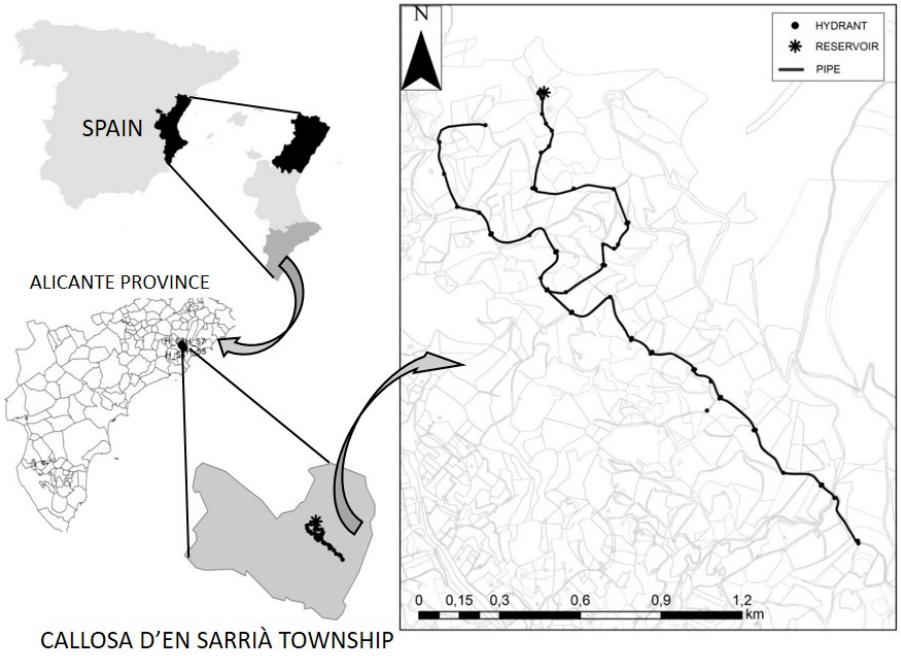

Figure 2. Location of the irrigation network

The most extended crop is loquat (*Eryobotrya japonica* [Lindl.]), although there is a small area with citrus and avocado pear trees. The water is accumulated in a reservoir with a capacity of 4000 m^3. The topography varies between 273 and 102 m above sea level. The tank is located sufficiently high (278 m above the sea level) to ensure the minimum pressure head of 30 m in every irrigation point.

The pipelines of the network are built on asbestos cement pipes, with diameters ranging between 200 and 250 mm. The installation has 34 multiuser hydrants, supplying to 143 irrigation points, connected to steel collector in the hydrant by polyethylene pipes. Counters were placed to register the consumption volume in all hydrants. On the one hand, the data of a flowmeter installed in the main line of the network were registered for every 5 minutes in year 2015, summing up a total of 105120 values. On the other hand, the water manager has data enabling the definition of the inputs, previously described in the method (Figure 1):

- Data Set I - Quarterly consumption in each irrigation point. This pattern was obtained from records of the water metered at each irrigation point. In each plot, registers were taken quarterly corresponding to the months of March, June, September and December of year 2015. Irrigation area, number of irrigation sector, and type of crop was also known for each plot of crop the irrigation area.
- Data Set II - Weekly trend of irrigation patterns. The weekly trend of irrigation has been defined from flowmeters records. Ratio among daily consumed volume and weekly consumed volume were obtained for each day, defining 52 weekly trend of irrigations patterns (one per week of year).
- Data Set III - Pattern of maximum days between irrigations. These patterns have been developed from the farmers´ habits. These habits (based on patterns described in Pérez-Sánchez *et al.,* 2016, after a surveys campaign) were established by agronomic engineer, according to meteorological station data located at Experimental plot of Cooperative of Callosa d'en Sarrià.
- Data Set IV - Pattern of irrigation time. This time was determined by equation (3). The irrigation needs of crops were obtained throughout irrigation schedules which were provided by technical service of the irrigation community. These irrigation needs were adapted over year, considering climatic parameters as well as an application efficiency (defined as the ratio between accumulated volume in root bulb and applied volume in the plot) of 0.754. This datum has been obtained from river Jucar's basin management plan (BOE, 2016).

3. Results

3.1 Calibration parameters

Flow variability in irrigation networks is due to many factors which have been previously enumerated (*i.e.,* weekly trend of irrigation, watering duration, maximum days between irrigations, and hour of time to start irrigation). Among them, the *i* was determinant, as can be observed in Figure 3a. This figure shows the obtained result of maximum estimated flows when the factors (maximum days between irrigations and *i*) were changed in the case study.

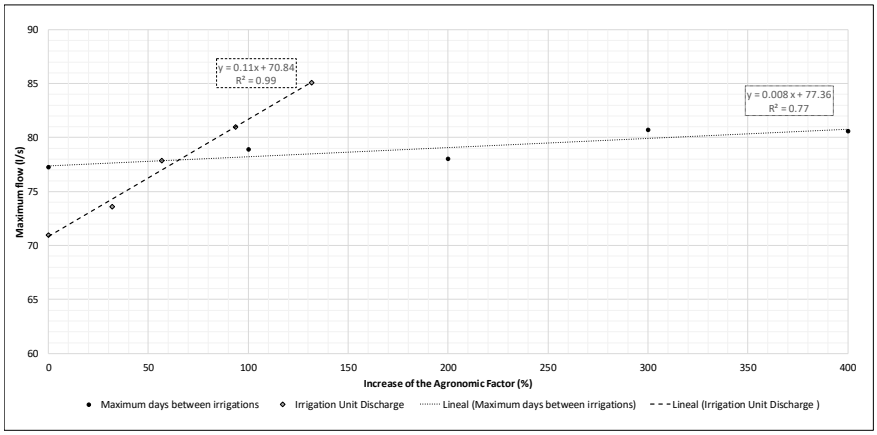

(a)

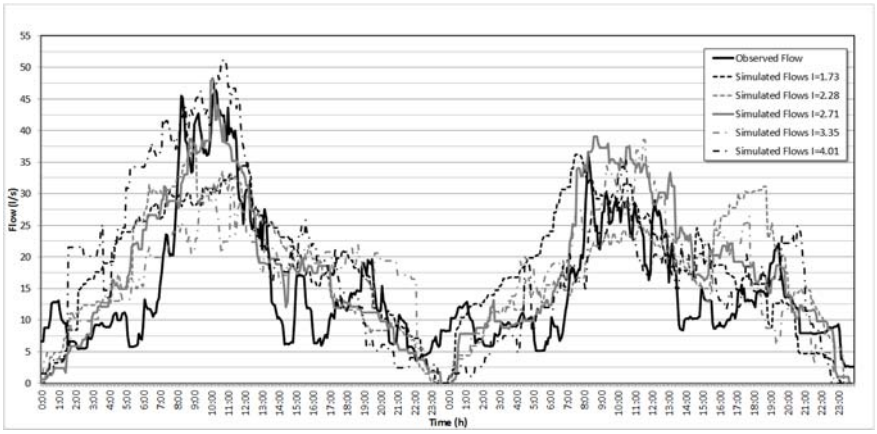

(b)

Figure 3. (a) Maximum flow *vs* increment of different irrigation unit discharges (*i*) and maximum days between irrigations in Callosa d'en Sarrià. (b) Observed and simulated flows with different irrigation unit discharges (*i*).

The importance of *i* in the maximum flow values was obvious when simulated values were compared with observed data. Other factors (*e.g.,* maximum days between irrigations) were not so sensitive to changes in maximum flow rates.

These variations can be seen in Figure 3b, where the variation of the *i* modified the estimated flow significantly, when these flows were compared to observed ones.

3.2 Calibration results

Once the flow was calculated at each line, the goodness of fit was evaluated using the observed data. Irrigation characteristics were considered (*i.e.,* maximum days between irrigation, weekly trend of irrigation, and patterns of start irrigation) for 2015, with

different values for i as a calibration parameter. Irrigation supply value was established from different planting layouts, number and characteristics of drippers used in the area. Table 2 shows the *i* values that depend on the different parameters defined by equation (2). These parameters were selected according to the common agricultural design in different plots of crop, considering irrigated surface.

Table 2. Irrigation unit discharge (*i*) depending on planting layouts

Planting layout (m × m)	n_p **(tree/ha)**	n_d **(dripper/tree)**	d_d **(l/h)**	i_i **(l/(s·ha))**
6.0 × 6.0	312.11	5	4	1.73
4.5 × 6.0	410.26	5	4	2.28
4.5 × 5.0	487.67	5	4	2.71
4.0 × 4.5	603.78	5	4	3.35
3.0 × 5.0	721.00	5	4	4.01

The exposed procedure in section 'Evaluation of goodness of fit' was used in the analyses. Figure 4a shows the values of *E* depending on irrigation amount (defined in Table 2) and different hourly intervals calculations (from 1 h to 336 h). This analysis allowed determining *i* that best simulates the maximum flows compared to the maximum observed flows for the studied interval. *E* values oscillated between -0.1 and 0.65 (Figure 4a) depending on i and time interval. *E* values obtained were positive in all range when *i* was 2.28, 2.71, or 3.35 l/(s·ha). According to Table 1, if $E > 0.2$, the goodness of fit is satisfactory.

Figure 4b shows *PBIAS* values obtained; i=1.73 l/(s·ha) had *PBIAS* values between 5 and 20%. If irrigation supply was 2.28 l/(s·ha), the index oscillated within 3% and 15%. *PBIAS* obtained was near to zero when i was 2.71 l/(s·ha), and the majority of times, *PBIAS* was below to 5% (except the interval of 12 and 24 h). *PBIAS* were negative with *i* values of 3.35 and 4.01 l/(s·ha), in which *PBIAS* oscillated between 0 and -10% (except for the time interval of 12 and 24 h, with irrigation supply of 3.35 l/(s·ha), in which *PBIAS* value was 3.01% and 4.25%, respectively).

Figure 4c shows *RRSE* values for calibration evaluation. These *RRSE* values oscillated between 0.60 and 1.05, depending on i and time interval. Results obtained for *i*=2.71 l/(s·ha) presented values between 0.6 and 0.80 in all range of time interval (Figure 4c).

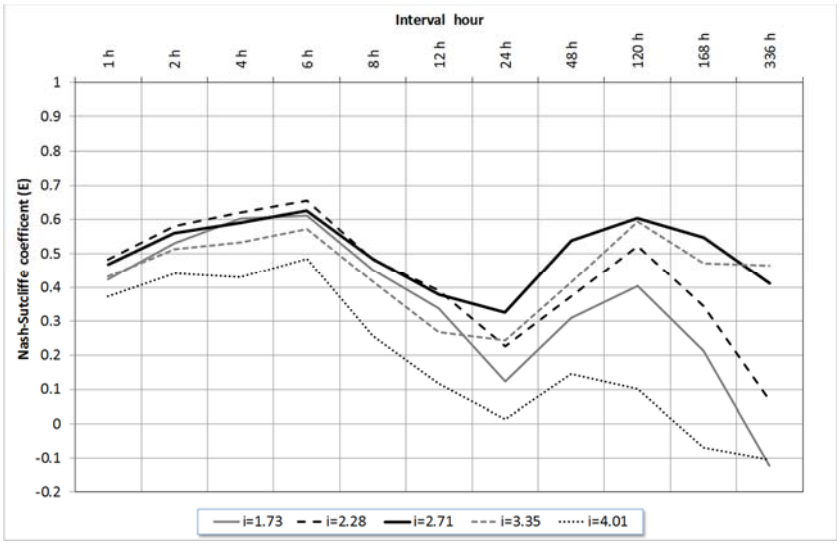

(a)

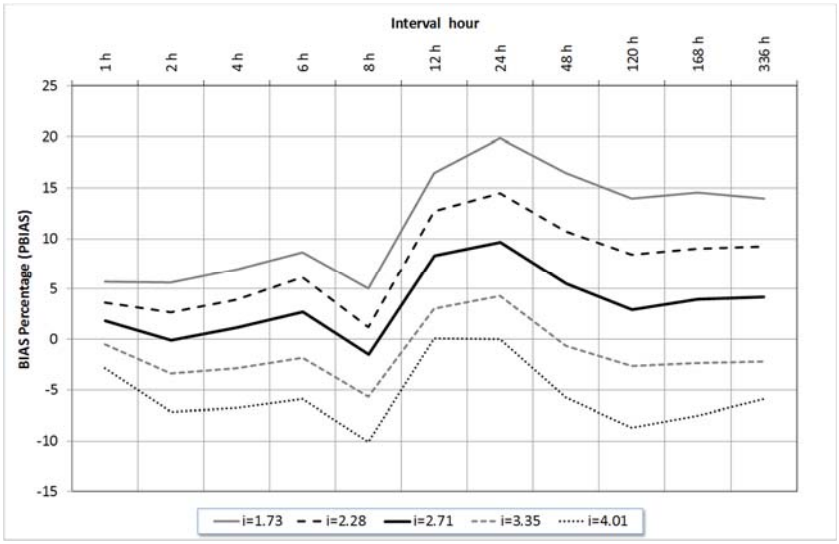

(b)

Figure 4. Nash-Sutcliffe coefficient, *E* (a), bias percentage, *PBIAS* (b) and root relative squared error, *RRSE* (c) depending on irrigation unit discharge (*i*) predicting maximum flows. (Continue in next page)

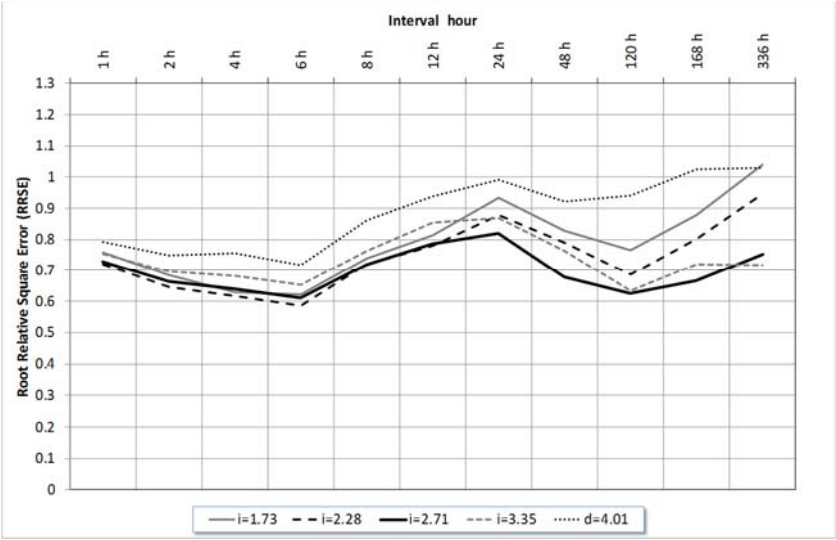

(c)

Figure 4. (Cont.) Nash-Sutcliffe coefficient, *E* (a), bias percentage, *PBIAS* (b) and root relative squared error, *RRSE* (c) depending on irrigation unit discharge (*i*) predicting maximum flows

Figure 5 depicts observed flow data and simulated values, considering *i*=2.71 l/(s·ha). This figure represents averaged hourly flow (observed *vs* simulated), and they present a $R^2 = 0.503$. This figure completes the necessary parameters to evaluate the goodness of fit of a temporal series according to the method described in section 'Evaluation of goodness of fit' (graphic representation, non-dimensional index, error index and tendency index).

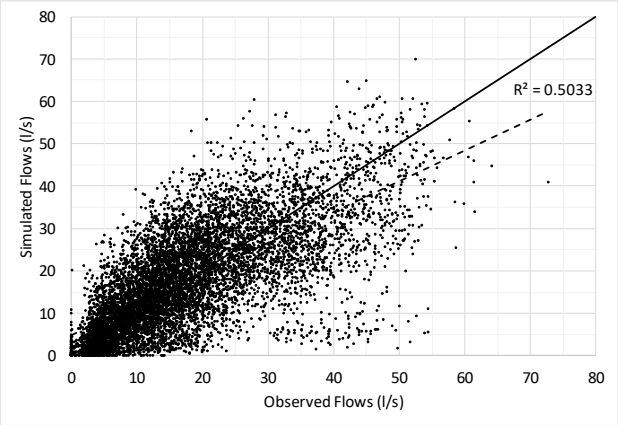

Figure 5. Visual comparative between average observed flows and average simulated flow with irrigation amount equal to 2.71 l/(s·ha).

Finally, Figure 6 shows the range of oscillation obtained in all *KPIF* parameters when the case study was simulated 200 times, considering i=2.71 l/(s·ha). The randomness in the opening of the irrigation points was only factor that varied along different simulations. *KPIF* parameters oscillation can be observed within very constrained intervals in Figure 6. This variability did not affect the results of goodness of fit of the series. Average *E* value oscillated between 0.30 and 0.63. Average *PBIAS* value was below 10% (very good, Table 1) in all the range. *RRSE* (root relative square error) presented average values between 0.65 and 0.80.

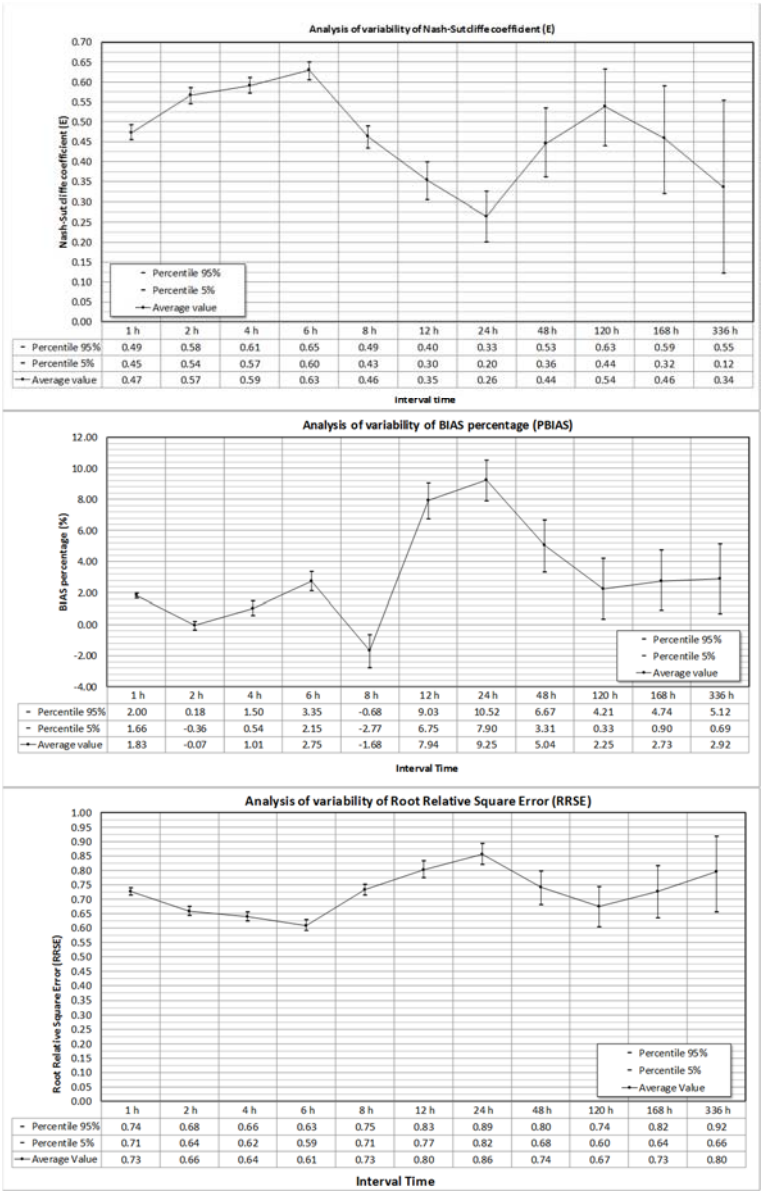

	1 h	2 h	4 h	6 h	8 h	12 h	24 h	48 h	120 h	168 h	336 h
Percentile 95%	0.49	0.58	0.61	0.65	0.49	0.40	0.33	0.53	0.63	0.59	0.55
Percentile 5%	0.45	0.54	0.57	0.60	0.43	0.30	0.20	0.36	0.44	0.32	0.12
Average value	0.47	0.57	0.59	0.63	0.46	0.35	0.26	0.44	0.54	0.46	0.34

	1 h	2 h	4 h	6 h	8 h	12 h	24 h	48 h	120 h	168 h	336 h
Percentile 95%	2.00	0.18	1.50	3.35	-0.68	9.03	10.52	6.67	4.21	4.74	5.12
Percentile 5%	1.66	-0.36	0.54	2.15	-2.77	6.75	7.90	3.31	0.33	0.90	0.69
Average value	1.83	-0.07	1.01	2.75	-1.68	7.94	9.25	5.04	2.25	2.73	2.92

	1 h	2 h	4 h	6 h	8 h	12 h	24 h	48 h	120 h	168 h	336 h
Percentile 95%	0.74	0.68	0.66	0.63	0.75	0.83	0.89	0.80	0.74	0.82	0.92
Percentile 5%	0.71	0.64	0.62	0.59	0.71	0.77	0.82	0.68	0.60	0.64	0.66
Average Value	0.73	0.66	0.64	0.61	0.73	0.80	0.86	0.74	0.67	0.73	0.80

Figure 6. Analysis of key performance indicators for goodness of fit (*KPIFs*) variation with an irrigation amount equal to 2.71 l/(s ha) and predicting maximum flows with two-hundred randomness simulations

4. Discussion

In this research, a method to determine irrigation circulating flow along the time in the network has been implemented (Pérez-Sánchez *et al*., 2016). This method allows water managers to know the flows in any pipe of a pressurized system discretized in the time, considering from irrigation needs and farmer's habit (*i.e.,* weekly trend of irrigation, maximum days between irrigation, irrigation time and pattern of start irrigation) when flow measurements are not available. *RN* generation (defined in Step B). Calculation of the P_I. Fig. 1 is uniform, varying between zero and one, when the P_I was determined by equation (1). This equation considers weekly trend irrigation and maximum days between irrigation and, therefore, indirectly, the distribution of climatic variables was also considered. This fact can be observed if the relative frequency histogram of flow is drawn when this method is applied (Pérez-Sánchez *et al*., 2016).

Proposed method randomly determined the opening time at each irrigation point, based on farmer's habits (Data Sets II and III). Unlike traditional methods (Clément, 1965; Boissezon & Haït, 1965; Soler *et al*., 2016), operating probabilities were constant at each tap for the analyzed time interval (Soler *et al*., 2016). Described method also determines the instantaneous flow, whilst other traditional methods only obtain the maximum flow (*e.g.,* if the applied method is Clément, the obtained flow is the value corresponding with the percentile of 95%).

A sensitivity analysis was performed, determining that unit discharge was the most important parameter in the flow assignment in lines, over other considered aspects for calibration. This parameter depends on type of crops, planting layout, installed irrigation system, and other agricultural factors (Granados, 2013), being essential to determine the maximum circulating flow in different design methods used in irrigation networks (Granados *et al*., 2015). Demand flow at each irrigation point depended on *i* when Clément first formula was applied (Clément, 1966). Figure 3a shows this sensitivity analysis of maximum flows when i and maximum days between irrigation were varied. As can be seen, on the one hand when Δi=100%, the variation of maximum flow was 11 l/s (15.49% of main flow). This hypothesis was confirmed when the maximum flow was calculated by the generalized Clément first formula, in which probabilities values are directly proportional to *i* (Lamaddalena & Sagardoy, 2000). In contrast, when the increment of maximum days between irrigations was 100%, the variation of maximum flow was 1.6 l/s (2.15% of main flow). The analysis of flows variation depending on maximum days between irrigations were described in Pérez-Sánchez *et al*. (2016). The obtained results in the sensitivity analysis showed that variation of flows was minimum, when maximum days between irrigation were modified. This variation was negligible when compared to the measurement errors of the flowmeter and water meters.

According to the foregoing, Figure 3b shows the variability of the simulated flows when they were compared with the observed values (13-14 Oct, 2015). A first visual comparison shows that some irrigation values for unit discharge underestimated the results of flow (*e.g.,* 1.73 l/(s ha)), while other i values (*e.g.,* 4 l/(s ha)) overestimated

main flow when compared to observed data. In Figure 3b also shows the importance of the irrigation supply in the maximum flows, meaning that goodness of fit evaluation must consider maximum flows along time, whilst minimum flows were trivial (null or close to zero). Therefore, maximum flows were almost insensitive to big variations of maximum days between irrigation. On the contrary, these flows substantially changed when i was slightly modified. As a consequence, here, the parameter to be adjusted in this calibration strategy was i, in order to fit the predictions to the observed values.

As a novelty, in this calibration process for irrigation *WDNs* modeling, some parameters have been proposed for estimating the goodness of fit. These have been called 'key performance indicators for goodness of fit (*KPIF*) (*i.e., E, RRSE* and *PBIAS*). These parameters have usually been used in hydrological analysis with good results (Legates & McCabe, 1999; McCuen *et al*., 2006). As previously justified, the calibration of the proposed method has only been established depending on *i*. This agronomic parameter is the most important one in the pipe´s sizing in networks (Granados *et al*., 2015), considering that others factor as irrigation time and irrigated volume depend on it (Clément, 1966). In addition, *i* is a crucial factor in the analysis of flows over year (Fig. 3b).

According to Figure 4 the model simulation had an optimal fit when i was 2.71 l/(s·ha). For this value, *KPIF* parameters were the best in the calculated series. If i <2.71 l/(s·ha), *PBIAS* values were higher than 5%. These positive *PBIAS* values indicate that the proposed method slightly undervalued the maximum flows (Moriasi *et al*., 2007). When irrigation supply reached values greater than 2.71 l/(s·ha), the simulation overestimated maximum flows values (Figure 3b). If *PBIAS* values are compared with the obtained index by these researchers (Moriasi *et al*., 2007), the first ones were nearer to zero and, therefore, the proposed calibration made better estimations. When *E* was analyzed, the optimal values were obtained for i = 2.71 l/(s·ha). Values obtained were positive (higher than 0.45 for maximum flows) for all studied interval time, being more precise when they were compared to values obtained in the hydrologic model proposed by Ritter *et al*. (2008), as well as the obtained indexes in the hydrologic and hydroclimate model developed by Legates & McCabe (1999). Obtained parameters were lower and even negative when other i values were considered. Negative values indicated that the goodness of fit was unsatisfactory, as stated in Cabrera (2009).

Finally, the lowest values of *RRSE* corresponded to i = 2.71 l/(s ha) (Figure 4c), which is the optimal fit. *RRSE* values were greater if these were compared to values obtained in the hydrologic calibration developed by Singh *et al*. (2005).

In this case, the necessary number of data included in the different Data Sets was high because the objective was an exhaustive calibration process. However, if Data Sets I, II or III are not exactly defined, then, *KPIF's* results are satisfactory for predicting average flows, but non-satisfactory for predicting maximum flows, which are the most important.

As instance, in the first place, when Data Set I was varied (considering double irrigation needs), *KPIF* results were 0.63, 0.61, and -0.01 (*E*, *RRSE* and *PBIAS* respectively) for average flows. These values were considered satisfactory according to Table 1. With these values for irrigation needs, *KPIF* values to maximum flows were: 0.47, 1.21, and 12.42 (*E*, *RRSE* and *PBIAS* respectively). These values were considered satisfactory according to Table 1.

In the second place, when Data Set II was simplified (uniform irrigation trend), obtained *KPIF* values were 0.93, 0.23, and 0.14 (*E*, *RRSE* and *PBIAS* respectively) for average flows. These values were considered satisfactory according to Table 1. Same Data Set II were used to obtain *KPIF* values for maximum flows. In this assumption, *E*, *RRSE*, and *PBIAS* were -0.02, 1.01, and 11.78 respectively. These values were considered non-satisfactory according to Table 1.

In the third place, when Data Set III was simplified (with uniform interval of 1 day between irrigations), *KPIF* values related to average flows were 1.00, 0.01, and -0.01 for *E*, *RRSE*, and *PBIAS*, respectively. These values were considered satisfactory according to Table 1. If *KPIF* values to maximum flows were determined, obtained results were 0.38, 0.78, and 5.64 for *E*, *RSR*, and *PBIAS*, respectively. These values were considered non-satisfactory according to Table 1.

When *KPIF* parameters were estimated for this *WDN* by means of reiterations (simulated 200 times), the goodness of fit was considered satisfactory for time intervals lower than 2 and 4 h. The intervals of 1 h and 8 h had satisfactory indexes of *E* and *PBIAS*, but *RRSE*> 0.70 (the range of values was 0.71-0.75 in Fig. 6). If greater time intervals were considered (>8 h), *E* and *PBIAS* values continued positive ($E > 0.2$ and $PBIAS < \pm 15\%$). These values established a satisfactory goodness of fit according to Moriasi *et al*., (2007) and Cabrera (2009), but the values of *RRSE* were higher than 0.70 (oscillating between 0.72 and 0.87).

If the average simulated flows were analyzed with i=2.71 L/(s ha), *E* oscillated between 0.37 and 0.41 for interval of one hour (these values were extracted of the variability analysis). *PBIAS* for this interval was -0.008% and *RRSE* varied between 0.76 and 0.78 (Fig. 4). These values have a good goodness of fit, except the *RRSE* value. If time interval greater than one hour was considered, *E* was higher than 0.47, $PBIAS = 0.008\%$, and $RRSE < 0.69$ (these values were for time interval of 2 h; if the interval time increased, the statistical parameters improved the goodness of fit). Goodness of fit was considered good and very good for average flow and interval of 1 and 2 h, according to criteria presented in Table 1. *E* obtained by Moriasi *et al*., (2007) for average flows were lower than obtained values in this calibration. The obtained results with average flows were more precise than statistical indexes obtained with maximum flows, considering in both cases $i = 2.71$ l/(s ha).

The statistical analysis finalized with the verification of the visual goodness of fit, which was confirmed in Figure 5, in which the determinant coefficient of maximum flows

observed versus maximum flows estimated was $R^2 = 0.503$. This value was similar to the obtained value in the hydrological calibration of temporal series in synthetic models (Abbasi *et al*., 2004). R^2 was used to carry out the first visual comparison between observed and simulated values.

The reiteration of the performed analysis (Figure 6) showed method proposed was robust. If flow values obtained were compared to those obtained by Clément's Method (Clément, 1966), results were similar. The results used to compare both methods were the flow values obtained on June (month in which irrigation needs were maximum). On the one hand, the Clément's flow was 52.87 l/s (Clément, 1966), according to individual probability at each tap (Figure 7). The opening probabilities oscillate between 0.08 and 0.32 in this network, according to characteristics in each one of 143 taps. On the other hand, the maximum obtained flow with proposed method to estimate flows over time varied between 47.67 and 54.09 l/s, depending on habit's farmers. These probabilities were different and independent to Clément's method. When 200 repetitions were considered, the average obtained flow was 50.17 l/s. The cumulated frequency of flow depicted in Figure 7 showed a better fit (when compared to observed values) than cumulated frequency obtained by Clément's method.

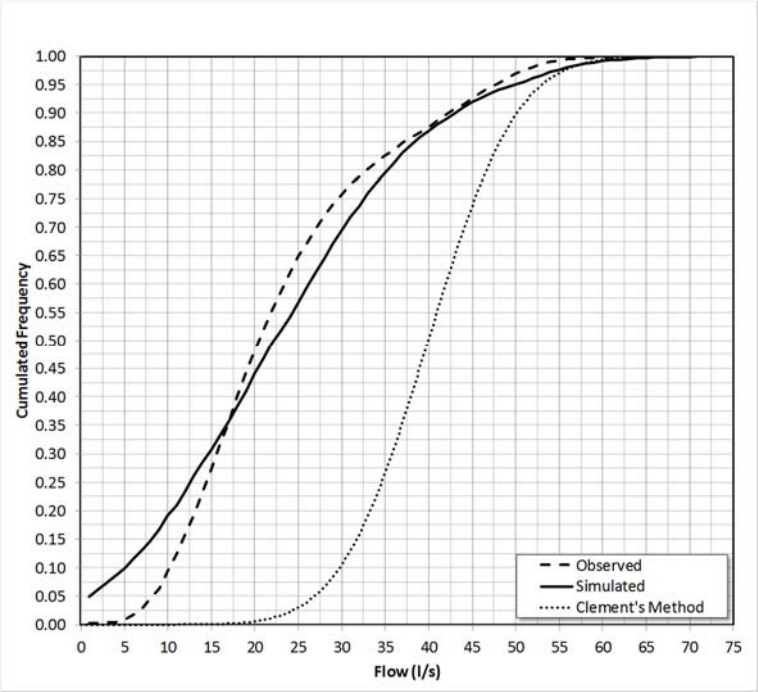

Figure 7. Comparison of cumulated frequency between observed, simulated and Clément's method to maximum irrigation needs on June

KPIF variations obtained were lower (in percentage) than those obtained by Mulligan & Brown (1998). This fact confirms proposed method is able to simulate the circulating flows over time in any pipeline of a pressurized irrigation network.

This method can be used in pressurized networks when water managers are developing the design stage or when the network is operating, and they want to improve the hydraulic and energy efficiency. In addition, the method can be used to optimize pumped systems according to histogram of circulating flow frequency. The knowledge of flows range allows the selection of optimal pump as well as operation rules, considering not only maximum obtained flow but the more frequent ones. In the case of design of pressure networks distributed by gravity, it could be applied with the same criteria.

This method can also be used by water managers, when pumped systems are oversized. In these cases, a new design is needed to reduce the electrical operating costs. In the case of gravity networks, the predicted flows can be used to select the operation range of the pressure reduction valves, or to analyze the possibility to recover energy in the locations where the pressure is greater than minimum pressure for irrigation. In the last case, the method allows the determination of the range and frequency flows used to calculate the theoretical recovered energy (Pérez-Sánchez *et al*., 2016). This permits multipurpose system in these infrastructures, increasing the energy efficiency and reducing the exploitation costs and consumed water.

In conclusion, a new method to calibrate flows rate over time in hydrological process has been presented in this contribution. This method has been successfully applied to calibrate the circulating flows in a particular *WDN*. The obtained values in this calibration verify a satisfactory, good or very good goodness of fit according to time intervals considered. This calibration method may have great utility in determining circulating flows inside networks when no measurement devices exist in the main lines.

Acknowledgments: This paper has been possible with the free collaboration of the "Comunidad de Regantes Torreta-Segarra" in the township of Callosa d'en Sarrià (Alicante, Spain). Authors also thank Laura Romero Marrero for her collaboration in the editing of this contribution.

Author Contributions: Conceived and designed the method to estimate flows and calibration strategy: MPS, PALJ and FJSR. Performed the calculus: MPS and FJSR. Analyzed the data: MPS, and PALJ. Statistical analysis: MPS, FJSR, and PALJ. Wrote the paper: MPS, HR, and PALJ. Critical revision of the manuscript for important intellectual content: HR. Supervising the work and coordinating the research project: PALJ

Conflicts of Interest: The authors declare no conflict of interest. The founding sponsors had no role in the design of the study, in the collection, analyses, or interpretation of data, in the writing of the manuscript, and in the decision to publish the results.

References

Abbasi F, Feyen J, Van Genuchten MT, 2004. Two-dimensional simulation of water flow and solute transport below furrows: Model calibration and validation. J Hydrol 290: 63-79.

Allen RG, Pereira LS, Raes D, Smith M, 2006. Crop evapotranspiration: Guidelines for computing crop water requeriments. FAO. Ed. Estudio FAO Riego y Drenaje. Rome, Italy. pp323

Arbat G, Pujol J, Pelegrí M, Puig-Bargués J, Duran-Ros M, Cartagena FR, 2013. An approach to costs and energy consumption in private urban Spanish Mediterranean landscapes from a simplified model in sprinkle irrigation. Span J Agric Res 11 (1): 244-257.

BOE, 2016. Royal decree 1/2016, of 8 January, that approved the revision of the Hydrological Plan Júcar River Basin Districts. Boletín Oficial del Estado (Spain) No. 439, 08/01/16.

Boissezon J, Haït JR, 1965. Calcul des débits dans les réseaux d'irrigation. La Houille Blanche 2: 159-164.

Braun JV, Ruel MT, Gillespie S, 2010. Calibration of hydraulic of network model. In: Water distribution systems handbook; Mays LW (ed), pp: 279-304. McGraw-Hills, Arizona, USA.

Butera I, Balestra R, 2015. Estimation of the hydropower potential of irrigation networks. Renew Sustain Energ Rev 48: 140-151.

Cabrera E, Cobacho R, Soriano J, 2014. Towards an energy labelling of pressurized water networks. Procedia Eng 70: 209-217.

Cabrera J, 2009. Calibración de modelos hidrológicos. Instituto para la Mitigación de los Efectos del Fenómeno el Niño, Lima, Perú.

Carravetta A, Del Giudice G, Fecarotta O, Ramos HM, 2012. Energy production in water distribution networks: A PAT design strategy. Water Resour Manag 26: 3947-3959.

Carravetta A, Del Giudice G, Oreste F, Ramos HM, 2013. PAT design strategy for energy recovery in water distribution networks by electrical regulation. Energies 6: 411-424.

Carravetta A, Fecarotta O, Del Giudice G. Ramos HM, 2014. Energy recovery in water systems by PATs: A comparison among the different installation schemes. Procedia Eng 70: 275-284.

Choulot A, 2010. Energy recovery in existing infrastructures with small hydropower plants. FP6 Project Shapes (work package 5- WP5). European Directorate for Transport and Energy.

Clark C, Wu ZY, 2006. Integrated hydraulic model and genetic algorithm optimization for informed analysis of a real water system. 8th Annual Water Distribution Systems Analysis Symposium, Cincinnati, OH, USA.

Clément R, (1955). Le calcul des débits dans les réseaux d'irrigation fonctionnant à la demande Journées d'études sur l'irrigation. 27-30 juin. Association Amicale des Anciens Élèves de l'Ecole National.

Clément R, 1966. Calcul des débits dans les réseaux d'irrigation fonctionnant à la demande. La Houille Blanche 5: 553-575.

Corominas J, 2010. Agua y energía en el riego, en la época de la sostenibilidad. Ingeniería del Agua 17 (3): 219-233.

Datta RSN, Sridharan K, 1994. Parameter estimation in water-distribution systems by least squares. J Water Resour Plan Manage 120 (4): 405-422.

Davidson JW, Bouchart FJC, 2006. Adjusting nodal demands in SCADA constrained real-time water distribution network models. J Hydraul Eng 132 (1): 102-110.

Delgoda D, Malano H, Saleem SK, Halgamuge MN, 2016. Irrigation control based on model predictive control (MPC): Formulation of theory and validation using weather forecast data and AQUACROP model. Environ Model Softw 78: 40-53.

Emec S, Bilge P, Seliger G, 2015. Design of production systems with hybrid energy and water generation for sustainable value creation. Clean Technol Environ Policy 17: 1807-1829.

Ghiass M, Zimbra DK, Saidane H, 2008. Urban water demand forecasting with a dynamic artificial neural network model. J Water Resour Plan Manage 134 (2): 138-146.

Granados A, 1986. Redes colectivas del riego a presión. Escuela de Ingenieros de Caminos y Puertos, Univ. Politécnica, Madrid.

Granados A, 2013. Criterios para el dimensionamiento de redes de riego robustas frente a cambios en la alternativa de cultivos. Doctoral Thesis, Univ. Politécnica, Madrid.

Granados A, Martín-Carrasco FJ, Jalón SG, Iglesias A, 2015. Adaptation of irrigation networks to climate change: Linking robust design and stakeholder contribution. Span J Agric Res 13 (4): e1205.

Gupta HV, Sorooshian S, Yapo PO, 1999. Status of automatic calibration for hydrologic models: Comparison with multilevel expert calibration. J Hydrol Eng 4: 135-143.

Lamaddalena N, Sagardoy JA, 2000. Performance analysis of on-demand pressurized irrigation systems. FAO, Roma, Italy. 132 pp.

Legates DR, McCabe GJ, 1999. Evaluating the use of “goodness-of-fit" measures in hydrologic and hydroclimatic model validation. Water Resour Res 35: 233-241.

Martínez-Solano J, Iglesias-Rey PL, Pérez-García R, López-Jiménez PA, 2008. Hydraulic analysis of peak demand in looped water distribution networks. J Water Resour Plan Manag 134: 504-510.

McCuen RH, Knight Z, Cutter AG, 2006. Evaluation of the Nash-Sutcliffe efficiency index. J Hydrol Eng 11: 597-602.

Moreno MA, Planells P, Ortega JF, Tarjuelo J, 2007. New methodology to evaluate flow rates in on-demand irrigation networks. J Irrig Drain Eng 133: 298-306.

Moriasi DN, Arnold JG, Van Liew MW, Binger RL, Harmel RD, Veith TL, 2007. Model evaluation guidelines for systematic quantification of accuracy in watershed simulations. T ASABE 50: 885-900.

Mulligan AE, Brown LC, 1998. Genetic algorithms for calibrating water quality models. J Environ Eng 124: 202-211.

Nash JE, Sutcliffe JV, 1970. River flow forecasting through conceptual models part I: A discussion of principles. J Hydrol 10: 282-290.

Pardo MA, Manzano J, Cabrera E, García-Serra J, 2013. Energy audit of irrigation networks. Biosyst Eng 115: 89-101.

Pérez-Sánchez M, Sánchez-Romero F, Ramos H, López-Jiménez P, 2016. Modeling irrigation networks for the quantification of potential energy recovering: A case study. Water 8: 1-26.

Preis A, Whittle A, Ostfeld A, 2009. Online hydraulic state prediction for water distribution systems. World Environ Water Resour Congr 2009: 1-23.

Pulido-Calvo I, Roldán J, López-Luque R, Gutiérrez-Estrada JC 2003. Water delivery system planning considering irrigation simultaneity. J Irrig Drain Eng 129: 247-255.

Ramos H, Borga A, 1999. Pumps as turbines: an unconventional solution to energy production. Urban Water 1: 261-263.

Ramos H, Mello M, De PK, 2010a. Clean power in water supply systems as a sustainable solution: from planning to practical implementation. Water Sci Technol Water Supply 10: 39-49.

Ramos H, Vieira F, Covas DIC, 2010b. Energy efficiency in a water supply system: Energy consumption and CO_2 emission. Water Sci Eng 3: 331-340.

Ritter A, Muñoz-Carpena R, Regalado C, 2009. Capacidad de predicción de modelos aplicados a ZNS: Herramienta informática para la adecuada evaluación de la bondad-de-ajuste con significación estadística. IX Jornadas sobre Investigación de la Zona no Saturada del Suelo - ZNS'09. Editores: Orlando Silva Rojas y Jesús Carrera Ramírez. Actas de las VII Jornadas sobre Investigación de la Zona no Saturada del Suelo. 18-20 noviembre. Barcelona (España)

Rodriguez-Diaz JA, Camacho-Poyato E, Carrillo-Cobo MT, 2010. The role of energy audits in irrigated areas. The case of "Fuente Palmera" irrigation district (Spain). Span J Agric Res 8 (2): 152-161.

Rossman LA, 2000. Epanet Manual. Cincinnati, OH, USA.

Sanz G, Pérez R, 2014. Demand pattern calibration in water distribution networks. Procedia Eng 70: 1495-1504.

Sanz G, Pérez R, 2015. Comparison of demand calibration in water distribution networks using pressure and flow sensors. Procedia Eng 119: 771-780.

Singh J, Knapp HV, Demissie M, 2005. Hydrologic modelling of the Iroquois River watershed using HSPF and SWAT. Water Resour Assoc 41: 343-350.

Soler J, Latorre J, Gamazo P, 2016. Alternative method to the Clément's first demand formula for estimating the design flow rate in on-demand pressurized irrigation systems. J Irrig Drain Eng 142 (7): 1-9.

Tabesh M, Jamasb M, Moeini R, 2011. Calibration of water distribution hydraulic models: A comparison between pressure dependent and demand driven analyses. Urban Water J 8: 93-102.

Willmott CJ, 1981. On the validations models. Phys Geogr 2 (2): 184-194.

This page is intentionally left blank.

Appendices

Appendix IV

WATER-ENERGY NEXUS. ENERGY OPTIMIZATION IN WATER DISTRIBUTION SYSTEM. CASE STUDY 'POSTRASVASE JÚCAR-VINALOPÓ (SPAIN)

Author version document which was published in index JCR Journal "Tecnologías y Ciencias del Agua" ISSN 2007-2422. Impact Factor 0.108. Position 83/85 (Q4). Water Resources.

Pérez-Sánchez, M., Sánchez-Romero, F., López-Jiménez, P., 2017. Water-energy nexus. Energy Optimization in water distribution system. Case study 'Postrasvase Júcar-Vinalopó (Spain)'. *Accepted date 27/03/2017. The manuscript will be published in Volume VIII (4) July-August 2017*

This page is intentionally left blank.

ABSTRACT

Nowadays, making interbasin transfers of water flow is the only solution to the water shortage for some agricultural areas. This is the case of the Spanish Mediterranean region, namely the southern province of Alicante. This area has historically presented a water balance deficit between irrigation needs and resources, resulting in overexploitation of aquifers. To alleviate this environmental impact, some water volumes between the basin of the Júcar and Vinalopó rivers were transferred. A hydraulic pressure system was responsible for transferring water between basins and distributing it to the irrigated areas. In this article, a methodology used to optimize water-energy system is described, developing a calibrated model using *EPANET* as a tool operating system. This model allows managers to analyze the distribution of volumes and flow dependence on the existing agricultural demand in each receiver reservoir. Attached to the hydraulic distribution, a thorough study of the possible hydro-energy relations in the whole system is carried out, obtaining a maximum theoretical value of recoverable energy 18 418 MWh/year. Overall, the feasibility of hydraulic jumps leverage is determinant to increase overall efficiency in the whole distribution system.

Keywords: Water-energy nexus, recoverable energy, Júcar-Vinalopó Post-transfer

1. Introduction

In the Spanish Mediterranean zone, concretely the South of the province of Alicante, are located the municipality of Alto Vinalopó, Medio Vinalopó, Bajo Vinalopó, and L'Alacantí (Figure 1). This area presents climatic conditions, which are very favourable to grow horticultural crops and woody crops such as wine grape, table grape, pomegranate, among others (Murillo Díaz *et al.,* 2009). The benevolence of the temperature contrasts with the lack of hydric resources, existing large interval time without precipitations. This lack of rain causes the totality of the crops are irrigated, obtaining the necessary hydric resources through spring and groundwater (Bru Ronda, 1993).

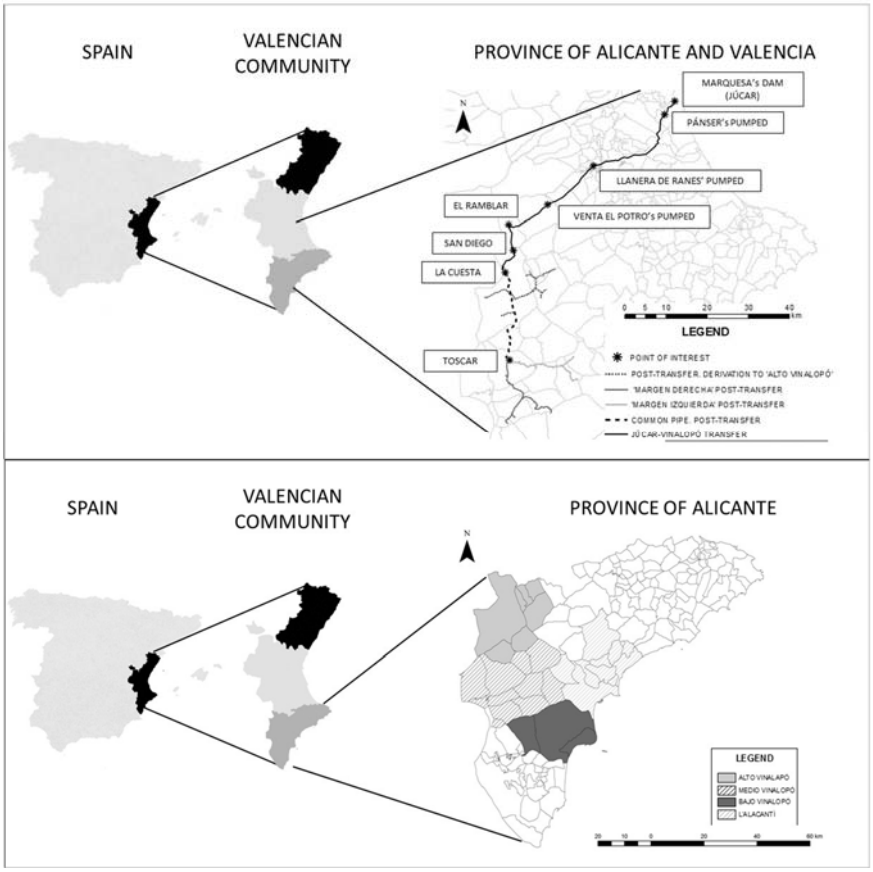

Figure 2. Vinalopó Basin (up). Jucar-Vinalopó Transfer and Júcar-Vinalopó Post-transfer (bottom)

Particularly in this Spanish area, the over-exploited aquifers were pronounced in the late 20th century in which the piezometric levels went down strongly and some cases, the aquifers salinized by marine intrusion (Ramón Morte, Olcina Cantos, & Rico Amorós, 1990). The environmental problems (over-exploited aquifers and low quality of the irrigation water) aggravated in the early 21st century. To try to solve these problems, Spanish government (IDAE, 2005) developed a strategic plan to change the irrigation open channels flow by drip irrigation. This developed plan was supported both Spanish government and autonomous community (Generalitat Valenciana) through European economic help. Parallelly, Jucar Basin Plan and National Hydrological Plan established Vinalopó Basin needs transfers from Jucar basin (Espín, 1997). This water transfer was established in 80 hm^3/year from Jucar River to irrigated area of the Vinalopó Basin. The objective of this transfer is to reduce the hydric deficit of 52 399 hectares as well as to guarantee the supply in the towns of this area.

The regulation of the open channels flow networks was a problem, which is already described in the bibliography (De Leon Mojarro, Verdier, Piquereau, Ruiz-Carmona, & Rendon Pimentel, 2002). Sometimes, the only solution is the water transfer between basins (Silva-Hidalgo, Aldama, Martín-Dominguez, & Alarcón-Herrera, 2013). In this case, to solve the lack of hydric resources, the water transfer is also the considered solution. To perform this transfer, a water system was built between basins. This pressurized water system connected Marquesa's Dam (Cullera, Valencia-Spain) and Ramblar Tank (Font de la Figuera, Valencia-Spain). Three pumped groups were installed in this water systems to raise from 1.5 m (water level in Marquesa Dam) to 655 m (water level in Ramblar's Tank). Once the water was in the Ramblar Tank, the water system operated by gravity. This built finished 9000 m downstream when the pipeline connected with San Diego reservoir. The previously described infrastructure was called Jucar Vinalopó Transfer (*TJV*) (Abreu, Cabrera, Espert, García-Serra, & Sanz, 2012). The function of this infrastructure was the water captation and storage in the head of the second infrastructure (here so called Jucar-Vinalopó Post-Transfer (*PJV*)) in the San Diego reservoir.

The *PJV* was the hydraulic infrastructure, which distributed the flows between different irrigation communities and municipalities. This pressurized water system completely operated by gravity and was integrated by 140 km of pipelines (Figure 2). This system was composed of a communal pipe, a branch so-called 'Margen Derecha', and other branch so-called 'Margen Izquierda'. The communal pipe had a length of 38 km and its diameter varies between 1900 and 1000 mm. The 'Margen Derecha' had a length of 60 km, varying its diameter between 1000 and 400 mm. The 'Margen Izquierda' had a length of 42 km (this branch is not currently built) (Figure 1).

The development of the irrigation modernization caused an increase of the hydraulic efficiency of the systems (Luis de Nicolás, Laguna-Peñuelas, & Viduera, 2014), but also, an increase in energy consumption (Corominas, 2010). The need to increase and to evaluate the hydraulic and energy efficiency in the pressurized water systems (Cabrera, Cobacho, & Soriano, 2014; Carravetta, Del Giudice, Fecarotta, & Ramos, 2012; Pardo, Manzano, Cabrera, & García-Serra, 2013; Salazar-Moreno, Rojano-Aguilar, & López-Cruz, 2014) to reduce the greenhouse emissions caused the need that the water systems had to be multipurpose systems (Choulot, 2010). However, the first objective of these systems must be to guarantee the demand in the system, being the second objective the energy generation and therefore, the reduction of energy footprint of water (Emec, Bilge, & Seliger, 2015; Gilron, 2014) as well as the proposal of systems more sustainable.

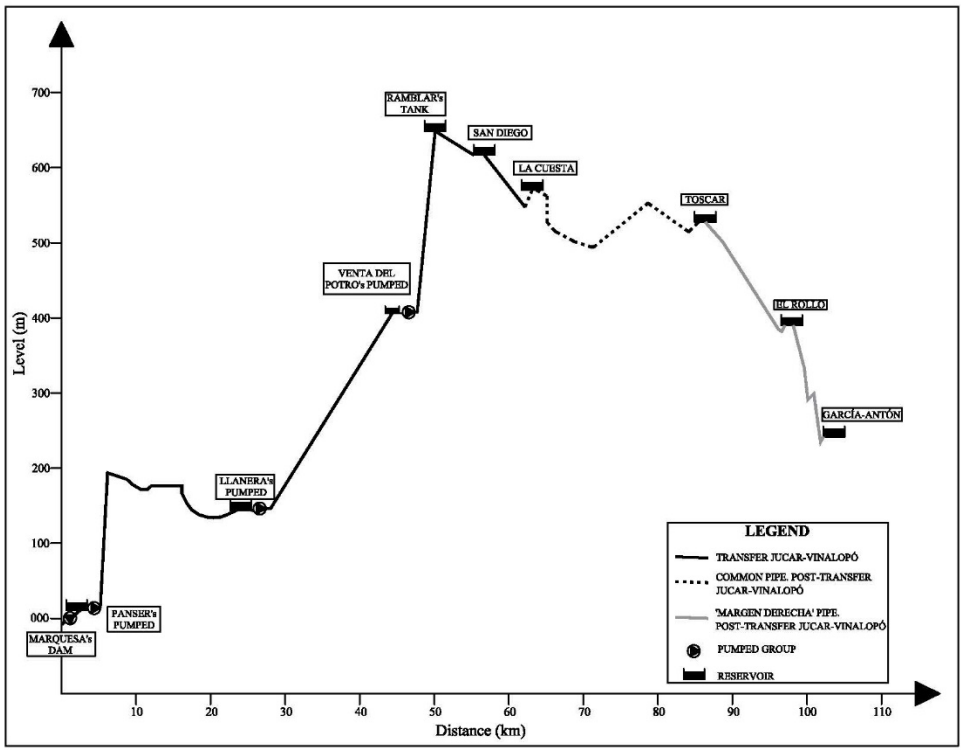

Figure 2. TJV and PJV profile schemes

The objectives of this analysis were to optimize the volumes transfer to minimize the use of groundwater and to analyse the theoretically recoverable energy in the system, considering the consumption (farmer's demand and urban demand). To develop these objectives, the used data were hydric resources in the Jucar River, the capacity of flow transfer, the regulation volume, and characteristic of the pressurized water system. Besides, the analysis of new infrastructure to increase the use of available resources and energy recovery were developed in this manuscript. Therefore, the developed stage in this paper were:

- To study of water management in the system *TJV*;
- To model the pressurized water system of the *TJV* and *PJV*, considering the demands and regulation volume;
- To analyze if current infrastructures, they satisfy the farmer's demand, considering different scenes of consumption as well as introducing the contribution of own hydric resources (*e.g.,* groundwater, regenerated water) in each irrigation community;

- To analyse and to plan the improvement in the system, which are derived of previous cited bullets. These improvements could be installed in the future to maximize the exploitation of the hydric resources and built infrastructures; and
- To study and to analyze the energy recovery in the different existing waterfalls between reservoirs. The use of these energy recoveries increases the energy efficiency of the system Jucar-Vinalopó Transfer-Post-Transfer.

2. Methods and Materials

2.1. Data collection. Existing infrastructures in the volume regulation, external contribution of water and pumped group

2.1.1. Data collection. Pumped group

To do the model with accurate, the available information in official document were consulted. In addition, this information was completed with interviews, which was developed in all irrigations communities (59) and their objective was to collect information of consumptions, own hydric resources, and existing volume regulations. This information was classified in each irrigation community through the following parameters: reservoir identification, supplied users, municipality, up and bottom level of the reservoir, useful volume, volume curve of the reservoir, own resources (*e.g.,* regenerated water, groundwater, other external transfers), farmer's demand over time, electrical tariff contract, and irrigated area.

2.1.2. Data collection. *Determination of irrigation needs*

The irrigation needs are calculated based on exposed methodology by Food and Agriculture Organization of the United Nations (Doorembos, J; Pruitt, 1977). The method is described in Table 1.

The irrigation needs are determined depending on the main crop in the different municipalities (*i.e.,* Alto Vinalopó, Medio Vinalopó, Bajo Vinalopó, and L'Alacantí). The calculus of the irrigation needs is simplified by considering three homogenous areas. These zones are related to wine grape (part of irrigated area of Medio Vinalopó), table grape (part of irrigated area of Medio Vinalopó), and wine grape (Alto Vinalopó). A little area of citric is also considered in the Bajo Vinalopó.

To determine the evapotranspiration, the meteorological data are taken from Spanish meteorological agency (AEMET). Data of measurement station located in Pinoso and Mónovar (Alicante, Spain) are used to wine grape. The located stations in Novelda and Monforte del Cid (both townships of Alicante, Spain) are used to table grape. Finally, the located stations in Elche and Alicante are used to citric.

Table 1. Methodology to determine the irrigation needs depending on crop

METHODOLOGY TO DETERMINE THE IRRIGATION NEEDS			
1. Obtaining the evapotranspiration of the crop (ET_{crl}) by equation (1):			
$ET_{crl} = ET_o K_C K_{vc} K_{ad} K_{loc}$ (1)			
where:			
ET_o is the reference evapotranspiration			
K_c is the crop coefficient, which is obtained according to Doorembos and Pruitt, (1977)			
K_{vc} is the coefficienct of climatic variation = 1,2, according to Doorembos and Pruitt, (1977)			
K_{ad} is the advection coefficient =1, according to Doorembos and Pruitt, (1977)			
K_{loc} is the drip coefficient, according to Doorembos and Pruitt, (1977)			
K_{loc} is determined by average value, which is obtained according to the following equations (Pizarro, 1996).			
$K_{loc} = 1.34 \cdot A$ (2)	$K_{loc} = 0.1 + A$ (3)	$K_{loc} = A + 0.5(1 - A)$(4)	$K_{loc} = A + 0.15(1 - A)$(5)
where A is the ratio of shaded soil area by vegetal cover in the middle day in the summer solstice. In this case, the adopted value is 0.35 for wine grape, 0.60 for table grape, and 0.7 for citric.			
2. Obtaining of the effective rain. This value is based on proposed method by United States Departament of Agriculture (*USDA*) Soil Conservation Service (Doorembos and Pruitt, 1977).			
3. Obtaining the monthly hydric balance to determine the irrigation net needs.			
4. Obtaining the irrigation needs by using the uniformity coefficient (0.9). This needs are increased 10% to consider the leaching of salts (Pizarro, 1996).			

Once the irrigation needs are determined, these endowments are compared to obtained values in the interviews. These values are also compared to the published information for these areas in the National Hidrological Plan (Table 2). If irrigation needs are compared to the real endowment, the values are similar. The values of wine and table grape are also similar if they are compared to National Hydrological Plan (*PHN*). In citric, the *PHN* value is lower than obtained irrigation needs. Finally, the following amounts are adopted, which are monthly distributed according to the Table 2:

- Demand 1; the wine grape amount is increased until 3461 m^3/ha to consider a little percentage of other crops (fruit trees, mainly).
- Demand 2; the considered table grape endowment is 4333 m^3/ha, which is adjusted to real consumption.
- Demand 3; the considered citric endowment is 5560 m^3/ha.

Table 2. Comparison of amounts (Ferrer, Sánchez-Romero, Torregrosa, & Zapata, 2002)

DEMAND	Theoretically Irrigation need (m^3/ha)	Real amount (m^3/ha)	PHN amount (m^3/ha)	Adopted amount (m^3/ha)
Wine grape [Demand 1]	2 029.62	2 524	4 060	3 461
Table grape [Demand 2]	4 335	4 356	4 270	4 333
Citric [Demand 3]	6 940	6 936	4 700	5 650

Monthly adopted demand (m^3/ha)			
Demand	**1**	**2**	**3**
January	78.0	127.5	212.5
February	97.5	158.5	265.0
March	148.0	253.0	359.5
April	185.0	309.5	519.5
May	343.0	418.0	625.5
June	495.0	546.5	740.0
July	663.0	733.5	817.0
August	623.0	694.5	741.0
September	411.0	460.5	548.0
October	252.5	303.0	382.5
November	93.0	189.0	221.5
December	72.0	139.5	218.0
Total (m^3/ha)	**3 461.0**	**4 333.0**	**5 650.0**

2.1.2. Data collection. Jucar's flow and pipelines

There are a lot of studies related to Jucar's flow. However, any study is conclusive to determine the available volume to transfer to another basin (Cabezas, 2006; Espert, 2009; López Ortiz & Melgarejo Moreno, 2010). These flows depended on hydrological year and minimum ecological flow established in the basin plan. The analyzed studies established an available transferred volume between 25 and 60 hm3/year. These transferred volumes vary depending on the considered assumptions, a number of pumps turns on, ecological flow, and used flow to irrigate in the caption point (Espert, 2009). Figure 3 showed the Jucar's flow and the transferred volumes depending on considered

assumption. These data were based on measured flow in the Huerto Mullet's dam (Sueca, Valencia, Spain). In each assumption, the irrigation consumption of this area was deducted on circulating flow in the Mullet's dam. In the analysis, four assumptions were considered (A, B, C and D). Each assumption establishes a return percentage, which comes from irrigation channels flow. This percentage is 25, 50, 75, and 100% (assumption A, B, C, and D, respectively). The last assumption was not realistic and therefore, it was rejected on the analysis. Considering these assumptions, the average flow can be observed in Figure 3. The transferred volumes depending on the number of connected pumps and ecological flow. Related to a number of connected pumps, three different assumptions were considered. Assumption 1, the pumped flow was 1.56 m^3/s. Assumption 2, in which the pumped flow was 2.85 m^3/s and the number of connected pumps was two. Assumption 3, in which, three pumps operated and the pumped flow was 3.80 m^3/s.

Figure 3 showed the difficult to transfer 80 hm^3/year. This volume can only be transferred when the returns of the irrigation open channels flow were very favourable and all pumps were connected. However, an objective of the manuscript was to establish the necessarily transferred volume depending on demand scene, therefore, in all analyzed cases, the model supposed the *TJV* was able to provide the demanded volume in the *PJV*. However, the transferred volume was always below to 80 hm^3/year (upper limit allowed in the *TJV*). The flow function, which kept with this limit, was shown in Figure 3.

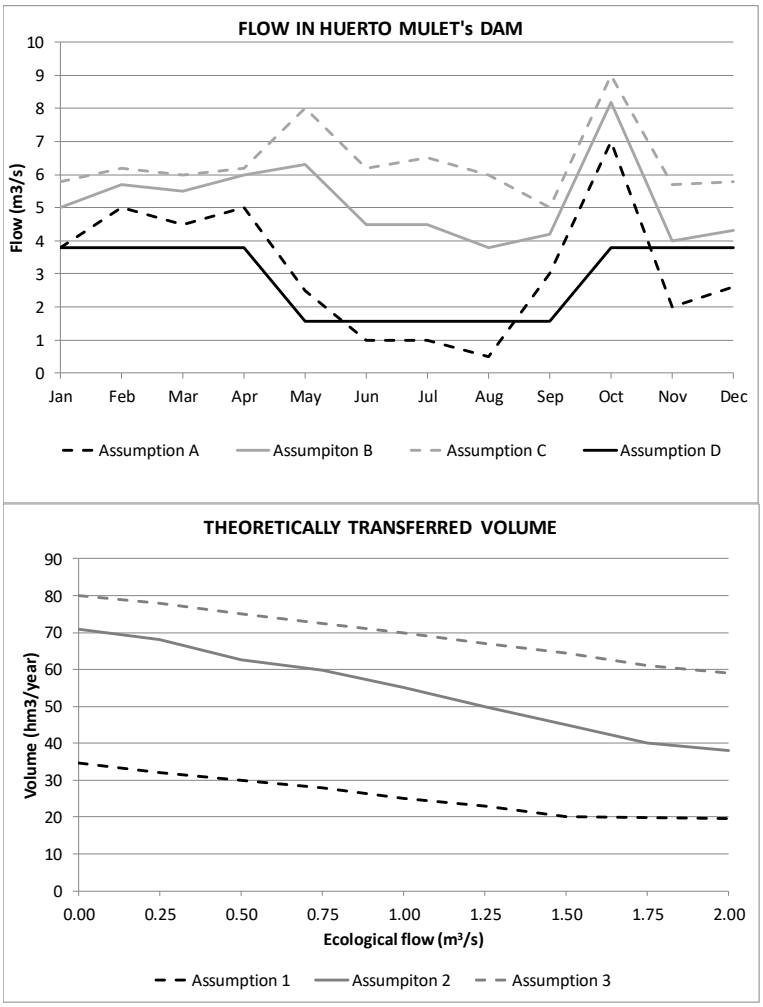

Figure 3. Average flow (up) and theoretically transferred volumes (bottom) depending on considered assumption

Related to hydraulic infrastructures (pipelines), an inventory to determine length, diameter and morphology of the system was done in all pressurized system (*i.e., TJV*, *PJV*, and irrigation communities). This inventory allowed for the modelling and the knowledge of distributed flow from Jucar's river to each crop area of the users.

2.1.3 Development of the model

The optimization model to distribute the volumes between different regulation reservoir was developed by using software *EPANET* (Rossman, 2000). The modelling allowed for the simulation of the current situation of this hydraulic system by using of the own

element (e.g. tank, reservoir, valves). However, the developed model had to be complemented by auxiliary systems which established the particular operating conditions in each existing regulation element. These singular points were mainly the input of the reservoirs and the input of own resources in each irrigation community.

The model was formed by 489 lines and 464 nodes, in which control rules were declared to develop the exploitation in the future. These operation laws, whose operating restrains were shown in Figure 4, enabled the establishment of transferred volume for *TJV*, the operating time of groundwater resources as a function of electrical contract rate, the provided volume from own resources (*e.g.,* regenerated water, surface water resource, desalinated water).

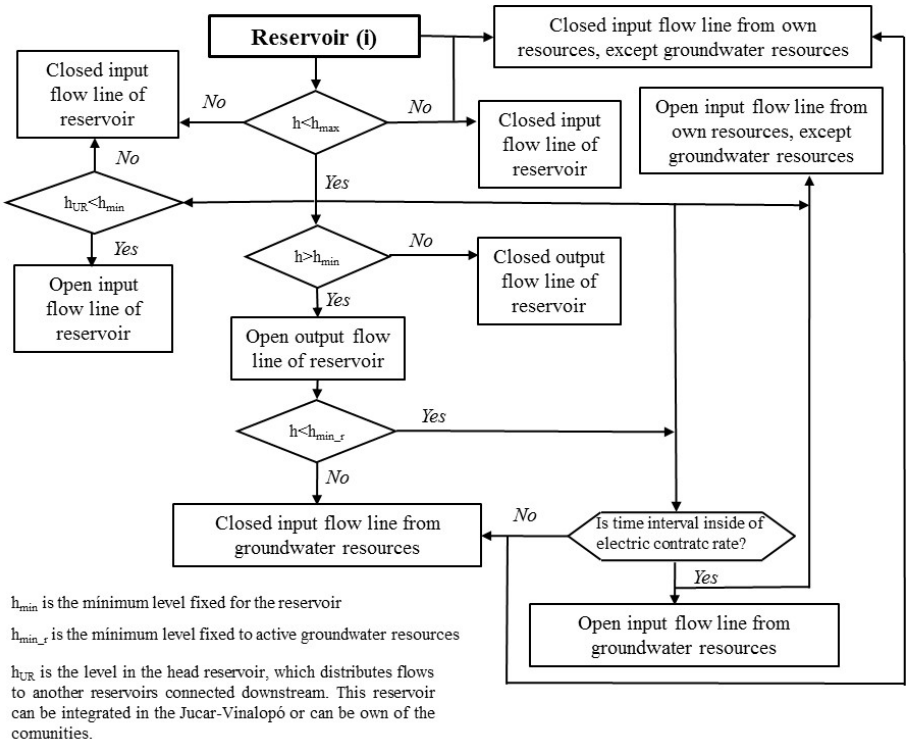

Figure 4. Control rules to optimize the flow distribution in *PJV*

The development of control rules was crucial to model the exploitation of the hydraulic system because the model's programming made possible to maximize the transferred volume from *TJV*. Depending on these transferred volumes, the developed model minimized (or voided when it was possible) the extracted volume from groundwater. This strategy pursues *PJV* contributed to the recovery of groundwater's piezometric level in a medium-long term, reaching one of the proposed objectives. The development of

the system modelling, which was focused on in the water management of the system, contributed to establish the operating rules of *TJV*, once the flows and demanded volumes by *PJV* were known.

When the control rules for each integrated reservoir in the system were established according to available resources, the input and output flows were established for each origin (*e.g, PJV*, groundwater, regenerated water) depending on irrigated area, which was associated with each reservoir. To define the agricultural demand, a consumption joint was used in each one of the reservoir. This junction was defined by annual modulation curve, which establishes the annual consumption flow's pattern. This pattern was defined for each reservoir according to the type of demand (Table 2) and the irrigated area, which was associated with the analyzed reservoir.

To develop an exhaustive analysis of the flow distribution in the system and to analyze the distribution of the volumes as a function of actual irrigated area, a base demand was assigned between 0 and 1 in each junction, according to the studied scene. This demand assignation allowed for the analysis of transferred volumes in each community when irrigated area varied from 10% (the base demand is 0.1) to 100% (the base demand is 1). Besides, to establish the irrigated area in each reservoir exactly made possible to have an updated model, which could be used by water managers along the exploitation according to the crops evolution and their irrigations needs.

The modelling of the regulation valves inside of the system made possible to develop an energy analysis of the theoretically recoverable energy to take advantage of the dissipated energy currently. This analysis considered both technical and economical considerations. The technical considerations defined the operating zone of the machine according to obtained results in the modelling for each assumption as well as the theoretically recovered energy. The economic considerations included the first analysis of viability according to Diversification and Energy Saving Institute (*IDAE*) (Castro, 2006). The objective of this analysis was to establish the viability of the different analyzed hydraulic jump.

To do the economic analysis, the economic consideration was defined according to Castro (2006), who established an average investment ratio of 1500 €/kW, an operating cost of 0.014516 €/kW, being the lifespan of 25 years. The incomes were established according to established price in Spain according to Ministerial Order ITC/3353/2010. This price was 8.4234 c€/kWh and didn't consider the hourly discrimination in the system because the main objective of the pressurized water systems is the distribution of the volumes, being the generation of renewable energy a secondary objective. However, a current water management should lead to purpose systems, increasing the energy efficiency (Choulot, 2010). The feasibility of each analyzed hydropower was established according to payback period (*PSR*) and energy index (*EI*). *PSR* related the investment and annual profit in the facility. EI linked the investment and annual generated energy (kWh/year). The hydropower's feasibility was defined positively when *PSR* is lower than six years and *EI* was between 0.4 and 0.7 €/kWh.

3. Results and discussion

The obtained results of the developed model were structured on hydraulic and energy point of view. The hydraulic results analysed, on the one hand, the transferred flow and volumes. On the other hand, the necessary flows and volumes of own resources were also analysed and determined. The energy results estimated the theoretically recovered energy in the *PJV*.

3.1. Results. Hydraulic modeling

Related to hydraulic modelling, although can be obtained numerous scenes considering different assumption of irrigated area, the objective of the study was to present the results that the model was able to obtain (flow and volumes), according to analysed demand as well as the transferred volumes from *TJV*, considering the maximization of this transfer when the operation rules are established.

The model allowed for the quantification of necessary volume to provide of own resources in each irrigation community, which were external to *TJV* (*e.g.,* groundwater, regenerated water). This knowledge of necessary volume determined if the own resources were enough to supply the demand in each assumption. The individual analysis for each one of the reservoirs, which were integrated into the water system, can be developed through obtained results. An example of these results was shown in Figure 5. If the figure was analyzed, different considerations can be determined such as the need to increase the regulation volumes or the determination of hydric deficit for each demand scene, calculating the necessary volume of groundwater resources and minimizing the extracted volume through control rules.

The shown example determines that there was not a problem that was related to regulation volume because the maximum level didn't reach in the reservoir. In contrast, there were supply problems along summer month and the end of the year. The figure showed the incapacity to transfer water volume to other reservoir located downstream between weeks 24 and 32. Related to demand, along these weeks (from 24 to 32), the irrigation needs have to be supplied through own resources, being the provided volume near to 250000 m^3/year (Figure 5). As the hydraulic conclusion, for this example, the analysis established the input flow in the reservoir must be upper than 0.35 m^3/s. to guarantee the irrigation needs as well as the transferred flow to others reservoir which are connected downstream. Similar analyses to Figure 5, can be developed through obtained results of the modelling for each one of 59 reservoirs of the *PJV* and for each considered assumption of irrigated area. The individual analysis for each reservoir can be extrapolated and performed to the different irrigation communities considering all their reservoirs. The analysis considering municipality or every system can also be developed. These analyses allowed water managers to develop water management plan (infrastructure and actuation plan) which can be defended the sustainable used of this infrastructure as well as the groundwater resources of these municipalities.

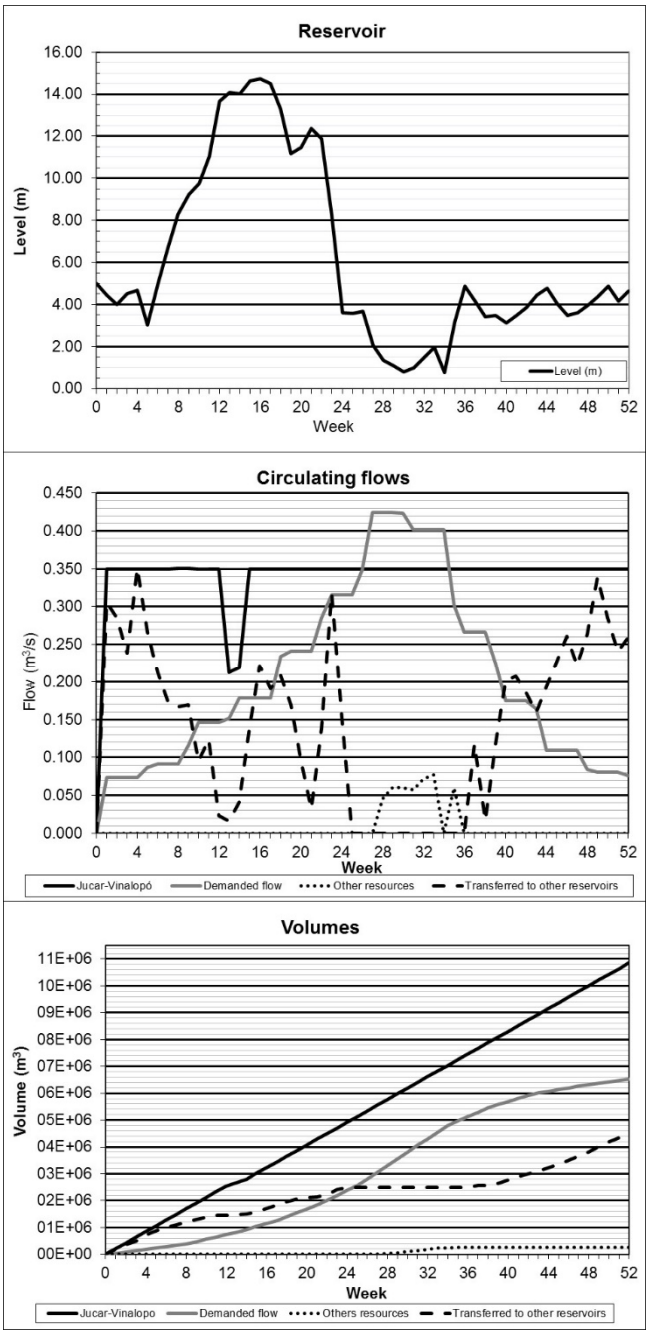

Figure 5. Example of obtained results through modelling for each reservoir connected to *PJV*

Figure 6 showed the variation of the inlet flow, demanded flow (considering the variability of the user's demand), level of the reservoir, as well as the theoretical generated power in one of the reservoir in the PJV. In the figure, the inlet flow was constant and its value was 0.35 because the reservoir was filling up. The generated power is 0.225 MW, being practically uniform because the recovered head remained constant, varying between 93.22 and 95.41 m w.c. as a function of the distributed flow. In contrast, the demanded flow by the users varied between 0 and 420 l/s and its average value was 147 l/s. This value coincided with the weekly demand, shown in the Figure 5 between the week 5 and 8.

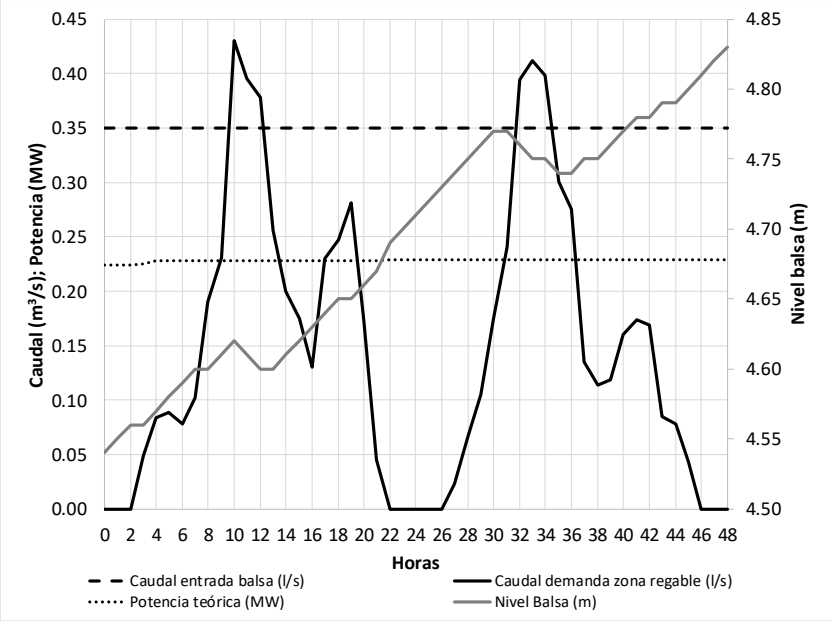

Figure 6. Theoretically generated power, circulating flow and the reservoir level over time

Finally, the developed hydraulic model made possible to analyze the system *TJV-PJV* in a global point of view (Figure 7) for each irrigated area. This figure showed that assumptions, which considered irrigated area between 50% and 100%, the *TJV* was not able to provide the necessary volume to satisfy the irrigations needs. These results justify the need to continue using own resources (which mainly come from groundwater).

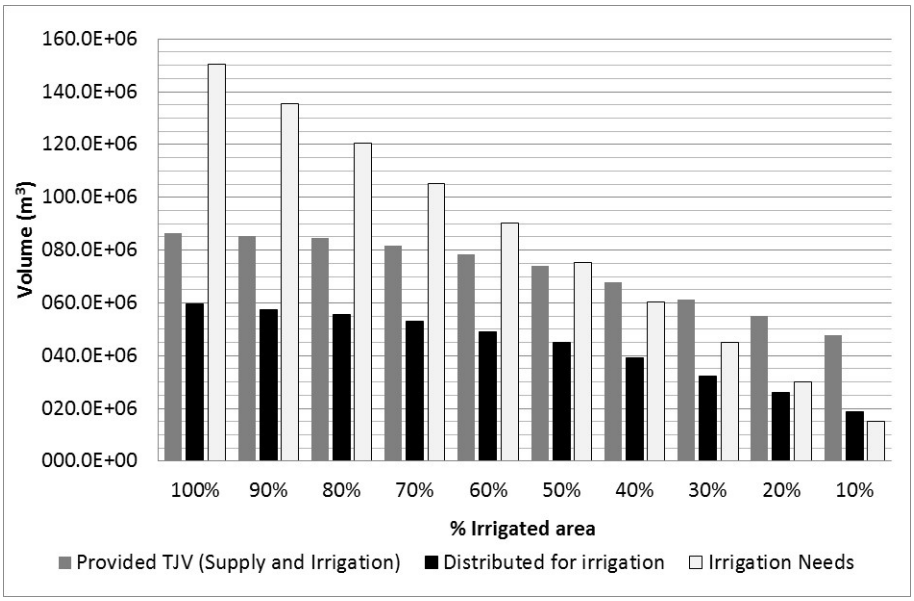

Figure 7. Global analysis of transferred volumes in the *TJV-PJV* system depending on irrigated area

3.2. Results. Theoretically recovered energy in the PJV system

The estimation of theoretically recovered energy in the system *PJV* presented the advantage that the input flow in each reservoir was fixed by water manager. Therefore, the operating point was fixed, excluding the available head, which was established by the developed model depending on circulating flow over time as well as the reservoirs' levels connected upstream and downstream. Figure 8 showed the theoretical operating zone of the hydraulic machine, which should be installed in the head reservoir of the *PJV* (here so called 'La Cuesta'). The same figure also showed the operating zone for another reservoir, which was located in the middle of the *PJV's* system. These results can be determined the same way in any of twenty recovery points analyzed using the developed model.

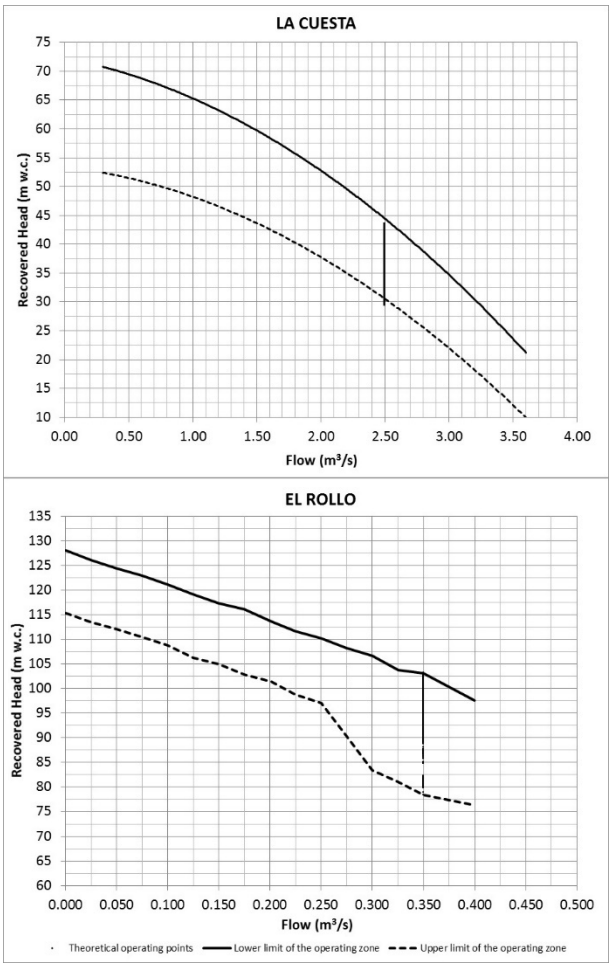

Figure 8. Examples of operating zone (recovered head vs flow) in different recovery points

The developed modelling for ten different assumptions of irrigated area made possible to define the upper and lower limits of the operating zone (Figure 8) for every recovery points studied. These two lines defined the operating zone (head and flow) of the hydraulic machine to install in the future. The more real situation was to work with permanent flows, which were defined according to control rules by the water managers of the *PJV* system. Figure 8 showed the most probable situation to 'La Cuesta' (reservoir 1) and 'El Rollo' (reservoir 2). If a hydraulic machine was installed in reservoir 1, the theoretically recovered head oscillated between 60 and 30 m w.c., being the flow range between 1.00 and 2.50 m^3/s, respectively. If available head in reservoir 2 was analyzed, the theoretically recovered head oscillated between 120 and 80 m w.c., while the flow range was contained between 0.1 and 0.35 m^3/s respectively.

The developed model also made possible to establish the theoretically recoverable energy depending on the considered scene of irrigated area. Therefore, for each scene and each recovery point of twenty analyzed, the water manager could determine maximum and minimum operating flow, maximum and minimum recovered head, maximum and minimum generated power of the machine, annual theoretically recoverable energy (kWh/year), annual volume (hm^3/year), as well as the economic parameter to define the feasibility of the recovery point (*PSR* and *EI*). Table 3 showed the obtained results for reservoir 2 (El Rollo), for which the theoretically recovered energy oscillated between 725 and 2625 MWh/year depending on analyzed assumption.

Table 3. Example of recovery parameter in reservoir 2, including feasibility parameters

Assumption of demand	**100%**	**70%**	**50%**	**30%**	**10%**
Q_{max} (m^3/s)	0.43	0.43	0.43	0.43	0.43
H_{max} (m)	106.6	119	120.4	120.5	120.6
P_{max} (kW)	449.7	502	507.9	508.6	508.9
Q_{min} (m^3/s)	0.4	0.39	0.38	0.38	0.4
H_{min} (m)	89.2	85.4	84.5	83.8	90.8
P_{min} (kW)	346.1	324.9	318.8	313.4	352.3
Energy (GWh/year)	2.6	2.58	2.19	1.49	0.73
V_{TURB} (hm^3)	12.81	12.35	10.33	6.69	3.11
t_{TURB} (h)	8 761	8 408	7 008	4 485	2 058
Incomes (€/year)	220 972	217 147	184 333	125 459	61 035
Expenses (€/year)	38 086	37 427	31 771	21 624	10 520
***PSR* (year)**	3.69	4.19	4.99	7.35	15.11
***EI* (€/kWh)**	0.26	0.29	0.35	0.51	1.05

Table 3 showed the feasibility of the recovery project is positive, being *PSR* lower than six years and *EI* was below to 0.4 kWh/year when the irrigated area was above 40%. Similar analyses can be done in the different studied recovery points.

Once the recovery points whose feasibility are defined, Figure 9 showed the consumed energy by the *TJV* system; the theoretically recovered energy in the *PJV* system, being the maximum value of 18 418 MWh/year; and the percentage which represents the recovered energy compared to consumed energy. The consumed energy was related to necessary energy to transfer the flow from Marquesa dam to San Diego reservoir as a function of transferred volume. The recovered energy showed the theoretically recovered energy, when the recovery systems are installed in the obtained feasible five recovery points, considering an efficiency of one.

Finally, the percentage of recovered energy showed the ratio between theoretically recovered energy and consumed energy for each transferred volume. Figure 9 showed the percentage of recovered energy is below to 7% when transferred volume was smaller than 80 hm^3. The development of these recovery points theoretically supposed to reduce the energy footprint of the water in the *TJV* system from 2.45 to 2.28 kWh/m^3.

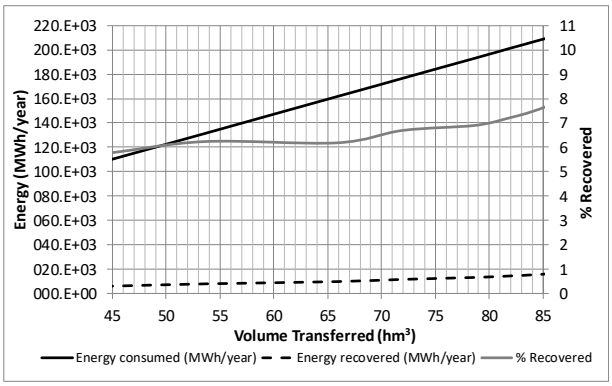

Figure 9. Consumed vs recovered energy depending on volume transferred

4. Conclusions and future developments

This contribution establishes the analysis of discretized flows over time in a greater distribution water system in Spain so-called Jucar-Vinalopó Transfer-Post-transfer. The objective of this infrastructure is to guarantee the supply in 50 000 irrigated hectares as well as the population of these municipality (Alto, Medio, Bajo Vinalopó, and L'Alacantí) and to recover the piezometric levels of the groundwater in the medium-long term.

To satisfy these objectives, a methodology was developed to optimize the pressurized water system by using software *EPANET* through a specific model developed. This simulation used own tools of the software as well as virtual hydraulic systems, which connected with main water system allow for the analysis of the water network. This simulation considered the transfer capacity as well as the regulation of volumes in the infrastructure.

The developed model was interesting because, once the model will be calibrated, it could be used as water management tool when the *TJV-PJV* system begins to operate, determining the control rules in the exploitation of the system. This model establishes the water management of the system depending on irrigation demand, supply demand and volume regulation of the connected infrastructure in the system. This tool also makes possible the decisions making, which maximize the distribution of the volumes in the *PJV* system.

The joint analysis of the system allowed the form to quantify the capacity of the *TJV* to guarantee the irrigation demand in the 59 reservoirs of the water system depending on irrigated area, the input of own hydric resources (mainly groundwater). When the system was analyzed, the study determines that there were not objective criteria which determine the closure of wells. This affirmation was supported on the analysis of annual transferred volume in each reservoir and each irrigation community.

The present work concluded developing a deep study of possible relations between water and energy in the joint system. If economic feasibility was considered in the possible recovery points, the maximum value of theoretically recovered energy was 18 418 MWh/year, considering the five feasible recovery points. This recovered energy was 7% of the provided energy to transfer the water volume from Marquesa dam to San Diego reservoir.

The future developments can be considered, using this recovered energy to complement processes in which was necessary electric energy (*e.g.,* desalation of wastewater) and currently, they cannot be used for irrigation due to the necessary economic cost to use it. If these analyses were developed, self-consumption systems could be established inside on irrigation communities. The development of these strategies made possible to reduce the hydric deficit, to minimize the extractions of groundwater, to improve the quality of water used, and to reduce the demanded energy to external resources.

Referencias

Abreu, J., Cabrera, E., Espert, V., García-Serra, J., & Sanz, J. (2012). *Transitorios Hidráulicos. Del regimen estacionario al golpe de ariete.*

Bru Ronda, C. (1993). La sobreexplotación de acuíferos y los planes de ordenación hidráulica en la cuenca del río Vinalopó: Alicante. *Investigaciones geográficas*. Instituto Interuniversitario de Geografía. Retrieved from ,https://dialnet.unirioja.es/servlet/articulo?codigo=111583&info=resumen&idioma=ENG

Cabezas, F. (2006). Trasvase Júcar-Vinalopó. Análisis de alternativas. Junta Central de Usuarios del Vinalopó, L'Alacantí y Marina Baixa.

Cabrera, E., Cobacho, R., & Soriano, J. (2014). Towards an Energy Labelling of Pressurized Water Networks. *Procedia Engineering*, *70*, 209–217. http://doi.org/10.1016/j.proeng.2014.02.024

Carravetta, A., Del Giudice, G., Fecarotta, O., & Ramos, H. M. (2012). Energy Production in Water Distribution Networks: A PAT Design Strategy. *Water Resources Management*, *26*(13), 3947–3959. http://doi.org/10.1007/s11269-012-0114-1

Castro, A. (2006). *Minicentrales Hidroeléctricas*. Madrid: Instituto para la Diversificación y Ahorro de la Energía. Retrieved from http://www.energiasrenovables.ciemat.es/adjuntos_documentos/Minicentrales_hidroelectricas.pdf

Choulot, A. (2010). Energy recovery in existing infrastructures with small hydropower plants. FP6 Project Shapes (work package 5- WP5), European Directorate for Transport and Energy. FP6 Project Shapes (work package 5- WP5).European Directorate for Transport and Energy.

Corominas, J. (2010). Agua y Energía en el riego en la época de la sostenibilidad. *Ingeniería Del Agua*, *17*(3).

De Leon Mojarro, R., Verdier, J., Piquereau, A., Ruiz-Carmona, V., & Rendon Pimentel, L. (2002). Regulación de una red de canales de riego. *Ingeniería Hidráulica En México*, *XVII*(4), 21–35.

Doorembos, J; Pruitt, W. O. (1977). *Las necesidades de agua de los cultivos* (FAO).

Emec, S., Bilge, P., & Seliger, G. (2015). Design of production systems with hybrid energy and water generation for sustainable value creation. *Clean Technologies and Environmental Policy*, *17*(7), 1807–1829. http://doi.org/10.1007/s10098-015-0947-4

Espert, J. (2009). Estudio de las estrategias óptimas de operación de la conducción del Trasvase Xúquer – Vinalopó. Proyecto Final de Carrera.

Espín, J. M. G. (1997). EL REGADÍO EN EL UMBRAL DEL SIGLO XXI: PLANES DE MEJORAS Y MODERNIZACIÓN. *Papeles de Geografía*.

Ferrer, C., Sánchez-Romero, F., Torregrosa, J., & Zapata, F. (2002). Plan de Obras y Actuaciones para la Comunidad General del Medio Vinalopó y L'Alacantí. Generalitat Valenciana.

Gilron, J. (2014). Water-energy nexus: matching sources and uses. *Clean Technologies and Environmental Policy*, *16*(8), 1471–1479. http://doi.org/10.1007/s10098-014-0853-1

IDAE. (2005). Ahorro y Eficiencia Energética en Agricultura de Regadío. (IDAE, Ed.). Madrid, Spain.

López Ortiz, M. I., & Melgarejo Moreno, J. (2010). El trasvase Júcar-Vinalopó: una respuesta a la sobreexplotación de acuíferos. *Investigaciones Geográficas*, *51*, 203–233. http://doi.org/10.14198/INGEO2010.51.09

Luis de Nicolás, V., Laguna-Peñuelas, F., & Viduera, P. (2014). Criterio para la optimización energética de redes ramificadas de agua. *Tecnología Y Ciencias Del Agua*, *5*(6), 41–54.

Murillo Díaz, J. M., Sánchez Guzmán, J., Castaño Castaño, S., Amayor Cachero, J. L., Gómez Gómez, J. de D., Roncero, J., … Corral Lledó, M. del P. (2009). *Alternativas de Gestión en el sistema de explotación Vinalopó-L'Alacantí*. (IGME, Ed.).

Pardo, M. A., Manzano, J., Cabrera, E., & García-Serra, J. (2013). Energy audit of irrigation networks. *Biosystems Engineering*, *115*(1), 89–101. http://doi.org/10.1016/j.biosystemseng.2013.02.005

Pizarro, C. F. (1996). Riegos localizados de alta frecuencia (RLAF). Goteo, micro aspersión y exudación. (Mundi-Pren). Madrid, Spain.

Ramón Morte, A., Olcina Cantos, J., & Rico Amorós, A. M. (1990). El cultivo de la uva de mesa en el Medio Vinalopó: recursos hídricos y riegos localizados de alta frecuencia. *Investigaciones geográficas*. Instituto Universitario de Geografía.

Rossman, L. A. (2000). *Epanet Manual*. (U. E. P. A. Risk Reduction Engineering Laboratory. Office of Research and Development, Ed.). Cincinnati, Ohio.

Salazar-Moreno, R., Rojano-Aguilar, A., & López-Cruz, I. L. (2014). La eficiencia en el uso del agua en la agricultura controlada. *Tecnología Y Ciencias Del Agua*, *V*(2), 177–183.

Silva-Hidalgo, H., Aldama, Á. A., Martín-Dominguez, I. R., & Alarcón-Herrera, M. T. (2013). Metodología para la determinación de disponibilidad y déficit de agua superficial en cuencas hidrológicas: aplicación al caso de la normativa mexicana. *Tecnología Y Ciencias Del Agua*, *IV*(1), 27–50.

Appendices

Appendix V

ENERGY FOOTPRINT OF WATER DEPENDING ON CONSUMPTION PATTERNS

Author version document which was sent to publish in Extended-JCR Journal "Ingeniería del Agua" ISSN 1134-2196.

Pérez-Sánchez, M., Sánchez-Romero, F., López-Jiménez, P.

[Accepted with changes 28/03/2017]

ABSTRACT

The energy audits are tools which make possible the analysis of the state of the water distribution network where the energy consumption depends on annual flow pattern (*RQ*). The present research develops a methodology to compare the energy footprint of water (*EWF*) through an energy balance with different *FPs*. The aim is to determine the energy behaviour of a network based on *FP* value. The study analyses four networks (two drinking and two irrigation networks), showing a lower total energy consumption (5.22, 3.21, and 4.01%) and a lower friction energy (28.57, 21.42, and 25%) those networks with *FP* less variable when these networks are compared with the network with more variability *FP*. As a novelty, the research defines a non-dimensional *EWF* parameter, which allows comparing *EWF* between different networks. This parameter can be introduced as sustainability index in the networks sizing in addition to technical and economic criteria.

Keywords: Energy footprint of water (*EWF*); consumption pattern; energy efficiency; pressurized water distribution networks

1. Introduction

The efficiency increase in the water cycle (*e.g.,* capitation, distribution or final use) is a prior objective to reach the development of sustainable systems (Corominas, 2010). The efficiency improvement in pressurized water systems has firstly been focused on the increase of hydraulic efficiency. Directly related to the improvement of hydraulic efficiency, the energy efficiency has also increased (Cabrera *et al.,* 2014). Nowadays, the improvement of energy efficiency is the main objective in pressurized distribution water systems as consequence as the increase in energy costs. Therefore, the energy analysis of water systems by the development of energy audits is a habitual technique which is used by water managers in pressurized water distribution networks (Gómez, 2016).

Initially, the energy studies were focused on drinking systems (Cabrera *et al.,* 1998) but the increase of energy consumption in pressurized irrigation networks as consequence as the development of drip irrigation causes a greater energy consumption in these irrigation networks (Abadia *et al.,* 2008). This growth of the consumed energy in addition to the increase of energy cost justify the need to develop strategies, which are supported in energy audits, to improve the efficiency of the network and to reduce the energy consumption in water networks. This need is justified when the evolution of energy and water consume is considered. From 1950 to 2013, irrigation water consumption grew

172%, improving 23% the hydraulic efficiency. At the same period time, energy consumption increased 1450% (Berbel et al., 2014).

Energy audits are priority to define the action objectives in the analyzed water systems. Once the energy audits are developed, the energy improvement should be tackled (Cabrera *et al.,* 2010; Pardo *et al.,* 2013). These objectives are mainly reduction of leakages in the water systems (Araujo *et al.,* 2006), improvement of pumped installations (Cabrera *et al.,* 2014), and development of methodology to minimize the pump's head when the system is pumped (Jiménez-Bello *et al.,* 2015; Moreno *et al.,* 2010). The energy recovery can be considered in addition to previously cited objectives (*e.g.,* pump as working turbines (*PATs*)) (Carravetta *et al.,* 2014, 2013a, 2013b; Ramos and Borga, 1999). The development of *PATs* allows for generating sustainable renewable energy (McNabola *et al.,* 2014; Ramos *et al.,* 2010), reducing the energy footprint along distribution phase of the water cycle either as direct ecological indicator in the water use or as indirect indicator in industrial process (Vanham and Bidoglio, 2013).

The establishment of efficiency thresholds in the water distribution systems is a difficult task. This difficulty is due to the determinants in each water networks (*e.g.,* topography, design criteria, consumption patterns) are different and inherent to the system. Therefore, at the beginning, a water network could only be compared to itself, being difficult the comparison between different water systems. In this sense, the present research looks for indicators, which allow for proposing comparison strategies based on non-dimensional parameters which are used to compare pressurized water systems. An energy balance is developed in four synthetic networks in which the topography and demand base are equal, using four different consumption pattern (two irrigation patterns and two supply patterns). The research shows the difference in the energy consumption depending on consumption patterns. Based on the developed analysis, the present manuscript proposes one sustainability energy index through energy footprint of water (*EWF*). The objective is to introduce this sustainability index in the future in addition to design and analysis criteria (*e.g.,* pressure, velocity, economical) of water networks to consider the headloss of friction energy as one additional criterion in the study and sizing of networks.

2. Methods and Materials

2.1. Methodology. Characterization of synthetic networks (Phase from 1 to 4)

The developed methodology in this section describes the different phases to do an energy balance in pressurized water networks which have similar design and operating conditions. Figure 1 shows these proposed phases. From phase 1 to 4, the synthetic network is developed while the last phase (phase 5) considers the energy balance of the system. The objective of the methodology is to obtain the characterization of synthetic networks with the same design criteria, which is based on consumption patterns of each analyzed networks. This characterization is necessary to develop the energy balances in

each network inherently to analyzed systems, making possible the comparison of energy values as a function of consumption patterns.

The necessary data to characterize the network are:

- Input 1: registered flow in main line of the network. In this case, recorded flows are hourly discretized.
- Input 2: characterization of the network. Consumption nodes, topographic heads, demand base and pipe length are defined. These parameters remain invariable in all study cases presented.

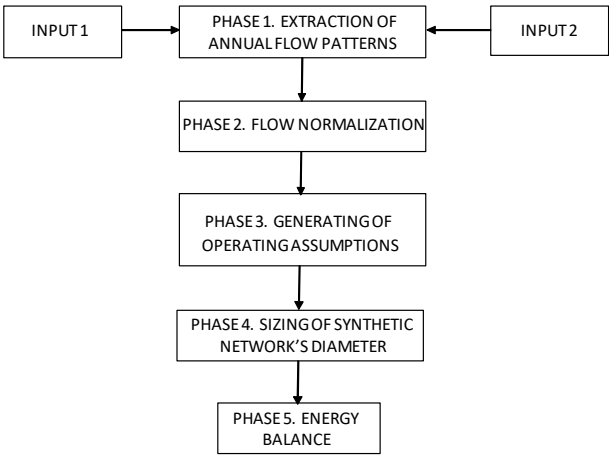

Figure 1. Characterization methodology of the synthetic networks and energy balance for each analyzed case study

Once the input data are described, the applied methodology in each consumption patterns is described:

1. Extraction of annual flow pattern (*FP*); For each registered flow (Input 1; Figure 1), an annual hourly operating pattern is obtained in the synthetic network. This pattern is consecutively defined for each hour by equation (1):

$$FP_j = \frac{Q_j}{Q_{100\%}} \quad (1)$$

where Q_j is the flow in the main line of the network in the instant *j* (m^3/s); $Q_{100\%}$ is the flow, whose value is the total demand of the consumption nodes (m^3/s). $Q_{100\%}$ is defined by equation (2):

$$Q_{100\%} = \sum_{i=1}^{i=n} Q_i \quad (2)$$

where *i* is each consumption node of the network. *i* varies between 1 and *n*, being *n* the total number of consumption node; Q_i is the demand of each

consumption node (m^3/s). The demand of consumption nodes is established by Input 2 (Figure1).

Once *FP* is obtained over year, this pattern is applied on all consumption nodes of the synthetic networks, obtaining the annual flow curve for the main line of the water network. The flow curve in this line has the same trend that the consumption node curve introduced.

2. Flow normalization; the obtained flow values in the main line are normalized. The main aim of normalization phase is to compare the same consumption situation each analysed pattern. This normalization is carried out adjusting the circulating flow to the integer number of above flow value. In the presented case study, the adjust is performed at intervals of 5 l/s to avoid to increase the number of generation of operating assumption to study. Once flow values in the main line are normalized, the hourly frequency distribution is obtained in each case study.
3. Generating of operating assumptions; for each normalized flow, different operating assumption are generated (the number of assumption in this case study are 31348). The consumption nodes are randomness opened or closed, increasing the number of opened nodes until the flow in the main line is equal to normalized flow studied (*e.g.,* 5, 10, 15 l/s). In some situations, the partial opening in the last consumption node is necessary to obtain the identical normalized flow value. To define the consumption node, which is opened, random integer number are generated between one and the total number of consumption nodes, being the generated number who establishes the opening node. This randomness opening continues consecutively until the getting of normalized flow in the main line without to consider the opened nodes previously.
4. Sizing of synthetic network's diameter; If the energy balance considering different *FP* is compared, all compared networks is necessary that they have the same design criteria. If the last sentence is considered, the synthetic network has to be sized for each considered *FP*. However, previous to define pipelines' diameter, the knowledge of sizing flow is necessary.

4.1. Determination of the sizing flows; the flow distribution in each line depends on the location of the opened consumption nodes. To obtain this distribution, different annual situations of opening consumption nodes are performed. These situations present the same annual frequency of normalized flow than the main line of the network in section 2. (100 situations are performed for each analyzed *FP* in this case study). These annual patterns are generated through the ensemble of operating assumption in section 3. The selection of the operating assumption is performed by generating random integer numbers (between one and a total number of calculated operating assumptions for each normalized flow). Each hypothesis is selected pertinently and the process

continues until the obtaining the total number of operating assumption for that normalized flow, which is defined by annual consumption pattern flow. In each selection, all assumptions are considered, although the assumption had previously been considered. For each generated pattern, the sizing flow is determined in each line as a function of the number of consumption nodes downstream (Q_{dc}), according to attached criterion in Table 1 (Granados García, 2013).

Table 1. Sizing criteria

Number of consumption nodes	Considered Flow (Q_{dc})
From 1 to 5	Cumulated flow equal to addition to all consumption nodes
From 6 to 25	Cumulated flow equal to percentile of 99%
>25	Cumulated flow equal to percentile of 95%

The maximum obtained flow is selected between all generated patterns for each line according to exposed criteria in Table 1. The used flow to size (Q_{dim}) will be the biggest value between previous calculated flow and obtained flow in the line connected downstream (Q_{dl}). Q_{dim} is defined by equation (3):

$$Q_{dim} = \max(Q_{dc};\ Q_{dl}) \tag{3}$$

4.2. Sizing pipelines' diameter. The sizing of the network is carried out by Excel worksheet which is programmed in Visual Basic (Walkenbach, 2010). This application determines the ensemble of diameters and resistance head of the network, minimizing the annual amortization cost by using the method of the economical series (Munizaga, 1976; Pérez-García, 1993) and considering the design conditions in pressure and velocity terms. The minimum pressure in the consumption nodes is 20 m w.c., being 10 m w.c. for those nodes whose consumption is null. Related to velocity criteria, the maximum and minimum velocity are 2.5 and 0.5 m/s, respectively. In each analyzed network, an only flow scene for each line is established as well as its pertinent solution of selected diameter.

2.2. Methodology. Energy Balance (Phase 5)

2.2.1. Determination of the resistance head of the network.

Particularly in this case as the network is pumped, the calculus of resistance head of the network is necessary before to do the energy balance. This head guarantees the minimum service pressure in each one of the operating assumptions, considering that for each operating assumption, the minimum service pressure is different as a function of the

location of opened nodes although the flow is identical. This head variation supposes the study of necessary resistance heads for the ensemble of generated assumptions, determining their variability according to the most unfavorable consumption point. For each normalized flow, the different pairs of data of flow (Q) and head (H) are obtained. The selected pair of data is that corresponds to 95% percentile value *(López-Cortijo et al.,* 2007; Pulido-Calvo *et al.,* 2003) of the ensemble pairs of data determined. This value represents the rule pressure, which must be provided by the pumped group as a function of flow in the main line (Planells and Ortega, 2006).

2.2.2. Energy balance

To perform the mathematical approximation in the problem solution, the energy equation through Reynolds Theorem (White, 2008) is used. This equation is defined by equation (4) when only supply point is considered (reservoir, if the network operates by gravity or pump if the network operates by pumped group) (Figure 2).

$$\gamma Q_O H_O \Delta t = \sum_{i=1}^{n} \gamma Q_i H_i \, \Delta t + \rho(\sum_{i=1}^{n}(Q_i u_i - Q_{oi} u_{oi}))\Delta t \quad (4)$$

where γ is the specific weight of the fluid in kN/m^3; Q_0 is the total demanded flow in the network in m^3/s; H_0 is the piezometric head of the water surface in the reservoir in m w.c.; Q_i is the demanded flow for each consumption point in m^3/s; H_{0i} is the piezometric head of consumption head i in m w.c., which is the addition of pressure (P_i) and geometrical level (z_i); $\gamma Q_O H_O$ is the total energy (E_T) provided by the reservoir or the pump group in kW; Δt is the considered interval time in s; $\sum_{i=1}^{n} \gamma Q_i H_i$ is the total consumed energy for each one of n consumption nodes of the network in kW; and $\rho(\sum_{i=1}^{n}(Q_i u_i - Q_{0i} u_{0i}))$ is the exchange of internal energy. If the system is adiabatic, internal energy is friction energy (E_{FR}) in kW.

The leakages are not considered because the objective of the methodology is to compare the energy balance as a function of the *FP*. However, leakages should be considered when energy audits are developed in a real network (Cabrera *et al.,* 2014; Pardo *et al.,* 2013).

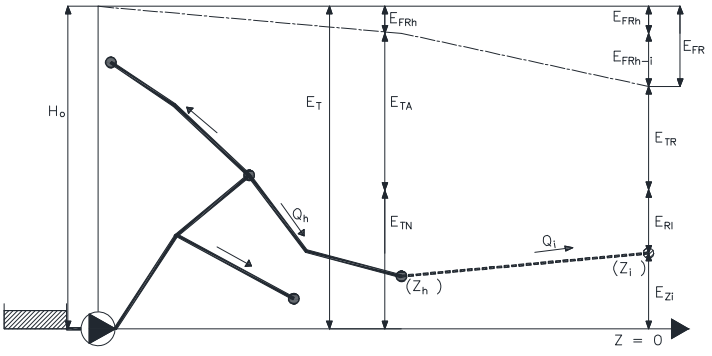

Figure 2. Energy scheme in a pressurized water system (adapted from Pérez-Sánchez *et al.,* 2016)

Pérez-Sánchez *et al.* (2016) differenced the global energy balance of the equation (4) in different energy terms for each line and type of consumption node (hydrant or user final) through equation (5):

$$E_{Ti} = E_{FRi} + E_{TNi} + E_{TAi} \tag{5}$$

where E_{Ti} is the provided energy to the system for each consumption node (i) in kWh; E_{FRi} is the dissipated friction energy in the network from origin to each consumption node in kWh; E_{TNi} is the minimum energy to guarantee the supply (pressure and flow) in the unfavourable consumption point in kWh, which is allocated downstream of the study point. This energy considers the geometrical energy more unfavourable in the pertinent point according to geometrical level (z_i), the minimum required pressure (P_{RIi}) as well as the friction headlosses from study point to more unfavourable point; E_{TAi} is the available energy in a consumption point or line in kWh. The totality of this energy is not necessary to carry out the supply. This energy can be divided on theoretically recoverable energy (E_{TRi}) and theoretically non-recoverable energy (E_{NTRi}). In the particular case of final consumption point, the totality of available energy is theoretically recoverable. The different described energies (E_{Ti}; E_{FRi}; E_{TNi}; E_{TAi}) are defined by the equations from (6) to (9):

$$E_{T_i}(kWh) = \frac{9.81}{3600} Q_i H_0 \Delta t \tag{6}$$

$$E_{FR_i}(kWh) = \frac{9.81}{3600} Q_i (H_o - H_i) \Delta t \tag{7}$$

$$E_{TN_i}(kWh) = \frac{9.81}{3600} Q_i H_{min_i} \Delta t \tag{8}$$

$$E_{TA_i}(kWh) = \frac{9.81}{3600} Q_i \left(H_i - H_{min_i}\right) \Delta t \tag{9}$$

where H_o is the provided head by the system (reservoir or pumped group) in m w.c.; H_{min_i} is the minimum piezometric head in a line or consumption node to guarantee the minimum pressure required to the unfavorable point downstream in m w.c.

The development of the proposed energy balance previously, allow for the determination of energy footprint of water (*EWF*). *EWF* is the dissipated friction energy per distributed unit of volume in the network (kWh/m^3). This *EWF* can be analysed for each network as a function of normalized flow. However, the given information by *EWF* doesn't allow for the comparison between pressurized water systems because the flow distribution and diameters are different in each network, and therefore, the friction energy values are also different. To be able to compare these values, non-dimensional energy footprint of water is defined (EWF_A) by equation (10):

$$EWF_{\mathrm{A}} = \frac{EWF}{EWF_{\mathrm{d}}} \tag{10}$$

where *EWF* is the energy footprint of water for each normalized flow value in kWh/m^3 and EWF_d is the obtained energy footprint of water for an only scene of flow by line, considering the scene of flow for which the network has been sized in kWh/m^3.

The determination of EWF_{A} possibilities the knowledge of one interval of energy footprint. This interval is inherent to the network and allows for comparing the obtained results between different networks. EWF_{A} can be determined for each value of normalized flow in each operating assumption. The comparison can be established when non-dimensional flow (Q_{A}) is associated with each EWF_{A} value. Q_{A} is defined by equation (11):

$$Q_{\mathrm{A}} = \frac{Q_{Ni}}{Q_{\mathrm{d}}} \tag{11}$$

where Q_{A} is the non-dimensional flow; Q_{Ni} is the normalized flow in each studied case (m^3/s); Q_{d} is the sized flow of the main line (m^3/s), according to defined criterion in Table 1.

2.3. Case study

The presented case study analyzes the behaviour of four different consumption patterns by applying described methodology previously. The patterns are obtained through registered data, which were recorded using an installed flowmeter in the main line in each of the four networks. These readings were recorded in two irrigation networks (here so called Network A and B) and two supply network (here so called Network C and D). Network A and B are systems, which were designed to demand. The existent crops in this irrigated area are different regarding irrigation needs and irrigation cultural techniques. Network C corresponds with a municipality network in which the population is uniform over the year, while Network D corresponds with a municipality network in which the population grows due to the township is touristic, increasing the population from June to October.

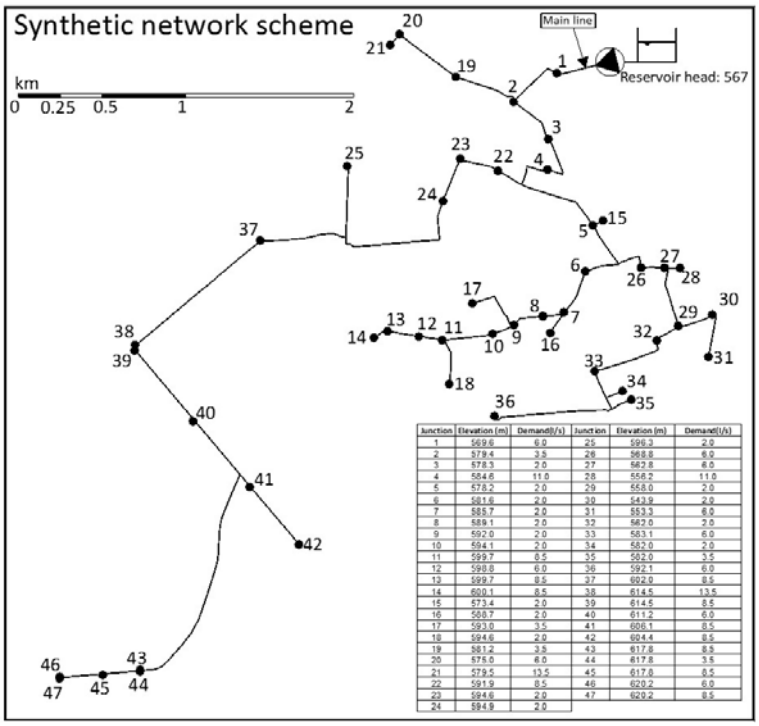

Junction	Elevation (m)	Demand(l/s)	Junction	Elevation (m)	Demand(l/s)
1	569.6	8.0	25	596.3	2.0
2	579.4	3.5	26	568.8	6.0
3	578.3	2.0	27	562.8	6.0
4	584.6	11.0	28	556.2	11.0
5	578.2	2.0	29	558.0	2.0
6	581.6	2.0	30	543.9	2.0
7	585.7	2.0	31	553.3	6.0
8	589.1	2.0	32	562.0	2.0
9	592.0	2.0	33	583.1	6.0
10	594.1	2.0	34	582.0	2.0
11	599.7	8.5	35	582.0	3.5
12	598.8	6.0	36	592.1	6.0
13	599.7	9.5	37	602.0	9.5
14	600.1	8.5	38	614.5	13.5
15	573.4	2.0	39	614.5	8.5
16	586.7	2.0	40	611.2	6.0
17	593.0	3.5	41	606.1	8.5
18	594.6	2.0	42	604.4	8.5
19	581.2	3.5	43	617.8	8.5
20	575.0	8.0	44	617.8	3.5
21	579.5	13.5	45	617.8	8.5
22	591.9	8.5	46	620.2	6.0
23	594.6	2.0	47	629.2	9.5
24	594.9	2.0			

Figure 3. Synthetic network's topology

Regarding network's topology (Figure 3), the pressurized water system is a branch network which provides the energy necessary by a pumped group. The network's model has 155 lines and 154 junctions, of which 47 junctions are consumption points. The network's elevation oscillates between 543.9 and 620.2 m, being pumped group's elevation 567 m.

3. Results and discussion

3.1. Annual flow patterns and synthetic network

The obtained annual flow patterns for each analysed network (A, B, C, and D) are shown in Figure 4 in which daily average *FP* are drawn. The four hourly patterns are different which are applied on $Q_{100\%}$ of 254 l/s. Network A (irrigation network) presents a flow pattern which has a similar trend of theoretical irrigation needs. These irrigation needs are minimum in the winter's months and they are maximum in summer's months, varying *FP* between 0 and 0.290 in July and obtaining an annual median *FP* of 0.015. Network B which is also an irrigation system presents a typical annual pattern of an irrigation network, in which, irrigation cultural techniques are applied promoting high frequency of irrigations along spring and autumn. Maximum *FP* is obtained in February, oscillating between 0 and 0.459. The annual median pattern is 0.095.

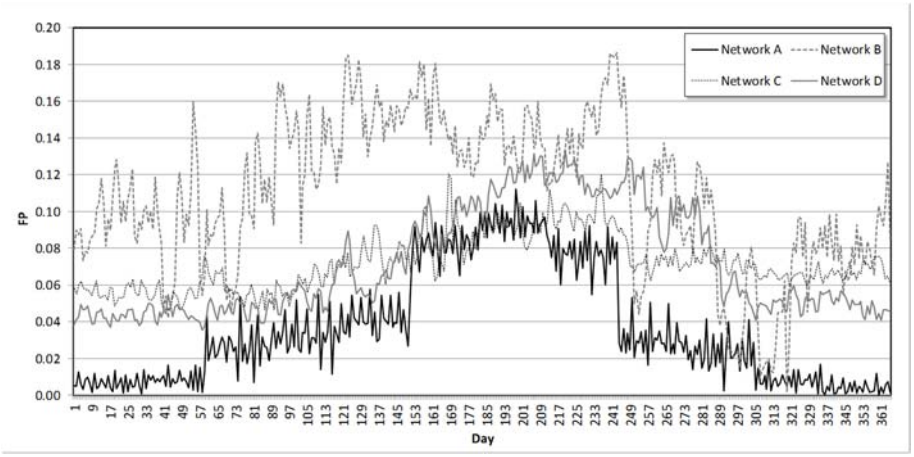

Figure 4. Daily average flow pattern for networks A, B, C, and D

Network C (drinking system) presents a pattern very uniform. This network supplies non-touristic township, keeping constant the population. *FP* oscillates between 0.015 and 0.206 in August (the month in which *FP* is maximum). The median value is 0.069. Finally, Network D corresponds a supply system of a touristic municipality with a high occupancy between June and October. *FP* varies between 0.004 and 0.258, being the annual median equal to 0.065.

When *FP* is determined for each network, the normalized flow's frequency is developed in each system. The relative frequency (*FR*) and cumulative frequency (*FC*) are shown for each network in Figure 5.

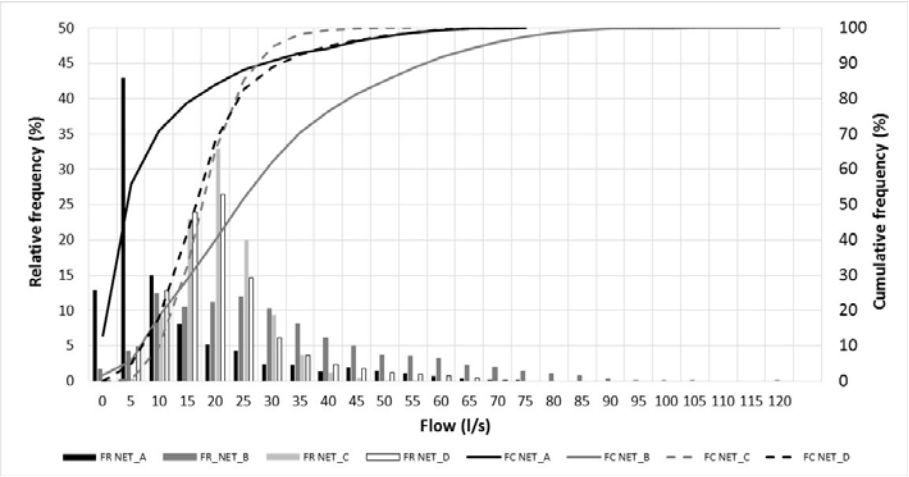

Figure 5. Relative (*FR*) and cumulative frequency (*FC*) of normalized flows

Figure 5 shown relative frequency are different between Network A and B. The cumulative frequency is 70.75% with flows between 0 and 10 l/s in the Network A. In contrast, Network B presents a cumulative frequency of 18.21% in the same flow range, showing a cumulative frequency of 52.04% between 10 and 35 l/s. This difference of values establishes a different behaviour in the demanded flows, justifying the difference between analyzed patterns. Whereas, networks C and D present a similar flow frequency (relative and cumulative). The cumulative frequency in these networks is 65.35 and 68.16% respectively when the flow range varies between 0 and 20 l/s. In all cases, the cumulative frequency is 100% when the normalized flow is above 60 l/s, except Network B, which has a cumulative frequency of 91.50% when the flow is 60 l/s. This difference of relative frequencies in each network has direct implications in the maximum flows and sizing of pipelines.

Table 2. Flow, pumped head, and selected diameter in each synthetic network

NETWORK	**A**	**B**	**C**	**D**
Flow in main line (l/s)	44.98	69.97	35.00	45.00
Head (m w.c.)	101.55	102.36	101.60	101.30
Diameter (mm)	**Network A Length (m)**	**Network B Length (m)**	**Network C Length (m)**	**Network D Length (m)**
DN40	0.00	0.00	0.00	0.00
DN50	2902.99	2902.99	3178.49	3178.49
DN63	782.00	782.00	506.50	506.50
DN75	334.63	334.63	334.63	334.63
DN90	1965.38	1965.38	1965.38	1965.38
DN110	1639.30	1267.06	1844.49	1844.49
DN125	433.33	435.73	369.84	369.84
DN150	1836.43	2400.93	1762.69	1562.03
DN200	2407.80	2109.14	2003.95	2204.61
DN250	2717.53	2821.53	4912.95	3053.42
DN300	2717.87	2387.57	893.86	2753.39
DN350	35.52	365.82	0.00	0.00
DN400	0.00	0.00	0.00	0.00

Table 2 summarizes sizing flows and pumped heads in the main line, which are obtained when each network is sized. The length of each selected diameter is also shown depending on the network. Related to design parameters, the sized flow oscillates

between 35 and 69.97 l/s and pumped head between 101.30 and 102.36 m w.c. The selected diameter range oscillates between 50 and 350 mm in all cases, although the length is different depending on the sized network.

3.2. Energy balance

According to methodology, firstly, the pumped head should be determined as a function of flow. Figure 6 shows obtained values (*e.g.,* there are 31348 pairs of data in the case study of Network B) for each analysed network and normalized flows. This figure draws the covering line, which guarantees the 95% percentile of resistance head. Figure 6 also shows the optimum point of pumped in the network. This point is used to size the network considering the energy costs.

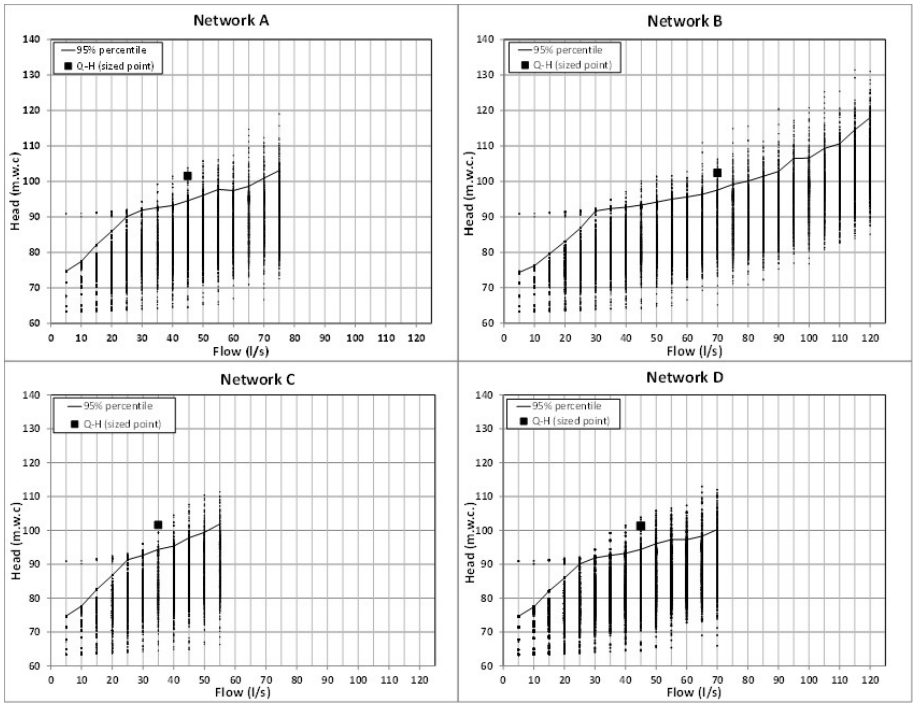

Figure 6. Resistance head as a function of normalized flow depending on consumption flow pattern (A, B, C, or D) and operating assumptions

The resistance head as a function of flow oscillates between 75 and 100 m w.c. when flow oscillates between 5 and 70 l/s in networks A, C (maximum normalized flow is 55 l/s), and D. The resistance head in Network B is greater as a consequence as the circulating flows are also greater than rest of networks. Network B reaches values near to 120 m w.c. when the flow is 120 l/s. If normalized flow range is analysed between 5

and 70 l/s, Network B presents a resistance head lower than obtained values in Network A, C, and D due to Network B has a greater length of the big diameter.

When diameters are known, which are determined by the same technical and economic criteria, as well as the resistance head of the system as a function of normalized flow and ensemble of operating assumptions, the energy balance can be developed in each analyzed network, obtaining the different values of energy. The annual obtained results of total energy (E_T), friction energy (E_{FR}), theoretically necessary energy (E_{TN}), and theoretically available energy (E_{TA}) are shown in Table 3.

These annual values are obtained by equations from (6) to (9) as a function of the annual operating hour for each normalized flow considering the annual flow pattern in each case.

Table 3. Energy balance developed for each consumption pattern

NET.	E_T		E_{FR}		E_{TN}		E_{TA}	
	kWh	kWh/m^3	kWh	kWh/m^3	kWh	kWh/m^3	kWh	kWh/m^3
A	89026.3	0.236	7544.3	0.020	65519.4	0.173	15962.6	0.042
B	240568.5	0.249	27056.7	0.028	154812.1	0.160	58699.7	0.061
C	157302.4	0.241	14106.9	0.022	116161.6	0.178	27033.9	0.041
D	156978.4	0.239	13598.3	0.021	114421.5	0.175	28958.7	0.044

The annual results of the energy balance are shown in Table 3 for each of energy terms as a function of considered consumption patterns (Network A, B, C, and D). However, each network has a different distributed volume. This difference impedes the comparison of energy values. Therefore, to compare these energy values between networks, the energy has to be defined by the unit of distributed volume. According to Table 3, Network B has the highest of total energy 240568.5 kWh (0.249 kWh/m^3). E_T ratio oscillates between 0.236 kWh/m^3 for the Network A and 0.249 kWh/m^3 for the Network B. E_{FR} varies between 0.020 kWh/m^3 for the Network A and 0.028 kWh/m^3 for the Network B. E_{TN} oscillates between 0.160 kWh/m^3 for the Network B and 0.178 kWh/m^3 for the Network C. Finally, E_{TA} varies between 0.041 kWh/m^3 for the Network C and 0.061 kWh/m^3 for the Network B.

If friction energy is known, the annual hourly energy footprint of water can be calculated through average obtained values of the operating assumptions generated. Figure 7 shows the relative (*FR*) and cumulated frequency (*FA*) of the *EWF* for each of the four consumption patterns. The main value of *EWF* is 0.1 kWh/m^3, which is inside of published average values range (between 0.1 and 0.3 kWh/m^3) on different networks. *FR* is 85.31% and 82.73% for the Network C and D respectively, being 75.36% for Network A and 51.85% for Network B. If cumulated frequency is observed, the reached values are 94.32%, 98.31% and 94.84 % for Networks A, C and D respectively, while Network B presents a cumulated frequency of 76.42%. Network B has a value near to

95% when *EWF* is 0.6 kWh/m^3. The analysis of the figure shows that the consumption pattern B has the highest EWF values, being in some cases close to 1.6 kWh/m^3.

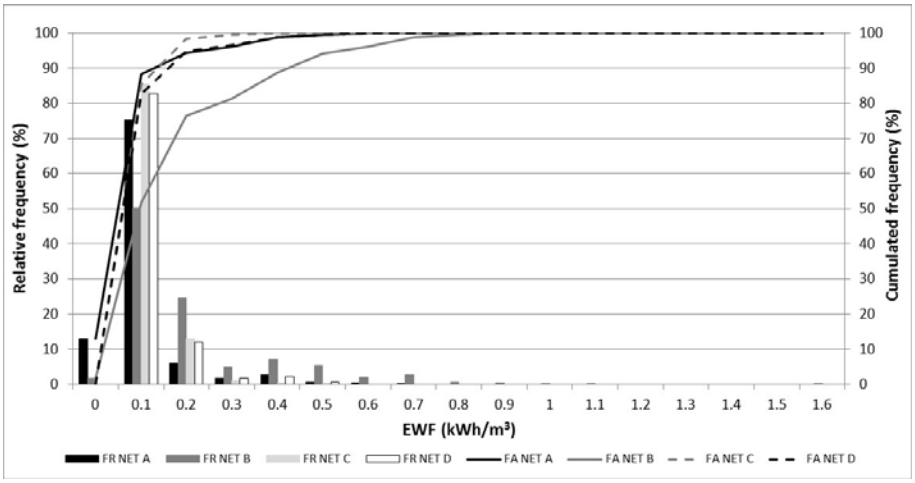

Figure 7. Annual relative and cumulated frequency of the EWF depending on consumption pattern.

Table 3 and Figure 7 show that the consumption pattern with more variable values of *FP* (Network B) has the highest consumption of energy in the majority of their terms (E_T, E_{FR} y E_{TN}). The *EWF* analysis for each of the four patterns can inherently be studied to the analyzed system. If the comparison between patterns is developed, EWF_A and Q_A should previously be determined. The sized flows are 44.98, 69.97, 35 y 45 l/s for Networks A, B, C, and D respectively (Table 2). EWF_d values are 3.08, 3.36, 2.85 and 2.86 kWh/m^3 for the networks A, B, C, and D respectively.

Figure 8 shows EWF_A values for each of the four analyzed patterns. Network B present the highest EWF_A value throughout the range of Q_A values, being the maximum EWF_A value 0.45. In contrast, Network C (which has more uniform *FP* values) presents the lowest EWF_A value throughout the range of Q_A values. In Network C, the maximum EWF_A value is 0.16. According to Figure 8, Network A and C present similar values of EWF_A, being the maximum close to 0.20.

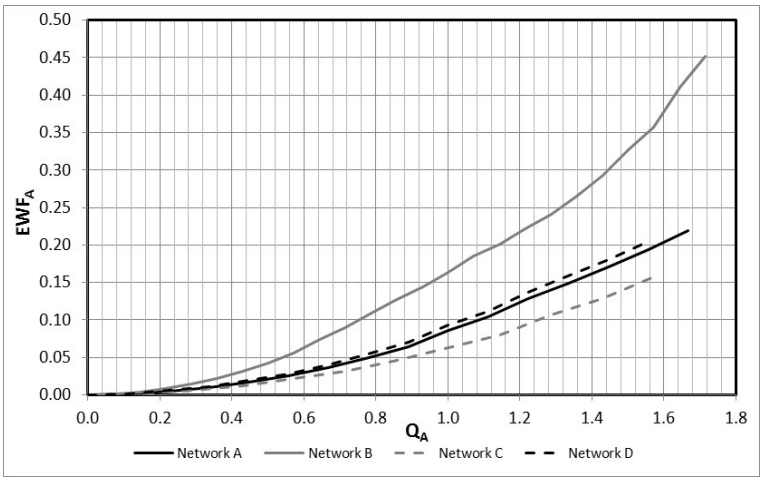

Figure 8. EWF_A as a function of Q_A for each one of the consumption patterns

If Figure 8 is analyzed according to shown values, when Q_A is 0.25, the minimum EWF_A value is 0.0048 kWh/m^3 in the Network C. Networks A and D present EWF_A values, which are above 32.49% and 44.72%, respectively, while EWF_A is 0.0114 kWh/m^3 in the Network B (141.14% upper than obtained value in Network C, which is the network with smaller non-dimensional energy footprint of water). When Q_A is 0.50, the results are similar. The minimum value of EWF_A is obtained in the Network C, being this value 0.0168 kWh/m^3. If the rest of EWF_A values is compared to Network C, the EWF_A value is 28.15% higher in the Network A, 155.36% higher in the Network B, and 41.07% higher in the Network C. If obtained results are analyzed when Q_A is 1.00, Network C present the minimum EWF_A value again. In this case, the EWF_A value is 0.0629 kWh/m^3. The obtained values of EWF_A are 36.72%, 159.62%, and 48.17% higher in the Networks A, B, and D, respectively. In the last case, when Q_A is 1.50, the EWF_A values are 27.10%, 128.71%, and 34.51% higher in the Networks A, B, and D if they are compared to Network C, whose EWF_A value is 0.1428 kWh/m^3.

Finally, if average EWF_A values in Networks A, B, and D are compared to obtained values in Network C for different values of Q_A, the average EWF_A are 31.53%, 149.38% y 42.59%, respectively. Therefore, the EWF_A analysis establishes that the network with the highest variability of *FP* (Network B) presents the highest EWF_A value comparing with *FP* more uniform.

.4. Conclusions

The developed manuscript allows for establishing different conclusions based on described results previously. The need to reduce the energy consumption is accepted by the society and therefore, the development of energy audits in distribution networks is a basic tool to detect the different defects in a water system studied. However, to try to

establish efficiency thresholds is a complex process which implies an exhaustive analysis of a lot of networks.

A methodology to develop a synthetic network with the same the technical and economic criteria through parameterized consumption patterns (*FP*). This methodology can be extrapolated to the study of any network, determining the *FP* value of the network, considering the base demand of the same. The definition of *FP* as a function of total demands of the consumption nodes ($Q_{100\%}$), the normalization of flows, the randomness process in the opening or closure of consumption points to generate the different operating assumptions considering the relative frequency of flows in each network possibility the characterization of the synthetic network. This methodology can be applied to energy analysis in any network both in the design phase or operating networks.

The knowledge of *FP* and its application in a network, which has the same determinant (*e.g.,* the number of consumption nodes, topography, the length of lines) makes possible the comparison of the energy balance in four different consumption patterns. The obtained results in this manuscript show that networks with high variability in their *FP,* the global energy consumption is higher. Therefore, when the network is pumped, the necessary power to distribute the flows is also higher than networks in which the *FP* is more uniform. The attached values in Table 3 show consumption reductions of E_T, which are 5.22 %, 3.21%, and 4.01% in the networks A, C, and D respectively, if these are compared to total consumed energy in Network B, which its *FP* is more variable. If E_{FR} is analyzed, the reductions are 28.57%, 21.42%, and 25%, respectively, when these values are compared to obtained value in Network B.

Once the energy balance is developed, the relative and cumulative frequency of *EWF* is determined for each of the networks. These frequency histograms show that the *FP* with a greater variability (Network B) also presents higher values of *EWF*. Network B has an average value of *EWF* of 0.150 kwh/m^3. The *EWF* values for the rest of networks (A, C, and D) are 0.041 kWh/m^3, 0.071 kWh/m^3, and 0.072 kWh/m^3. However, the comparison can only be done by using of new defined parameters (EWF_A and Q_A). The drawn results in Figure 8 show that the network whose *FP* is more variable, EWF_A values are high if they are compared to networks who *FP* is more uniform. The average EWF_A values are 31.53%, 149.38% and 42.59% (Network A, B, and C) higher than average EWF_A value for the Network C.

Finally, the proposal of EWF_A can be used to develop comparisons of *EWF* between the different networks. This index can also be incorporated in sizing methodologies in distribution water networks in addition to technical and economic criteria, introducing this parameter as a sustainability index in the sizing of the network. However, before to be used, the index has to be checked with more operating networks. The establishment of design thresholds of this parameter with the help of the flow data base is crucial to incorporate EWF_A inside of design parameters of the water networks.

References

Abadia, R., Rocamora, C., Ruíz, C., 2008. *Protocolo de Auditoría Energética en Comunidades de Regantes.* IDAE, Madrid, Spain.

Araujo, L.S., Ramos, H., Coelho, S.T., 2006. *Pressure Control for Leakage Minimisation in Water Distribution Systems Management*. Water Resources Management. 20, 133–149. doi:10.1007/s11269-006-4635-3

Berbel, J., Gutiérrez-Martín, C., Camacho, E., Montesinos, P., Rodriguez, 2014. "Efectos de la modernización de regadíos en el consumo de agua, energía y coste" in*: Congreso de Regantes de Huelva. Universidad de Córdoba*.

Cabrera, E., Almandoz, J., Arregui, F., García-Serra, J., 1998. *Auditoría de Redes de Distribución de Agua*. Ingeniería del Agua 6(4) 387–399. doi:10.4995/ia.1999.2794

Cabrera, E., Cobacho, R., Soriano, J., 2014. *Towards an Energy Labelling of Pressurized Water Networks*. Procedia Engineering. 70, 209–217. doi:10.1016/j.proeng.2014.02.024

Cabrera, E., Pardo, M.; Cobacho, R., Cabrera Jr., E., 2010. *Energy audit of water networks*. Journal Water Resource Planning and Management. 136, 669–677. doi:10.1061/(ASCE)WR.1943-5452.0000077

Carravetta, A., Del Giudice, G., Fecarotta, O., Ramos, H., 2013a. *Pump as Turbine (PAT) Design in Water Distribution Network by System Effectiveness*. Water 5, 1211–1225. doi:10.3390/w5031211

Carravetta, A., Del Giudice, G., Fecarotta, O., Ramos, H., 2013b. *PAT Design Strategy for Energy Recovery in Water Distribution Networks by Electrical Regulation*. Energies 6, 411–424. doi:10.3390/en6010411

Carravetta, A., Fecarotta, O., Del Giudice, G., Ramos, H., 2014. *Energy Recovery in Water Systems by PATs: A Comparisons among the Different Installation Schemes*. Procedia Engineering 70, 275–284. doi:10.1016/j.proeng.2014.02.031

Gómez, E., 2016. *Caracterización y mejora de la eficiencia energética del transporte de agua a presión*. Universitat Politècnica de Valencia.

Granados García, A., 2013. *Criterios para el dimensionamiento de redes de riego robustas frente a cambios en la alternativa de cultivos*. E.T.S.I. Caminos, Canales y Puertos (UPM). doi:16101

Jiménez-Bello, M.A., Royuela, A., Manzano, J., Prats, A.G., Martínez-Alzamora, F., 2015. *Methodology to improve water and energy use by proper irrigation scheduling in pressurised networks*. Agricultural Water Management. 149, 91–101. doi:10.1016/j.agwat.2014.10.026

López-Cortijo, I., Esquiroz, J.C., Aliod, R., García, S., 2007. Determinación de los costes energéticos en el cálculo de redes a presión con bombeo directo in: *XXV Congreso Nacional de Riegos. Pamplona*.

McNabola, A., Coughlan, P., Corcoran, L., Power, C., Prysor Williams, A., Harris, I., Gallagher, J., Styles, D., 2014. *Energy recovery in the water industry using micro-hydropower: an opportunity to improve sustainability*. Water Policy 16, 168. doi:10.2166/wp.2013.164

Moreno, M., Córcoles, J., Tarjuelo, J., Ortega, J., 2010. *Energy efficiency of pressurised irrigation networks managed on-demand and under a rotation schedule*. Biosystems Engineering 107, 349–363. doi:10.1016/j.biosystemseng.2010.09.009

Munizaga, E., 1976. *Redes de agua potable: diseño y dimensionamiento*. Instituto Eduardo Torroja. Monografía num. 335.

Pardo, M.A., Manzano, J., Cabrera, E., García-Serra, J., 2013. *Energy audit of irrigation networks*. Biosystems Engineering. 115, 89–101. doi:10.1016/j.biosystemseng.2013.02.005

Pérez-García, R., 1993. *Dimensionado óptimo de redes de distribución de agua ramificadas considerando los elementos de regulación*. Universitat Politècnica de Valencìa.

Pérez-Sánchez, M., Sánchez-Romero, F., Ramos, H., López-Jiménez, P., 2016. *Modeling Irrigation Networks for the Quantification of Potential Energy Recovering: A Case Study*. Water 8, 1–26. doi:10.3390/w8060234

Planells, P., Ortega, J.F., 2006. *Selección de bombas en redes de riego a presión*. Ingeniería del Agua 6, 47–57.

Pulido-Calvo, I., Roldán, J., López-Luque, R., Gutiérrez-Estrada, J.C., 2003. *Water Delivery System Planning Considering Irrigation Simultaneity*. Journal Irrigation and Drainage Engineering 129, 247–255. doi:10.1061/(ASCE)0733-9437(2003)129:4(247)

Ramos, H., Borga, A., 1999. *Pumps as turbines: an unconventional solution to energy production*. Urban Water 1, 261–263. doi:10.1016/S1462-0758(00)00016-9

Ramos, H., Mello, M., De, P.K., 2010. *Clean power in water supply systems as a sustainable solution: from planning to practical implementation*. Water Science and Technology Water Supply 10, 39–49. doi:10.2166/ws.2010.720

Vanham, D., Bidoglio, G., 2013. *A review on the indicator water footprint for the EU28*. Ecological Indicators 26, 61–75. doi:10.1016/j.ecolind.2012.10.021

Walkenbach, J. 2010. Excel 2010. Programación con VBA. Editorial Anaya. Madrid

White, F.M., 2008. Fluid Mechanics, Sixth edit. ed. McGrau-Hill.

This page is intentionally left blank.

Appendices

Appendix VI

PATs SELECTION TOWARDS SUSTAINABILITY IN IRRIGATION NETWORKS: SIMULATED ANNEALING AS WATER MANAGEMENT TOOL

Author version document which was sent to publish to index JCR Journal "Renewable Energy" ISSN 0960-1481 for its potential publication (Registered Data: 10/09/2016) Impact Factor 3.404. Position 24/88 (Q2). Energy&Fuels

Coauthors: Pérez-Sánchez, M; Sánchez-Romero FJ; López-Jiménez PA.; Ramos, HM.

This page is intentionally left blank.

ABSTRACT

Irrigation networks involve many water and energy aspects, in which sustainability plays a paramount role. Nowadays, water tariff of distribution flows in irrigation networks suppose a high percentage within of farmers' costs due to low hydraulic and energy efficiency. Considering the installation of pump as turbines (*PATs*) allows reducing the pressure and generating energy at the same time and the development of strategies for water and energy savings becomes interesting for water managers. In this research, a new methodology of recovered energy maximization taking into account the real feasibility is proposed to allocate *PAT* within networks. Simulated annealing techniques are used, with different objective functions and number of installed machines. Once the maximum energy lines are defined, real machines are selected according to the available net head in each allocation. Furthermore, the use of *WaterGEMS*® software has allowed the simulation of circulating flows and pressure variation for the installed machines. *WaterGEMS*® with simulated annealing techniques and the proposed methodology are powerful water management tools towards the sustainability in irrigation networks. To illustrate the proposed methodology, a case study is shown with a group of PATs parallelly installed in a pipe, recovering 26.51 MWh/year (a 9.55 % of the provided energy).

Keywords: Energy; Irrigations Networks; Simulated Annealing; *PAT*

1. Introduction

Nowadays, the development of the actual society is conditioned to the implementation of renewable energies. This development is established by European Union's policy, which the objective of reducing the greenhouse gas emissions down to 20% (Kougias *et al.,* 2014). Therefore, taking account that the consumption in water pressurized systems represents approximately 2-3% of the consumption of energy (Nogueira and Perrella, 2014), the use of hydropower plants in these infrastructures becomes of paramount relevance (Ramos *et al.,* 2010) to make possible the energy recovery and as a consequence, the energy footprint of water is reduced in the distribution of flows. Also, these actions contribute to management more environmentally and economically sustainable (*i.e.,* reduction of leakage and pipe breaks, as well as the generation of renewable energy for sale or personal consumption) (Carravetta *et al.,* 2013a; Cabrera *et al.,* 2014).

The energy recovery in water supply systems has been studied by different authors in terms of replacing the pressure reduction valves *(PRVs*) by mini-hydropower station

(Carravetta *et al.,* 2012), selecting of the type of hydraulic machine where pump as turbines (*PATs*) can be a feasibility solution (Ramos *et al.,* 2010, Carravetta *et al.,* 2013a, 2013b), and maximizing the theoretical energy available (Samora *et al.,* 2016). Drinking systems are different to irrigation network because in the latter, the demand is more variable and it is function on agronomic parameters, being more difficult to determine the consumption patterns.

In pressurized irrigation networks, different researchers have analyzed the optimization of consumption of energy in pumped systems (Moreno *et al.,* 2010; Pardo *et al.,* 2013; Jiménez-Bello *et al.,* 2015),while others have developed strategies to perform energetic audits in pressurized systems (Abadia *et al.,* 2010; Rodriguez-Diaz *et al.,* 2010; Pardo *et al.,* 2013; Cabrera et al., 2014), but the analysis of the potential recovered energy has not been performed deeply. Regarding this topic, only preliminary studies have been made. Some of these studies considered the average flows (Estrada and Ramos, 2015) and others studies analyzed the discretized flows and calculated the theoretical recovered energy in some pipe branches of a network (*i.e.,* in line, in hydrant or in irrigation point) (Pérez-Sánchez *et al.,* 2016).

This research promotes the study of energy recovery considering several factors: the demand's farmer, which depends on different habits (*i.e.,* irrigation endowment, maximum days between irrigation, weekly trend of irrigation, and irrigation duration); choosing the location of the turbines, which maximizes the theoretical energy recovered in function of the numbers of turbines; the definition the type of hydraulic machine to install (*i.e.,* speed number, diameter of impeller, rotational speed); and the analysis of the energy recovered as function of performance of the machine.

Although different authors have proposed strategies more or less complexes for placing the machines, which are cited by Samora *et al.* (2016), the localization of these places is not perfectly defined. In similar problems, the use of stochastic methods have been used, such as: localization of *PRVs* (Araujo *et al.,* 2006); sizing the diameter of pipes in the network (Kuo *et al.,* 2003; Tospornsampan *et al.,* 2007; Reca *et al.,* 2008); minimizing energy in pumped networks (Prats *et al.,* 2011); and recently, the method has been applied to allocate of recovery machine in water distribution network (Samora *et al.,* 2016). However, the problematic in the resolution of the number of combinations, as consequence the high number of lines implies also a higher number of combinations of calculus.

This research proposes a methodology to localize a high number of turbines (which attain ten) in an irrigation network, maximizing the theoretical recovered energy. Later, this is carried out in a real case study, where the used machines are defined and the network is modelled with *WaterGEMS* software (Nazari and Meisami, 2008) to obtain the recovered energy. *WaterGEMS* is a private domain software that provides to users a decision support tool for water distribution networks improving the knowledge of how infrastructure behaves as a system. This software can represent different elements (*e.g.,* pipes, joints, pumps, turbines, valves) as well as optimization strategies to minimize

consumed energy in pumped systems or determining pipe sizes as function of the investment cost, circulating flows and restriction of pressure by means use of genetic algorithm. The software has others utilities to improve the water management.

2. Material and methods

2.1. Analysis of recovered energy with installed turbines in different lines

In this section, the mathematical analysis of recovery energy with installed turbines in series is performed. Assuming a pipe system in series, where a turbine can be installed in all pipes (Figure 1).

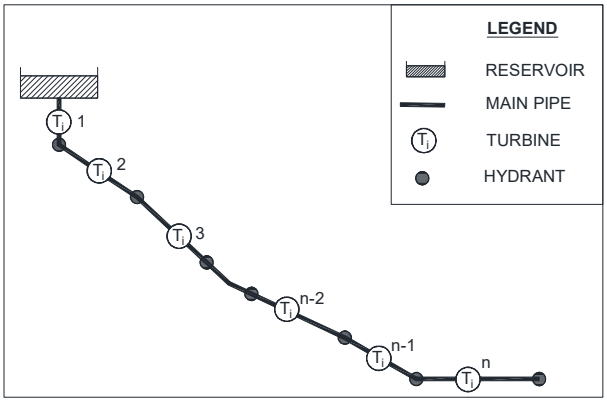

Figure 1. Pipe system with "n" turbines installed in series on all lines

If only a turbine is installed in the pipe system, the recovered energy is determined by equation (1):

$$E_{R_i} = \sum_{k=1}^{k=p} \eta\gamma Q_i \left(P_i - \max\left(P_{min_i}; P_{minI_i}\right)\right) \quad \Delta t = \sum_{k=1}^{k=p} \eta\gamma Q_i H_i \Delta t \tag{1}$$

where E_{R_i} is the recovered energy in line 'i' when an only turbine is installed in the pipe system (kWh); if subscript is *'R'*, this indicates that recovering value is obtained with a defined machine. When subscript is *'T'*, this indicates that recovering value is theoretical; i is the line of the system where the turbine is installed. 'i' varies between one and 'n'; k is the time interval analyzed. k varies between one and 'p'; p is the number analyzed intervals; η is the machine efficiency; γ is the specific weight of the fluid (N/m^3); Q_i is the circulating flow by a line (m^3/s); P_i is the service pressure in any point of the network when consumption exists (m w.c.); P_{min_i} is the minimum pressure of service of a line or hydrant to ensure the minimum pressure in the most disadvantageous consumption node (m w.c.); P_{minI_i} is the minimum pressure of service of an irrigation point required to ensure the irrigation water evenly (mw.c.); H_i is the value of head in irrigation point, hydrant or line (m w.c.); Δt is the time interval (s).

When several turbines are installed, the recovered energy in each line is equal to equation (2):

$$E_{Ri}^{s} = \sum_{\Delta t=0}^{\Delta t=p} \eta\gamma Q_i H_i \Delta t - \sum_{i=1}^{i=m}\left(\sum_{\Delta t=0}^{\Delta t=p} \eta\gamma Q_i H_i \Delta t\right) = \sum_{\Delta t=0}^{\Delta t=p} \eta\gamma Q_i \left(H_i - \sum_{i=1}^{i=m}(\mathrm{H}_i^{S})\right)\Delta t \quad (2)$$

where *n* is the number of turbines installed in the piping systems. If all lines have turbine, '*n*' is equal to '*i*'; *m* is the number of installed turbines upstream. *m* varies between 0 and '*n-1*'; E_{Ri}^{s} is the recovered energy by the turbine installed in the line 'i' with other turbines installed in series (kWh); H_i^{S} is the recovered head by other installed turbines in series with the line '*i*' in upstream lines (m w.c.).

As an example, if the pipe system has three lines (*n*=3), the recovered energy, according to equation (2) is:

In line 1 (i=1),

$$E_{R1}^{s} = \sum_{\Delta t=0}^{\Delta t=p} \eta\gamma Q_1 \left(H_1 - \sum_{i=1}^{i=0}(\mathrm{H}_i^{S})\right)\Delta t = \sum_{\Delta t=0}^{\Delta t=p} \eta\gamma Q_1 (H_1)\Delta t;$$

In line 2 (i=2),

$$E_{R2}^{s} = \sum_{\Delta t=0}^{\Delta t=p} \eta\gamma Q_2 \left(H_2 - \sum_{i=1}^{i=1}(\mathrm{H}_i^{S})\right)\Delta t = \sum_{\Delta t=0}^{\Delta t=p} \eta\gamma Q_2 (H_2 - \mathrm{H}_1^{S})\Delta t;$$

In line 3 (i=3),

$$E_{R3}^{s} = \sum_{\Delta t=0}^{\Delta t=p} \eta\gamma Q_3 \left(H_3 - \sum_{i=1}^{i=2}(\mathrm{H}_i^{S})\right)\Delta t = \sum_{\Delta t=0}^{\Delta t=p} \eta\gamma Q_3 (H_3 - \mathrm{H}_1^{S} - \mathrm{H}_2^{S})\Delta t;$$

Therefore, the total recovered energy with installed turbine in series (E_{RT}^{s}) is equal to $E_{R1}^{s} + E_{R2}^{s} + E_{R3}^{s}$. If the expression is generalized for '*n*' turbines in series in '*n*' lines, the E_{T}^{s} is defined by the equation (3):

$$E_{TR}^{s} = \sum_{i=1}^{i=n} E_{Ri}^{s} \quad (3)$$

If the analysis of the E_{TR}^{s} is performed in a branched network (Figure 2), E_{TR}^{s} is defined by the equation (4):

$$E_{TR}^{s} = tr[D] = tr\left[[A][B][C]\right] \quad (4)$$

where E_{TR}^{s} is the total theoretical recovered energy in the network (kWh); $[A]$ is the matrix (*nxi*) made up zero or one. The matrix has '*n*' rows, where '*n*' is the number of turbines and '*i*' columns, being *'i'* the number of lines of the network. This matrix defines where the turbines are installed in the network. If the value is one, a turbine is installed in this line, otherwise (value equal to zero), the line *'i'* has not installed a turbine; $[B]$ is the matrix (*ixi*), which defines the energy that could be recovered in a line, when another independent turbine upstream can exist. This matrix is constant in the network and this is defined by the number of lines of the network *(i)* and it is previously defined; $[C]$ is the matrix (*nxi*) made up zero or one, which defines the lines where the turbines upstream are placed. This matrix is generated according to the topology of the network. Only can present one in each column; $[D]$ is the matrix (*nxn*), which is the result to matrixes product [*A*][*B*][*C*]. When this product is calculated and the trace of the matrix *(tr)* [*D*] is

determined, the obtained value is the theoretical recovered energy in the network (E_{TR}^{S}). The trace is the addition of eigenvalues of the main diagonal of the matrix.

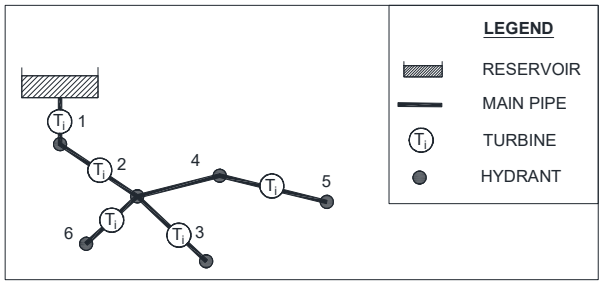

Figure 2. Branched network with *'n'* turbines installed

2.2 Optimization methodology for maximizing energy

Simulated Annealing is a search heuristic algorithm, which is based on the analogy with the physics process of annealing of metals and this is inspired in Monte-Carlo's method. Kirkpatrick *et al.* (1983) based on Metropolis's idea (Metropolis et al., 1953), applied it to the optimization problems of combination. This method, which is indicated as a powerful tool for both discrete as continuous problems (Tospornsampan *et al.,* 2007), can find robustly (Rutenbar, 1989; van Laarhoven and Aarts, 1987; Youssef *et al.,* 2001) the best solution (according to the defined objective function) of problems of different typologies and a high number of combinations.

Next, the flowchart to develop the maximization problem (Figure 3) is defined:

1. Definition of the objective function (ψ_i). In this research, are studied two functions to maximize and these are defined by the equation (5) and (6):

$$\psi_1 = E_{TR}^{S} \tag{5}$$

$$\psi_2 = \frac{E_{TR}^{S}}{PSR} \tag{6}$$

   where *PSR* is the payback period simple, which is lately defined in section 2.5. When the optimization is performed with the objective function defined in the equation (6), an averaged performance equal to 0.55 is considered, according to the author Castro (2006).

2. Generating of an ordered list of the lines in descendent order depending on objective function. For function defined by equation (5), the order is established according to theoretical energy recovery in a line (E_{Ti})

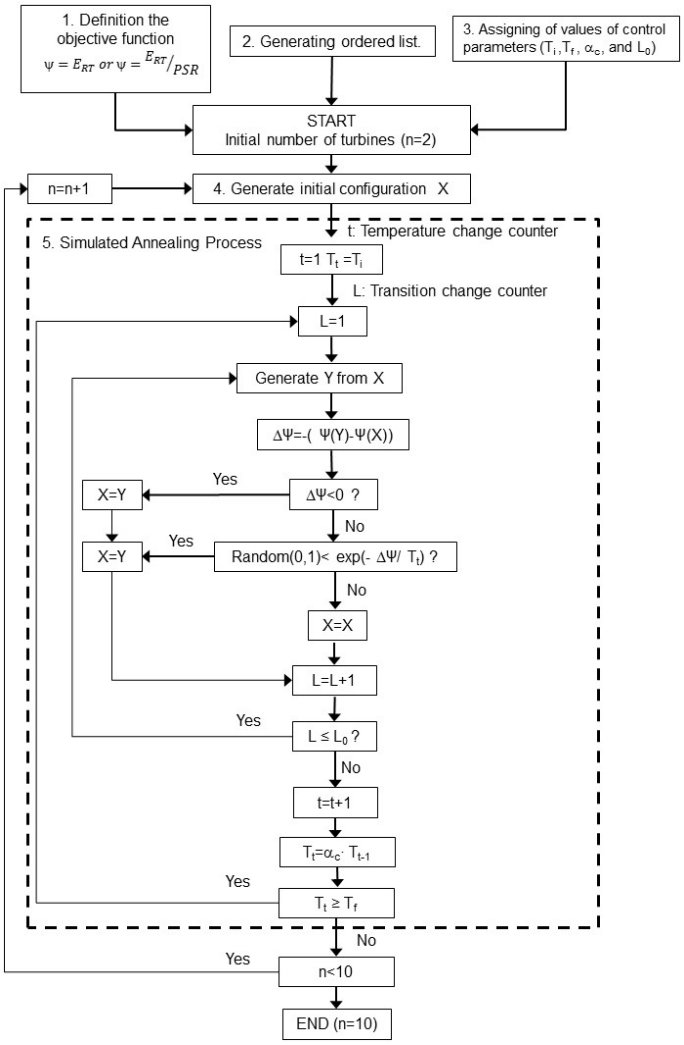

Figure 3. Flowchart for optimization of networks in the energy recovering process with "n" installed turbines

3. Assigning of values of control parameters which characterize the Simulated Annealing Process, defining the number of iterations. These parameters are: T_i is the initial temperature; T_f is the final temperature, α_c is the cooling rate; and L_0, which is the number of transitions in each temperature step (T_t). These parameters are fixed according to a sensitivity analysis performed previously and are changed depending on objective maximized function.

4. Establishment of the initial combination (*X*), $X = (x_1, x_2, .., x_n)$, in which '*n*' is the number of turbines and $'x_i'$ is the line where each turbine is located. For *n=2*, the lines selected are the first two lines. If the initial combination is to *n*>2, it starts with obtained solution for '*n-1*' turbines. The line with greater value of the objective function, is added to this initial result, which is not contained in the solution.
5. Developed Simulated Annealing Process, where a new combination (*Y*) is generated, according to the general process, which is described by (Tospornsampan *et al.,* 2007). For each iteration, randomly, a line is deleted of the combination and other line is randomly introduced taking account that the lines with better position in the ordered list (Step 2) have greater probability to be introduced in the new combination $Y = (y_1, y_2, .., y_n)$.

2.3 Selection of PATs

The selection of the hydraulic machine is very important in the energy recovering process, taking into account that the water manager has to guarantee the quality service to users, ensuring the minimum pressure established (normally, in irrigation network, this pressure is equal to 30 m w.c. in the consumption node).

In this sense, numerous authors have analyzed the use of *PATs* in non-conventional heads, where the flow and head are not constants. These have been proposed at remote areas (Ramos and Borga, 1999; Arriaga, 2010) and for small applications in pressurized systems of distribution, which are mainly allocated for drinking systems (Ramos et al., 2009, 2010; Carravetta et al., 2012, 2013a, 2013b, 2014; Imbernón and Usquin, 2014; Kougias *et al.,* 2014; Samora *et al.,* 2016) or irrigation (Estrada and Ramos, 2015; Pérez-Sánchez *et al.,* 2016). The use of these machines is due to: wide range of pumps existing in the actual market, low price, and high availability if *PATs* are compared with the conventional turbines (Ramos *et al.,* 2009).

Different authors (Singh, 2005; Rawal and Kshirsagar, 2007; Derakhshan and Nourbakhsh, 2008; Yang *et al.,* 2012) have analyzed characteristic curves of head (*Q-H*) and performance, for non-dimensional parameters of the hydraulic machines, such as the discharge number (φ) and the head number (ψ), being defined by the equations (7) and (8) (Mataix, 2009) as a function of impeller's diameter (*D*) and rotational speed of the machine (*N*):

$$\varphi = \frac{Q}{ND^3} \tag{7}$$

$$\psi = \frac{H}{N^2D^2} \tag{8}$$

Figure 4 shows the values of head number and performance (η) for some turbines depending on the discharge number, for different values of specific speed (*ss*) which is defined by equation (9):

$$ss = N\frac{\sqrt{P_R}}{H_R^{1.25}} \quad (9)$$

where: N is the rated rotational speed (rpm); P_R is the rated power (kW); H_R is the rated head (m w.c.); being *'R'* the pump design point or the best efficiency condition.

This figure confirms the high variation of the performance if the flow through the *PAT* varies. Also, the best efficiency point (*BEP*) trend line is drawn in this figure allowing to determine the *BEP* as function of the specific speed of the machine.

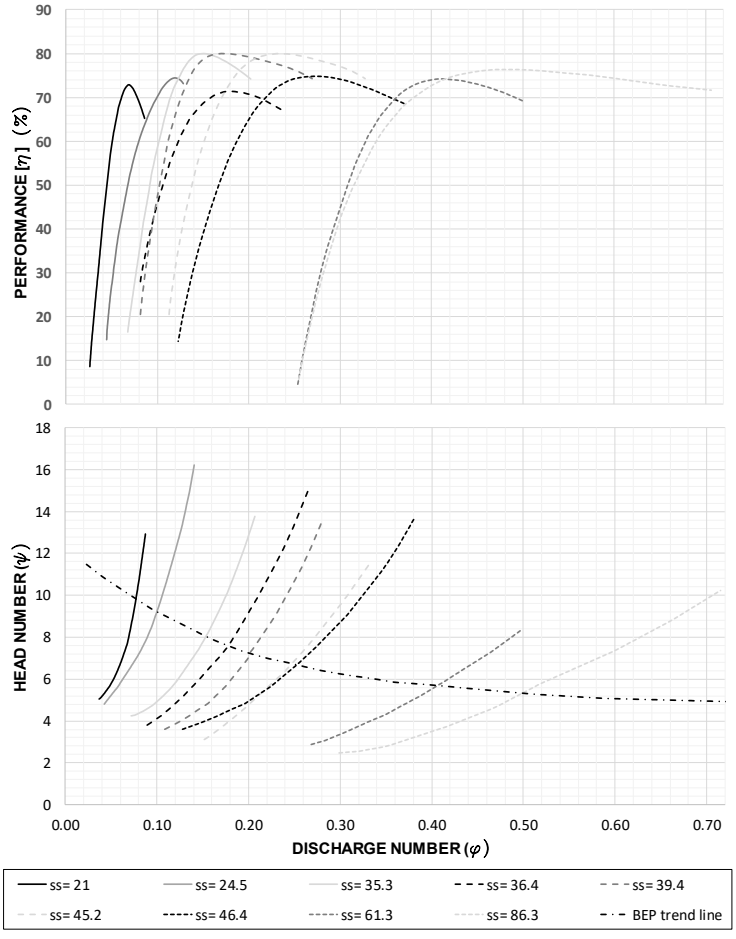

Figure 4. Head number and performance depending on the discharge number (adapted from Singh, 2005; Rawal and Kshirsagar, 2007)

The assignation of values of circulating flows and available net head (H_T) in each line are obtained through the methodology proposed by Pérez-Sánchez *et al.* (2016). These

flows have been determined on the basis of open probability of irrigation point according to farmers' habits.

Therefore, considering that the pressure must be ensured for users in all operating range, the selected machine cannot absorb more head than the H_T obtained. This premise must be considered always, and it prevails on the recovery of energy because the water distribution networks can be multipurpose systems, since the power generation is not the first objective (Choulot, 2010). Figure 5 shows the criterion of selection for the operation range of the machine, diameter of impeller (D) and rotational speed (N) have been fixed taking account the available net head.

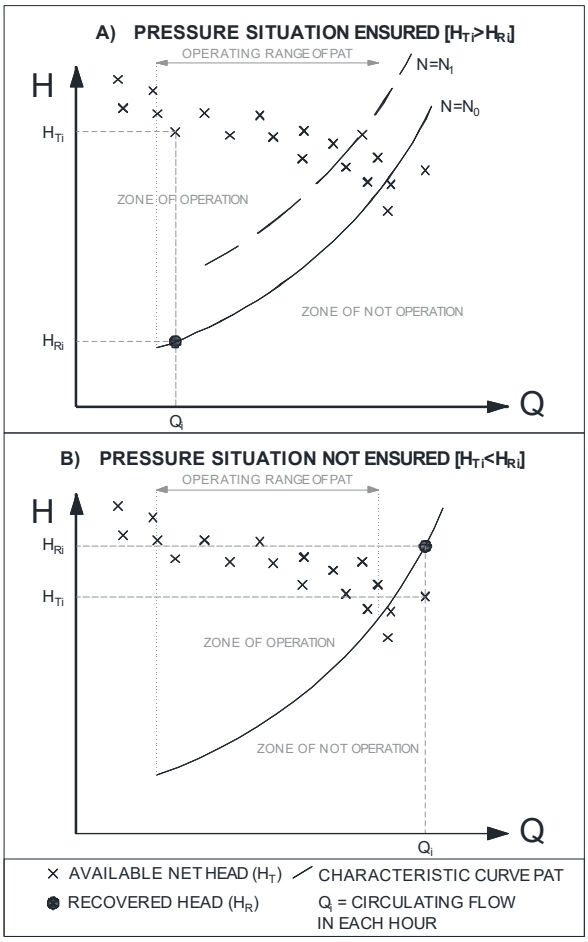

Figure 5. Criterion to select machine ensuring pressure in the irrigation points. (A) Ensured pressure. (B) Not ensured pressure

To select the upper limit of flow in the operation range of *PAT*, the arbitrary criterion adopted is to ensure at least 80% of the cumulative frequency of circulating flows in the studied line can be recovered. This criterion is defined considering the high variability of the *PAT* performance, when the flow varies. Particularly in these networks, the variability of flows along the time is very high. In order to increase the operation range, the installation of groups of *PAT* in parallel should be considered. The number of installed machines will depend on its characteristic curve considering a fixed rotational speed.

Figure 6 shows the proposed scheme for installing the *PATs* in each pipe line: one flowmeter, for measuring the instantaneous flows; isolation valves (*IV*), installed upstream to each *PAT* (its number is equal to the number of parallel *PATs* installed, plus one more pipe, corresponding to the by-pass when the system does not generate energy); and *PATs* that the number of the machines varies as a function of their characteristic curve for reaching 80% of the cumulative frequency of flow at least in each line.

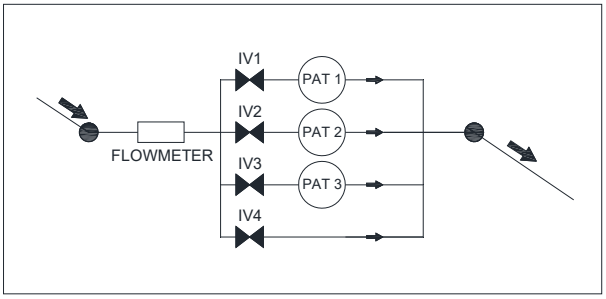

Figure 6. Scheme proposed for installing the *PATs* in parallel

The operation mode is described below, and this is shown in the Figure 7. For a particular *'k'* hour, the estimated flow ranges between minimum flow in line ($Q_{min\ in\ line}$) and minimum operation flow defined for one *PAT* (Q_{min_1PAT}), the isolation valve 4 *(IV4*) is open and the rest (*IV1*, *IV2*, and *IV3*) are closed. If the instant flow is between Q_{min_1PAT} and maximum operation flow defined for one *PAT* (Q_{max_1PAT}), *IV1* is open and *IV2*, *IV3* and *IV4* is closed. When the flow increases to Q_{max_1PAT}, the second *PAT* must be connected and *IV2* changes its state from closed to open. This position is maintained in the flow range with lower limit equal to the minimum operation flow defined for two *PATs* installed in parallel (Q_{min_2PAT}; $Q_{min\_2PAT} = Q_{max\_1PAT}$) and its upper limit equals to the maximum operation flow defined for two *PAT* installed in parallel (Q_{max_2PAT}). This situation is recurrent as function of the number of *PAT* installed. When the flow is higher than the maximum operation flow defined (in the Figure 7 is Q_{max_3PAT}), the isolation valve of the by-pass (*IV4*) is open and the rest closed in the range of flows between the maximum operation flow for *"n"* installed *PAT* (in Figure 7), the number of machines are equal to three (n=3) and the maximum circulating flow ($Q_{max\_in\_line}$).

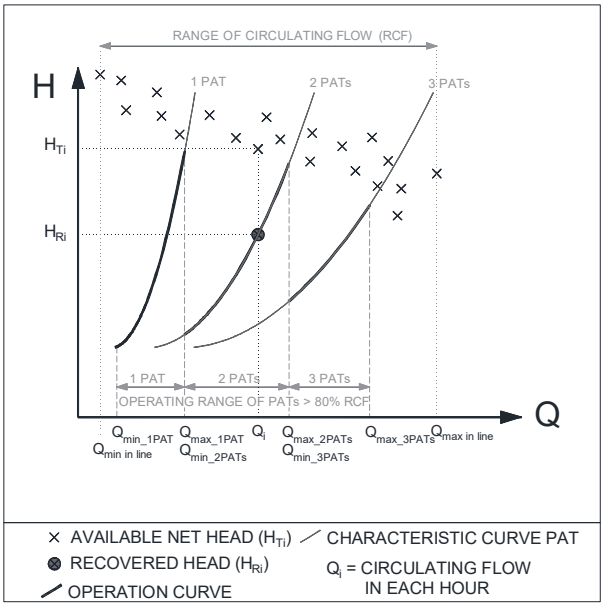

Figure 7. Scheme of Operation Zone

2.4 Selection of PATs

Once operation curves have been defined for the selected lines of in the network, where the machines have been allocated according to solution established in the optimization by simulated annealing, the next steps consist on the maximization of the energy recovered. To do so the network is modelled in *WaterGEMS* (Nazari and Meisami, 2008) in extended period simulation. The simulation is performed according to the demand's pattern in all consumption points and by implementing the *PAT's* operation schemes previously defined and the operation curves of recovering energy.

Subsequently, the obtained results of flow and recovered head are processed, determining the performance in each machine. This analysis allows to know: recovered energy (E_R); recovering coefficient (RC), defined as the ratio between recovered energy and theoretical energy (E_T) in the line, obtained for ideal machines (where every available energy can be recovered); maximum power installed (P_{max}), this value corresponds to the maximum instant power generated by the machine; minimum power installed (P_{min}), it refers to the minimum instant power performed by the machine; maximum performance (η_{max}), minimum performance (η_{min}) and weighted average performance (η_w) developed by the machine in all operating times; operating time of each machine (t_{nT}); total energy recovered (E_{TR}) in the network (taking account to the total number of installed turbines (n) in the parallel group in all lines); and total recovering coefficient (TRC) in the network.

2.4 Maximum number of turbines to be installed

Obviously, the installation of a larger number of turbines implies a greater recovered energy. However, the maximum number of turbines to be installed in a branching network will be established taking into account recovered energy and economic parameters. Although different authors (Castro, 2006; Zema et al., 2016) have used the economic criterion based on payback period of the investment, in Spain, Castro (2006) proposed as investment viability analysis the following indicators:

a) Period simple return (*PSR*). This indicator is defined by the equation (10):

$$PSR = \frac{IC}{I-C} \tag{10}$$

where: *IC* is the investment cost (€), Carravetta et al., (2013a) estimated the value of *IC* equal to 545 €/kW if pump as turbine (*PATs*) is used for installed power below to 10 kW; *I* is the annual income (€/year); C is the annual operating cost (€/year).

The annual income (*I*) is defined by the equation (11):

$$I = P_E E_{TR} \tag{11}$$

where P_E is the energy price (€/kWh); E_{TR} is the recovered energy obtained through the *WaterGEMS*. When the hydropower station injects the energy on the grid, P_E is the sale price of the energy. If the hydropower station is used for self-consumption, P_E is the purchase price of the electric energy for the consumer. In this case, the average price considered is equal to 0.0842 €/kWh.

The annual operating cost (*C*) is defined by the equation (12):

$$C = C_0 E_{TR} \tag{12}$$

where C_0 is the unit operating cost (€/kWh). Castro (2006) estimated this parameter in 0.0145 €/kW;

b) Energy index (*EI*) is the ratio between *IC* and E_{TR}, which is defined by equation (13):

$$EI = \frac{IC}{E_{TR}} \tag{13}$$

According to Castro (2006), these installations are viable if the *PSR* is less than six years and the energy index smaller than 0.6 €/kWh.

3. Case Study

3.1 Description

In order to apply the described methodology for determining the optimal number of turbines to be installed in a real network, a particular case study for a Spanish irrigation network is here described.

The modelled network is located in Vallada (Spain) and the surface irrigated is equal to 290.2 ha, being the citrus the main crop. The irrigation system (Figure 8) is designed as a branching network, which is designed with the criterion of irrigation to demand (the user can get the resource in sufficient quality and quantity necessary). The difference of topographic elevation between higher and lower irrigation point is equal to 130 m and the high reservoir ensures the minimum pressure of 30 m w.c. in all consumption points. The diameter of pipelines oscillates between 150 and 500 mm, being the pipe materials: asbestos cement, polyvinyl-chloride and ductile iron. The different irrigation points (the total number of consumption points is 371) are connected with pipes of polyethylene to multiuser hydrants, being 70 the total number of hydrants.

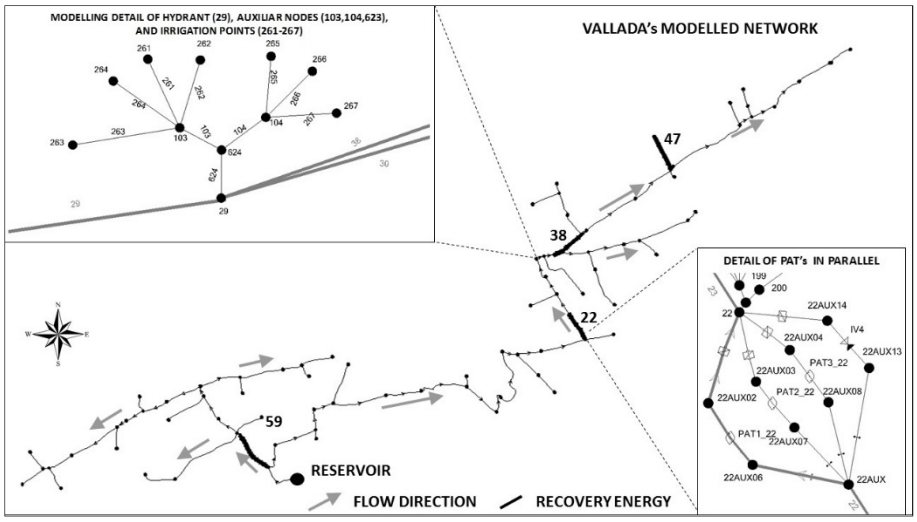

Figure 8. Case study. Vallada (Spain)

3.2 Assumptions

Although the maximization of the number of turbines to install in this network could arise up to ten, the maximum number of modelled lines is equal to four, due to the used feasibility criterion. If the analysis determines that it is necessary, more cases will be defined and including in the model. In this case, the modelled assumption has been:

a) Assumption A: Only one parallel group of turbines is installed in the network. According to results obtained in the theoretical maximization, the line with greater E_T is selected.

b) Assumption B: Two lines with group installed turbines are modelled in the network; these correspond to the theoretical combination where the recovering is maximum.

c) Assumption C: Following same criterion, three lines with turbines are modelled.

d) Assumption D: In this case, four lines with machines are simulated.

4. Results and Discussion

4.1. Model developed

Circulating flows have been calculated for any line, and adjusted to the available measurements, presenting a Nash-Sutcliffe index upper to 0.40, root relative squared mean error below 0.7 and percent bias below 5% (Pérez-Sánchez *et al.,* 2016) as calibration parameters. As a consequence, the model calibration is considered 'good' according Cabrera (2009) and Moriasi *et al.* (2007) and this values do not present signficative variability when the process is repeated. Therefore, with these premises, the circulating flows have been used to maximize the theoretical recovered energy and to analyze the selected machines, which are modelled in *WaterGEMS*.

The developed model (Figure 8) has a total of 647 lines, with 85 lines in the branched network, 341 lines correspond to pipes connecting hydrants and irrigation points, and the remaing are secondaries and auxiliars lines. The number of modelled juncions are equal to 646, these correspond to: 341 consumption nodes, 70 with multiuser hydrants and the others are auxiliar nodes.The definition of the demands' patterns have been adopted, according to the cited methodology in section 2.4, where these depend on farmers' habit. The total number of developed patterns are equal to 341 (one by each irrigation point), which have been discretized by hourly intervals along a complete year.

4.2. Maximization of the theoretical energy recovered

According to the optimization methodology, this study has analyzed the maximization with two different objective functions (E_{TR}^S and $\frac{E_{TR}^S}{PSR}$). Previously, the ordered list of E_{TR}^S and $\frac{E_{TR}^S}{PSR}$ must be generated. Table 1 shows the values of theoretical recovered energy, which have been sorted in descendent order. The line with greater recovered energy is the line 38 with 90.28 MWh/year. The list of sorted lines according to $\frac{E_T^S}{PSR}$, has been performed considering the values of recovered and *PSR*, and the maximum theoretical power.

Table 1. Ordered list taking account theoretical recovered energy in lines *(E_T)*

PIPE	E_T (MWh/year)	PIPE	E_T (MWh/year)	PIPE	E_T (MWh/year)	PIPE	E_T (MWh/year)
38	**90.28**	8	26.01	1	4.37	7	1.41
22	**83.75**	9	25.00	42	4.23	32	1.13
43	83.00	3	18.75	36	4.23	66	0.90
23	82.74	2	17.65	41	3.96	57	0.87
25	79.55	**47**	**16.19**	37	3.59	61	0.87
26	78.38	51	14.56	70	3.32	11	0.82
27	77.90	54	12.96	74	3.12	17	0.79
29	76.38	55	12.77	68	3.04	69	0.77
44	55.82	56	12.68	83	3.01	84	0.75
45	48.59	58	11.08	75	2.94	35	0.65
10	41.84	**59**	**10.62**	31	2.87	76	0.60
12	41.30	60	10.24	85	2.82	4	0.57
14	41.16	30	9.93	77	2.82	82	0.52
15	41.16	39	8.92	78	2.55	18	0.49
13	41.16	33	7.72	52	2.26	73	0.41
16	40.62	40	7.64	28	2.10	72	0.41
19	39.58	63	5.85	24	2.01	62	0.32
20	38.82	65	5.32	71	1.98	64	0.22
48	32.79	46	5.17	53	1.94	21	0.13
49	28.30	50	5.08	80	1.81	--	--
5	26.99	67	4.95	81	1.63	--	--
6	26.57	34	4.86	79	1.51	--	--

Once, the list has been established, the maximization can be carried out with two different objective functions. Previously, the sensitivity analysis has been performed by the different control parameters. The results of the optimization are shown in Table 2.

The obtained results in the maximization for one turbine are equals and correspond to the line 38. If the optimization is performed for two turbines, the solution in both objective function is the same (line 22 and line 38). When more than three turbines are considered, the solution depends on the chosen objective function, although in both, the lines 22 and 38 appear, and these lines represent a percentage of recovered energy upper to 78.60 (when E_{TR}^{S} is maximized) and 84.95 if the maximized function is the ratio between E_{TR}^{S} and *PSR*. This indicates that these lines are main locations for recovering energy. In all cases, the recovered energy is lower if the maximization has been optimized taking account *PSR* value. The increment of recovered energy oscillates between 1.10 % (minimum obtained in the solution of four turbines) and 8.09 % (maximum deviation obtained in the solution with ten turbines).

Table 2. Results of maximization according to the objective function.

OPTIMIZATION TAKING ACCOUNT MAXIMUM THEORETICAL E_{TR}													
T_i = 100; T_f =0.01; a =0.9; L = 10; Number of iterations=7128													
n	**LINES**										**E_{TR}^{s}* (MWh/year)**	***PSR***	**$\frac{E_{TR}^{s}}{PSR}$**
1	**38**										49.66	5.46	9.10
2	**22**	**38**									60.36	5.65	10.68
3	**22**	**38**	59								66.20	5.99	11.05
4	**22**	**38**	47	59							69.00	6.31	10.94
5	**5**	**22**	**38**	47	59						71.25	6.22	11.45
6	**5**	**22**	**38**	47	**58**	59					73.25	6.28	11.67
7	**5**	**22**	**38**	47	**58**	59	70				74.44	6.41	11.61
8	**5**	**22**	**38**	39	47	**58**	59	70			75.34	6.53	11.54
9	2	10	**22**	39	43	47	**58**	59	70		75.92	6.79	11.19
10	2	10	**22**	39	43	47	**58**	59	70	85	76.80	6.85	11.21
OPTIMIZATION TAKING ACCOUNT THE RATIO BETWEEN E_{TR} AND *PSR*													
T_i= 10; T_f=0.01; a=0.9; L= 10; Number of iterations=5346													
n	**LINES**										**E_{TR}^{s}* (MWh/year)**	***PSR***	**$\frac{E_{TR}^{s}}{PSR}$**
1	**38**										49.66	5.46	9.10
2	**22**	**38**									60.36	5.65	10.68
3	5	**22**	**38**								62.61	5.58	11.23
4	5	**22**	**38**	60							68.24	5.87	11.62
5	**5**	**22**	**38**	56	60						69.68	5.96	11.69
6	**5**	10	**22**	**38**	**58**	60					70.95	5.98	11.87
7	**5**	10	**22**	27	**38**	**58**	60				70.95	5.98	11.87
8	1	**5**	12	13	**22**	**38**	**58**	60			70.93	5.95	11.94
9	1	5	10	**22**	38	48	**58**	54	60		71.05	5.95	11.95
10	1	5	6	8	10	**22**	26	**38**	58	60	71.05	5.95	11.95

* For these calculus, averaged performance equal to 0.55 has been considered to determine the PSR index.

Finally, the option of maximum recovered energy has been chosen to model in *WaterGEMS* in extended period simulation along the time. The reasons of this selection are based on:

a) Both solutions contain main lines (22 and 38) and lines (5 and 58) since solution with five turbines.

b) The index *PSR* has been calculated from theoretical references, therefore, as results are similar, the recovered energy has been prioritized. In the case study, where the investment and maintenance costs are defined exactly with market' prices, the selection of lines by this objective function (ratio between E_{TR}^{s} and PSR) could be prioritized.

c) The indexes of *PSR* are similar, and the option E_{TR}^{s} has more available energy to be recovered.

d) It was verified in this network, line 5, the points of theoretical available head (H_T) are constant along the range of circulating flows. This causes that for covering at least 80% of operation range of flows, the number necessary of *PATs* to install will be very high (in this case, in line 5, minimum twelve machines) and which is not convenient in this network.

e) Related with the cited points b) and d), if the location of the machines is optimized taking account *PSR* index, search vector in the simulated annealing must contains restrictions in the lines where available machines to install cannot operate independently. For it, this objective function can be used when the economic parameters and available machines are exactly known.

f) In this particular case study, considering *PSR* index for the optimization, the obtained result placed many machines (5, 22, 38 and 58) in main branches of the network. As later described (section 4.3.2), when different machines are allocated in series, the operation zone of upstream installed machines (Q-H_T) is very variable when compared with non-series installed machines. It is due to demand's pattern are very variable along the time in the irrigation network (i.e. this does not occur in water supply systems where the demand's patterns are less variable along the time). Considering the optimization with E_{TR}^{S}, the positioning of machines is more variable in terms of branch' levels (*i.e.,* main, secondary, tertiary pipes).

The solution with four turbines (22+38+59+47; Table 2) recovers 69.00 MWh/year. This solution represents 90% of the E_{TR}^{S} when ten turbines are optimized (76.80 MWh/year; Table 2). Taking into account the solution with four turbines, in the following section an energy analysis is developed in the network (Figure 8) for Case A (line 38); B (lines: 22 and 38); C (lines: 22, 38, and 59); and D (lines: 22, 38, 59, and 47)

4.3. Energy Recovered with selected machines

4.3.1. Selection of *PATs*

PATs have been selected with the premises described in section 2.3. In these cases, H_R cannot be greater than H_T to ensure the minimum service pressure, and the operation range must cover at least 80% of time of circulating flow existing in analyzed line. Also, discharge and head numbers have been taken from Figure 4 previously presented. The characteristics of the selected machines are listed in Table 3. Selected *PATs* have specific speed between 24.50 and 46.40 rpm being their fixed rotational speed in: 2030 rpm (*PATs* simulated in line 59), 2500 rpm (*PATs* installed in line 38) and 2900 rpm (*PAT* in line 38 when it operates alone and line 22). *PATs* operate with fixed rotational speed in any time. The rotational speed has been defined to adjust recovered head to theoretical available head.

Table 3. Characteristics of selected *PATs*

	ASSUMPTION	A	B		C			D			
	LINE	**38**	**22**	**38**	**22**	**38**	**59**	**22**	**38**	**59**	**47**
CHARACTERISTICS OF PAT	**ss (rpm)**	24.50	24.50	46.40	24.50	46.40	39.40	24.50	46.40	39.40	35.30
	***N* (rpm)**	2900	2900	2500	2900	2500	2030	2900	2500	2030	2900
	***D* (m)**	0.14	0.14	0.10	0.14	0.10	0.10	0.14	0.10	0.10	0.10
	Q_{min} (l/s)	5.88	5.27	5.12	5.27	5.12	2.74	5.27	5.12	2.74	3.22
	Q_{max} (l/s)	16.98	14.12	15.03	14.12	15.03	9.11	14.12	15.03	9.11	9.76
	***BEP*- Q (l/s)**	13.24	11.87	10.58	11.87	10.58	6.91	11.87	10.58	6.91	7.46
	***BEP*-H (m)**	43.22	11.81	8.52	11.81	40.87	8.52	11.81	40.87	8.52	13.92
VALUES OF PATs IN PARALLEL	**LINE**	**38**	**22**	**38**	**22**	**38**	**59**	**22**	**38**	**59**	**47**
	n	3	3	3	3	3	3	3	3	3	3
	Q_{min} (l/s)	5.88	5.27	5.12	5.27	5.12	2.74	5.27	5.12	2.74	3.22
	Q_{max} (l/s)	50.94	42.36	45.09	42.36	45.09	27.33	42.36	45.09	27.33	27.20
	H_{Rmin} (m w.c.)	23.84	22.16	6.42	22.16	6.42	3.98	22.16	6.42	3.98	10.09
	H_{Rmax} (m w.c.)	63.40	52.09	21.30	52.09	21.30	14.47	52.09	21.30	14.47	27.50
	RANGE OF OPERATION OF PATs (%) (MIN 80 %)	89.28	80.01	86.91	80.01	86.91	85.10	80.01	86.91	85.10	99.91
THEORETICAL VALUES IN LINE	**LINE**	**38**	**22**	**38**	**22**	**38**	**59**	**22**	**38**	**59**	**47**
	H_{Tmax} (m w.c.)	79.40	56.35	24.12	56.35	24.12	18.60	56.35	24.12	18.60	41.76
	Q_{min} (l/s)	0.18	0.19	0.18	0.19	0.18	0.23	0.19	0.18	0.23	0.70
	Q_{max} (l/s)	106.00	137.27	106.00	137.27	106.00	76.07	137.27	106.00	76.07	28.74

The selected machines shown in Table 3 ensure the minimum pressure of service to user in all joints and time. Also, *PATs* can operate upper to 80% of the frequency of circulating flows reaching a 99.91%, the *PAT* installed in the line 47. The lines 38 and 59, when operate simultaneously, the range of operation is upper to 85%.

The values of discharge and head number and performance of these turbines will be used to select the more appropriate machine, in order to analyze the case study according to available head in each case. The values of performance will be used supposing that affinity between machines is total. The last affirmation is not absolutely certain, as only the geometric affinity exists. However, the use of variable performance in function of the discharge number is more interesting (although those determined by the laws of similarities are greater) because this can help to know the weighted average performance of this machines when the variability of flows is high.

4.3.2. Recovered Energy

Tables 4 and 5 contain the obtained results from *WaterGEMS*, when the different assumptions previously described in Section 4.2 have been considered for different scenarios.

Table 4. Balance of recovered energy in each PAT as function of assumptions and line

ASSUMPTION	LINE	BALANCE IN EACH PAT							VARIABLE	OPERATION			
		Q_{max} (l/s)	Q_{min} (l/s)	P_{max} (kW)	P_{min} (kW)	η_{max} (%)	η_{min} (%)	η_w (%)		PAT STOP	PAT1	PAT2	PAT3
A	38	16.99	6.05	7.83	0.27	74.15	19.29	68.46	t (h)	4566	4194	2020	565
									E_R (kWh/year)	--	10282.41	3530.99	907.23
									% E_R	--	69.85	23.99	6.16
B	22	14.00	5.01	5.34	0.11	74.58	9.86	65.85	t (h)	4600	4160	2191	619
									E_R (kWh/year)	--	6482.75	2420.60	908.47
									% E_R	--	66.07	24.67	9.26
	38	15.00	5.00	2.21	0.04	74.95	11.77	71.85	t (h)	4600	4160	2191	619
									E_R (kWh/year)	--	3016.88	1142.49	289.80
									% E_R	--	67.81	25.68	6.51
C	22	14.00	5.01	5.34	0.11	74.58	9.86	65.85	t (h)	4600	4160	2191	619
									E_R (kWh/year)	--	6482.75	2420.60	908.47
									% E_R	--	66.07	24.67	9.26
	38	15.00	5.00	2.21	0.04	74.95	11.77	71.85	t (h)	4600	4160	2191	619
									E_R (kWh/year)	--	3016.88	1142.49	289.80
									% E_R	--	67.81	25.68	6.51
	59	9.00	3.03	0.97	0.02	81.06	15.35	75.78	t (h)	5846	2914	1415	534
									E_R (kWh/year)	--	809.56	316.44	112.42
									% E_R	--	65.37	25.55	9.08
D	22	14.00	5.01	5.34	0.11	74.58	9.86	65.85	t (h)	4600	4160	2191	619
									E_R (kWh/year)	--	6482.75	2420.60	908.47
									% E_R	--	66.07	24.67	9.26
	38	15.00	5.00	2.21	0.04	74.95	11.77	71.85	t (h)	4600	4160	2191	619
									E_R (kWh/year)	--	3016.88	1142.49	289.80
									% E_R	--	67.81	25.68	6.51
	59	9.00	3.03	0.97	0.02	81.06	15.35	75.78	t (h)	5846	2914	1415	534
									E_R (kWh/year)	--	809.56	316.44	112.42
									% E_R	--	65.37	25.55	9.08
	47	8.99	4.41	1.92	0.34	84.90	69.64	82.53	t (h)	6931	1319	461	49
									E_R (kWh/year)	--	961.73	427.09	68.04
									% E_R	--	66.01	29.32	4.67

Table 5. Balance of recovered energy in each line and global in the network as a function of assumptions (Continue in next page).

ASSUMPTION	LINE	BALANCE IN THE LINE									BALANCE IN THE NETWORK			
		P_{max} (kW)	VARIABLE	OPERATION				E_R (MWh/year)	E_{TR} (MWh/year)	RC	P_{max} (kW)	E_R (MWh/year)	E_{TR} (MWh/year)	TRC
				PAT STOP	1PAT	2PATs	3PATs							
A	38	23.42	t (h)	4566	2174	1455	565	25.41	90.29	0.28	23.42	25.41	90.28	0.28
			E_R (kWh/year)	--	6.75	5.25	2.72							
			% E_R	--	45.86	35.65	18.49							
B	22	16.00	t (h)	4600	1969	1572	619	18.29	83.75	0.22	22.60	26.18	109.75	0.24
			E_R (kWh/year)	--	4062.15	3024.28	2725.40							
			% E_R	--	41.40	30.82	27.78							
	38	6.60	t (h)	4600	1969	1572	619	7.89	26.00	0.30				
			E_R (kWh/year)	--	1874.39	1705.39	869.39							
			% E_R	--	42.13	38.33	19.54							
C	22	16.00	t (h)	4600	1969	1572	619	18.29	83.75	0.22	25.50	28.50	120.37	0.24
			E_R (kWh/year)	--	4062.15	3024.28	2725.40							
			% E_R	--	41.40	30.82	27.78							
	38	6.60	t (h)	4600	1969	1572	619	7.89	26.00	0.30				
			E_R (kWh/year)	--	1874.39	1705.39	869.39							
			% E_R	--	42.13	38.33	19.54							
	59	2.90	t (h)	5846	1499	881	534	2.32	10.62	0.22				
			E_R (kWh/year)	--	493.11	408.04	337.27							
			% E_R	--	39.82	32.95	27.23							
			E_R (kWh/year)	--	1197.95	236.22	22.68							
			% E_R	--	82.23	16.21	1.56							

Table 5. *(Cont.)* Balance of recovered energy in each line and global in the network as a function of assumptions.

ASSUMPTION	LINE	BALANCE IN THE LINE									BALANCE IN THE NETWORK			
		P_{max} (kW)	VARIABLE	OPERATION				E_R (MWh/year)	E_{TR} (MWh/year)	RC	P_{max} (kW)	E_R (MWh/year)	E_{TR} (MWh/year)	TRC
				PAT STOP	1PAT	2PATs	3PATs							
D	22	16.00	t (h)	4600	1969	1572	619	18.29	83.75	0.22	31.00	30.52	125.46	0.24
			E_R (kWh/year)	--	4062.15	3024.28	2725.40							
			% E_R	--	41.40	30.82	27.78							
	38	6.60	t (h)	4600	1969	1572	619	7.89	26.00	0.30				
			E_R (kWh/year)	--	1874.39	1705.39	869.39							
			% E_R	--	42.13	38.33	19.54							
	59	2.90	t (h)	5846	1499	881	534	2.32	10.62	0.22				
			E_R (kWh/year)	--	493.11	408.04	337.27							
			% E_R	--	39.82	32.95	27.23							
	47	5.49	t (h)	6931	1829	510	49	2.02	5.09	0.40				
			E_R (kWh/year)	--	1197.95	236.22	22.68							
			% E_R	--	82.23	16.21	1.56							

Table 4 shows the characteristic values of operation of each installed *PAT*, depending on the line and assumption. The instant maximum developed power (7.83 kW) occurs when *PATs* are only installed in line 38. This scenario presents the highest values of power in each machine. The recovered energy by each *PAT* can be visualized in Table 4, and its operation time along the year as well as the maximum, minimum and weighted performance in each case.

The results contained in Table 5 are referred to analysis of energy recovery in lines and total in the network, depending on the considered assumptions. The maximum recovered energy in a line takes place when case A is considered (25.41 MWh/year). If this value is compared to the theoretical recovered energy (E_{TR}) in the same scenario, the line presents a recovery coefficient (*RC*) equal to 0.28. Therefore, in this situation, a total of 28% of the available energy can be recovered with a weighted average performance equal to 68.46 % (this value obtained on Table 4).

Figure 9 (A and B) shows an example of the operation zone in the line 38, when a *PAT* is installed in series in the line 22. The theoretical available head in line 38 varies substantially, as Figure 9 illustrates, when *PAT* is installed or not in line 22. If *PATs* are connected in series, the points of the operation zone are more dispersed if the same line is compared with non-serial machines. This spread of theoretical work points causes a reduction of the operation time, which can be analyzed in Table 4. However, the weighted performance is similar because the selected machines are different in each

simulated assumption (to maximize the recovered energy as function of the theoretical available head).

If assumption A and B are simulated again, assuming that installed machines in line 38 are equals to analyze the effect caused by the installation of *PATs* in series, *RC* is 0.09 in line 38 when PATs in line 22 do not operate. This result is due to a high range of available head. If Figure 9 (B) is observed, the available head oscillates between 23 and 80 m w.c. when the machines are installed in series (only the operation range is considered since 5.12 to 45.09 l/s), when the energy is only recovered in line 38, H_T oscillates between 70 and 80 m w.c. for the same operation range of flows.

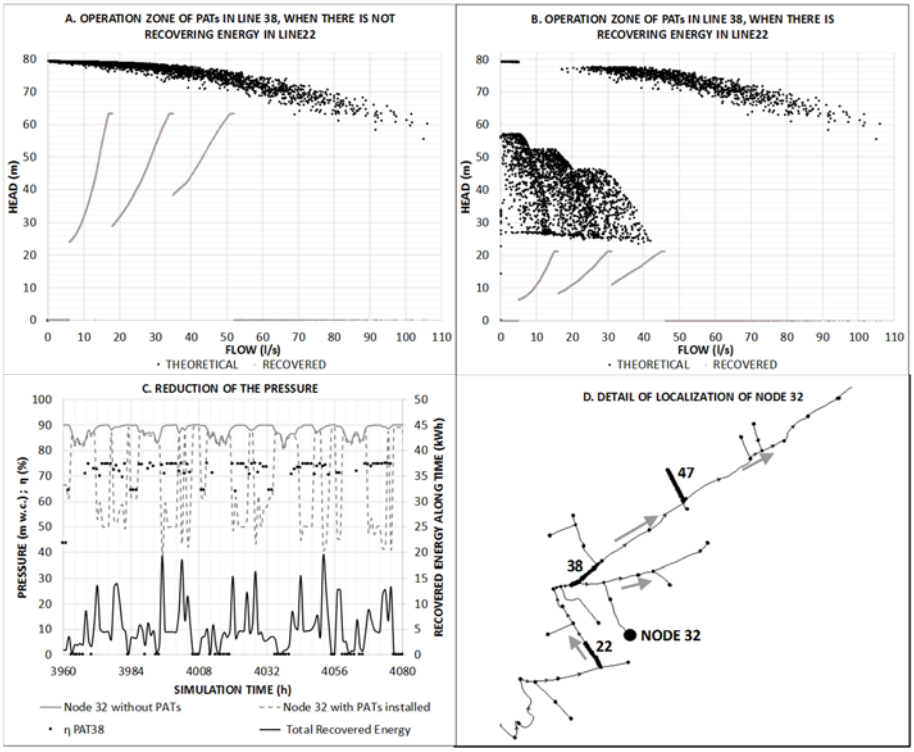

Figure 9. Variation of H_T with machines installed in series

Also, Figure 9 (C) shows the pressure in node 32 (this junction simulates a hydrant) such as an interval of five days, where the pressure value is reduced when the turbines are operated. The pressure in the hydrant has a variation from 85 m w.c. (when *PATs* are not operated) to 40 m w.c. (when *PATs* operate). As well as, the total recovered energy can be seen along the time by the four groups of installed *PATs*, even the instant performance of installed *PAT* in line 38 in each interval has values near to 75%. Similar information can be obtained from all nodes, lines and installed machines.

Figure 10 shows the different work points of recovered head and performance in each *PAT*, which have been obtained from the simulation with *WaterGEMS*. This figure shows that when the selected machine has a short interval of flows, the performance is higher (*e.g., PATs* in line 47, where the performance is upper to 70% in all range of application, which is between 4.2 and 8.2 l/s). However, the other *PATs*, which have a greater operation range of flows its performance oscillate between 15 and 75 %, being the range of flows in the interval 5-15 l/s, approximately.

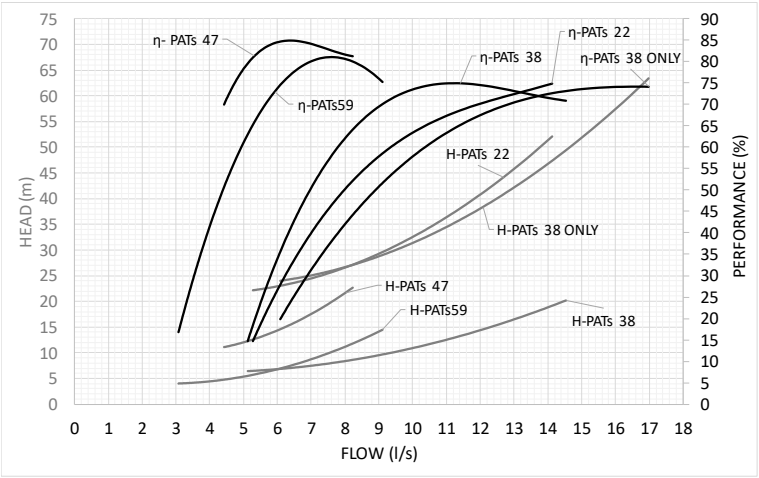

Figure 10. Head (H_R) and performance (η) obtained with *WaterGEMS*® depending on PAT installed

Table 5 allows modelers to determine the operation time and recovered energy of each *PAT*, when these operate in parallel with the other of *PATs*. If the total recovered energy in the network is analyzed, the highest recovery energy takes place in assumption D, when four groups of turbines are working along the year. In this case, the recovered energy is equal to 30.52 MWh/year and the total recovery coefficient (*TRC*) in the network is 0.24. However, if this value is compared with case A (25.41 MWh/year in Table 5), the increase of recovered energy is 5.11 MWh (20.11 %), but installed power necessary varies from 23.42 to 30.11 (an increase of 28.56%). If the analysis is performed with theoretical recovered energy, the increase of E_{TR} is equal to 38.76%. This value shows that the increase of the number of *PATs* installed in different lines reduce the *TCR* values in the network.

This is shown by the Figure 11, where E_{TR} and E_R are drawn. In this figure the trend of energy in both cases can be observed (theoretical and recovered), resuming the values contained in Table 5 and showing that the increase of recovered energy is smaller than the theoretical, when the number of lines with recovering systems grows in the network. If this is compared taking into account the economics indexes, which establish the feasibility, the case B presents the best economics indexes (*PSR* = 5.47 and *EI*=0.47) below of 6 and 0.6, respectively. Therefore, the viability of the project could be considered. All studied cases are feasible, except assumption D, which presents a *PSR*

of 6.44. In this figure is observed that the variation between theoretical and recovered indexes is not important. Theoretical and recovered *PSR* values varies between 5.5 and 6.5 (theoretical: Case A =5.46; B=5.65; C=5.58; and D=5.87); recovered: A=5.85; B=5.48; C=5.68; and D=6.44). This difference is due to consider the efficiency of the machine function of circulating flow along the time.

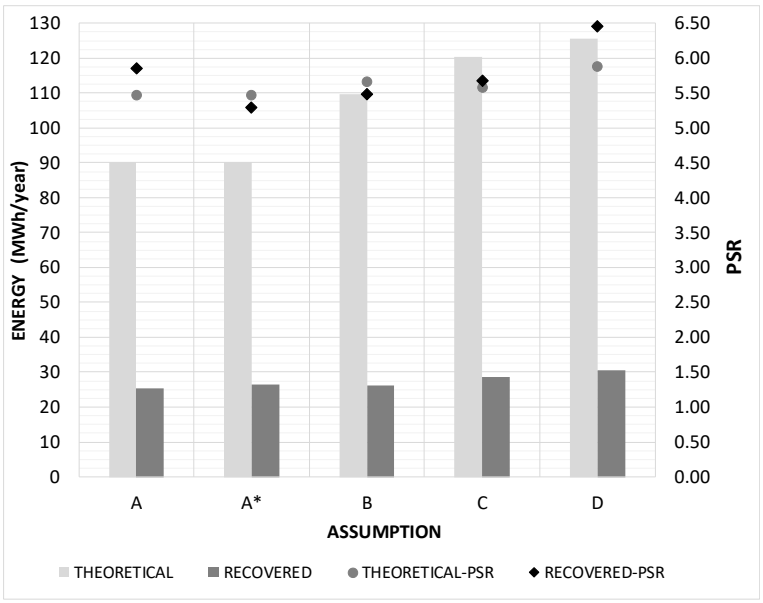

Figure 11. E_{TR}, E_R, *PSR*, and *EI* depending on analyzed cases

If the case A is recalculated again with the *PAT1* is a machine with variable rotational speed which has a fixed rotational speed (n_0) equal to 2900 rpm (this new calculus has been denominated 'Case A*'), keeping specifics speed (*ss*) and diameter of impeller.

The rotational speed of *PAT1* varied in the following ranges: 1450 rpm ($\alpha = \frac{n}{n_0} = 0.5$) in the interval of flows between 2.94 l/s and 5 l/s; 2320 rpm ($\alpha = 0.8$) between 5 and 9 l/s; 2900 rpm ($\alpha = 1.0$) between 9 and 14 l/s; and 3480 rpm ($\alpha = 1.2$) between 14 and 18.5 l/s. For this situation, when circulating flows are upper to 18.5 l/s the machines (*PAT1*, *PAT2*, and *PAT3*) operate with the same rotational speed (2900 rpm) to ensure the minimum pressure to users and the machines recover the same head and losses. In this case, the recovered energy is equal to 26.52 MWh/year. This value is 4.33% higher than the assumption in which all machines are with non-variable rotational speed (25.41 MWh/year in Table 5). Also, the use of variable speed in line 38 allows obtaining grater recovered energy than case B, which is integrated by two groups of *PATs* in parallel. In this case, the existence of a single group of installed machines enables the exploitation of the network as well as a lower of maintenance's costs.

Finally, if the energy balance is performed considering the solution of assumption A with variable rotational speed, the energy is distributed in the followings terms: 4.10% is dissipated by friction, 27.45% is necessary to ensure the irrigation service, 58.90 % is non-recoverable, and 9.55% of the provided energy can be recovered when the machines are installed in line 38. This value of recovered energy, when the annual consumption in the network is equal to 927553 m^3, supposes an average index of recovering equal to 0.03 kWh/m^3.

6. Conclusions

In this research, it has shown that the recovering energy in agricultural water networks is a technologically feasible alternative to improve the energetic efficiency of these systems and be a sustainability alternative for use in self-consumption or sale. On the one hand, a methodology of optimization to maximize recovered energy has been proposed making use of simulated annealing algorithm. As novelty, the maximization has been performed with an objective function that it takes account both maximum recovered energy as feasibility index (*PSR*). If result of this criterion is compared with the obtained values when objective function is maximum recovered energy, these are similar in values of total recovered energy and *PSR*. However, the use of *PSR* in the maximization can be introduced when the water management get the market's prices and characteristics curve of the available machines. If the manager knows these parameters, they may establish criterion in the simulated annealing to discriminate the lines where the recovering is not possible and thus, the solution of maximization avoids incorrect solutions. On the other hand, the analysis of the real case study has determined that machines are installed in series in main lines, the operation zone is modified by installed machine upstream. This modification affects to greater dispersion of data pairs (*Q,H*), and it causes decrease of operation time of the machine because more points are out of range. Therefore, a possible criterion of discrimination in the maximization can be that machines are not installed in the same branch's levels.

The analyzed cases in this research present a *TCR* between 0.28 and 0.24, decreasing when the number of turbines is increased. In this case, case B is the solution more viable considering fixed rotational speed in the *PATs*. On instead, if the rotational speed is variable (case A*; with only groups of *PATs*) recovers more energy than B. If same assumption A is compared (with/without variable speed), the recovered energy increases 4.33% for variable speed. If the energetic balance in the network is performed, a 9.55 % of the provide energy to the network initially versus dissipated energy by friction, which represents a 4.10% in the balance. Therefore, case A* with only one group of three turbines in parallel which is located in line 38 is the solution more viable, being the assumption where the recovered energy is maximum and equal to 26.51 MWh/year and the *PSR* is minimum and equal to 5.28.

Finally, the use of this proposed methodology allows to use to water managers, with the simulated annealing as a helpful tool, ensuring the quality service all the time, towards sustainability in irrigation networks, through maximization of recovering energy.

References

Abadia, R., Rocamora, M.C., Corcoles, J.I., Ruiz-Canales, A., Martinez-Romero, A., Moreno, M.A., 2010. Comparative analysis of energy efficiency in water users associations. Spanish J. Agric. Res. 8, 134. doi:10.5424/sjar/201008S2-1356

Araujo, L.S., Ramos, H., Coelho, S.T., 2006. Pressure Control for Leakage Minimisation in Water Distribution Systems Management. Water Resour. Manag. 20, 133–149. doi:10.1007/s11269-006-4635-3

Arriaga, M., 2010. Pump as turbine – A pico-hydro alternative in Lao People's Democratic Republic. Renew. Energy 35, 1109–1115. doi:10.1016/j.renene.2009.08.022

Cabrera, E., Cobacho, R., Soriano, J., 2014. Towards an Energy Labelling of Pressurized Water Networks. Procedia Eng. 70, 209–217. doi:10.1016/j.proeng.2014.02.024

Cabrera, J., 2009. Calibración de Modelos Hidrológicos [WWW Document]. Imefen.Uni.Edu.Pe. URL http://www.imefen.uni.edu.pe/Temas_interes/modhidro_2.pdf

Carravetta, A., Del Giudice, G., Fecarotta, O., Ramos, H., 2013a. PAT Design Strategy for Energy Recovery in Water Distribution Networks by Electrical Regulation. Energies 6, 411–424. doi:10.3390/en6010411

Carravetta, A., Del Giudice, G., Fecarotta, O., Ramos, H., 2013b. Pump as Turbine (PAT) Design in Water Distribution Network by System Effectiveness. Water 5, 1211–1225. doi:10.3390/w5031211

Carravetta, A., Del Giudice, G., Fecarotta, O., Ramos, H.M., 2012. Energy Production in Water Distribution Networks: A PAT Design Strategy. Water Resour. Manag. 26, 3947–3959. doi:10.1007/s11269-012-0114-1

Carravetta, A., Fecarotta, O., Del Giudice, G., Ramos, H., 2014. Energy Recovery in Water Systems by PATs: A Comparisons among the Different Installation Schemes. Procedia Eng. 70, 275–284. doi:10.1016/j.proeng.2014.02.031

Castro, A., 2006. Minicentrales Hidroeléctricas. Instituto para la Diversificación y Ahorro de la Energía., Madrid.

Choulot, A., 2010. Energy recovery in existing infrastructures with small hydropower plants. FP6 Project Shapes (work package 5- WP5), European Directorate for Transport and Energy.

Derakhshan, S., Nourbakhsh, A., 2008. Experimental study of characteristic curves of centrifugal pumps working as turbines in different specific speeds. Exp. Therm. Fluid Sci. 32, 800–807. doi:10.1016/j.expthermflusci.2007.10.004

Estrada, F., Ramos, H., 2015. Micro-hydro solutions in Alqueva Multipurpose Project (AMP) towards water-energy-environmental efficiency improvements. Dissertation Project at IST. ESCOLA TÉCNICA SUPERIOR D'ENGINYERIA INDUSTRIAL DE BARCELONA.

Imbernón, J.A., Usquin, B., 2014. Sistemas de generación hidráulica. Una nueva forma de entender la energía, in: II Congreso Smart Grid.

Jiménez-Bello, M.A., Royuela, A., Manzano, J., Prats, A.G., Martínez-Alzamora, F., 2015. Methodology to improve water and energy use by proper irrigation scheduling in pressurised networks. Agric. Water Manag. 149, 91–101. doi:10.1016/j.agwat.2014.10.026

Kirkpatrick, S., Gelatt, C., Vecchi, M., 1983. Optimization by simmulated annealing. Science (80-.). 220, 671–680.

Kougias, I., Patsialis, T., Zafirakou, A., Theodossiou, N., 2014. Exploring the potential of energy recovery using micro hydropower systems in water supply systems. Water Util. J. 7, 25–33.

Kuo, S.-F., Liu, C.-W., Chen, S.-K., 2003. COMPARATIVE STUDY OF OPTIMIZATION TECHNIQUES FOR IRRIGATION PROJECT PLANNING. J. Am. Water Resour. Assoc. 39, 59–73. doi:10.1111/j.1752-1688.2003.tb01561.x

Mataix, C., 2009. Turbomáquinas Hidráulicas. Universidad Pontificia Comillas, Madrid.

Metropolis, N., Rosenbluth, A., Rosenbluth, M., Teller, A., Teller, E., 1953. Simulated annealing. J. Chem. Phys. 21, 1087–1092.

Moreno, M., Córcoles, J., Tarjuelo, J., Ortega, J., 2010. Energy efficiency of pressurised irrigation networks managed on-demand and under a rotation schedule. Biosyst. Eng. 107, 349–363. doi:10.1016/j.biosystemseng.2010.09.009

Moriasi, D.N., Arnold, J.G., Van Liew, M.W., Binger, R.L., Harmel, R.D., Veith, T.L., 2007. Model evaluation guidelines for systematic quantification of accuracy in watershed simulations. Trans. ASABE 50, 885–900. doi:10.13031/2013.23153

Nazari, A., Meisami, H., 2008. Instructing WaterGEMS Software Usage. Tehran.

Nogueira, M., Perrella, J., 2014. Energy and hydraulic efficiency in conventional water supply systems. Renew. Sustain. Energy Rev. 30, 701–714. doi:10.1016/j.rser.2013.11.024

Pardo, M.A., Manzano, J., Cabrera, E., García-Serra, J., 2013. Energy audit of irrigation networks. Biosyst. Eng. 115, 89–101. doi:10.1016/j.biosystemseng.2013.02.005

Pérez-Sánchez, M., Sánchez-Romero, F., Ramos, H., López-Jiménez, P., 2016. Modeling Irrigation Networks for the Quantification of Potential Energy Recovering: A Case Study. Water 8, 1–26. doi:10.3390/w8060234

Prats, A.G., Picó, S.G., Alzamora, F.M., Bello, M.Á.J., 2011. Random Scenarios Generation with Minimum Energy Consumption Model for Sectoring Optimization in Pressurized Irrigation Networks Using a Simulated Annealing Approach. http://dx.doi.org/10.1061/(ASCE)IR.1943-4774.0000452.

Ramos, H., Borga, A., 1999. Pumps as turbines: an unconventional solution to energy production. Urban Water 1, 261–263. doi:10.1016/S1462-0758(00)00016-9

Ramos, H., Mello, M., De, P.K., 2010. Clean power in water supply systems as a sustainable solution: from planning to practical implementation. Water Sci. Technol. Water Supply 10, 39–49. doi:10.2166/ws.2010.720

Ramos, H.M., Borga, A., Simão, M., 2009. New design solutions for low-power energy production in water pipe systems. Water Sci. Eng. 2, 69–84. doi:10.3882/j.issn.1674-2370.2009.04.007

Rawal, S., Kshirsagar, J., 2007. simulation on a pump operating in a turbine mode, in: Proceedings of the 23rd International Pump Users Symposium. Houston: Texas A & M University, pp. 21–27.

Reca, J., Martínez, J., Gil, C., Baños, R., 2008. Application of Several Meta-Heuristic Techniques to the Optimization of Real Looped Water Distribution Networks. Water Resour. Manag. 22, 1367–1379. doi:10.1007/s11269-007-9230-8

Rodriguez-Diaz, J.A., Camacho-Poyato, E., Carrillo-Cobo, M.T., 2010. The role of energy audits in irrigated areas. The case of "Fuente Palmera" irrigation district (Spain). Spanish J. Agric. Res.

Rutenbar, R.A., 1989. Simulated annealing algorithms: an overview. IEEE Circuits Devices Mag. 5, 19–26. doi:10.1109/101.17235

Samora, I., Franca, M., Schleiss, A., Ramos, H., 2016. Simulated Annealing in Optimization of Energy Production in a Water Supply Network. Water Resour. Manag. 30, 1533–1547. doi:10.1007/s11269-016-1238-5

Samora, I., Franca, M.J., Schleiss, A.J., Ramos, H.M., 2016. Simulated Annealing in Optimization of Energy Production in a Water Supply Network. Water Resour. Manag. 30, 1533–1547. doi:10.1007/s11269-016-1238-5

Singh, P., 2005. Optimization of the Internal Hydraulic and of System Design in Pumps as Turbines with Field Implementation and Evaluation. University of Karlsruhe.

Tospornsampan, J., Kita, I., Ishii, M., Kitamura, Y., 2007. Split-Pipe Design of Water Distribution Network Using Simulated Annealing. World Acad. Sci. Eng. Technol. Int. J. Environ. Chem. Ecol. Geol. Geophys. Eng. 1, 28–38.

van Laarhoven, P.J.M., Aarts, E.H.L., 1987. Simulated annealing, in: Simulated Annealing: Theory and Applications. Springer Netherlands, Dordrecht, pp. 7–15. doi:10.1007/978-94-015-7744-1_2

Yang, S.S., Derakhshan, S., Kong, F.Y., 2012. Theoretical, numerical and experimental prediction of pump as turbine performance. Renew. Energy 48, 507–513. doi:10.1016/j.renene.2012.06.002

Youssef, H., M. Sait, S., Adiche, H., 2001. Evolutionary algorithms, simulated annealing and tabu search: a comparative study. Eng. Appl. Artif. Intell. 14, 167–181. doi:10.1016/S0952-1976(00)00065-8

Zema, D.A., Nicotra, A., Tamburino, V., Zimbone, S.M., 2016. A simple method to evaluate the technical and economic feasibility of micro hydro power plants in existing irrigation systems. Renew. Energy 85, 498–506. doi:10.1016/j.renene.2015.06.066

Appendices
Appendix VII

MODIFIED AFFINITY LAWS IN HYDRAULIC MACHINES TOWARDS THE BEST EFFICIENCY LINE

Author version document which was sent to publish to index JCR Journal "Water Resources Management" ISSN 0920-4741 for its potential publication (Registered Data: 08/12/2016). Impact Factor 2.437. Position 12/85 (Q1). Water Resources

Coauthors: Pérez-Sánchez, M; López-Jiménez PA.; Ramos, HM.

This page is intentionally left blank.

ABSTRACT

The development of hydraulic and optimization models in analyses of water networks to improve the sustainability and efficiency through the installation of micro or pico hydropower is swelling. Hydraulic machines involved in these models have to operate with different rotational speed, in order that in each instant to maximize the recovered energy. When the changes of rotational speed are determined using affinity laws, the errors can be significant. Detailed analyses are developed in this research through experimental tests to validate and propose new affinity laws in different reaction turbomachines. Once the errors have been analyzed, a methodology to modify the affinity laws is applied to radial and axial turbines. An empirical method to obtain the best efficiency line (*BEL*) in proposed (i.e. based on all the best efficiency points (*BEPs*) for different flows). When the experimental measurements and the calculated values by the empirical method are compared, the mean errors are reduced 81.81 %, 50%, and 86.67% for flow, head, and efficiency parameters, respectively. The knowledge of *BEL* allows managers to define the operation rules to reach the *BEP* for each flow, improving the energy efficiency in the optimization strategies to be adopted.

Keywords: affinity laws, best efficiency line (*BEL*), variation operating strategies, energy recovery

1. Introduction

Nowadays, the development of mathematical models to analyze the behavior of hydraulic systems requires theoretical and experimental laws. In some cases, the direct application of these equations can lead to erroneous results (Simpson and Marchi, 2013), being necessary to correct them in order to consider the necessary simplifications in the initial assumptions (*e.g.,* viscosity effects, friction losses, turbulence, vortex). In water distribution networks, the model simulation with installed hydraulic machines is very common, and the energy analyses have a great significance due to the increasing price of the energy (Corominas, 2010) and the need to reduce the energy consumption and the system efficiency to satisfy the European standards requirements (Pasten and Santamarina, 2012).

Traditionally, these optimizations of energy consumption in water systems have been focused on the reduction of consumed power by installed pumps. Hence, some authors have worked in the development of pumped systems to adapt the rotational speed of the machine to reduce the energy consumption (Sarbu and Borza, 1998; Moreno *et al.,* 2010; Simpson and Marchi, 2013; Jiménez-Bello *et al.,* 2015) and the pressure in the system (Kevin, 1990; Giustolisi *et al.,* 2008; Cabrera *et al.,* 2014). These reductions are of paramount importance in economic and environmental savings, which have been

analyzed through different algorithms and software such as *EPANET* (Rossman, 2000) or *WaterGEMS* (Nazari and Meisami, 2008), providing significant tools for water management in pipe systems.

In the last years, different authors have developed researches using new technologies to leverage the pressure reduction in water distribution networks, increasing the global efficiency in the water system (Abbott and Cohen, 2009; Dannier *et al.,* 2015). Araujo *et al.,* (2006) and Giugni *et al.,* (2014) enumerate different algorithms to optimize the location the optimal place of the pressure reduction valves (*PRVs*) in a network for leakages control. The initial development of studies of pump working as turbines (*PATs*) installed in water systems to replace *PRVs* (Ramos and Borga, 1999) has allowed modellers to analyze the turbine behavior according to different aspects such as:

- The morphology of the machine (Yang *et al.,* 2012; Carravetta *et al.,* 2013a; Shi *et al.,* 2015);
- The design of installation schemes and operation strategies (Carravetta *et al.,* 2012, 2013b, 2014b; Fontana *et al.,* 2012);
- The design of machines, adapted to specific work conditions (*i.e.,* low head and high range of flows) in these water drinking network such as the tubular propeller (Ramos *et al.,* 2013; Samora *et al.,* 2016b);
- The analysis of potential recovered energy according to circulating flow along the time through of simulated annealing techniques (Pérez-Sánchez *et al.,* 2016; Samora *et al.,* 2016a); and
- The economic and feasibility analyses of these installations showing the sustainability and environmental profit of these solutions (Ramos *et al.,* 2010; McNabola *et al.,* 2014).

Furthermore, the study of the performance behavior of these machines, Singh (2005) and Derakhshan and Nourbakhsh (2008) proposed the efficiency and head curves as function of flow according to the specific rotational speed of the machine. These curves can be used in the simulations of energy analyses with good results when the hydraulic machine operates in its nominal rotational speed. However, if the energy studies consider operation strategies with variation of speed, the use of affinity laws in the simulations can bring erroneous results of recovered energy in the system (Sarbu and Borza, 1998; Gulich, 2003) since the turbines do not behave as the similarity described. Taking into account the need to know the efficiency of the machine as function of rotational speed, the first aim of this research is to obtain the errors between measured and calculated efficiency through the application of affinity laws.

This analysis has been developed for two machines (with axial and radial impellers) based on experimentation. The second objective is to develop modified affinity laws to establish the best efficiency line (*BEL*) and the best efficiency head (*BEH*) of each machine as function of flow. *BEL* and *BEH* establish the rotational speed of the machine

when the variable operating strategies (*VOS*) are used (Carravetta *et al.,* 2013b), claiming for each flow the best operation point (*BEP*).

2. Material and methods

2.1. Type of hydraulics machines

A general typification of hydraulic machines refers to action or reaction, according to the exchange of energy between fluid and impeller at atmospheric pressure or not. Inside the group of the reaction machines, a second classification can be established according to the impeller shape and the specific rotational speed. This parameter is defined as the rotational speed of a similarity turbine (geometrically) to generate one kW when the head is equal to one. The specific rotational speed establishes the impellers' typology and it is defined by equation (1):

$$n_s = n\frac{P^{1/2}}{H^{5/4}} \tag{1}$$

where n_s is the specific speed of the machine in (m, kW); n is the rotational speed of the machine in rpm; P is the power in shaft, which is measured in (kW); and H is the recovered head in (m w.c.).

Based on the specific speed, the impellers can be: radial, semi-axial, or axial according to Figure 1. The radial or centrifugal impeller are those where the fluid enters in the machine in radial direction and exists in axial direction. This type of machines has a specific speed number between 36 and 93 rpm. For n_s between 93 and 176 rpm, the machine is called diagonal or semi-axial. In this sort of machine, the inlet of the fluid is diagonal, while the outlet has an axial direction. Finally, the axial machines, with a specific speed greater than 176 rpm, present the fluid direction both inlet and outlet with axial direction.

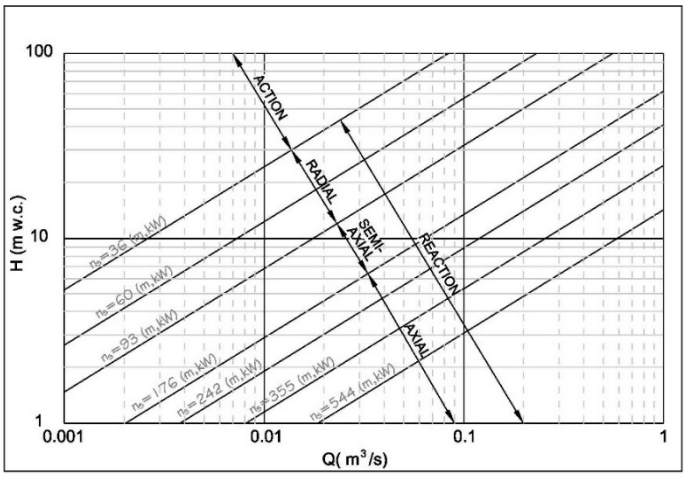

Figure 1 Type of impeller according to specific rotational speed (adapted from Alexander et al. 2009)

2.2. Theoretical approximation: affinity laws

The study of the behavior of turbomachines with equal specific rotational speed can be tackled if the conditions of similarity (geometrical, kinematic and dynamic) are entailed. The first condition is satisfied, when the study is focused on analyzing the behavior of a machine with different rotational speed. Kinematic condition establishes that in the inlet and outlet impeller, the triangles are similar. These two conditions are defined by equations (2) to (4):

$$\frac{Q_1}{Q_0} = \left(\frac{D_1}{D_0}\right)^3 \frac{N_1}{N_0} \tag{2}$$

$$\frac{H_1}{H_0} = \left(\frac{D_1}{D_0}\right)^2 \left(\frac{N_1}{N_0}\right)^2 \tag{3}$$

$$\frac{P_1}{P_0} = \left(\frac{D_1}{D_0}\right)^2 \left(\frac{N_1}{N_0}\right)^3 \tag{4}$$

where Q_1 is the flow in the new conditions of rotational speed in m^3/s; Q_0 is the flow in nominal rotational speed in m^3/s for the *BEP*; D_1 is the diameter of the impeller in new situation of rotational speed in m; D_0 is the nominal diameter of the impeller in m; N_1 is the new rotational speed in rpm; N_0 is the nominal rotational speed of the impeller in rpm; H_1 is the head in new condition in m w.c.; H_0 is the head in the nominal conditions in m w.c.; P_1 is the shaft power in new conditions in kW; and P_0 is the shaft power in the nominal condition in kW.

Therefore, if hydraulic parameters of the turbomachine (flow, head, and power) can be related through affinity laws (Mataix 2009), the efficiency of the machine can be indirectly determined for different rotational speeds, keeping the impeller's size. Based on this assumption, equations from (2) to (4) can be simplified into equations from (5) to (7):

$$\frac{Q_1}{Q_0} = \frac{N_1}{N_0} = \alpha \tag{5}$$

$$\frac{H_1}{H_0} = \left(\frac{N_1}{N_0}\right)^2 = \alpha^2 \tag{6}$$

$$\frac{P_1}{P_0} = \left(\frac{N_1}{N_0}\right)^3 = \alpha^3 \tag{7}$$

where α is the ratio between N_1 and N_0.

The nominal characteristic curve of a turbomachine (as a second-degree polynomial) can be written by equation (8):

$$H_0 = AQ_0^2 + BQ_0 + C \tag{8}$$

where A, B, and C are coefficients of the characteristic curve.

The efficiency curve can be also established by a second (Mataix 2009) or by third-degree polynomial if a discretized range of flows is considered (Ulanicki *et al.,* 2008). The nominal efficiency curve is then defined by equation (9):

$$\eta_0 = EQ_0^3 + FQ_0^2 + GQ_0 + I \tag{9}$$

where η_0 is the efficiency of the machine for a flow equal to Q_0; E, F, G, and I are coefficients of efficiency curve.

When the affinity laws are applied to equations (8) and (9), the new curves of the turbomachines are defined by equations (10) and (11):

$$H_1 = AQ_1^2 + \alpha BQ_1 + \alpha^2 C \tag{10}$$

$$\eta_1 = \frac{E}{\alpha^3}Q_1^3 + \frac{F}{\alpha^2}Q_1^2 + \frac{G}{\alpha}Q_1 + I \tag{11}$$

where η_1 is the efficiency of the turbine for a flow equal to Q_1.

2.2. Experimental approximation: efficiency curves

The prediction of head and flow values in turbines working with different rotational speeds has a reasonable approximation. Nevertheless, as the affinity laws do not consider the viscosity effects of the fluid inside of the impeller (third condition of similarity), the use of these laws is limited (Simpson and Marchi 2013). Hence, these equations cannot be applied in all flow range to predict the performance, obtaining good results in turbines for ranges between +/- 20% around of the best efficiency point. As the viscosity effect has to be considered, the dynamic similarity is important in these cases. This effect must be taken into account together with geometrical and kinematic similarity. To consider the dynamic condition, different researchers (Sarbu and Borza 1998; Gulich 2003; Simpson and Marchi 2013) have proposed equations to define the performance as function of the rotational speed variation. Gulich (2003) proposed the equation (12), which predicts the performance according to the variation of Reynolds number between both rotational speeds of the machine.

$$\frac{1-\eta_1}{1-\eta_0} = K + (1-K)\left(\frac{Re_1}{Re_0}\right)^2 \tag{12}$$

where Re_1 is the Reynolds number for the rotational speed N_1; Re_0 is the Reynolds number for the rotational speed N_0; K is the loss coefficient in the impeller as function of the Reynolds number.

Similar equation was proposed by Sarbu and Borza (1998), who also related the Reynold number as function of the rotational speed, defined in equation (13):

$$\frac{1-\eta_1}{1-\eta_0} = \left(\frac{N_1}{N_0}\right)^{0.1} \tag{13}$$

Equations (12) and (13) were tested by Simpson and Marchi (2013), obtaining good results in the prediction of the efficiency, if the rotational speed is not reduced under to 70% of the nominal speed. This is due to the empirical expression exponent changes with viscosity and friction effects in the impeller.

When variable operating strategy (*VOS*) is applied, the final objective is to determine the best efficiency line (*BEL*) as function of the rotational speed for each flow (Figure 2). The operation point should be fixed in the available maximum point to maximize the efficiency of the recovery system. The knowledge of *BEP* for each flow along the time (*i.e.,* Q_i, Q_{i+1}) as well as the available net head (H_{Ti}) will allow researchers to know the best efficiency head line (*BEH*) of the installed machine ($H_{Ri,N0}$, $H_{Ri+1,N1}$) for the recovery system. Both lines allow to recover the maximum energy, helping to define the *VOS* in the system for the necessary rotational speed (*i.e.,* N_0, N_2, …, N_i) in each time.

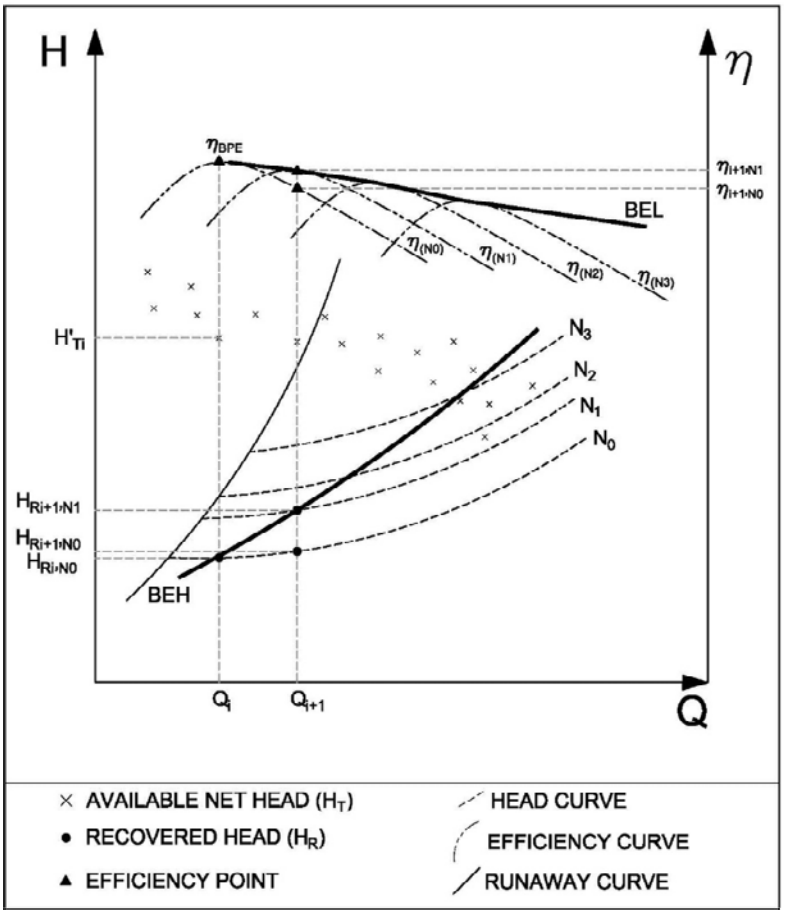

Figure 2. Operating points

Traditionally, these variations have been predicted by affinity laws, but only near the *BEP*. In this *BEL*, different authors (Carravetta *et al.,* 2014a, 2014b; Fecarotta *et al.,* 2016) have proposed modifications in the affinity laws to improve the prediction of the *BEP* depending on the rotational speed. This proposal was developed for some semi-axial machines with specific rotational speed between 120 and 162 (m, kW). As proposed, the modification of the affinity laws is developed according to the equations (5) to (7) as well as the use of the Suter parameters (*SP*), which were defined by Suter (1966)by equations (14) and (15):

$$\text{Head SP; } WH = \frac{h}{n^2+q^2} \tag{14}$$

$$\text{Torque SP; } WT = \frac{b}{n^2+q^2} \tag{15}$$

where *h*, *q*, *n*, and *b* are the head, discharge, velocity, and torque coefficients defined by equations from (16) to (19), respectively.

- Head coefficient;

$$h = \frac{H}{H_0} \tag{16}$$

- Discharge coefficient;

$$q = \frac{Q}{Q_0} \tag{17}$$

- Velocity coefficient;

$$n = \frac{N}{N_0} \tag{18}$$

- Torque coefficient;

$$b = \frac{T}{T_0} \tag{19}$$

Finally, the performance coefficient (*e*) (which is also called efficiency ratio) is defined by equation (20):

$$e = \frac{\eta}{\eta_B} = \frac{bn}{qh} = \tan\varphi \frac{WT}{WH} \tag{20}$$

where $\tan\varphi$ is the ratio between q and n, according to the third quadrant ($\pi<\varphi<3\pi/2$), when the machine is working as turbine (*PAT*). In this case, h and b are positive, while n and q are negative. According to expert references (Carravetta *et al.,* 2014a, 2014b; Fecarotta *et al.,* 2016), the affinity laws can be modified as:

$$q = \frac{Q_1}{Q_0} = f_1(\alpha) \tag{21}$$

$$h = \frac{H_1}{H_0} = f_2(\alpha) \tag{22}$$

$$p = \frac{P_1}{P_0} = f_3(\alpha) \tag{23}$$

where f_1, f_2, and f_3 are fitted functions, which depend on the experimental data according to α.

2.3. Theoretical vs experimental: error definition

The determination of the errors is evaluated by equations (24) and (25). Three comparisons have been done: a) experimental data versus classic affinity laws; b) experimental data versus modified affinity laws; and experimental data versus empirical method. Equation (24) defines the absolute relative error between the experimental data and estimated measurements for the same flow value (head or efficiency) and equation (25) defines the mean square error, which is determined according to the number of measured data:

$$Absolute\ relative\ error\ (\varepsilon_i) = \left|\frac{X_{est}-X_{exp}}{X_{exp}}\right| \tag{24}$$

$$Mean\ square\ error\ (\sigma_i) = \frac{1}{m}\sqrt{\sum_{i=1}^{m}\left(\frac{X_{est}-X_{exp}}{X_{exp}}\right)^2} \tag{25}$$

where i is the tested parameter, which can be q, h, p, or e; X_{est} is the estimated value through affinity laws or empirical method; X_{exp} is the measured value; and m is the number of measurements.

3. Developed test

3.1. Tested impellers

The experimental tests have been carried out in *CERIS*-Hydraulic Lab of Instituto Superior Técnico at the University of Lisbon with two different machines. In both cases the discharge was measured by an electromagnetic flowmeter, the pressure was registered by pressure transducers, and the power by multimeter which was connected to the generator, while the rotational speed was measured by a frequency meter.

Two different machines have been tested (Figure 3). On the one hand, an axial machine with an impeller's size of 85 mm with five blades. This machine has the best efficiency point for a flow of 4.44 l/s and head of 0.24 m w.c., being the specific speed number of 283 (m, kW) (Equation (1)). On the other hand, a radial machine with an impeller size of 139 mm, with the best efficiency point for 3.36 l/s and 4 m w.c. and the specific rotational speed 51 (m, kW).

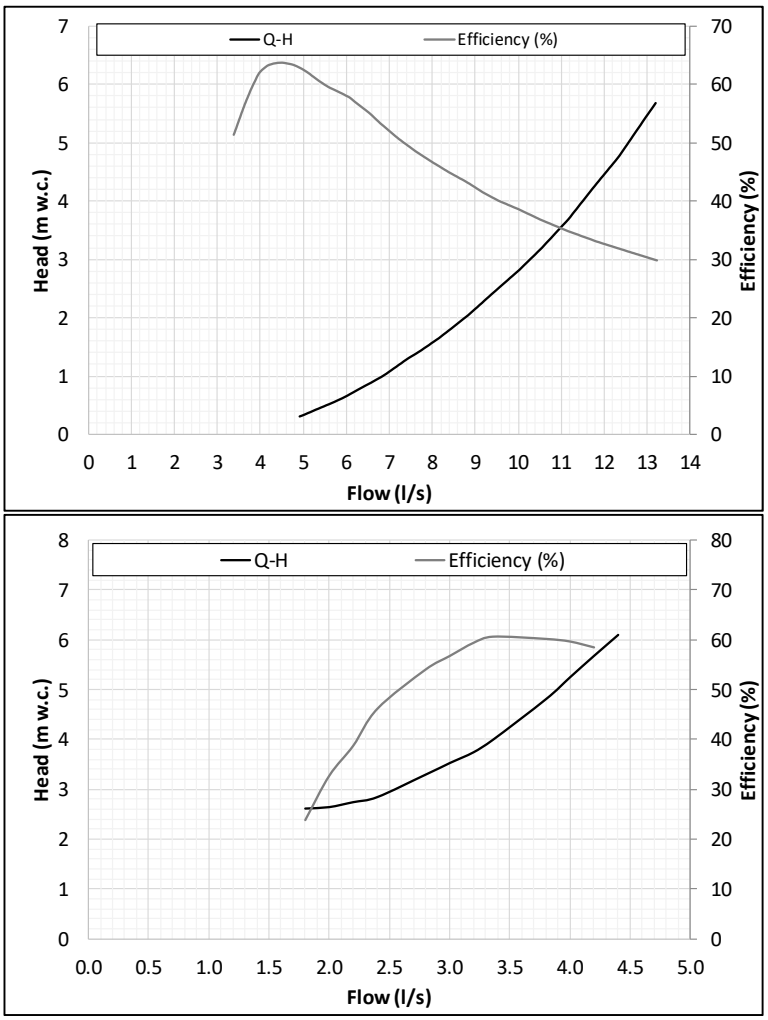

Figure. 3 Experimental curves. (Up) Axial machine for 750 rpm. (Bottom) Radial machine for 1020 rpm

3.2. Rotational speed variation

In Figure 4, the efficiency and head curve for different rotational speed are shown according to the performed tests in the axial machine. In this case, this figure shows the head values and the efficiency as function of the flow for different rotational speeds (500, 750, 1000, 1250, and 1500 rpm), as well as the runaway curve.

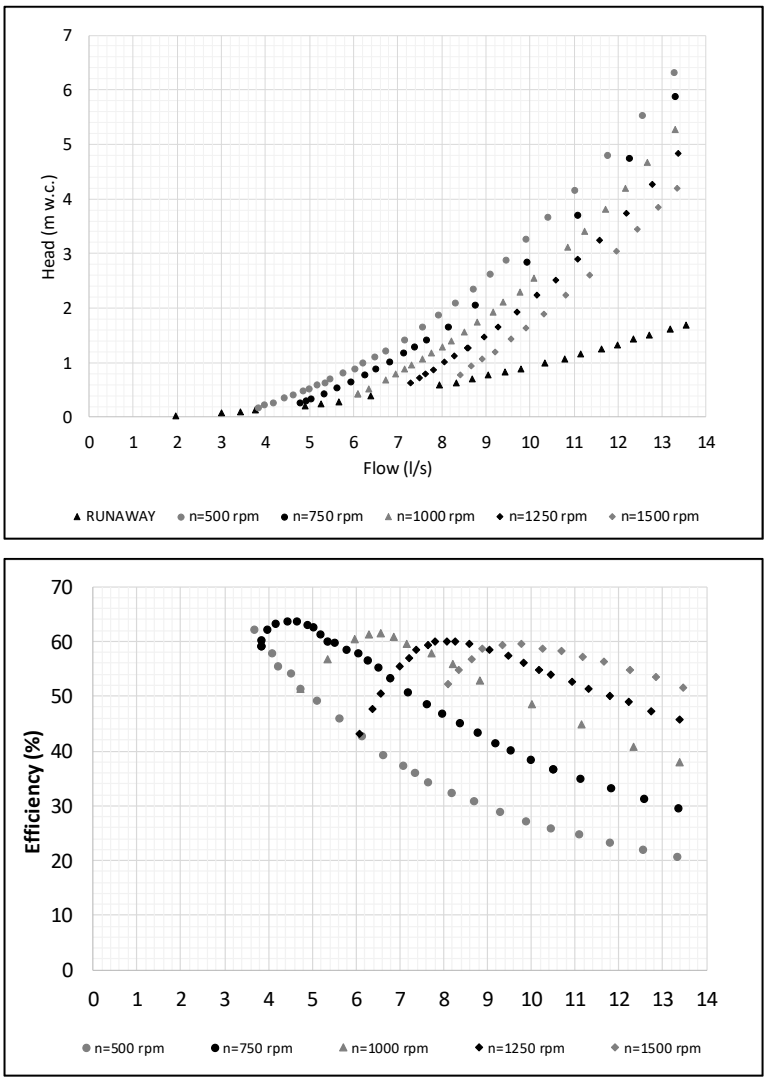

Figure 4. Experimental data for axial machine. Head (Up) and Efficiency (Bottom) as a function of the rotational speed

These characteristic curves for a rotational speed of 750 rpm can be fitted by polynomial equations (26) and (27):

- Head curve (m w.c.);

$$H = 0.047Q^2 - 0.219Q + 0.272 \ (R^2 = 0.998) \ [4.40<Q<13.30 \text{ l/s}] \quad (26)$$

- Efficiency (%);

$$E = -0.058Q^4 + 1.942Q^3 - 23.690Q^2 + 118.381Q - 143.852$$

(R^2=0.995). [4.40 < Q <13.30 l/s] (27)

When the machine is operating in its nominal rotational speed, the flow range oscillates between 4.40 l/s and 13.30 l/s, varying the recovered head between 0.26 and 5.88 m w.c. For this range of flows, the efficiency of the machine oscillates between 63.65 % and 29.62%, being the maximum efficiency of 63.65%, when the flow is 4.44 l/s.

Figure 5 shows similar results according to tests carried out with the radial machine. In this case, the machine was tested for 600, 900, 1020, and 1200 rpm. The characteristic curve is presented for a rotational speed of 1020 rpm, being defined by the following equations (28) and (29):

- Head curve (m w.c.):

$$H = 0.431Q^2 - 1.310Q + 3.553 \quad (R^2 = 0.995) \quad [1.80 < Q < 4.40 \text{ l/s}] \tag{28}$$

- Efficiency (%):

$$E = -11.145Q^2 + 80.698Q - 84.535 \quad (R^2 = 0.995) \quad [4.80 < Q < 13.30 \text{ l/s}] \tag{29}$$

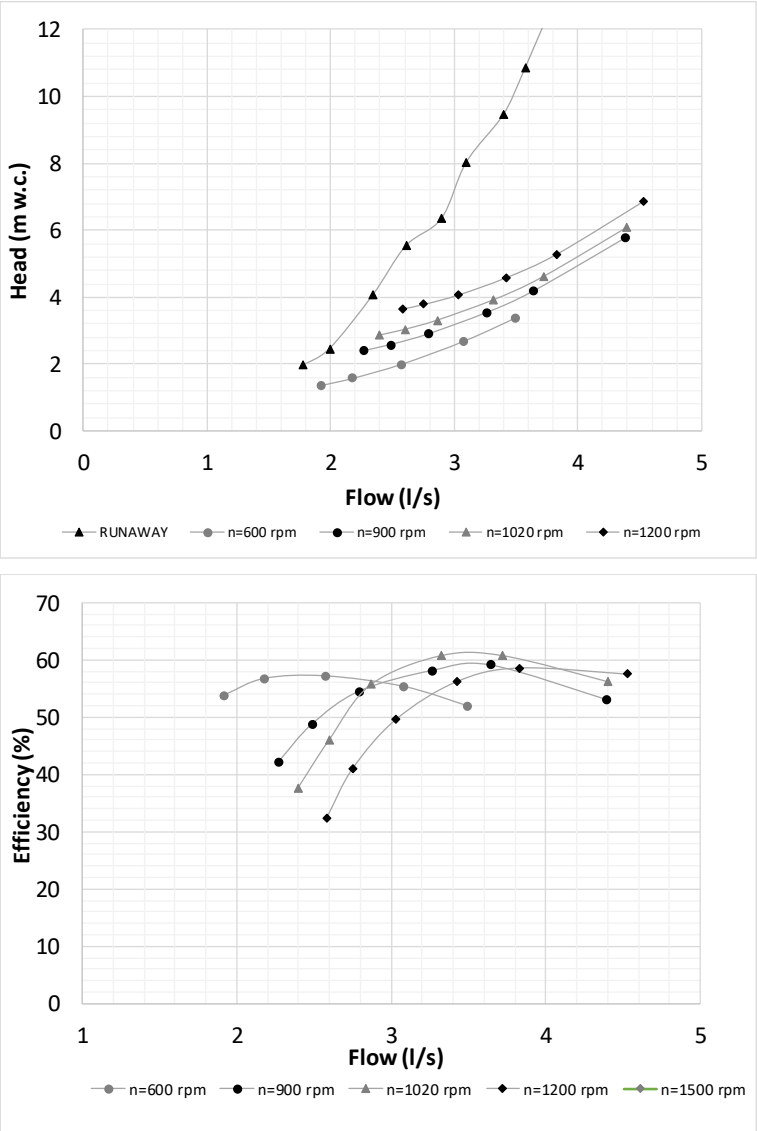

Figure 5 Experimental data for the radial machine. Head (Up) and Efficiency (Bottom) as function of the rotational speed.

For this type of machine, the maximum efficiency is 60.5% for a flow of 3.36 l/s.

The runaway curves are also shown in Figures 4 and 5 for the both machines (axial and radial). When these curves are analyzed, a significative difference can be determined taking into account the *VOS*. If a same value of the recovered head is established, a

reduction of the flow with a high rotational speed can lead to cause the runaway condition in radial machines (Figure 5). In the case of the axial machine (Figure 4), an increasing of the flow keeping the recovered head can be attained the runaway conditions.

3.3. Analytical versus experimental curves

The need to know the head and efficiency values of each machine can lead to develop new curves with different rotational speeds through affinity laws or Suter parameters, when the water manager uses *VOS*. The obtained results in analyses of axial and radial machines are shown in Figures 6 and 7, respectively. In both figures, the head values of the affinity laws can be observed, being coincident in a great range of flow conditions. Therefore, the use of these laws to develop new equation of recovered head curve can be used. Otherwise, if water managers want to determine the efficiency, the affinity laws can fail. Figures 6 and 7 show the predicted efficiencies given by the affinity laws, which are different, especially when the maximum values are considered (*i.e.,* maximum efficiency and flow value).

As shown in Figure 6, in the axial machine when the rotational speed is 750 rpm, the maximum efficiency is 63.60% for a flow of 4.66 l/s, while the maximum efficiency by affinity laws is 62.19%. For the rotational speed of 1000 rpm, the maximum efficiency is 61.56% when the flow is 6.56 l/s, being the maximum efficiency by the affinity laws 62.27% when the flow is 6.03 l/s. This error raises with rotational speeds of 1250 and 1500 rpm. For the rotational speed of 1250 rpm, the maximum measured efficiency is 59.98% and the maximum estimated efficiency is 62.27 %, being the flow values of 8.28 and 7.21 l/s, respectively. Similar tendency can be observed in Figure 6 when the rotational speed is 1500 rpm.

Figure 7 shows results between measured efficiencies and estimated values by affinity laws for different rotational speeds of 600, 900, 1020, and 1200 rpm in the radial machine, not being coincident the *BEP* for each rotational speed (e.g. when the rotational speed is 900 rpm, the maximum measured efficiency is 59.23% and the maximum estimated efficiency is 61.82%, being the flows 3.65 l/s and 3.25 l/s, respectively).

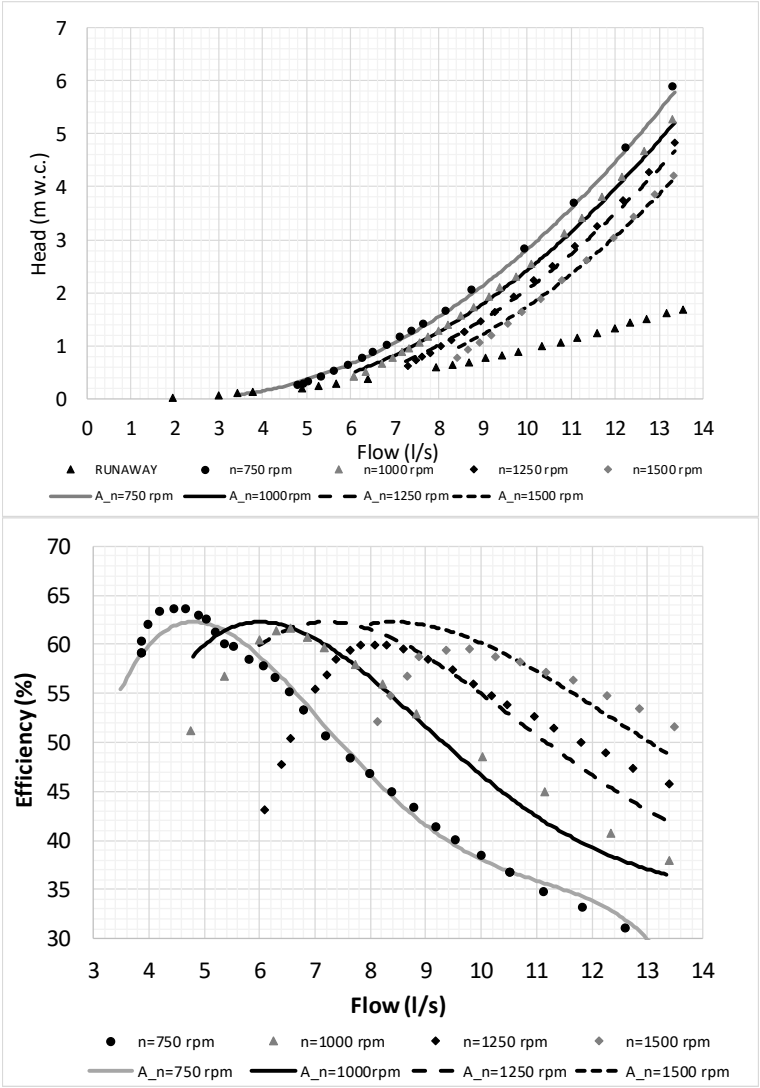

Figure 6 Experimental *vs* affinity laws in the axial machine: head and efficiency as a function of rotational speed

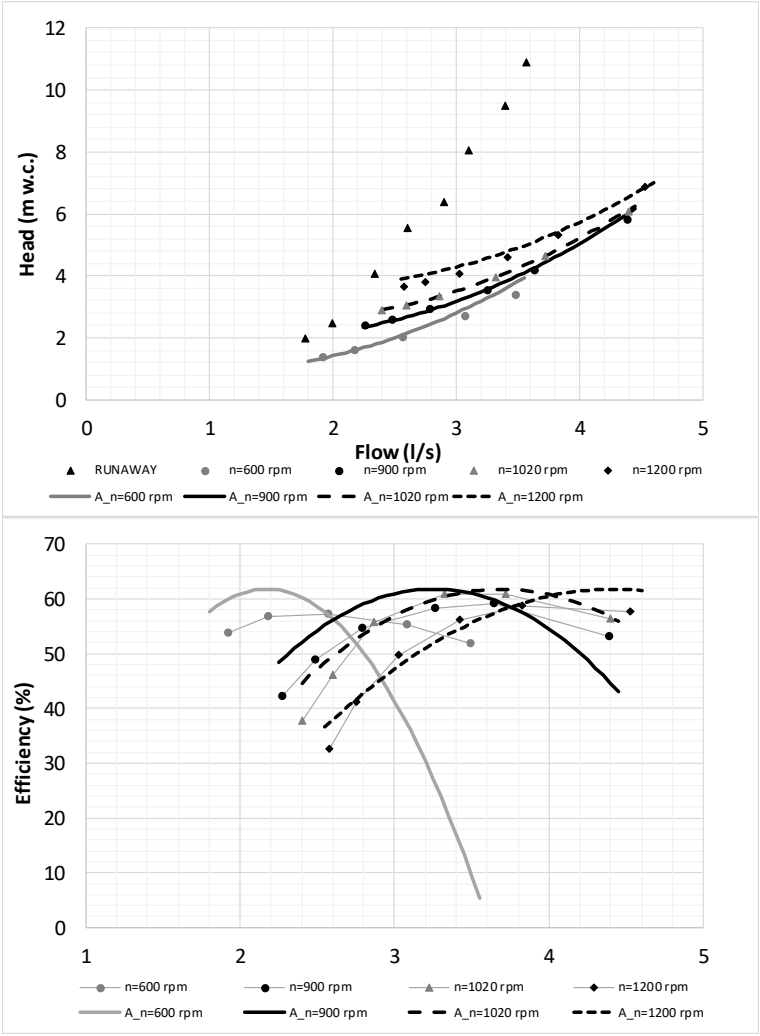

Figure 7 Experimental vs affinity laws in the radial machine: head and efficiency as a function of rotational speed

Figure 8 shows the absolute relative error between experimental data and estimated values by affinity laws used to predict head and efficiency for flows (Q) and rotational speeds (N) in the axial machine. The majority of head errors can attain 10% in both cases (axial and radial machines). If efficiency errors are analyzed, the best fits are located in low value zone of efficiency curve, being these errors below to 1%.

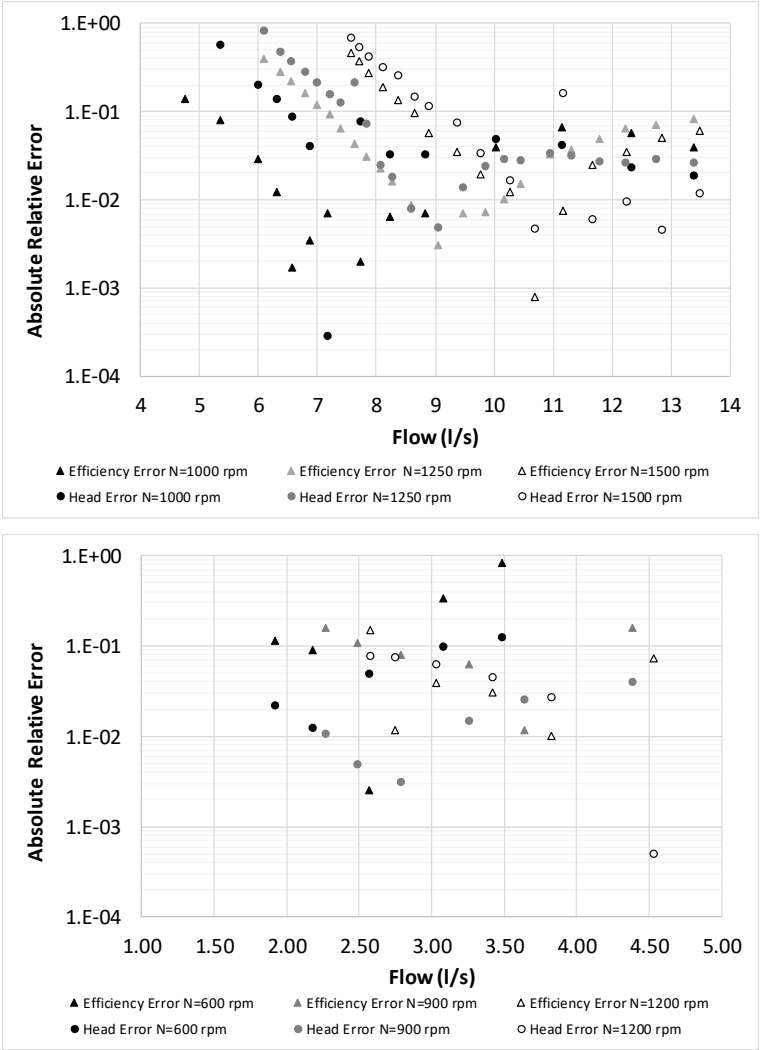

Figure. 8 Absolut relative error as function of the flow and rotational speed in axial (left) and radial (right) machines

This can be observed in Figure 6, being the maximum errors near to the maximum efficiency point. In the case of radial machine, this trend does not occur as for axial machine. These efficiency errors are important to be considered, because when the mean errors are averaged taken into account for all flow range, the obtained mean error is lower than the absolute relative error near the *BEP* (e.g. when the radial machine is run to 900 rpm, the absolute relative error is 0.06 and the mean square error is 0.02). Therefore, if

the mean error is determined for each speed, this can mislead to erroneous analyses. In the axial machine, the mean square errors are 0.05, 0.04, and 0.06 for rotational speeds of 1000, 1250, and 1500 rpm, respectively. These error values are not representative to analyze the maximum efficiency in the machine when the recovery system is operating by *VOS*. The mean square errors in radial machine are 0.09, 0.02, and 0.01 for speed of 600, 900, and 1200 rpm, respectively.

3.4. Empirical method towards new affinity laws

If the shown errors in the Figure 8 are taken into account, it is necessary to search for new solutions, which allow modelers to determine functions with a less error, to be used in the energy studies based on Suter Parameter (*SP*). To fit the affinity laws, the described methodology in section 2.3 allows to obtain such functions (f_1, f_2, and f_3). These functions lead for the determination of the *BEH* and the *BEL* in both machines, maximizing the efficiency in all ranges of flow by rotational speed variations.

Figures 9 and 10 show the proposed fitted functions for the axial and radial machines, respectively. To do a better analysis, other maximum values of efficiency were measured in the machine for rotational speeds of 250, 1750, 2000, and 2250 rpm.

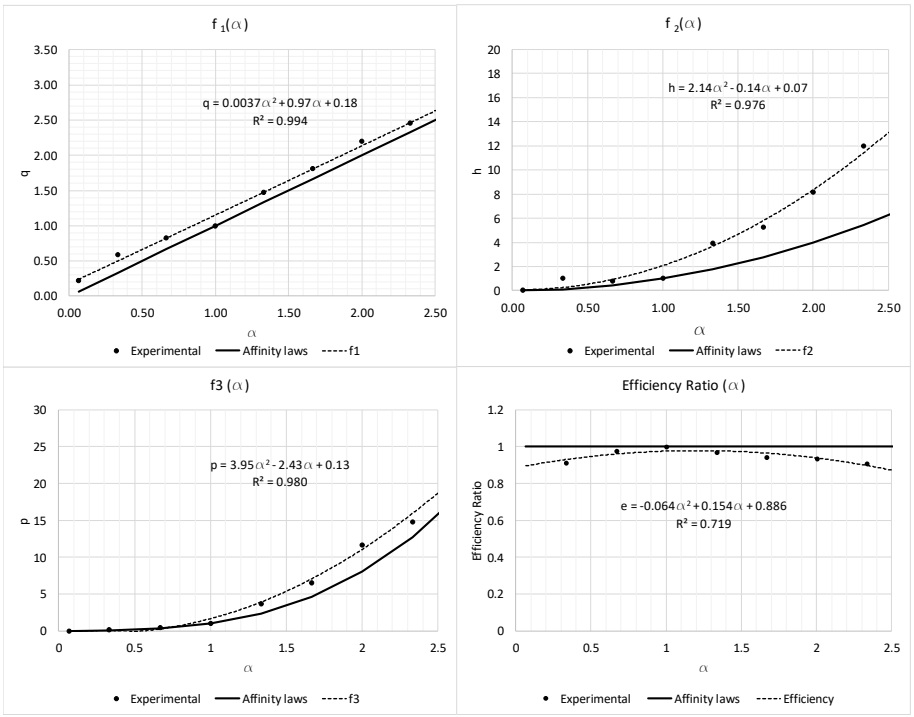

Figure 9 Proposed functions for axial machine

In the case of the radial machine, the maximum efficiency for the rotational speed of 1500 rpm has also been measured. In both machines, the obtained functions present good regression indexes, being higher to 0.94 to parameters of q, h, p, and efficiency ratio, except the value of efficiency ratio in axial machine, which is 0.719.

Once the functions for each parameter have been adjusted by least squares, the errors can be calculated, obtaining in the Figure 11 the results for both machines. The errors of q, h, p, and efficiency ratio (e) are shown when the parameters are determined by affinity laws (*AL*), the proposed empirical method (*EM*), and Sarbu-Borza's Method (*SB*) (since this method is only used to determine efficiency values according to equation (13)). In all cases the less error is obtained by *EM*. The obtained errors with SB are between the *AL* and *EM*. For the *EM*, the mean square errors are 0.02, 0.02, 0.004 for q, h, and efficiency ratio in the radial machine. If these values are determined for the axial machine, 0.02, 0.03, and 0.008 are obtained, respectively. The mean square error by *SB* is 0.02 for both machines.

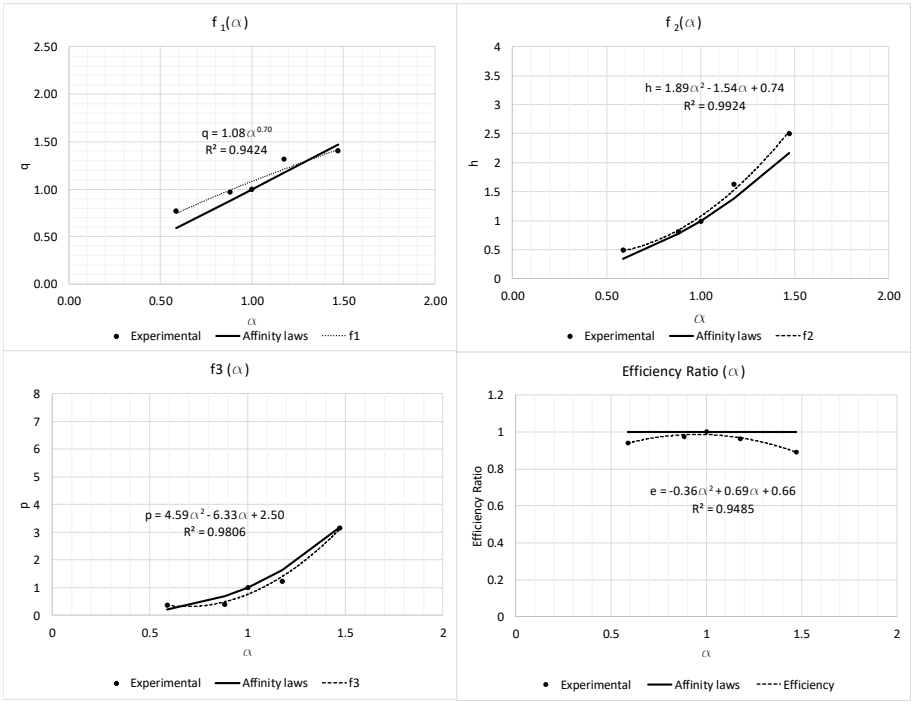

Figure 10 Proposed functions for radial machine

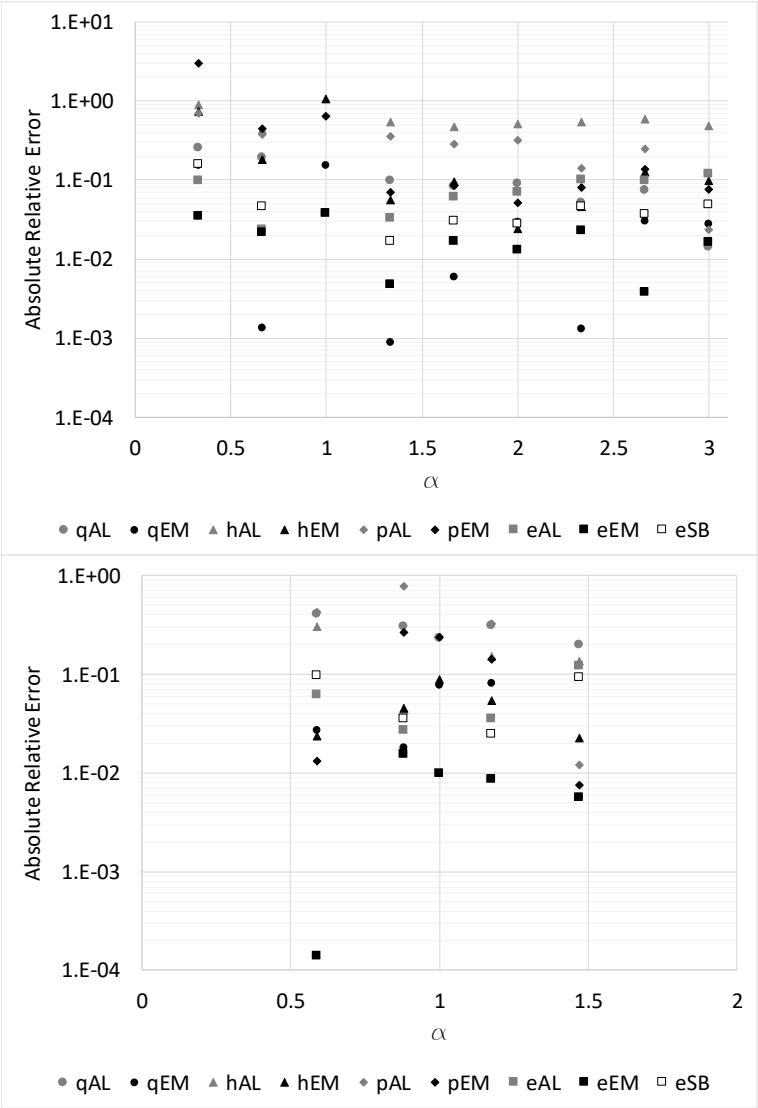

Figure 11 Absolute error in axial (up) and radial bottom) machines when the parameters are determined by affinity laws (*AL*), empirical method (*EM*), and Sarbu-Borza method (*SB*)

Once the errors have been analyzed, and the functions (f_1,f_2, and f_3) are known depending on the rotational speed, the *BEL* and *BEH* of each machine can be drawn. Figure 12 shows these lines for the axial and the radial machines as function of flow, according to *VOS* described in Figure 2. In the particular case of the radial machine, the *BEL* indicates that recovery system is working upper to 55% in the all range of flows. *BEL* and *BEH*

are significant information in the optimization methodologies for water managers to develop the *VOS* in each hydraulic machine, maximizing the system efficiency.

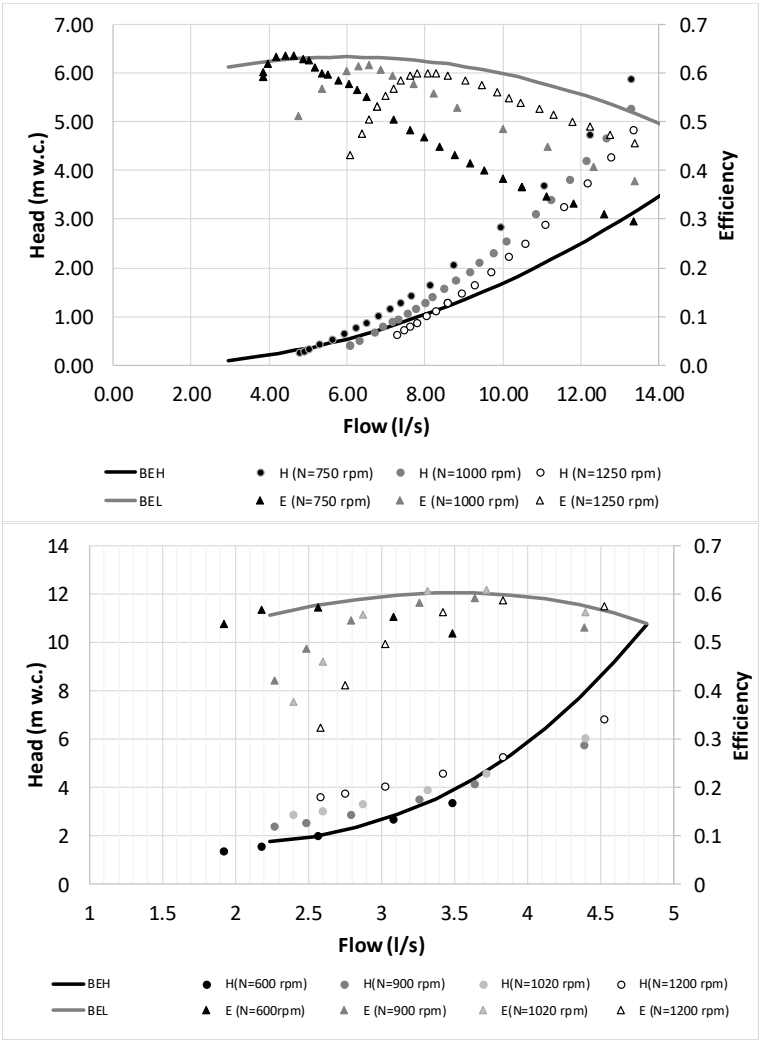

Figure 12 *BEH* and *BEL* for axial (up) and radial (bottom) hydraulic machines

Finally, joining the depicted procedure to modify the affinity laws with the analysis developed for semi-axial machines by Fecarotta *et al.,* (2016), different functions can be drawn (*i.e., f_1, f_2, f_3* and *e*) depending on the rotational speed. This analysis is shown in Figure 13 which correlates functions (*i.e., f_1, f_2, f_3* and *e*) with the variables: velocity ratio and specific rotational speed.

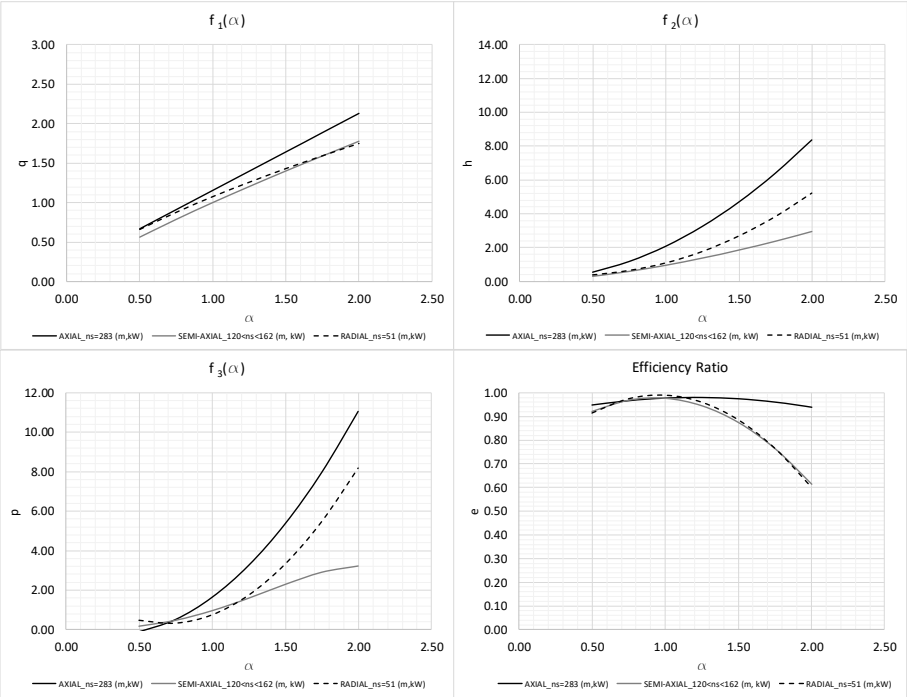

Figure 13. Fit function to different hydraulic machines

These functions (f_1, f_2, f_3 and e) present relative and mean errors smaller than affinity laws and Sarbu-Borza's method when they are used to predict the real behavior of hydraulic turbines. If the radial machine is analyzed, the empirical mean square errors are 0.02, 0.02, and 0.004 for q, h, and e parameters and the mean square error of affinity laws are 0.11, 0.04, and 0.03, respectively. Therefore, the application of this empirical method reduces the mean error values in 81.81%, 50%, and 86.67% respectively. For the axial machine, the empirical mean errors are 0.02, 0.03, and 0.008, for q, h, and e parameters respectively. Against, these errors are 0.06, 0.18, and 0.03 when the efficiency is determined by affinity laws, reducing them to 66.67%, 83.33%, and 73.33%, respectively.

4. Conclusions

This research presents developed experimental tests for two different hydraulic turbines, axial and radial, with specific rotational speed of 283 and 51 (m, kW) respectively, in which the characteristic curves (flow-head, flow-mechanical power, and flow-efficiency) have been obtained for different rotational speeds. The variable operating strategies (*VOS*) in recovery systems of water distribution networks implicate the need to predict the efficiency and head curve of each machine for different rotational speeds, to develop viability studies based on energy and economic analyses.

The prediction of the efficiency with different rotational speeds by the classic affinity laws can imply significant erroneous values. These errors induce the need to develop a modification in the affinity laws to take into account losses in the impeller of each machine. New modified functions are proposed to know the flow, head, power and efficiency parameters depending on the rotational speed ratio for radial and axial machines.

These functions (f_1, f_2, f_3 and e) have been validated for the tested hydraulic machines, presenting relative and mean errors smaller than affinity laws and the Sarbu-Borza's method. When the radial machine is analyzed, the mean errors are reduced 81.81%, 50%, and 86.67% for q, h, and e parameters when compared with the affinity laws. For the axial machine, the mean errors are reduced 66.67%, 83.33%, and 73.33% respectively, when compared with affinity laws.

The knowledge of these functions allows to develop the *BEL* and *BEH* lines of each machine as function of the flow, helping managers to choose the best operating rules in order to achieve the best efficiency point for each flow. These rules maximize the real recovered energy under optimization strategies. Regarding the rotational speeds the analysis when the flows are reduced keeping a constant head the rotational speed increases in radial machine. This phenomenon can cause that *PAT* reaches the runaway conditions when the machine is installed in a line or point of a network with significant variable flows.

Finally, the need to correlate the rotational speed and the specific speed with the different characteristic parameters (q, h, p, and e) is of utmost importance. The development of similar studies for different specific rotational speeds will allow to define the *BEL* and *BEH* and to choose the best hydraulic machine for each system characteristics.

Acknowledgments

This research is supported by Program to support the academic career of the faculty of the Universitat Politècnica de Valencia 2015/2016 in the project "Methodology for Analysis of Improvement of Energy Efficiency in Irrigation Pressurized Network".

Compliance with Ethical Standards

Conflict of Interest The authors declare that they have no conflict of interest.

References

Abbott M, Cohen B, (2009) Productivity and efficiency in the water industry. Util. Policy 17:233–244.

Alexander KV, Giddens EP, Fuller AM (2009) Radial- and mixed-flow turbines for low head microhydro systems. Renew Energy 34:1885–1894. doi:10.1016/j.renene.2008.12.013

Araujo LS, Ramos HM, Coehlo ST (2006) Pressure Control for Leakage Minimisation in Water Distribution Systems Management. Water Resources Management 20:133–149. doi: 10.1007/s11269-006-4635-3

Cabrera E, Cobacho R, Soriano J (2014) Towards an Energy Labelling of Pressurized Water Networks. Procedia Eng 70: 209–217. doi:10.1016/j.proeng.2014.02.024

Carravetta A, Conte MC, Fecarotta O, Ramos HM (2014a) Evaluation of PAT performances by modified affinity law. Procedia Eng 89:581–587. doi:10.1016/j.proeng.2014.11.481

Carravetta A, Del Giudice G, Fecarotta O, Ramos H (2013a) Pump as Turbine (PAT) Design in Water Distribution Network by System Effectiveness. Water 5:1211–1225. doi:10.3390/w5031211

Carravetta A, Del Giudice G, Fecarotta O, Ramos H (2013b) PAT Design Strategy for Energy Recovery in Water Distribution Networks by Electrical Regulation. Energies 6:411–424. doi:10.3390/en6010411

Carravetta A, Del Giudice G, Fecarotta O, Ramos H (2012) Energy Production in Water Distribution Networks: A PAT Design Strategy. Water Resour Manag 26:3947–3959. doi:10.1007/s11269-012-0114-1

Carravetta A, Fecarotta O, Martino R, Antipodi L (2014b) PAT efficiency variation with design parameters. Procedia Eng 70:285–291. doi:10.1016/j.proeng.2014.02.032

Corominas J (2010) Agua y Energía en el riego en la época de la sostenibilidad. Ing del Agua 17.

Dannier A, Del Pizzo A, Giugni M, Fontana N, Marini G, Proto D (2015) Efficiency evaluation of a micro-generation system for energy recovery in water distribution networks. Int. Conf. Clean Electr Power 689–694. doi:10.1109/ICCEP.2015.7177566

Derakhshan S, Nourbakhsh A (2008) Experimental study of characteristic curves of centrifugal pumps working as turbines in different specific speeds. Exp Therm Fluid Sci 32:800–807. doi:10.1016/j.expthermflusci.2007.10.004

Fecarotta O, Carravetta A, Ramos HM, Martino R (2016). An improved affinity model to enhance variable operating strategy for pumps used as turbines. J Hydraul Res 1686:1–10. doi:10.1080/00221686.2016.1141804

Fontana N, Giugni M, Portolano D (2012) Losses Reduction and Energy Production in Water-Distribution Networks. J Water Resour Plan Manag 138:237–244. doi:10.1061/(ASCE)WR.1943-5452.0000179

Giugni M, Fontana N, Ranucci A (2014) Optimal Location of PRVs and Turbines in Water Distribution Systems. J Water Resour Plan Manag 140:06014004. doi:10.1061/(ASCE)WR.1943-5452.0000418

Giustolisi O, Savic D, Kapelan Z (2008). Pressure-Driven Demand and Leakage Simulation for Water Distribution Networks. J Hydraul Eng 134:626–635. doi:10.1061/(ASCE)0733-9429(2008)134:5(626)

Gulich J (2003) Effect of Reynolds number and surface roughness on the efficiency of centrifugal pump. J Fluid Eng 125:670–679.

Jiménez-Bello MA, Royuela A, Manzano J, Prats AG, Martínez-Alzamora F (2015) Methodology to improve water and energy use by proper irrigation scheduling in pressurised networks. Agric Water Manag 149:91–101. doi:10.1016/j.agwat.2014.10.026

Kevin B (1990) Optimization m o d e l for w a t e r distribution system design 115:1401–1418.

Mataix C (2009) Turbomáquinas Hidráulicas. Universidad Pontificia Comillas, Madrid.

McNabola A, Coughlan P, Corcoran L, Power C, Prysor Williams A, Harris I, Gallagher J, Styles D (2014) Energy recovery in the water industry using micro-hydropower: an opportunity to improve sustainability. Water Policy 16:168. doi:10.2166/wp.2013.164

Moreno M, Córcoles J, Tarjuelo J, Ortega J (2010) Energy efficiency of pressurised irrigation networks managed on-demand and under a rotation schedule. Biosyst Eng 107:349–363. doi:10.1016/j.biosystemseng.2010.09.009

Nazari A., Meisami H, (2008) Instructing WaterGEMS Software Usage. Tehran.

Pasten C, Santamarina JC (2012). Energy and quality of life. Energy Policy 49:468–476. doi:10.1016/j.enpol.2012.06.051

Pérez-Sánchez M, Sánchez-Romero F, Ramos HM, López-Jiménez PA (2016) Modeling Irrigation Networks for the Quantification of Potential Energy Recovering: A Case Study. Water 8:1–26. doi:10.3390/w8060234

Ramos HM, Borga A (1999). Pumps as turbines: an unconventional solution to energy production. Urban Water 1:261–263. doi:10.1016/S1462-0758(00)00016-9

Ramos HM, Mello M, De PK (2010) Clean power in water supply systems as a sustainable solution: from planning to practical implementation. Water Sci Technol Water Supply 10:39–49. doi:10.2166/ws.2010.720

Ramos HM, Simão M, Borga A (2013) Experiments and CFD Analyses for a New Reaction Microhydro Propeller with Five Blades. J Energy Eng 139:109–117. doi:10.1061/(ASCE)EY.1943-7897.0000096

Rossman LA, 2000. EPANET 2: User's manual, U.S. EPA. ed. Cincinnati.

Samora I, Franca M, Schleiss A, Ramos HM (2016a). Simulated Annealing in Optimization of Energy Production in a Water Supply Network. Water Resour Manag 30:1533–1547. doi:10.1007/s11269-016-1238-5

Samora I, Hasmatuchi V, Münch-Alligné C, Franca MJ, Schleiss AJ, Ramos HM (2016b). Experimental characterization of a five blade tubular propeller turbine for pipe inline installation. Renew Energy 95: 356–366. doi:10.1016/j.renene.2016.04.023

Sarbu I, Borza I (1998) Energetic optimization of water pumping in distribution systems. Period Polytech Ser Mech Eng 42:141–152.

Shi G, Liu X, Yang J, Miao S, Li J (2015) Theoretical research of hydraulic turbine performance based on slip factor within centripetal impeller. Advances in Mechanical Engineering 7(7):1–12. doi:10.1177/1687814015593864

Simpson AR, Marchi A (2013). Evaluating the Approximation of the Affinity Laws and Improving the Efficiency Estimate for Variable Speed Pumps. J Hydraul Eng 139:1314–1317. doi:10.1061/(ASCE)HY.1943-7900.0000776

Singh P (2005) Optimization of the Internal Hydraulic and of System Design in Pumps as Turbines with Field Implementation and Evaluation. University of Karlsruhe.

Suter P (1966) Representation of pump characteristics for calculation of water hammer. Sulzer Tech Rev 66:45–48.

Ulanicki B, Kahler J, Coulbeck B (2008) Modeling the Efficiency and Power Characteristics of a Pump Group. J. Water Resour Plan Manag 134:88–93. doi:10.1061/(ASCE)0733-9496(2008)134:1(88)

Yang SS, Derakhshan S, Kong FY (2012) Theoretical, numerical and experimental prediction of pump as turbine performance. Renew Energy 48:507–513. doi:10.1016/j.renene.2012.06.002

Appendices
Appendix VIII

PATs OPERATING IN WATER NETWORKS UNDER UNSTEADY FLOW CONDITIONS: CONTROL VALVE MANEUVER AND OVERSPEED EFFECT

Author version document which was sent to publish to index JCR Journal "Renewable Energy" ISSN 0960-1481 for its potential publication (Registered Data: 20/02/2017) Impact Factor 3.404. Position 24/88 (Q2). Energy&Fuels

Coauthors: Pérez-Sánchez, M; López-Jiménez PA.; Ramos, HM.

This page is intentionally left blank.

ABSTRACT

The knowledge of transient conditions in pressurized water networks, which are equipped with pump as turbines (*PATs*) is of the utmost importance and it is becoming a priority for safety reasons and good design implementation of these new renewable solutions. This research characterizes the water hammer phenomenon in the design of *PAT* systems, in order to emphasize transient events that can occur during a normal operation. This is based on project concerns towards a stable and efficient operation associated to the normal dynamic behavior of a flow control valve closure or by induced overspeed effect. Basic concepts of mathematical modelling, characterization of control valves behavior, damping effects in the wave propagation and runaway conditions of *PATs* are currently associated to an inadequate design. The correct evaluation of basic operating rules depends upon the system and components type, as well as the safety level required during each operation.

Keywords: Energy recovery systems; Runaway conditions; Unsteady flow; Water hammer

1. Introduction

The need to increase the efficiency in pressurized water networks has allowed to develop new water management strategies (Kougias *et al.,* 2014; Nogueira & Perrella, 2014). These strategies have been focused on two different directions according to water pressurized network type (*i.e.,* pumped or gravity systems). In pump solutions, the increase of efficiency in the network is directly correlated with the reduction of the manometric head (Moreno *et al.,* 2010; Jiménez-Bello *et al.,* 2015), the operation rules correction and the design of facilities (*e.g.,* pump efficiency, leakage control, establishment of optimum schedules - Pardo *et al.,* 2013; Cabrera *et al.,* 2014). In gravity systems, the efficiency improvement has been related with the reduction of leakage level through the installation of pressure reduction valves (Araujo *et al.,* 2006; Abbott & Cohen, 2009; Giugni *et al.,* 2014; Dannier *et al.,* 2015). Ramos and Borga (1999) proposed the replacement of *PRVs* by hydraulic machines, which could also generate energy. These systems provide two benefits, on the one hand, *PATs* reduce the pressure in the system and therefore, leakages are also reduced by the operation of *PRV*s; on the other hand, the generated energy contributes to improve the energy balance of these water systems, increasing the efficiency in the water networks as well as improving the performance indicators (Mamade *et al.,* 2017). However, the infrastructures design of

these energy recovery has to be planned and calculated correctly, considering the current computational tools (Su and Karney 2014)

Commonly, a hydraulic machine when proposed to replace the *PRVs* has been pump working as turbines (*PATs*). Numerous researchers have analyzed the behavior of these machines in steady flow conditions. Review of available technologies has been developed by Senior et al. (2010), Razan et al. (2012), Elbatran et al. (2015) and Pérez-Sánchez *et al.,* (2017). The analysis of performance and modelling in *PAT* were tackled by Nourbakhsh & Jahangiri (1992); *Arriaga (2010); Simão and Ramos (2010); Razan et al.,* (2012); Fecarotta *et al.,* (2016) among others, while the analysis of these machines in water distribution network was studied by Ramos *et al.,* (2009); Caxaria *et al.,* (2011); Carravetta *et al.,* (2014); Butera and Balestra (2015), designing an innovative strategy to maximize the recovered energy when the flows vary along the day Carravetta *et al.,* 2013, 2014; Fecarotta *et al.,* 2014, 2016; Sitzenfrei *et al.,* 2015) as well as their economic feasibility (Zema *et al.,* 2016). These strategies have been applied to determine and to maximize the theoretical recovered energy in both drinking and irrigation water systems (Samora *et al.,* 2016; Pérez-Sánchez *et al.,* 2016). The last case studies consider the significance of the changes in flow over time to predict the generated power in these facilities when they are installed in pressurized water networks (Corcoran *et al.,* 2016).

Nowadays, the study of unsteady flow in these systems is poorly analyzed and the installation of *PATs* in pilot plant (Imbernón & Usquin 2014; McNabola *et al.,* 2014) induces the need to analyze the unsteady flow conditions in order to better estimate the overpressures that can put in risk the facilities. As novelty, this paper analyzes the effective percentage of closure (effective %) in valve manoeuvres, the start-up and shutdown of radial and axial *PATs* of small size (*i.e.,* with low inertia) through experimental data collection. The runaway conditions induced by the overspeed effect are also presented. The overpressure and the flow cut effects are emphasized in the overspeed of radial machines, as well as the flow increasing in axial machines. These effects were also denoted in Ramos (1995) developed for conventional turbines but in this case, the small inertia of *PATs* has an important influence.

2. Material and methods

2.1. Basic hydraulic modelling of the transient conditions

The unsteady flow in pressurized pipe systems with higher length than diameter can be analyzed, considering the one-dimensional (1D) model type, through the mass and momentum conservation equations which derive from the Reynolds transport theorem (White 2008). These principles are defined by differential equations (1) and (2) (Wylie *et al.,* 1993):

$$\frac{\partial H}{\partial t} + \frac{c^2}{gA}\frac{\partial Q}{\partial x} = 0 \quad (1)$$

$$\frac{\partial H}{\partial x} + \frac{1}{gA}\frac{\partial Q}{\partial t} + \frac{4\tau_w}{\rho g D} = 0 \quad (2)$$

where H is the piezometric head in m w.c.; t is the time in s; c is the pressure wave speed in m/s, which is defined by the equation (3); g is the gravity acceleration in m/s^2; A is the inner area of the pipe in m^2; Q is the flow in m^3/s; x is the coordinate along the pipeline axis; τ_w is the shear stress at the pipe wall in N/m^2; ρ is the density of the fluid in kg/m^3; and D is the inner diameter of the pipe in m.

$$c = \sqrt{\frac{K}{\rho(1+(K/E)\psi)}} \quad (3)$$

where K is the fluid bulk modulus of elasticity in N/m^2; E is the Young's modulus of elasticity of the pipe in N/m^2; and ψ is the dimensionless parameter that takes into account the cross-section parameter of the pipe and supports constraint.

The considered assumptions applied in the classical one dimensional water hammer models are (Almeida and Koelle, 1992):

- The flow is homogenous and compressible;
- The changes of density and temperature in the fluid are considered negligible when these are compared to pressure and flow variations;
- The velocity profile is considered pseudo-uniform in each section, assuming the values of momentum and Coriolis coefficients constant and equal to one;
- The behavior of the pipe material is considered linear elastic; and
- Head-losses are calculated by uniform flow friction formula, which is used in steady flow.

The differential equations (1) and (2) can be simplified into a hyperbolic system of equation (Ramos 1995; Chaudhry 1987). These equations can be presented as a matrix (4):

$$\frac{\partial U}{\partial t} + \frac{\partial F(U)}{\partial x} = D(U) \quad (4)$$

being:

$$U = \begin{bmatrix} H \\ Q \end{bmatrix}; F(U) = \begin{bmatrix} \frac{c^2}{gA} & Q \\ gA & H \end{bmatrix}; D(U) = \begin{bmatrix} 0 \\ \frac{-JgA}{Q^2} Q|Q| \end{bmatrix} \quad (5)$$

where J is the hydraulic gradient.

The solution of these equations is obtained through a discretized time interval for each time step 'Δt' at a specific point of the pipe for each 'Δx', fulfilling the Courant condition (C_r=1) (6):

$$\frac{\Delta x}{\Delta t} = a \quad (6)$$

The differential equation (4) can be transformed into linear algebraic equations, obtaining the equations (7) and (8). The application of these equations is denominated the "Method of Characteristics" (*MOC*).

$$C^+: H_i^{n+1} - H_{i-1}^n + \frac{A}{c}\left(V_i^{n+1} - V_{i-1}^n\right) + \frac{f_{i-1}^n \Delta x}{D} V_{i-1}^n |V_{i-1}^n| = 0 \quad (7)$$

$$C^-: H_i^{n+1} - H_{i-1}^n - \frac{A}{c}\left(V_i^{n+1} - V_{i-1}^n\right) - \frac{f_{i-1}^n \Delta x}{D} V_{i-1}^n |V_{i-1}^n| = 0 \quad (8)$$

where H_i^{n+1} is the piezometric head in m w.c. at pipe section '*i'* and time instant '*n+1*'; V_i^{n+1} is the velocity in m/s at pipe section '*i'* and time instant '*n+1*; where H_{i-1}^n is the piezometric head in mw.c. at pipe section '*i-1*' and time instant '*n*'; V_{i-1}^n is the velocity in m/s at pipe section '*i-1*' and time instant *'n'*; f_{i-1}^n is the friction factor in the section *'i-1'* at time instant *'n'*.

2.2. Control valves

The valves are system components, which are responsible to change the flow when its opening degree changes. Any operation in a valve modifies the opening degree and varies the loss coefficient of the valve causing a flow variation in the system, being one of the origin of hydraulic transients. The closure time as well as the valve type influence the type of water hammer (i.e., fast or slow manoeuvers) for a system characterized by its diameter, length and pipe material.

For any maneuver, the loss coefficient of the valve is a function of the opening degree ($K_v(\theta)$) (Abreu et al. 1995) and the behavior of the valve can be defined by equation (9):

$$Q = K_v(\theta)\sqrt{\Delta H} \quad (9)$$

where Q is the flow rate in m^3/s; K_v is flow loss coefficient as a function of the opening degree (θ) in $m^{5/2}/s$. This coefficient can be obtained from manufacture and ΔH is the head loss in the valve in m w.c.

The ratio between the flow loss coefficient for a determined opening degree and for the nominal flow loss coefficient (*i.e.,* K_{v0} flow coefficient for completely opened valve), can be defined by equation (10):

$$\varphi(\theta) = \frac{K_v}{K_{v0}} \quad (10)$$

This ratio can be also defined as a function of the time, using the parameter τ between the flow coefficient for determined opening degree $K_v(t)$ and the one corresponding to the initial state $K_v(0)$. This parameter is defined by equation (11) (Abreu *et al.,* 1995):

$$\tau(t) = \frac{K_v(t)}{K_v(0)} = \frac{\varphi(t)}{\varphi(0)} \quad (11)$$

When the closure or opening maneuver is total, the parameter τ is one when the steady

flow is established (at initial time) and is zero when the time (t) is higher than the closure (or opening) time (T_c).

The variation of parameters $\varphi(\theta)$ and $\tau(t)$ along the maneuver time depends on the type of valve, with consequences in the pressure values of the transient regime due to the closure law. This parameter can be estimated by the equation (12):

$$\varphi(\theta) = \theta^b \tag{12}$$

where b is an integer number greater than zero. In a closure law of a valve, θ is 1 or 0 when the valve is opened and closed respectively.

Then the equation (9) can be rewritten as equation (13).

$$\varphi(t) = \left(1 - \frac{t}{T_c}\right)^b \tag{13}$$

Figure 1 shows different closures as a function of b exponent. If the exponent is one, the closure law is linear and the variation of the flow loss coefficient is continuous. When the exponent is less than one, the variation of the flow loss coefficient is higher at the end of the closure time (e.g. diaphragm valve - Figure 1. left (f)).

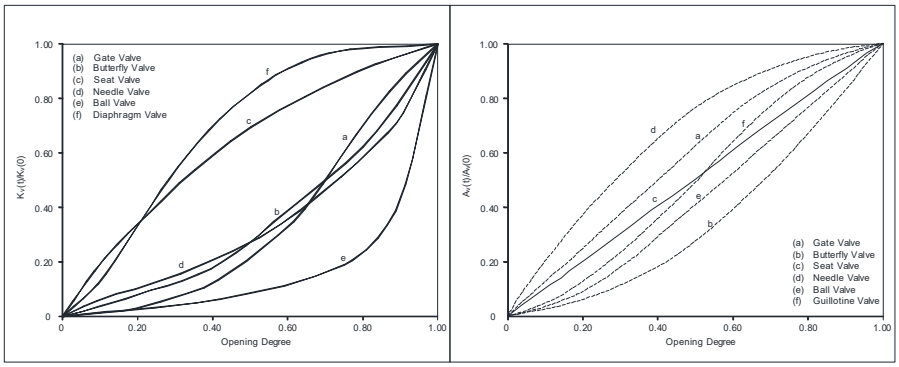

Figure 1. Type of closure as function of the valve type of flow coefficient (left) (Iglesias-Rey et al., 2004) and ratio between area as function of the opening degree (right) (Abreu et al., 1995)

If the exponent is greater than one, the closure is higher at the beginning of the maneuver (*e.g.,* butterfly valve), causing higher overpressures due to the main closure occurs at the beginning when the velocity of the fluid is greater. Considering the equation (10), the maneuver can be an instantaneous closing ($b \to \infty$), convex closure ($0<b<1$), linear *($b=1$)*, and concave closure (b>1) (Subani and Amin 2015). Although the closure law is known depending on the opening degree, this is not enough to establish the boundary condition, even knowing the ratio of free area as a function of the opening degree, which differs according to the type of the valve. Therefore, the valve installed in a pipe system has a great significance in the generated transient.

The duration of the valve maneuver, the diameter, the type of closure law (linear or non-linear) and the actuator type will influence the shape and values of the piezometric line envelopes. The effective time closure (T_{ef}) is the real time of valve closure (lesser than the total time (T_C)), which can induce high discharge reduction, responsible by extreme water hammer phenomenon (see the effective closure % in Figure 2). This time is, mathematically, defined in the equation (14) by the tangent to the point of the curve where *dq/dt* is highest:

$$T_{ef} = \frac{\Delta Q}{\left(\frac{dq}{dt}\right)_{max}} \tag{14}$$

where q is the ratio Q/Q_o (relative discharge value), ΔQ is the discharge variation in the hydraulic system, and Q_o is the discharge for total opening.

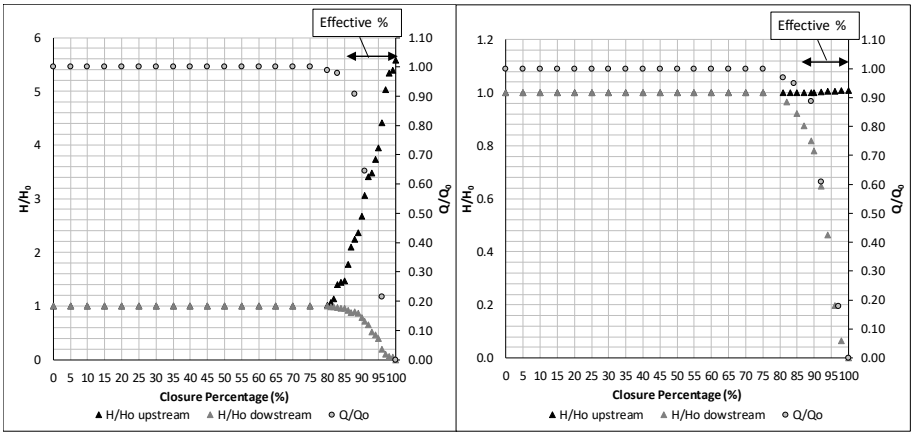

Figure 2. H/H_0 (upstream and downstream) variation and Q/Q_0 in a ball valve for turbulent flow (left; *Re*=100000) and laminar flow (right; *Re* = 1000). Comparison between effective closure % and total closure

2.3. Damping effects

Water hammer analysis usually focuses on the estimation of the extreme pressures associated with valves' maneuvers, pumps trip-off or turbines shutdown or start-up. The correct prediction of the pressure wave propagation, in particular, the damping effect, is not always properly accounted for. The latter will influence the system re-operation, the advanced model calibration and the dynamic behaviour of the system response. Transient solvers, commercially available, are not capable of predicting the pressure surge damping observed in real systems.

A new simplified approach of the surge damping is presented taking into account the pressure peak damping in time. This damping can be a combined effect of the non-elastic behaviour of the pipe-wall and the unsteady friction effect. This technique aims at the characterization of energy dissipation through the variation of the extreme piezometric head in time (Ramos *et al.,* 2004).

In a rigid pipe with an elastic behavior, the energy dissipation of the system in time for a rough turbulent flow, in a dimensionless form, varies with h^2 (due to almost exclusively friction effects). Based on the well-known upsurge given by Joukowsky formulation through equation (15):

$$\Delta H_j = \frac{cQ}{gS} \tag{15}$$

the time head variation ($h = \frac{H}{\Delta H_j}$) can be obtained according to equation (16):

$$h = \frac{1}{\frac{1}{h_0} + K\Delta h_0(\tau - \tau_0)} \tag{16}$$

assuming $\tau = \frac{t}{2L/c}$, being h_o the dimensionless head at initial time, $\tau_0 = \frac{t_0}{2L/c}$, and t_0 the time for the first pressure peak where the head is maximum.

According to the same type of analysis, in a plastic pipe with a non-elastic behaviour associated (*e.g.,* PVC, HDPE), the pipe-wall retarded-behaviour is the main responsible for the pressure damping. Thus, the energy dissipation can adequately be reproduced if proportional to the head, with mathematic transformations (Ramos et al. 2004) by the following equation (17):

$$h = h_0 e^{-K\Delta h_0(\tau - \tau_0)} \tag{17}$$

This equation is in accordance with the typical behaviour of a viscoelastic solid. For systems with combined effects (i.e. elastic and plastic), the surge damping can be evaluated by a combination of both former effects by the equation (18) (Ramos et al. 2004):

$$h = \frac{1}{\left(\frac{K_{elas}}{K_{plas}} + \frac{1}{h_0}\right) e^{K_{plas}\Delta h_0(\tau - \tau_0)} - \frac{K_{elas}}{K_{plas}}} \tag{18}$$

where K_{plas} and K_{elas} are decay coefficients for the plastic and elastic effects, respectively (Ramos 2003).

2.4. Runaway conditions

The specific rotational speed (n_s) is given by equation (19):

$$n_s = n\frac{P^{1/2}}{H^{5/4}} \tag{19}$$

where n_s is the specific speed of the machine in (m, kW); n is the rotational speed of the machine in rpm; P is the power in the shaft, which is measured in (kW); and H is the recovered head in (m w.c.). Therefore, n_s is a characteristic parameter about the runner shape and its dynamic behavior associated. In reaction turbines with low specific speed the flow drops with the transient overspeed. Conversely, for turbines with high specific speed the transient discharge tends to increase (Ramos, 1995, 2000).

The flow across a runner is characterized by three types of velocities: absolute velocity of the water (*V*) with the direction imposed by the guide vane blade, relative velocity (*W*) through the runner and tangential velocity (*C)*, of the runner.

For an uniform velocity distribution assumed at inlet (section 1) and outlet (section 2) of a runner, the application of Euler's theorem enables obtaining the relation between the motor binary and the momentum moment between these two sections 1 and 2 by equation (20):

$$BH = \rho Q(r_1 V_1 cos\alpha_1 - r_2 V_2 cos\alpha_2) \tag{20}$$

being α and *r* the angle and radius, respectively (see Figure 3).

The output power in the turbine shaft is a result of the multiplication of the binary by the angular speed ω, being defined by equation (21).

$$P = BH\omega \tag{21}$$

where *BH* is the hydraulic torque in Nm and *P* the output power in W.

It yields in the following equation (22) after some transformations to obtain the discharge variation (Ramos 1995):

$$Q = A\frac{\eta}{n} + Bn \tag{22}$$

where η is the turbine efficiency, coefficients A and B are defined by equations (23) and (24), respectively:

$$A = \frac{\frac{60\ gH_0}{2\pi r_2}}{\left(\frac{1}{2\pi b_0 r_2 \tan\alpha_0} + \frac{1}{A_2 \tan\beta_2}\right)} \tag{23}$$

$$B = \frac{\frac{2\pi r_2}{60}}{\left(\frac{1}{2\pi b_0 r_2 \tan\alpha_0} + \frac{1}{A_2 \tan\beta_2}\right)} \tag{24}$$

depending upon the rotational speed value and the characteristic of each runner.

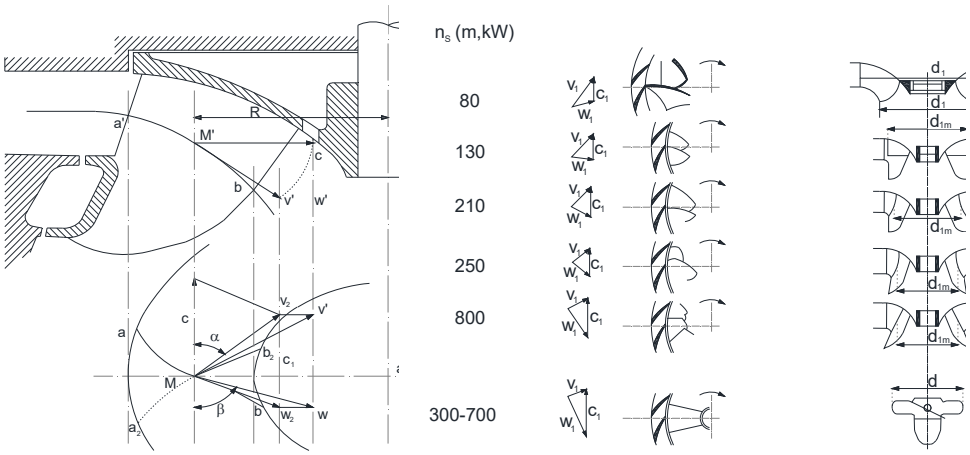

Figure 3. Velocity components across a reaction turbine runner (adapted from Mataix, 2009)

The subscript '*o*' denotes outlet from the wicket gate; the subscripts "1" and "2" are at inlet to and outlet from the runner; b_o is the runner height (or free-area) in m; r is the radial distance in m; α is the angle that the velocity vector (V) makes with the rotational velocity (C) in degrees; β is the angle that the runner blades makes with the C direction in degrees; and A_2 is the exit flow cross-section area in square meters.

Looking to this equation, the discharge regulation can be obtained by the variation of b_o, α_o or β_2. The b_o variation is a fixed characteristic of a runner (related to the height of the runner). According to Ramos (1995), the ratio (Q_{RW}/Q_0) between the flow discharge in runaway conditions (Q_{RW}) and the discharge for initial conditions of total opening (Q_0) tends to increase linearly with the increase of the specific speed (Figure 4).

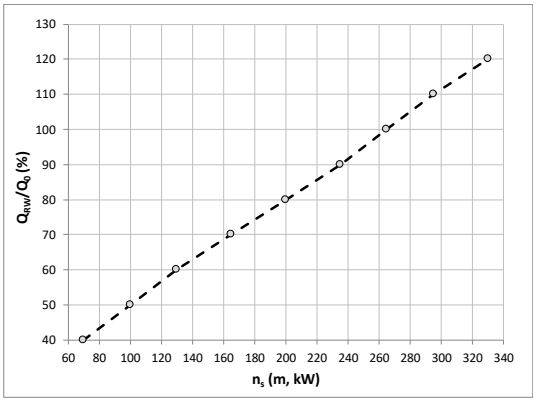

Figure 4. Overspeed effect on the discharge variation of reaction turbines (adapted from Ramos, 1995)

Furthermore, Ramos (1995, 2000) determined the variations of the ratio Q/Q_{BEP} as a function of N/N_{BEP} for constant values of h (H/H_{BEP}) in radial and axial conventional turbines machines based on Suter parameters (Figure 5) which are in accordance with the dynamic behavior associated with the runner shape.

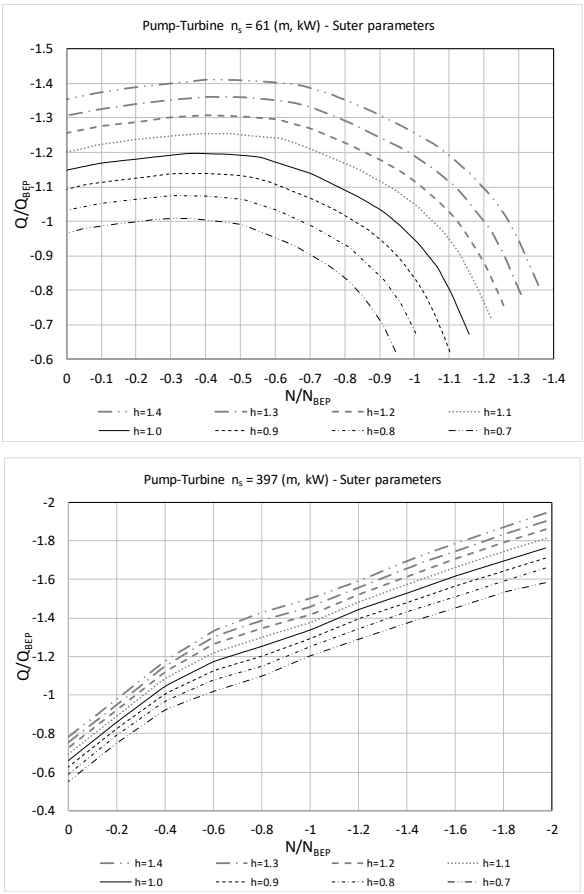

Figure 5. Q/Q_{BEP} as function of N/N_{BEP} and h for radial and axial machine (adapted from Ramos and Almeida, 2001)

2. Experiments and simulations developed

Experimental tests in small inertia hydraulic machines have been carried out in *CERIS*-Hydraulic Lab of Instituto Superior Técnico at the University of Lisbon for a radial and an axial one. In both cases the discharge was measured by an electromagnetic flowmeter; the pressure was registered by pressure transducers, through the Picoscope data acquisition system; the power was measured by a multimeter which was connected to

the generator; and the rotational speed was measured by a frequency meter.

The used machines were a radial pump working as turbine (*PAT*), with a rotational specific speed of 51 rpm (in m, kW); and an axial one, with a rotational specific speed of 283 rpm (in m, kW) (Figure 6). Each machine has been tested in different hydraulic circuits according to the available facilities. The radial machine scheme is composed by a reservoir to stabilize the flow; a pump to recirculate the flow; an air-vessel tank to control and stabilize the system pressure, which has 1 m^3 of capacity; an electromagnetic flowmeter; a hundred meters of polyethylene high density (*HDPE*) pipe, with 50 mm of nominal diameter; a *PAT* which is connected downstream of the *HDPE* loop pipe; and a ball valve located at downstream the *PAT*.

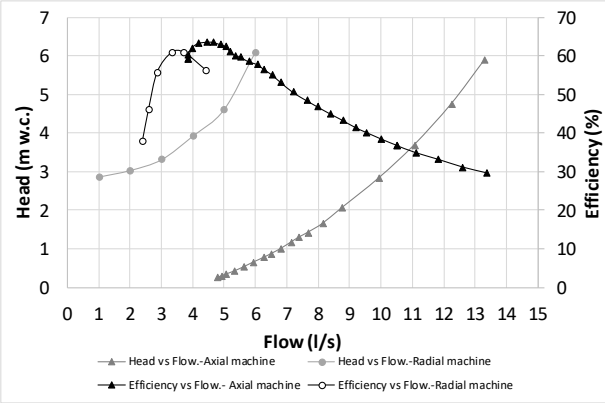

Figure 6. Experimental Head and Efficiency curves of axial (N_0=750 rpm) and radial (N_0=1020 rpm) machine.

This ball valve was connected with the reservoir by a *PVC* pipe. Pump and air vessel were joined by a *PVC* pipe of 7.40 m of length and 50 mm of nominal diameter. Air vessel and flowmeter were joined by other rigid *PVC* pipe with 1.80 m of length. Two pressure sensors were installed upstream and downstream the *PAT* to estimate the net head.

For the axial machine the scheme is similar to the previous one. The facility was composed by a reservoir, a pump to recirculate the flow, an air vessel tank to maintain a quasi-uniform pressure (the capacity of this tank is also 1 m^3), an electromagnetic flowmeter to measure the flow, the axial machine followed by a butterfly valve to isolate the facility. The pump and the air vessel were joined by a steal pipe with a length of 3.50 m and 80 mm of diameter, respectively. The axial machine and the butterfly valve were connected by a serial pipe, which is composed by a corrugated *PVC* (4.90 m and 110 mm of diameter) and a steal pipe (4.50 m and 80 mm of diameter). The butterfly valve and the reservoir were connected by a steal pipe, being its length equal to 2 m and its diameter equal to 80 mm. Two pressure sensors were installed upstream and downstream the axial machine.

These schemes (Figure 7) have been simulated with *Allievi* software (ITA 2010) according to the system characteristics in each facility previously described. The inner diameter and the wave speed are shown in Table 1 according to the pipe material.

Table 1. Basic parameters for the simulation

Material	Inner Diameter (m)	Wave speed (m/s)
HDPE	0.044	280
Corrugated *PVC*	0.110	385
Rigid *PVC*	0.047	527
Steal	0.068	1345

Flow and head in the pump, and pressure in the air vessel have been fitted in each developed simulation according to the registered experimental data for each test type. When the radial machine has been tested, the flow values oscillate between 2 and 5.15 l/s and the pressure between 15 and 30 m w.c.. In the axial machine, the tested flow varies between 5 and 14.10 l/s and the pressure in the air-vessel between 10 and 20 m w.c., as previously designed (Ramos *et al.,* 2009, 2013).

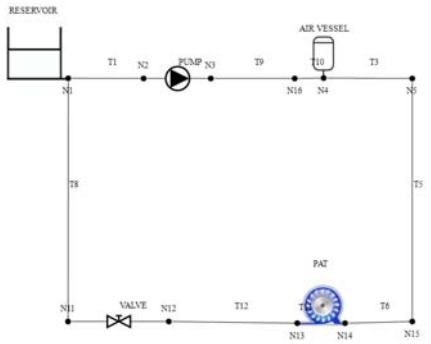

Figure 7. Simulation scheme used in *Allievi* model (*ITA*, 2010)

3.1. Control valve closure and PAT trip-off

This section shows the flow and the rotational speed variation when a fast shutdown is carried out downstream of the *PATs*. Figure 8 shows four tests with different initial flow values in the radial machine and three tests for the axial one. The values rapidly vary from the nominal values (flow and rotational speed) to zero. The closure time is around two seconds in all maneuvers considered as fast maneuvers.

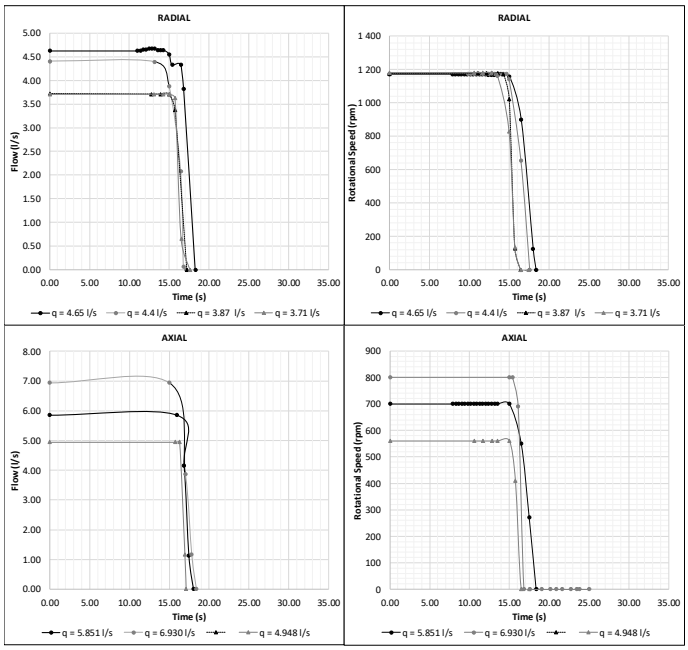

Figure 8. Experimental data recorded for the fast closure of the downstream control valve in radial (up) and axial (bottom) schemes.

According to the installed systems, the model has been implemented in *Allievi* (ITA, 2010) software as presented in Figure 7. The model has been calibrated to take into account the damping effects associated to the characteristic parameters of the system and the type of hydraulic machines.

Comparisons between experimental and simulated pressure values (upstream and downstream) present a very good fit. In Figure 9, the experimental overpressure in the radial machine is 69.85 m w.c. while the simulated overpressure is 70.52 m w.c. The result in the first depression wave is similar, where the minimum experimental value is 24.54 m w.c. and the simulated is 19.73 m w.c. The axial machine presents values of experimental overpressure around 46.23 m w.c. and simulated of 49.24 m w.c. The minimum experimental depression value is 36.54 m w.c. while the simulated value is 33.63 m w.c.. These results show the dynamic behavior of the radial and axial machines when a transient induced downstream attain the runners. The transient wave pass through the runners and the pressure variation are upstream and downstream are essentially both in phase.

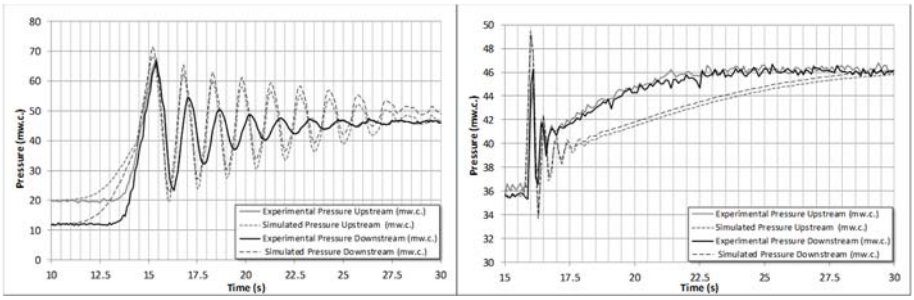

Figure 9 Experimental and simulated pressure values along time in a fast closure maneuver (t=2 s): radial (left) and axial (right)

3.2. Control valve opening and PAT start-up

Flow, rotational speed, and pressure values (upstream and downstream) have been recorded over time (Figures 10 and 11). Figure 10 shows the fast opening of the downstream control valve for each system. Some variations can be observed, where the rotational speed of the machine reaches 2235 rpm, the double of the nominal rotational speed of the machine for 4.65 l/s for the radial machine and 1500 rpm for the axial machine, being 6.93 l/s the nominal flow, and 800 rpm the nominal rotational speed.

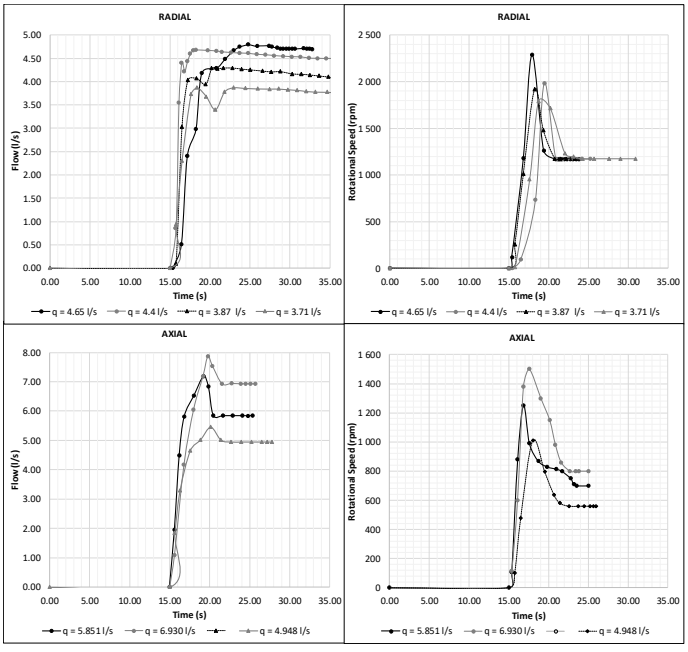

Figure 10. Experimental data recorded for the fast opening of the downstream control valve in radial (up) and axial (bottom) schemes

The trend in the valve opening for *PAT* start-up is similar in all cases: firstly, the machine increases the rotational speed upper its nominal value. When the overspeed is reached with a flow value near to 4.00 l/s for the radial and 7.86 l/s for the axial, the rotational speed decreases to the nominal one. In this time, the flow attains the nominal flow with the maximum valve opening degree. If the pressure variation is analyzed during the valve opening, the behavior is similar a fast maneuver. In this case, with the valve opening a downsurge wave in both machines is observed (radial and axial). This depression depends on the flow and the opening time. This value has also been simulated with *Allievi* (ITA, 2010), obtaining very interesting and quite accurate results (Figure 11).

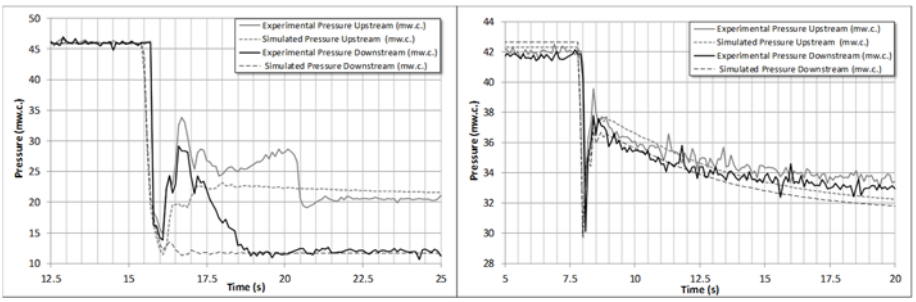

Figure 11. Experimental data and simulation for fast opening downstream control valve of radial (left) and axial machine (right)

3.3. Overspeed effects in PATs

Some interesting conclusions can be drawn for both types of runners. Figure 12 presents the obtained values of flow, rotational speed, and pressure (upstream and downstream) for the overspeed conditions. The flow value decreases over time in all tests induced by the runner shape associated to the low specific speed value as previously it is mentioned from Figure 3 to 5. This decrease of the flow is related to an increase of the rotational speed, being the minimum flow attained when the runaway conditions are reached (*e.g.,* for an initial flow of 4.67 l/s, the rotational speed varies from 1150 to 2235 rpm, while the flow reduces to 2.4 l/s). This flow value (2.4 l/s) can be checked in Figure 13, correspondent to runaway conditions.

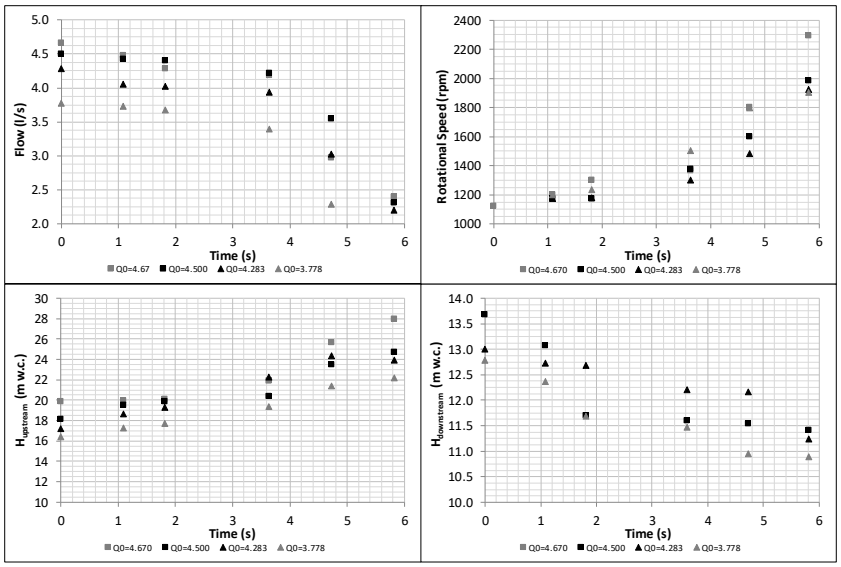

Figure 12. Experimental data of flow, rotational speed, and upstream and downstream head in the radial machine under the overspeed effect

Regarding the pressure variation, some issues can be observed: the upstream pressure value increases being the maximum pressure when the machine reaches the runaway conditions and consequently the downstream pressure decreases (Figure 12). There is a flow cut effect induced by the radial runner under overspeed conditions.

The experimental data under runaway conditions can be expressed by different parameters: the discharge flow, the pressure and the rotational speed for total opening valve degree (Q_0, H_0, N_0). Furthermore, the experimental results can be associated to the values of best efficiency point of the machine in turbine mode (Q_{BEP}, H_{BEP}, N_{BEP}). These variations are shown in Figure 13. If Q_{RW}/Q_0 versus N_{RW}/N_0 (the subscripts '*RW*' indicates runaway conditions) is observed, the values are almost constant for all experimental data denoting a typical characteristic of the radial machine. In this case, the ratio Q_{RW}/Q_0 is close to 0.514. This value means there a flow reduction of around 50% of the rated conditions as presented in Figure 4, showing the characteristic of this radial machine under the overspeed effect.

Similar conclusions can be obtained if the upstream and downstream pressure are analyzed with values near to 1.40 and 0.85, inducing an upsurge and a downsurge at upstream and downstream of the machine, respectively. If the values are compared with the best efficiency point of the radial machine, under the overspeed effect, the flow decreases for a constant value of h ($h=H/H_{BEP}$). All cases have the same tendency for different h values in Figure 13.

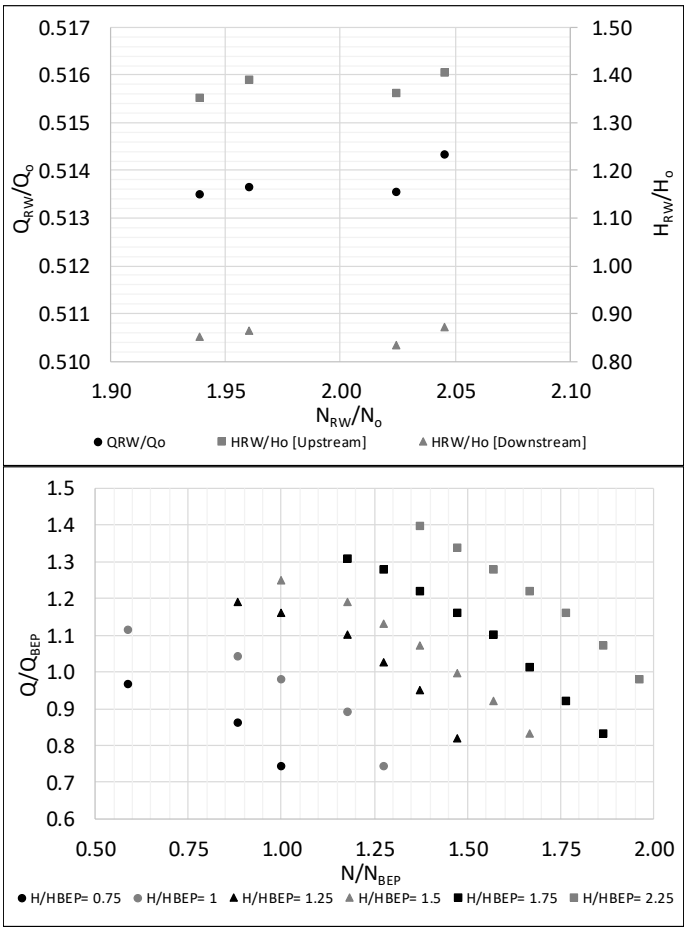

Figure 13. Q_{RW}/Q_0 and H_{RW}/H_0 as function of N_{RW}/N_0 (up) and Q/Q_{BEP} as function of N/N_{BEP} and H/H_{BEP} (bottom) for the radial machine

Converse results are obtained when the experimental data are analyzed for the axial machine (Figure 14). The flow rises over time as the rotational speed increases until to reach the runaway value. In these cases, the upstream and downstream pressure remain almost constant over time.

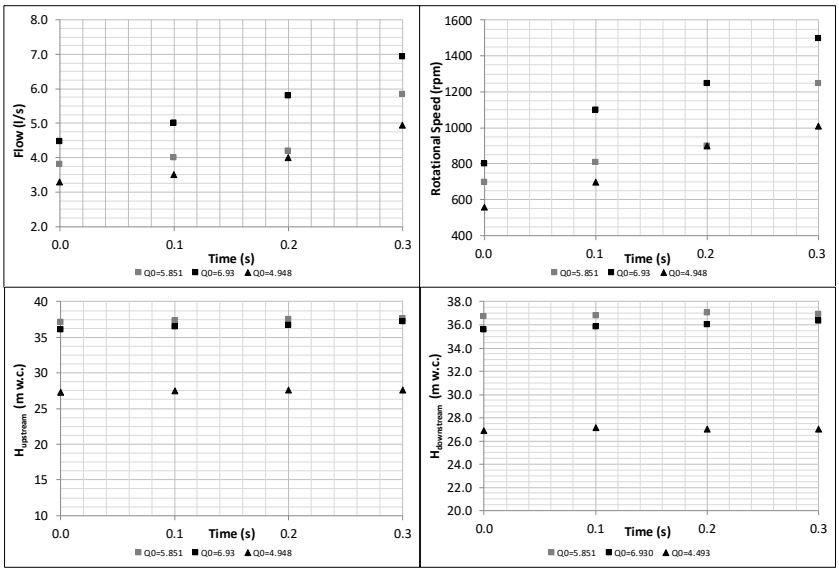

Figure 14. Experimental data of flow, rotational speed, and upstream and downstream head in the axial machine under the overspeed effect

As for the radial machine, Figure 15 shows the experimental data for the discharge flow, pressure, and the rotational speed variation for the total valve opening (Q_0, H_0, N_0) during the overspeed conditions. In this case, the ratio Q_{RW}/Q_0 shows an increasing of flow equal to 1.52. This value is upper than in the one getting from Fig. 4, where the Q_{RW}/Q_0 is 105% (1.05) for n_s equal to 280 rpm (in m, kW).

The experimental data have also been correlated with the values of the best efficiency point (Q_{BEP}, H_{BEP}, N_{BEP}). The obtained results are contrasting to the radial machine. If a constant value of h ($h=H/H_{BEP}$), the flow grows when the rotational speed increases. All cases analyzed for a constant h value are shown in Figure 15, presenting the same tendency.

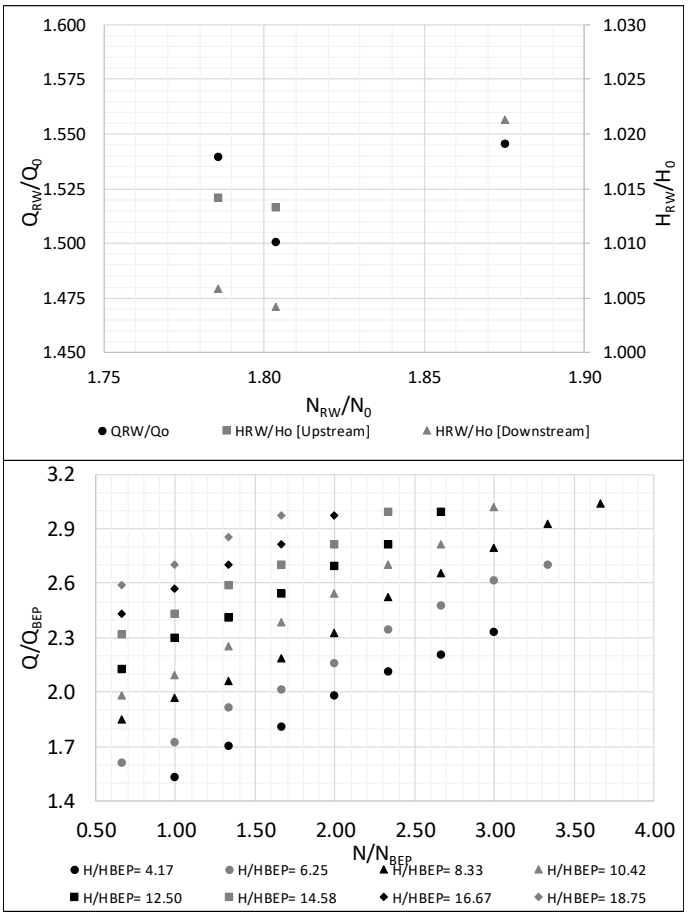

Figure 15. Q_{RW}/Q_0 and H_{RW}/H_0 as a function of N_{RW}/N_0 (up) and Q/Q_{BEP} as a function of N/N_{BEP} according to $h=H/H_{BEP}$ (bottom) for the axial machine

4. Conclusions

Based on the experience, a large number of criteria to deal with the design and hydraulic transients of micro hydropower systems are addressed. The type of analysis will be influenced by the design stage and the complexity of each system. Hence, based on each hydraulic system characteristics, for the most predictable maneuvers, the designers will be able to define exploitation rules according to expected safety levels. In fact, convenient operational rules need to be specified in order to control the maximum and minimum transient pressures. These specifications will mainly depend on the following factors:

- the characteristics of the pipe system to be protected; in fact, these characteristics based on head loss and inertia of the water column can adversely modify the system behaviour and the same valve closure time can induce whether a slow or a rapid flow change;
- the intrinsic characteristics of the valve: a butterfly valve (*e.g.,* for medium heads) and a spherical valve (*e.g.,* for high heads) have different effects on the dynamic flow response for the same closure law;
- since *PATs* have no guide vane, the flow control is made through valves where the closure and opening laws are crucial in the safety system conditions, as the type of the valve actuator; and
- based on the characteristics of the pump as turbine machine (radial or axial), different dynamic behavior will be associated to:
    - the small inertia of the rotating masses induces a fast overspeed effect under runaway conditions imposed by a full load rejection.
    - the overspeed effects provoke flow variations (*i.e.,* flow reduction in low n_s machines and increasing in the high n_s machines) and pressure variations that can propagate upsurges to upstream of a radial machine and downsurges downstream of it.

Therefore, based on data obtained during this intensive experimental campaign, important information is presented and utilized for some specific *PAT* transient state conditions. This analysis requires a mathematical transformation of available data of pumps (based on experiments especially developed for this study) into characteristic curves of discharge variation, Q/Q_{BEP}, with the rotating speed, N/N_{BEP} (Figures 12 and 15, for radial and axial machines, respectively). This procedure makes easier the understanding of the dynamic pump as turbine behavior under unsteady conditions.

The feasibility of pumps operating as turbines seems to be proved, based on typical performed control analyses. The dynamic behavior of those machines is quite similar to the classical reaction turbines, regarding the flow variation due to the runner type, generally characterized by its specific rotational speed (n_s) (through the studies of Ramos, 1995, 2000; Ramos and Almeida, 2001, 2002).

These *PAT* solutions can be adopted instead of energy dissipation devices in conveyance pipe systems with excess available energy at some pipe sections. Therefore, the use of reverse pumps in drinking, irrigation and sewage or drainage water systems can be a quite interesting solution in some cases, taking the advantage of the available head that in other way would be dissipated.

Hence, the integrated system response depends on the disturbance or the excitation type as well the interaction of different components that can induce potential instabilities as presented herein. Being computer analyses a common place in the design process, the

sophistication modelling needed for the capability analyses by *Allievi* (*ITA*, 2010) depends on the type of events and phenomena associated to each system characteristic as presented in this research.

Acknowledgments

This research is supported by Program to support the academic career of the faculty of the Universitat Politècnica de València 2015/2016 in the project "Methodology for Analysis of Improvement of Energy Efficiency in Irrigation Pressurized Network".

Competing interests

The authors have declared that no competing interests exist.

References

Abbott, M. & Cohen, B., 2009. Productivity and efficiency in the water industry. *Utilities Policy*, 17(3-4), 233–244.

Abreu, J., Guarga, R. & Izquierdo, J., 1995. Transitorios y oscilaciones en sistemas hidráulicos a presión J. Abreu, R. Guarga, & J. Izquierdo, eds., Valencia: U.D. Mecánica de Fluidos. Universidad Politécnica de Valencia.

Almeida, A.B. & Koelle, E., 1992. Fluid transients in pipe networks. *Computational Mechanics Publications*. Elsevier Applied Science, Amsterdam, Netherlands

Araujo, L., Ramos, H. & Coelho, S., 2006. Pressure Control for Leakage Minimisation in Water Distribution Systems Management. *Water Resources Management*, 20(1), 133–149.

Arriaga, M., 2010. Pump as turbine – A pico-hydro alternative in Lao People's Democratic Republic. *Renewable Energy*, 35(5), 1109–1115.

Butera, I. & Balestra, R., 2015. Estimation of the hydropower potential of irrigation networks. *Renewable and Sustainable Energy Reviews*, 48, 140–151.

Cabrera, E., Cobacho, R. & Soriano, J., 2014. Towards an Energy Labelling of Pressurized Water Networks. *Procedia Engineering*, 70, 209–217.

Carravetta, A., Fecarotta, O., Del Giudice, G., & Ramos, H., 2013. PAT Design Strategy for Energy Recovery in Water Distribution Networks by Electrical Regulation. *Energies*, 6(1), 411–424.

Carravetta, A., Del Giudice, G., Fecarotta, O., & Ramos, H.M, 2014. Energy Recovery in Water Systems by PATs: A Comparisons among the Different Installation Schemes. *Procedia Engineering*, 70, 275–284.

Caxaria, G., de Mesquita e Sousa, D., & Ramos, H.M., 2011. Small Scale Hydropower: Generator Analysis and Optimization for Water Supply Systems. pp.1386–1393. Available at: http://www.ep.liu.se/ecp_article/index.en.aspx?issue=57;vol=6;article=2.

Chaudhry, M., 1987. *Applied Hydraulic Transients* 2nd ed. V. N. R. Company, ed.,

Corcoran, L., McNabola, A. & Coughlan, P., 2016. Predicting and quantifying the effect of variations in long-term water demand on micro-hydropower energy recovery in water supply networks. *Urban Water Journal*, 9 (6), 1–9.

Dannier, A., Del Pizzo, A., Giugni, M., Fontana, N., Marini, G., & Proto, D., 2015. Efficiency

evaluation of a micro-generation system for energy recovery in water distribution networks. 2015 International Conference on Clean Electrical Power (ICCEP), pp.689–694. Available at: http://ieeexplore.ieee.org/lpdocs/epic03/wrapper.htm?arnumber=7177566.

Elbatran, A.H., Yaakob, O.B., Ahmed, Y.M., & Shabara, H.M., 2015. Operation, performance and economic analysis of low head micro-hydropower turbines for rural and remote areas: A review. *Renewable and Sustainable Energy Reviews*, 43, pp.40–50.

Fecarotta, O., Aricò, C., Carravetta, A., Martino, R., & Ramos, H.M., 2014. Hydropower Potential in Water Distribution Networks: Pressure Control by PATs. *Water Resources Management*, 29(3), pp.699–714.

Fecarotta, O, Carravetta, A., Ramos, H.M., & Martino, R., 2016. An improved affinity model to enhance variable operating strategy for pumps used as turbines. *Journal of Hydraulic Research*, 1686(October), pp.1–10.

Giugni, M., Fontana, N. & Ranucci, A., 2014. Optimal Location of PRVs and Turbines in Water Distribution Systems. Journal of Water Resources Planning and Management, 140(9), p.06014004.

Iglesias-Rey, P., Izquierdo, J., Fuertes, V., & Martínez-Solano, F., 2004. Modelación de transitorios hidráulicos mediante ordenador. Grupo Mult., Universidad Politécnica de Valencia.

Imbernón, J.A. & Usquin, B., 2014. Sistemas de generación hidráulica. Una nueva forma de entender la energía. In II Congreso Smart Grid Madrid, Spain 27-28th October 2014. https://www.smartgridsinfo.es/biblioteca/libro-de-comunicaciones-del-ii-congreso-smart-grids

ITA, 2010. Allievi. Available at: www.allievi.net.

Jiménez-Bello, M.A., Royuela, A., Manzano, J., Prats, A.G., Martínez-Alzamora F., 2015. Methodology to improve water and energy use by proper irrigation scheduling in pressurised networks. *Agricultural Water Management*, 149, pp.91–101.

Kougias, I., Patsialis, T., Zafirakou, A., & Theodossiou ,N., 2014. Exploring the potential of energy recovery using micro hydropower systems in water supply systems. *Water Utility Journal*, 7, pp.25–33.

Mamade, A., Loureiro, D., Alegre, H., & Covas, D., 2017. A comprehensive and well tested energy balance for water supply systems. *Urban Water Journal*. Available at: http://dx.doi.org/10.1080/1573062X.2017.1279189 [Accessed February 19, 2017]

Mataix, C., 2009. *Turbomáquinas Hidráulicas*, Madrid: Universidad Pontificia Comillas.

McNabola, A., Coughlan, P., Corcoran, L., Power, C., Prysor, A.,Harris, I., Gallagher, J., & Styles, D., 2014. Energy recovery in the water industry using micro-hydropower: an opportunity to improve sustainability. *Water Policy*, 16(1), 168-183.

Moreno, M., Córcoles, J., Tarjuelo, J., & Ortega, J., 2010. Energy efficiency of pressurised irrigation networks managed on-demand and under a rotation schedule. *Biosystems Engineering*, 107(4), 349–363.

Nogueira, M., Perrella, J., 2014. Energy and hydraulic efficiency in conventional water supply systems. Renew. Sustain. Energy Rev. 30, 701–714. doi:10.1016/j.rser.2013.11.024

Nourbakhsh, A. & Jahangiri, G., 1992. Inexpensive small hydropower stations for small areas of developing countries. In Conference on Advanced in Planning-Design and Management of Irrigation Sistems as Related to Sustainable Land use. Louvain, Belgium, pp. 313–319.

Pardo, M.A., Manzano, J., Cabrera, E., & García-Serra, J., 2013. Energy audit of irrigation networks. *Biosystems Engineering*, 115(1), 89–101.

Pérez-Sánchez, M., Sánchez-Romero, F., Ramos, H., & López-Jiménez, P.A., 2017. Energy Recovery in Existing Water Networks: Towards Greater Sustainability. *Water*, 9(2), 97-117.

Pérez-Sánchez, M., Sánchez-Romero, F., Ramos, H., & López-Jiménez, P.A., 2016. Modeling Irrigation Networks for the Quantification of Potential Energy Recovering: A Case Study. *Water*, 8(6), 1–26.

Ramos, H., 2003. Design concerns in pipe systems for safe operation. *Dam Engineering*, 14(1), 5–30.

Ramos, H., 2000. *Guidelines for Design of Small Hydropower Plants*; WREAN (Western Regional Energy Agency &Network) and DED (Department of Economic Development), Belfast, North-Ireland.

Ramos, H., 1995. *Simulation and Control of Hydrotransients at Small Hydroelectric Power Plants*. PhD Thesis, IST, Portugal.

Ramos, H.M., Borga, A., & Simão, M., 2004. Surge damping analysis in pipe systems: modelling and experiments. *Journal of Hydraulic Research*, 42(4), 413–425.

Ramos, H. & Almeida, A.B., 2001. Dynamic orifice model on water hammer analysis of high or medium heads of small hydropower schemes. *Journal of Hydraulic Research*, 39(4), 429–436.

Ramos, H. & Almeida, A.B., 2002. Parametric Analysis of Water-Hammer Effects in Small Hydro Schemes. *Journal of Hydraulic Engineering, ASCE*, 128(7), 689–696.

Ramos, H. & Borga, A., 1999. Pumps as turbines: an unconventional solution to energy production. *Urban Water*, 1(3), 261–263.

Ramos, H.M., Borga, A. & Simão, M., 2009. New design solutions for low-power energy production in water pipe systems. Water Science and Engineering, 2(4), 69–84.

Ramos, H.M., Simão, M. & Borga, A., 2013. Experiments and CFD Analyses for a New Reaction Microhydro Propeller with Five Blades. *Journal of Energy Engineering*, 139(2), 109–117.

Razan, J.I., Islam, R.S., Hasan, R., Hasan, S., & Islam, F., 2012. A Comprehensive Study of Micro-Hydropower Plant and Its Potential in Bangladesh. *ISRN Renewable Energy*, 2012, 1–10.

Samora, I., Manso, P., Franca, M., Schleiss, A., Ramos, H., 2016. Energy Recovery Using Micro-Hydropower Technology in Water Supply Systems: The Case Study of the City of Fribourg. *Water*, 8(8), 344-359.

Senior, J., Saenger, N. & Müller, G., 2010. New hydropower converters for very low-head differences. *Journal of Hydraulic Research*, 48(6), 703–714.

Simão, M. & Ramos, H.M., 2010. Hydrodynamic and performance of low power turbines: conception, modelling and experimental tests. *International Journal of Energy and Environment*, 1(3), 431–444.

Sitzenfrei, R., Berger, D. & Rauch, W., 2015. Design and optimization of small hydropower systems in water distribution networks under consideration of rehabilitation measures. *Urban Water Journal*, 12 1–9.

Su, P.-A. & Karney, B., 2014. Micro hydroelectric energy recovery in municipal water systems: A case study for Vancouver. *Urban Water Journal*, 12(8), 678–690.

Subani, N. & Amin, N., 2015. Analysis of Water Hammer with Different Closing Valve Laws on Transient Flow of Hydrogen-Natural Gas Mixture. *Abstract and Applied Analysis*, 2, 12-19.

White, F.M., 2008. *Fluid Mechanics* Sixth edit., McGrau-Hill.

Zema, D.A., Nicotra, A., Tamburino, V., Zimbone, S.M., 2016. A simple method to evaluate the technical and economic feasibility of micro hydro power plants in existing irrigation systems. Renew. Energy 85, 498–506. doi:10.1016/j.renene.2015.06.066